UC Santa Cruz

UC Santa Cruz Electronic Theses and Dissertations

Title

Pharmacokinetic and Conformational Analysis of Naturally Inspired Cyclic Peptides

Permalink

https://escholarship.org/uc/item/7744s04p

Author

Schwochert, Joshua Allen

Publication Date

2017

Peer reviewed|Thesis/dissertation

eScholarship.org Powered by the California Digital Library
University of California

UNIVERSITY OF CALIFORNIA
SANTA CRUZ

Pharmacokinetic and Conformational Analysis of Naturally Inspired Cyclic Peptides

A dissertation submitted in partial satisfaction
Of the requirements for the degree of

DOCTOR OF PHILOSOPHY

in

CHEMISTRY AND BIOCHEMISTRY

by

Joshua Allen Schwochert

March 2017

The Dissertation of Joshua Allen Schwochert
is approved:

_____
Professor R. Scott Lokey, Advisor

_____
Professor Joseph P. Konopelski, Chair

_____
Professor Carrie L. Partch

_____
Tyrus Miller
Vice Provost and Dean of Graduate Studies

TABLE OF CONTENTS

1. Revisiting N-to-O Acyl Shift for Synthesis of Natural Product-like Cyclic Depsipeptides 1

1.1. Foreword 1

1.2. Introduction 1

1.3. *N*-to-*O* Rearrangement and Subsequent Acylation 3

1.3.1. Spectroscopic elucidation of the *N*-to-*O* Acyl Shift 3

1.3.2. *N*-Acylation of Isoacylthreonine 4

1.3.3. Generality of the Acid Catalyzed *N*-to-*O* Rearrangement in Cyclic Peptides 5

1.3.4. Conformational Requirements for the Rearrangement as Assessed by Molecular Dynamics 7

1.4. ADME Analysis of Depsipeptides 8

1.5. Conformational Analysis 9

1.5.1. Solution Conformations of 1 and 3 as Elucidated by NMR 9

1.5.2. X-ray Crystal Structure of 1 11

1.5.3. Temperature Shift Analysis of 1 and 3 11

1.6. Conclusion 12

1.7. Abbreviations 13

1.8. Methods 13

1.8.1. General Synthetic and Procedures 13

1.8.1.1. Overview 13

1.8.1.2. Automated Peptide Synthesis 14

1.8.1.3. Microwave Reaction Conditions 14
1.8.1.4. Loading of 2-Chlorotrityl resin 14
1.8.1.5. Automated On-Resin Fmoc Deprotection 15
1.8.1.6. Automated Amino Acid Coupling 15
1.8.1.7. On-Resin O-allyl and Fmoc deprotection 15
1.8.1.8. On-Resin Cyclization 16
1.8.1.9. On-Resin Selective Methylation 16
1.8.1.10. On-Resin Installation of o-Ns 16
1.8.1.11. On-Resin Installation of the TFA protecting group 17
1.8.1.12. N-Alkylation under Mitsunobu Conditions 17
1.8.1.13. On-Resin O-Ns Deprotection 17
1.8.1.14. On-Resin TFA Deprotection 18
1.8.1.15. Amino Acid Coupling to Hindered Amines under Microwave Condtions 18
1.8.1.16. Peptide Cleavage 18
1.8.1.17. Cyclization with COMU 19
1.8.1.18. Removal of Acid Labile Side Chain Protecting Groups 19
1.8.1.19. N-O Acyl shift 19
1.8.1.20. Coupling of 'tails' 20
1.8.1.21. Purification of Peptides 20
1.8.2. RRCK Cell Permeability 21
1.8.3. X-ray Crystal Structure of 1 22
1.8.3.1. Details of the Single-Crystal Data Collection, Structure solution and Refinement 23
1.8.4. NMR Analysis and Assignment 24
1.8.4.1. Acquisition Parameters 24
1.8.4.1. Temperature Coefficients 25

1.8.4.2. Spectral Assignment....26
1.8.4.3. Conformation Generation and DISCON Analysis....28
1.8.5. Molecular Dynamics of the N-to-O Acyl Rearrangement....31
1.8.6. Compound structures and synthetic considerations....32
1.8.7. HPLC MS data for compounds 1-15....47
1.8.8. Selected NMR Spectra....55
1.9. References....81
2. Investigation of Peptoid Substitutions in 1NMe3: ADME and Conformational Consequences....86
2.1. Foreword....86
2.2. Introduction....86
2.2.1. Preamble....86
2.2.2. Peptoids as Modular Building Blocks....87
2.2.3. Peptoids in Drug Discovery....89
2.3. Previous Results and Experimental Design....89
2.4. ADME Properties of Peptoid Analogs of 1NMe3....91
2.5. Structural Analysis of L2N and L3N....93
2.6. Diversification of the Y6 Position....95
2.7. Conclusions....97
2.7.1. Abbreviations....98
2.8. Methods....99
2.8.1. General Synthetic Prodcedures....99
2.8.1.1. Compound Specific Considerations....99
2.8.1.2. Microwave Reaction Conditions....99

2.8.1.3. Loading of 2-Chlorotrityl resin 99
2.8.1.4. Room Temperature Amino Acid Coupling 100
2.8.1.5. Room Temperature Amino Acid Coupling onto Secondary Amines 100
2.8.1.6. Amino Acid Coupling under Microwave Condtions 101
2.8.1.7. Amino Acid Coupling onto N-Methylated Amino Acids under Microwave Conditions 101
2.8.1.8. Coupling of Bromoacetic acid at Room Temperature 101
2.8.1.9. Coupling of Bromoacetic acid Under Microwave Conditions 102
2.8.1.10. Installation of Peptoid Sidechain 102
2.8.1.11. Removal of the N-Fmoc Protecting Group at Room Tempearture 103
2.8.1.12. Removal of the N-Fmoc Protecting Group Under Microwave Conditions 103
2.8.1.13. On-Resin Installation of the TFA protecting group 103
2.8.1.14. N-Alkylation under Mitsunobu Conditions 103
2.8.1.15. On-Resin TFA Deprotection 104
2.8.1.16. Peptide Cleavage 104
2.8.1.17. Cyclization with EDC and HOAt 105
2.8.1.18. Cyclization with COMU 105
2.8.1.19. Removal of Acid Labile Side Chain Protecting Groups 105
2.8.1.20. Purification of Peptides 106
2.8.2. RRCK Permeability 107
2.8.3. NMR Analysis and Assignment 108
2.8.4. DISCON Analysis: 112
2.8.5. Characterization of Compounds 116
2.8.6. Selected NMR Spectra 129
2.9. References 154

3. Naturally Derived Cyclic Peptides: Synthesis, Physiochemical and Spectroscopic Analysis. 164

3.1. Foreword 164

3.2. Introduction 165

3.2.1. Structural Elements and Cell Permeability 165

3.2.2. Cyclosporine and Solvent Dependent Conformations 166

3.3. Phepropeptins and Analogs 166

3.3.1. Introduction 166

3.3.2. Synthesis 167

3.3.3. ADME Properties 168

3.3.4. NMR Analysis 170

3.3.4.1. Temperature Shift Analysis 170

3.3.4.2. NMR Structure of Phepropetin C (**3**) in Chloroform 172

3.3.4.3. NMR Structure of Phepropeptin C in DMSO 175

3.4. Methods for the Preparation and Analysis of Phepropeptins and Analogs 177

3.4.1. General Synthetic Methods 177

3.4.1.1. Loading of 2-Chlorotrityl resin 177

3.4.1.2. Automated Peptide Synthesis 177

3.4.1.3. Automated On-Resin Fmoc Deprotection 177

3.4.1.4. Peptide Cleavage 178

3.4.1.5. Automated Amino Acid Coupling 178

3.4.1.6. Cyclization with COMU 178

3.4.1.7. Purification of Peptides 179

3.4.2. Methods for *in vitro* ADME assays 180
3.4.2.1. Plasma stability assay 180
3.4.2.2. Mechanistic permeability assay 180
3.4.2.3. Thermodynamic Solubility via "High Throughput Method" 181
3.4.2.4. LogD 7.4 182
3.4.3. HPLC-MS of Phepropeptins and Analogs 183
3.4.4. NMR Solution Structures 191
3.4.4.1. NMR Parameters 191
3.4.4.2. Molecular Dynamics and Conformer Analysis: 191
3.4.4.3. NMR Processing and Comparison of Conformations: 192
3.4.1. Selected NMR Spectra 202
3.4.1.1. Pairwise Comparisson in Chloroform of Epimers 210
3.5. Other Natural Products 219
3.5.1. Introduction 219
3.5.2. Cylindrocyclin 220
3.5.2.1. Introduction 220
3.5.2.2. Synthesis 221
3.5.2.3. NMR Analysis 223
3.5.2.4. Conclusion 224
3.5.3. Stylissamide G 225
3.5.4. Cordyheptapeptide B 226
3.5.5. Scytalidamide A 230
3.6. Abbreviations 232
3.7. Methods for Natural Product Synthesis 232
3.7.1. General Synthetic Strategies 232

3.7.2. Loading of 2-Chlorotrityl resin 233
3.7.3. Microwave Reaction Conditions 233
3.7.4. Amino Acid Coupling under Microwave Condtions 233
3.7.5. Amino Acid Coupling onto Sterically Demanding Amino Acids under Microwave Conditions 234
3.7.6. Difficult Amino Acid Coupling with BTC 234
3.7.7. Removal of the *N*-Fmoc Protecting Group Under Microwave Conditions 235
3.7.8. Peptide Cleavage 235
3.7.9. Cyclization with COMU 235
3.7.10. Purification of Peptides 236
3.7.11. NMR Analysis 236
3.7.12. HPLC-MS Characterization 237
3.7.13. Selected NMR Spectra 241
3.8. Conclusions 245
3.9. References 246
4. Bibliography 256

List of Figures

Figure 1-1 Structure of Kahalalide F 2

Figure 1-2 Acyl rearrangement and subsequent acylation..... 3

Figure 1-3 Mechanism of the *N*-to-*O* Acyl Rearrangement 4

Figure 1-4 Scatter plots representing 10 ns molecular dynamics simulations of **1** and **9**, respectively, monitoring the distance and angle between the Thr-OH and i-1 carbonyl carbon every 5 ps 7

Figure 1-5. Analysis of Molecular Dynamics a) Distance and angle measured between Thr-OH and i-1 carbonyl carbon b) graph of snapshots containing an –OH to C=O distance of < 4 Å and O-C-O angle within ±10˚ of the Burgi-Dunitz angle. .. 8

Figure 1-6 a, b) Major conformation of the DISCON ensemble for **1** and **3**, respectively. c) Conformation of **3**, highlighting tail to backbone hydrogen bond. d) Overlay of **1**, green, and **3**, orange. e,f) X-ray structrure of **1** and an overlay of the the X-ray structure, purple, and solution conformation, green. 10

Figure 1-7 ORTEP Images of 1 23

Figure 1-8 Temperature dependence of the amide protons of compound **1** 25

Figure 1-9 Temperature dependence of the amide protons of compound **3** 25

Figure 1-10 Minor conformations of **3** as determined by DISCON with their respective contribution to the ensemble listed below. 30

Figure 2-1 Structural Elements of Peptoids..... 87

Figure 2-2 FMOC SPPS versus Peptoid Synthesis..... 88

Figure 2-3 Peptoid Series and MDCK-LE Apparent Cell Permeability (average of 3 replicates, * denotes 2 replicates only) 91

Figure 2-4 a,b) NMR restrained solution conformations of **L2N** and **L3N**, respectively. c,d) 2D representation of the conformations of **L2N** and **L3N**, respectively, with the amide between positions 2 and 3 highlighted in yellow, peptoid residues highlighted in red. e, f) Electrostatic surfaces of the **L2N** and **L3N**, with the solvent exposed carbonyl of Leucine 1 highlighted with a dashed circle..... 93

Figure 2-5 Peptoid Series and MDCK-LE Apparent Cell Permeability (average of 3 replicates)..... 95

Figure 2-6 EPSA values (compared to RRCK) as caclulated in Goetz et al.[54]..... 96

Figure 3-1 Structure of the phepropeptins and analogs 167

Figure 3-2 *In vitro* cell permeability and solubility for the phepropeptins and epimeric analogs. 170

Figure 3-3 Temperature shift experiments for **1**, **3**, **5** and **7** in chloroform. Using the cutoff of -4 ppb/K peaks that are solvent exposed are noted in red, while those that are hidden from solvent are noted in green. Peaks that disappear and reappear are highlighted with a red line Note: only 4 peaks were observable for compounds **5** and **7**, with the 5th amide NH likely hidden under the phenylalanine sidechain protons at 7.2-7.3 ppm. 172

Figure 3-4 NMR structure of phepropeptin C (**3**) in chloroform a) table of NMR data for the NH protons of compound **3**, b) solution structure of **3** as found by molecular dynamics, ROESY, and 3*J* HNHA, c) surface showing solvent accessible polarity of

the structure in b, with the solvent exposed NH of phenyalanine 2 highlighted with a dashed circle..... 174

Figure 3-5 NMR structure of phepropeptin C (**3**) in DMSO a) table of NMR data for the NH protons of compound **3** in DMSO, b) two views of the solution structure of **3** in DMSO c) Box plots of solvation energy of the 10 best NMR structures in DMSO and chloroform..... 175

Figure 3-6 Numbering Scheme for Phepropeptin C (**3**)..... 194

Figure 3-7 Overlays of the 10 lowest RMSD structure in CDCl3..... 196

Figure 3-8 Overlays of the 10 lowest RMSD structures in DMSO..... 199

Figure 3-9 Comparisson of Phepropeptin A and Epiphepropeptin A in Chloroform210

Figure 3-10 Comparisson of Phepropeptin B and Epiphepropeptin B in Cholroform 211

Figure 3-11 Comparisson of Phepropeptin C and Epiphepropeptin C in Chloroform 211

Figure 3-12 Comparisson of Phepropeptin D and Epiphepropeptin D in Chloroform 211

Figure 3-13 Structure of cylindrocyclin A..... 221

Figure 3-14 Synthesis of cylindrocyclin A 223

Figure 3-15 Variable Temperature NMR Spectra for Cylindrocyclin A..... 224

Figure 3-16 Structure of Stylissamide G 225

Figure 3-17 Total Synthesis of Stylissamide G 226

Figure 3-18 Cordyheptapeptides A and B 227

Figure 3-19 Crystal Structure of Cordyheptapeptide C reported by Chen et al..... 228

Figure 3-20 Total Synthesis of Cordyheptapeptide B..... 229

Figure 3-21 Total Synthesis of Scytalidamide A..... 231

List of Tables

Table 1-1 Sequence and rearrangement efficiencies for cyclic peptides [a] 1 M ethanolic HCl, 50 °C, 15 h [b] 0.1M ethanolic HCl, 30 °C, 15 h. Bold indicates *N*-methylated amino acids. [c] as quantified by UV (220 nm) integration of HPLC spectra. 6

Table 1-2 *In vitro* cell permeability for selected compounds 9

Table 1-3 X-ray measurements, solution and refinement of structure **1**..... 22

Table 1-4 Temperature coefficients for **1** and **3**..... 25

Table 1-5 NMR Assignment of Compound **1**..... 26

Table 1-6 NMR Assignment of Compound **3**..... 27

Table 1-7 NOE correlations **1**..... 29

Table 1-8 NOE correlations **3**..... 30

Table 2-1 Compound **2** Assignment 109

Table 2-2 Compound **3** Assignment 110

Table 2-3 Compound **2** Minor Conformer Assignment..... 111

Table 2-4 ROE correlations **2** 113

Table 2-5 ROE correlations **3** 114

Table 2-6 Conformer Contribution NMR Spectra 115

Table 3-1 ADME Properties of phepropeptins and epiphepropetins ^{a}thermodynamic aqueous solubility pH 7.4, ^{b}average of A-B and B-A apparent permeability, Papp, reported in cm/sec x10^{-6}..... 169

Table 3-2 Experimental ROESY distances and computational structure (650) in $CDCl_3$. 195

Table 3-3 Experimental coupling constants and computational structure (650) in $CDCl_3$. 195

Table 3-4 10 lowest computational structures by RMSD and average over the entire run in $CDCl_3$. 196

Table 3-5 phepropeptin C (**3**) assignment in DMSO 197

Table 3-6 Experimental ROESY distances and computational structure (251) in DMSO. 198

Table 3-7 Experimental coupling constants and computational structure (251) in DMSO. 198

Table 3-8 10 lowest computational structures by RMSD and average over the entire run in DMSO 199

Table 3-9 Temperature Coefficient Data in ppb/K for Phepropeptin A (**3**) 200

Table 3-10 Temperature Coefficient Data in ppb/K for Phepropeptin C (**3**) 200

Table 3-11 Temperature Coefficient Data in ppb/K for Epiphepropeptin A (**5**) 200

Table 3-12 Temperature Coefficient Data in ppb/K for Epiphepropeptin C (**7**) 201

Table 3-13 Temperature Shift Analysis of Cylindrocyclin A 223

Abstract

Title: Pharmacokinetic and Conformational Analysis of Naturally Inspired Cyclic Peptides

Author: Joshua Allen Schwochert

Research into macrocycles as an emerging class of pharmaceutically relevant molecules has increased in recent years. Advances in combinatorial chemistry and screening have yielded a number of potent macrocycles against challenging protein targets. Although they often exhibit favorable target binding characteristics, with long off rates and high specificity, they generally tend to suffer from an inability to cross cellular membranes and are thus limited to extracellular targets. By contrast, some cyclic peptide natural products or derivatives thereof are cell permeable. This observation has led to a surge of interest in understanding the factors that govern ADME characteristics such as cell permeability, solubility and plasma stability, in medium- and large-ring macrocycles. Additionally, new synthetic strategies that allow for the synthesis of more diverse macrocycles, especially those mimicking natural products, are desired.

First we investigate a cyclic peptide scaffold able to undergo an *N*-to-*O* acyl rearrangement. Despite the prevalence of head-to-side chain threonine linkages in natural products, their incorporation has been underexplored in synthetic cyclic peptides. Upon acylation of the amine with diverse carboxylic acids, the resulting cyclic depsipeptides displayed favorable cellular permeability and a conformation

similar to the parent peptide. The rearrangement was found to be scaffold and conformation dependent as evidenced by molecular dynamics experiments.

Additionally, we report on the effect of peptide-to-peptoid substitutions on the passive membrane permeability of an *N*-methylated cyclic hexapeptide. In general, substitutions maintained permeability but increased conformational heterogeneity. Diversification with nonproteinogenic side chains increased permeability up to 3-fold. Additionally, the conformational impact of peptoid substitutions within a β-turn are explored. Based on these results, the strategic incorporation of peptoid residues into cyclic peptides can maintain or improve cell permeability, while increasing access to diverse side-chain functionality.

Finally, we identified the phepropeptins as natural product cyclic peptides with potential cell permeability. Synthesis of the phepropeptins and epimeric analogues revealed much more rapid cellular permeability for the natural stereochemical pattern. Despite being more cell permeable, the natural compounds exhibited similar aqueous solubility as the corresponding epimers, a phenomenon explained by solvent-dependent conformational flexibility among the natural compounds. When analyzing the polarity of the solution structures we found that neither the number of hydrogen bonds nor the total polar surface area accurately represents the solvation energies of the high and low dielectric conformations. This work adds to a growing number of natural cyclic peptides whose solvent-dependent conformational behavior allows for a balance between aqueous solubility and cell permeability, highlighting structural flexibility as an important consideration in the design of molecules in bRo5 chemical space.

Acknowledgements

The text of this dissertation includes whole or partial reprints of the following previously published material:

Schwochert, J.; Pye, C.; Ahlbach, C.; Abdollahian, Y.; Farley, K.; Khunte, B.; Limberakis, C.; Kalgutkar, A. S.; Eng, H.; Shapiro, M. J.; Mathiowetz, A. M.; Price, D. A.; Liras, S.; Lokey, R. S. Revisiting N-to-O Acyl Shift for Synthesis of Natural Product-like Cyclic Depsipeptides. *Org. Lett.* **2014**, 16 (23), 6088–6091.

The following co-authors are acknowledged for their contributions to the published work: Y. Abdollabian performed the X-ray crystallography. C. Ahlbach performed ADME analysis in house. C. Pye helped with conformational elucidation. K. Farley, B. Khunte, C. Limberakis, A. Kalgutkar, H. Eng, M. Shaprio, A. Mathiowetz, D. Price, and S. Liras performed ADME assays and helped with analysis. R. S. Lokey listed in this publication directed and supervised the research which forms the basis for the dissertation

Schwochert, J.; Turner, R.; Thang, M.; Berkeley, R. F.; Ponkey, A. R.; Rodriguez, K. M.; Leung, S. S. F.; Khunte, B.; Goetz, G.; Limberakis, C.; Kalgutkar, A. S.; Eng, H.; Shapiro, M. J.; Mathiowetz, A. M.; Price, D. A.; Liras, S.; Jacobson, M. P.; Lokey, R. S. Peptide to Peptoid Substitutions Increase Cell Permeability in Cyclic Hexapeptides. *Org. Lett.* **2015**, 17 (12), 2928–2931.

The following co-authors are acknowledged for their contributions to the published work: R. Turner initially conceived of the project and performed or oversaw most the synthesis. M. Thang, R. Berkeley, A. Ponkey, and K. Rodriguez helped with synthesis. S. Leung and M. Jacobson performed initial computational studies. B. Khunte, G. Goetz, C. Limberakis, A. Kalgutkar, H. Eng, M. Shaprio, A. Mathiowetz, D. Price, and S. Liras performed ADME assays and helped with analysis. R. S. Lokey listed in this publication directed and supervised the research which forms the basis for the dissertation

Schwochert, J.; Lao, Y.; Pye, C. R.; Naylor, M. R.; Desai, P. V; Gonzalez Valcarcel, I. C.; Barrett, J. A.; Sawada, G.; Blanco, M.-J.; Lokey, R. S. Stereochemistry Balances Cell Permeability and Solubility in the Naturally Derived Phepropeptin Cyclic Peptides. *ACS Med. Chem. Lett.* **2016**, 7 (8), 757–761.

The following co-authors are acknowledged for their contributions to the published work: Y. Lao performed most of the synthesis. M. Naylor performed some NMR experiments. C. Pye calculated computationally derived solvation energies. P. Desai, I. Gonzalez Valcarcel, J. Barret, G. Sawada, and M. Blanco conducted ADME analysis. R. S. Lokey listed in this publication directed and supervised the research which forms the basis for the dissertation

1. REVISITING N-TO-O ACYL SHIFT FOR SYNTHESIS OF NATURAL PRODUCT-LIKE CYCLIC DEPSIPEPTIDES

1.1. Foreword

This chapter contains text and figures from the following manuscript.

Schwochert, J.; Pye, C.; Ahlbach, C.; Abdollahian, Y.; Farley, K.; Khunte, B.; Limberakis, C.; Kalgutkar, A. S.; Eng, H.; Shapiro, M. J.; Mathiowetz, A. M.; Price, D. A.; Liras, S.; Lokey, R. S. Revisiting N-to-O Acyl Shift for Synthesis of Natural Product-like Cyclic Depsipeptides. *Org. Lett.* **2014**, 16 (23), 6088–6091.

The work was completed as a collaboration between all authors, though I prepared the manuscript, performed most of the synthesis and spectroscopic analysis. Yashar Abdollabian in collaboration with Indranil Chakraborty performed the X-ray crystallography. Chris Ahlbach helped with ADME analysis in house. Cameron Pye helped with conformation eludciation. The team at Pfizer conducted ADME assays and helped with analysis.

1.2. Introduction

Cyclic depsipeptides are a diverse class of natural products that have shown a wide variety of biological activities.[1–5] Many cyclic depsipeptides are defined by a single C-terminal-to-side-chain ester (*i.e.*, “depsi”) linkage through either a threonine or

serine residue. These linkages result in lariat-type structures in which the amino termini are further elongated and/or capped with diverse lipid tails. It has been shown in structure-activity studies with the kahalalides, Figure 1-1, for example, that both the depsi-linkage and tail are required for biological activity.[6–9]

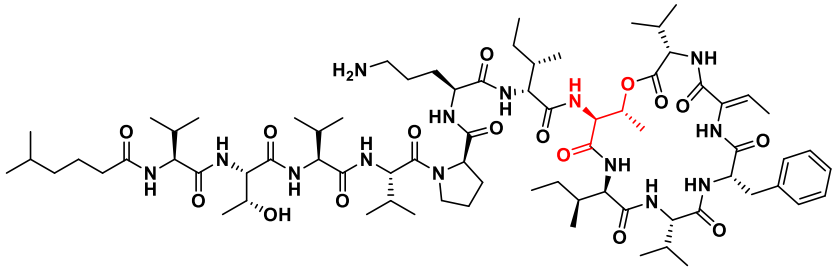

Figure 1-1 Structure of Kahalalide F

The *N*-acyl-*O*-acylthreonine linkages found in many cyclic depsipeptides[9] involve a significant backbone rearrangement of the parent homodetic peptides and allow for further diversification, by decoration of the exocyclic amine with any of a variety of peptide extensions and/or lipids caps. Cyclic peptide backbone elements, e.g., ring size, stereochemistry, and amide *N*-methylation, are known to have an impact not only on pharmacological activity, but also on ADME properties such as cell permeability and metabolic stability.[10–13] However, despite the ubiquitous presence of backbone-to-side chain linkages among cyclic peptide natural products, their effect on physicochemical and pharmacokinetic properties has not been investigated in detail.

Previously our laboratory undertook an investigation into the influence of side chain polarity on the permeability and metabolic stability of the cell permeable and orally bioavailable *N*-methylated cyclic hexapeptide cyclo[Leu1–D(NMe)Leu2–(NMe)Leu3–Leu4–DPro5–(NMe)Tyr6] (**1NMe3**).[13,14] The (NMe)Leu3 residue was substituted with

a variety of different amino acids, and the ADME properties of the derivatives were compared with those of the parent compound. We found that the derivative in which (NMe)Leu3 was replaced with (NMe)Thr, **1**,(Figure 1-2) had good oral bioavailability in rat (F = 24%), nearly equal to that of the parent compound. However, in the course of analysis via reversed phase HPLC, we found that **1** had partially converted to a more polar and less permeable isomer.

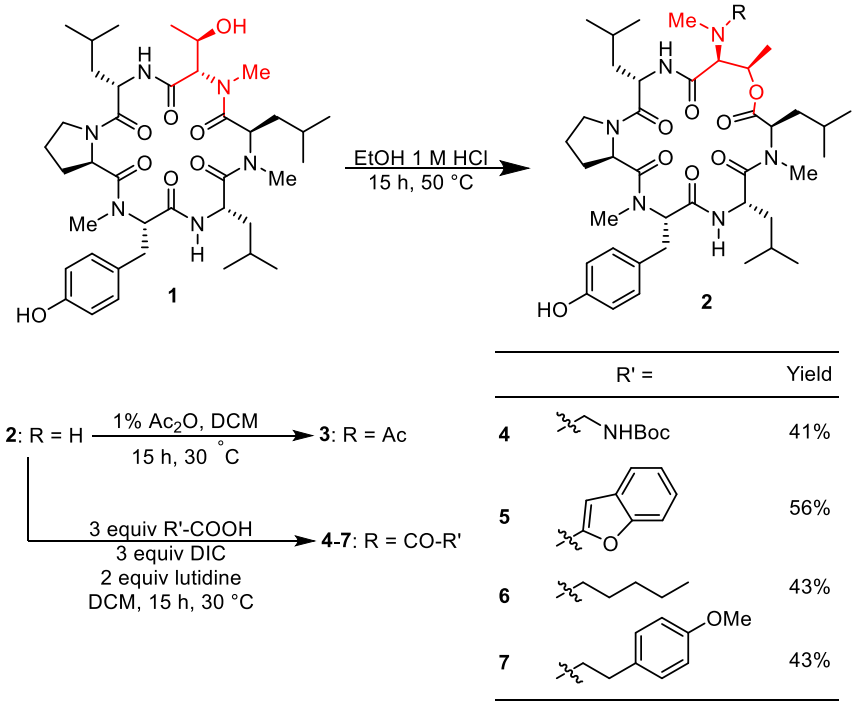

Figure 1-2 Acyl rearrangement and subsequent acylation

1.3. *N*-to-*O* Rearrangement and Subsequent Acylation

1.3.1. Spectroscopic elucidation of the *N*-to-*O* Acyl Shift

NMR analysis of this isomer revealed its structure to be compound **2**, Figure 1-2, the product of an *N*-to-*O* acyl migration from the main chain to the Thr side chain,

Figure 1-3. Since its discovery in 1922[15], this rearrangement has been used as a prodrug strategy to enhance the solubility of lipophilic peptides, and has been observed as a side reaction during the acidic deprotection of synthetic peptides that contain Thr and Ser residues.[16,17] In addition, this reaction has been explored as a degradation pathway of the clinically relevant drug cyclosporine A.[18] In light of the recent surge of interest in macrocycles as "beyond-rule-of-5" (bRo5) scaffolds in drug discovery[19] and the prevalence of depsipeptides among cyclic peptide natural products, we were compelled to investigate the potential of this unanticipated side reaction as entry into lariat peptides as a sub-genre of synthetic, cell-permeable macrocycles.

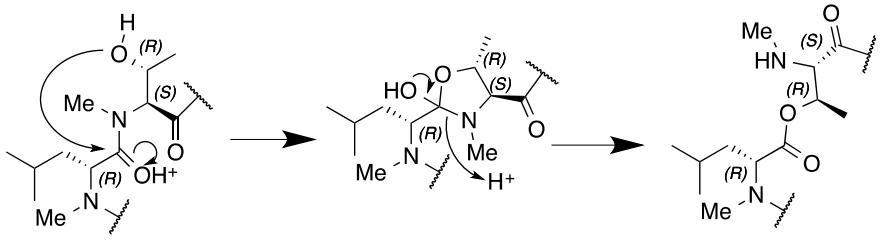

Figure 1-3 Mechanism of the *N*-to-*O* Acyl Rearrangement

1.3.2. *N*-Acylation of Isoacylthreonine

Although the isoacyl depsipeptide **2** was stable as its HCl salt, it quickly rearranged back to the amide upon neutralization in aqueous buffer.[18] To stabilize the ester and allow for a more direct comparison between the uncharged lactam **1** and the corresponding depsipeptide, the free amine **2** was acetylated with acetic anhydride to generate cyclic depsipeptide **3** in good yield (62% after HPLC purification) and purity. Compound **3** contains the same *N*-acetyl-*O*-acylthreonine moiety commonly found in

many bioactive cyclic peptide natural products such as the micropeptins, aspergillicins, xenobactin, and some members of the kahalahide series.[6–9]

Inspired by cyclic depsipeptides containing chemically diverse 'tails', we sought to explore functionalization of the exocyclic amine. To that end we synthesized a small set of compounds from the HCl salt of **2**, using standard carbodiimide coupling chemistry. The resulting cyclic depsipeptides were isolated in reasonable yield over two steps starting with **1** and in good purity after HPLC purification. The addition of Boc-glycine was used as a possible entry point into solution phase peptide synthesis that would allow for access to peptidic tails such as those observed in a majority of head-to-side chain cyclic depsipeptides. The addition of the lipidic hexanoic acid yielded a macrocycle similar to the lipopeptide antibiotics[20] and demonstrates the potential of this route for late stage diversification.

1.3.3. Generality of the Acid Catalyzed *N*-to-*O* Rearrangement in Cyclic Peptides

To explore the generality of this acyl rearrangement within different macrocycles, a series of cyclic peptides were synthesized and subjected to the acidic conditions employed in the acyl shift of **1**. These peptides were varied with respect to ring size, *N*-methylation pattern, and amino acid constitution. Since many cyclic depsipeptide natural products contain primarily hydrophobic residues, another series was designed that incorporated *N*-methyl Phe and Ala in addition to Leu, Tyr, and Pro. The peptides in Table 1-1 were synthesized using standard Fmoc-SPPS and subjected to either global

selective *N*-methylation[13] or in-sequence *N*-methylation using NBS- or TFA-protecting group strategies.[21,22]

compd	cond	1	2	3	4	5	6	7	Conv. %[c]
8	a	Thr	**dLeu**	**Leu**	Leu	dPro	**Tyr**		45.8
9	a	Leu	**dThr**	**Leu**	Leu	dPro	**Tyr**		0
1	a	Leu	**dLeu**	**Thr**	Leu	dPro	**Tyr**		100
10	b	Leu	**dLeu**	**Leu**	Thr	dPro	**Tyr**		6.4
11	b	Leu	dLeu	dThr	Leu	dPro	Tyr		19.2
12	b	Leu	**Leu**	**Thr**	Leu	dPro	**Tyr**		0.9
13	a	Leu	**Thr**	Ala	**Phe**	dPro			41.3
14	b	Leu	**Thr**	Ala	**Phe**	Leu	dPro		100
15	b	Leu	**Thr**	Ala	**Phe**	Leu	Leu	dPro	100

Table 1-1 Sequence and rearrangement efficiencies for cyclic peptides [a] 1 M ethanolic HCl, 50 °C, 15 h [b] 0.1M ethanolic HCl, 30 °C, 15 h. Bold indicates *N*-methylated amino acids. [c] as quantified by UV (220 nm) integration of HPLC spectra.

Purified peptides were then subjected to 1 M ethanolic HCl at 50˚C overnight. In some scaffolds these conditions were found to cause degradation, in which case gentler conditions (0.1 M ethanolic HCl at 30 ˚C overnight) were used. The depsipeptide-to-peptide ratio was quantified by HPLC. The sequences and rearrangement efficiencies are outlined in Table 1-1. Notably, compounds **14** and **15** rearranged quantitatively under the mild conditions. Although all compounds that quantitatively rearrange in the conditions tested contain an *N*-methyl Thr, *N*-methylation does not appear to be a requirement. Of the three compounds not containing an *N*-methyl Thr tested, **8**, **10** and **11** all rearrange to some extent, with **8** achieving nearly 50% conversion. Since *N*-

methylation impacts both conformation and electronics, it is difficult to draw any strong conclusions about the direct effect of *N*-methylation on the rearrangement efficiency.

1.3.4. Conformational Requirements for the Rearrangement as Assessed by Molecular Dynamics

Indeed, the dramatic difference in rearrangement efficiency between **1** and **9** (100% and 0% conversion, respectively), which have the same backbone geometry and differ only in the location (and stereochemistry) of the Thr side chain, suggested that the position of the Thr residue in the beta-turn (*i* + *1* for **9** vs. *i* + *2* for **1**) was the source of their differential reactivity. The optimal attack angle for nucleophilic attack at an sp^2 center is ~105˚, known as the Burgi-Dunitz angle[23]. We hypothesized that access to the productive conformer required for nucleophilic attack of the Thr-OH onto the *i* - *1* carbonyl carbon, defined by both the Burgi-Dunitz angle and the distance between the reacting groups, was related to the side chain's conformational preference with respect to the conformation of the backbone of the *i* – 1 residue.

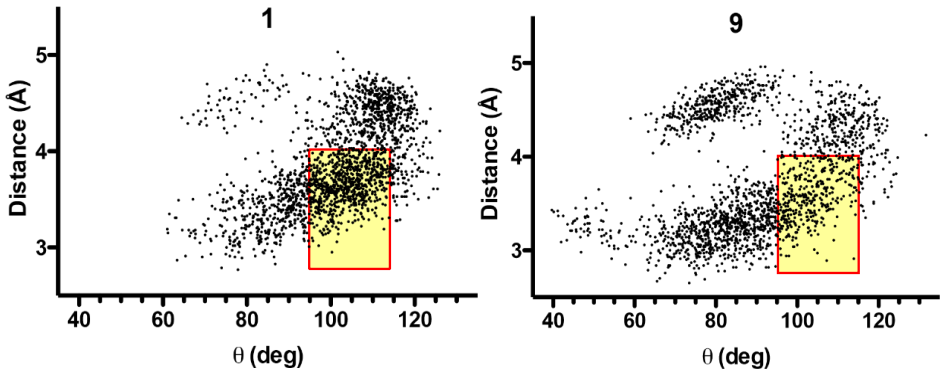

Figure 1-4 Scatter plots representing 10 ns molecular dynamics simulations of **1** and **9**, respectively, monitoring the distance and angle between the Thr-OH and i-1 carbonyl carbon every 5 ps

We ran molecular dynamics (MD) simulations on **1** and **9** (Figure 1-4) monitoring the distance and angle between the reacting atoms. Analysis of 2000 snapshots from each simulation showed that reactive conformations for **1** were sampled twice as frequently as they were for **9** (Figure 1-5). Thus, while the stereochemistry and/or *N*-Me status of the Thr and its neighboring residues may not, in themselves, be predictive of rearrangement efficiency, they may allow or disallow access to reactive conformations by virtue of their impact (along with other factors) on the global conformation of the macrocycle. Combined with the fact that under highly acidic conditions the reverse acyl shift is unlikely, the MD results point toward a kinetic rather than thermodynamic effect driving the observed differences in % conversion.

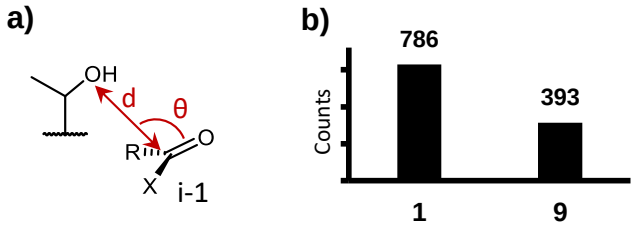

Figure 1-5. Analysis of Molecular Dynamics a) Distance and angle measured between Thr-OH and i-1 carbonyl carbon b) graph of snapshots containing an –OH to C=O distance of < 4 Å and O-C-O angle within ±10˚ of the Burgi-Dunitz angle.

1.4. ADME Analysis of Depsipeptides

In an attempt to gain a deeper understanding the biochemical properties imparted by the amide-to-ester transformation, the ADME properties of all depsipeptides were investigated in the MDCK-LE assay for passive cell permeability, Table 1-2. Despite its increased size and flexibility, the cell permeability of **3** was comparable to that of **1**.

The depsipeptides containing more complex tails, **4-7**, exhibited favorable cellular permeability as well, at least as high as that of the orally bioavailable cyclic peptide natural product **CSA**. In an attempt to explain the cell permeabilities of **1** and **3** we sought to solve their 3-dimensional solution conformations.

Table 1-2 *In vitro* cell permeability for selected compounds

compound	MDCK-LE (10^{-6} cm/s)
1	2.7
3	3.3
4	2.2
5	1.1
6	2.9
7	2.0
CSA	1.1
1NMe3	4.0

1.5. Conformational Analysis

1.5.1. Solution Conformations of 1 and 3 as Elucidated by NMR

Compound **1** and its acetylated depsipeptide analog **3** provide a model system with which to explore the effect of the depsipeptide linkage on backbone conformation and permeability. Peak assignments were made using COSY, TOCSY, HSQC, and HMBC experiments, and NOESY-derived interproton distances were calculated based on crosspeak volumes. ^{3}JH-H couplings were also used to provide dihedral information. Conformers were generated using molecular dynamics (MD) simulations and ensembles were fit to the distance and dihedral restraints using the "NMR analysis of

molecular flexibility in solution" (NAMFIS)[24] protocol in the program DISCON.[25,26] This algorithm fits NMR data to ensembles of conformers rather than *a priori* assuming the presence of a single, low energy conformation in solution.

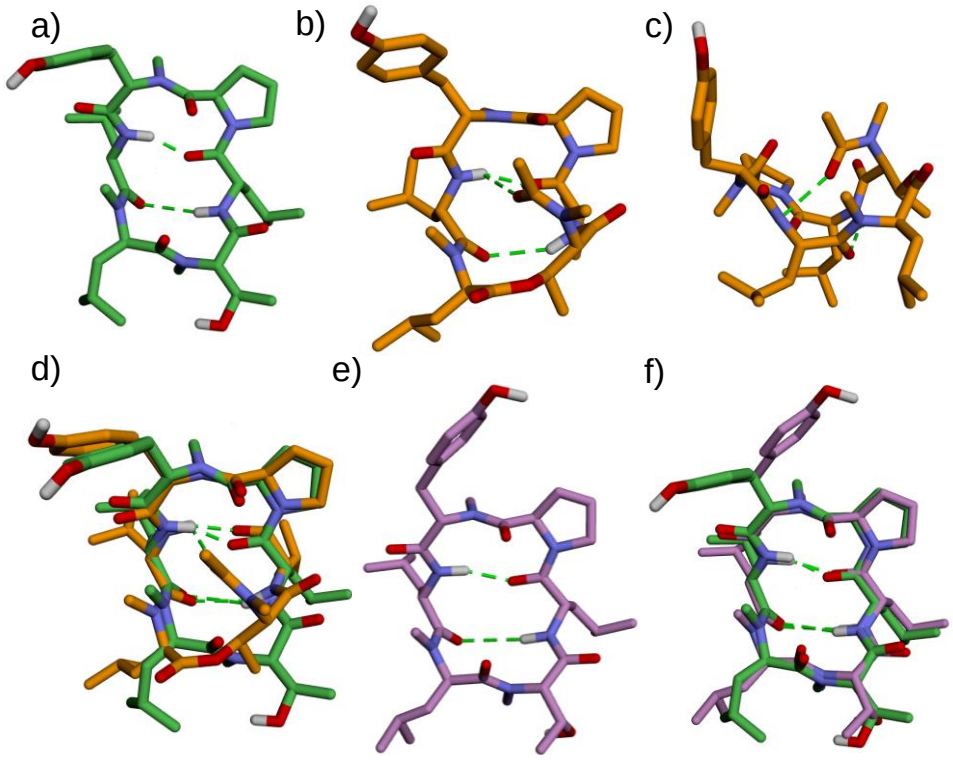

Figure 1-6 a, b) Major conformation of the DISCON ensemble for **1** and **3**, respectively. c) Conformation of **3**, highlighting tail to backbone hydrogen bond. d) Overlay of **1**, green, and **3**, orange. e,f) X-ray structrure of **1** and an overlay of the the X-ray structure, purple, and solution conformation, green.

Compound **1** showed a single, dominant conformer (98% of the ensemble) when analyzed with DISCON. In contrast, compound **3** showed a mixture of 4 different conformations with the major one constituting 54% of the ensemble. Minor conformations are shown in the methods, Figure 1-10. Interestingly, the major solution conformation of **3** showed a backbone conformation with transannular

hydrogen bonds flanked by β–turns, very similar to those of **1** and **1NMe3** despite the amide-to-ester ring expansion, Figure 1-6.

1.5.2. X-ray Crystal Structure of 1

In addition to the DISCON structure, crystallization of **1** by vapor diffusion between benzene and cyclohexane yielded X-ray diffraction-quality crystals. The X-ray structure of **1** was similar to that of the solution conformation (backbone and Cβ RMSD = 0.321 Å). In addition, both the X-ray and solution structure adopted a conformation similar to that of the solution structure previously determined for **1NMe3** in $CDCl_3$.[13] This conformation is defined by two transannular hydrogen bonds flanked on either side by opposing β-turns, Figure 1-6. The similarity in backbone conformation between **1** and **1NMe3** lends further support to the observation that stereochemistry and *N*-methylation are major determinants of backbone geometry in cyclic peptides in this size range.

1.5.3. Temperature Shift Analysis of 1 and 3

The presence of intramolecular hydrogen bonds has been shown to be a significant determinant of cell permeability in cyclic peptides[27,28] and are present in the major conformations of both **1** and **3.** Variable temperature experiments were conducted to independently assess the solvent exposure of the backbone amides. Both amide protons in **1** and **3** exhibited temperature coefficients consistent with their engagement in hydrogen bonds, Methods Table 1-4. The solution structure of **3** also shows a lower solvent exposed polar surface area compared to that of **1** (130 $Å^2$ vs 162 $Å^2$) and a

slightly decreased radius of gyration (5.1 Å versus 5.4 Å) both parameters which have recently been linked to passive membrane permeation.[29] Furthermore the acetyl carbonyl of **3** reaches back over the ring and forms another hydrogen bond with the amide proton of Leu1, decreasing its solvent accessibility. Scaffolds other than **1NMe3**, which do not contain transannular hydrogen bond in their homodedic form, may benefit more from the ring expansion and added flexibility afforded by the depsi-bond in accessing lipophilic conformations.

1.6. Conclusion

By exploiting the *N*-*O* acyl shift, often considered an unwanted side reaction in peptide synthesis, we have synthesized a diversifiable cyclic depsipeptide bearing striking resemblance to natural products aspergillicin and xenobactin, while maintaining the cellular permeability of the parent scaffold. In some cases the acid catalyzed acyl rearrangement may represent an effective synthetic strategy for either diversity oriented synthesis or total synthesis of natural products given the ability of about half of scaffolds presented here to undergo said rearrangement. Although this rearrangement was previously used in the synthesis of actinomycin precursors, it has not been explored in other scaffolds.[30] From the collection of compounds presented here it appears that this rearrangement may be used in some macrocycles, though there is a strong dependence of conversion efficiency on both conformation and ring size. Further studies will be directed at more fully exploring the scope of this chemistry in other scaffolds.

1.7. Abbreviations

ACN, acetonitrile; COMU, (1-Cyano-2-ethoxy-2-oxoethylidenaminooxy)dimethylamino-morpholino-carbenium hexafluorophosphate; DBU, 1,8- Diazabicyclo[5.4.0]undec-7-ene; DCM, dichloromethane; DIAD, diisopropyl azodicarboxylate; DMF, N,N-dimethylformamide; DIC, diisopropylcarbodiimide; DIPEA, diisopropylethylamine, DMSO, dimethylsulfoxide; DVB, divinylbenzene; EtOH, ethanol; Fmoc, 9-fluorenylmethoxycarbonyl; HBTU, N,N,N',N'-Tetramethyl-O-(1H-benzotriazol-1-yl)-uronium hexafluorophosphate; HOAt, 1-hydroxy-7-azabenzotriazole; IR, infrared; LCMS, liquid chromatography mass spectrometry; MeOH, methanol; N2, nitrogen; NMP, 1-methyl-2-pyrrolidinone; PTFE, Polytetrafluoroethylene; PyBOP, (benzotriazol-1-yloxy)tripyrrolidinophosphonium hexafluorophosphate; RP, reverse phase; SPPS, solid phase peptide synthesis; TFA, trifluoroacetic acid; THF, tetrahydrofuran

1.8. Methods

1.8.1. General Synthetic and Procedures

1.8.1.1. Overview

Peptides were prepared with the following procedures; **1**, **8**, **9**, **10**, and **11** were prepared via automated peptide synthesis followed by on-resin cyclization. **1**, **8**, **9**, and **10** were then subjected to on-resin selective methylation. **12**, **13**, **14**, and **15** were

prepared using a solution phase cyclization strategy with in-sequence *N*-methylation (TFA or o-Ns strategy) or installation of pre *N*-methylated Fmoc amino acids.

1.8.1.2. Automated Peptide Synthesis

Linear peptide intermediates were synthesized on a Protein Technologies Prelude peptide synthesizer, using advanced programming mode and 60 mL reaction vessels. The reaction procedures are described below.

1.8.1.3. Microwave Reaction Conditions

Microwave assisted reactions were done in a CEM Discover microwave reactor with an open reaction vessel. Reactions were heated to 50 °C with 12 watts of power while temperature was monitored with an IR probe from within the reaction vessel.

1.8.1.4. Loading of 2-Chlorotrityl resin

For resin bound for on-resin cyclization Fmoc-*O*-allyl-Tyr (0.954 g, 0.43 mmol) was added to a flame dried round bottom flask and dried in a vacuum dessicator with phosphorous pentoxide overnight. Cesium carbonate (2 g) was added to the flask and it was purged with N_2. Dry DCM (50 mL) was cannula transferred into the flask followed by DIPEA (2.5 mL). After sonication for 10 min, of 2-chlorotrityl resin (5 g) was added under a stream of N_2 and allowed to shake for 4 h. Resin was capped with a 15 mL solution of 1:2:17 MeOH:DIPEA:DMF (3 x 15 min). Resin was washed with

DMF (3 x 15 mL) followed by DCM (3 x 15 mL). Loading value was calculated by mass increase of dried, loaded resin.

1.8.1.5. Automated On-Resin Fmoc Deprotection

Resin was immersed in 5 mL of a solution of 2% piperidine and 2% DBU in DMF for 10 min under N_2 agitation twice. Resin was washed with DMF (6 x 3 mL).

1.8.1.6. Automated Amino Acid Coupling

A solution of Fmoc-Xaa (3 equiv), DIPEA (5 equiv), and HBTU (3 equiv) were added to the resin in 4.5 mL of DMF. The reaction was agitated via N_2 bubbling for 90 min. The resin was washed with DMF (6 x 3 mL) and DCM (3 x 3 mL).

1.8.1.7. On-Resin O-allyl and Fmoc deprotection

Air was run over resin until dryness followed by 3 washes of 10 mL of dry THF. A solution of $Pd(PPh_3)_4$ (1 equiv) with 20% piperidine in DMF was added to the resin under a head of N_2. This was shaken for 3 h after which the resin was washed with a solution of sodium diethyldithiocarbamate (0.833 g) and 0.833 mL of DIPEA in 16.67 mL of DMF for 3 x 20 min. The resin was washed with DMF (3 x 15 mL) and DCM (3 x 15 mL).

1.8.1.8. On-Resin Cyclization

A solution of PyBOP (3.8 equiv), DIPEA (5 equiv), and HOAt (5 equiv) were dissolved in DMF (10 mL per gram of resin). This was added to the resin and it was shaken overnight. The solution was drained and resin was washed with DMF (3x) and DCM (3x).

1.8.1.9. On-Resin Selective Methylation

The resin was dried under a stream of air followed by 3 washes of 10 mL of dry THF. A 1M solution of lithium *t*-butoxide in dry THF was filtered and added under a head of N_2 (10 mL per gram of resin) and shaken for 45 min. The solution was drained under a stream of N_2 and a 10% solution of methyl iodide in dry DMSO (10 mL per gram of resin) was added and shaken for 45 min. Resin was washed once with 15 mL of DCM, once with 15 mL of MeOH, 3 times with 15 mL of DMF, and 3 times with 15 mL of DCM. Reaction was monitored by LCMS and repeated until the tri-methylated product was dominant.

1.8.1.10. On-Resin Installation of o-Ns

O-nitrobenzenesulfonyl (Ns) (4 equiv) chloride was dissolved in a solution of 10 eq of collidine in NMP. This solution was added to the deprotected amino acid on resin and allowed to react for 15 minutes. The solution was drained and resin was washed 3 times with DMF and 3 times with DCM.

1.8.1.11. On-Resin Installation of the TFA protecting group

A solution of ethyltrifluoroacetate (10 equiv) and DBU (12 equiv) in THF was added to the deprotected amino acid on resin. The reaction was heated in a microwave reactor for 10 min at 50 °C. The solution was drained and resin was washed 3 times with DMF and 3 times with DCM.

1.8.1.12. N-Alkylation under Mitsunobu Conditions

The resin was washed 3 times with dry THF (5 mL). Triphenylphosphine (5 equiv) was dissolved in a minimum volume of dry THF and MeOH (10 equiv, stored over molecular sieves) was added. This mixture was added to the resin and vortexed while DIAD (5 equiv, stored over molecular sieves) was added dropwise. The reaction was sealed and allowed to proceed for 10 min at rt under gentle rocking. The resin was washed once with dry THF and the procedure was repeated (2-5 times) until no more starting material was observed by LCMS. Prior to the removal of the TFA or *O*-Ns group the resin was washed 3 times with DMF and 3 times with DCM.

1.8.1.13. On-Resin O-Ns Deprotection

A solution of 2-mercaptoethanol (10 equiv) and DBU (5 equiv) in NMP was added to the resin was agitated by gentle rocking for 5 min. This reaction was repeated twice with a single wash of NMP in between. The solution was drained and resin was washed

3 times with DMF and 3 times with DCM. This procedure was repeated (1-3 times) until no more starting material was observed by LCMS.

1.8.1.14. On-Resin TFA Deprotection

A 1:1 solution of dry THF and dry EtOH was added to the resin. A large excess (10-40 equiv) of sodium borohydride was added and the reaction was allowed to proceed at room temperature for one hour. This procedure was repeated (1-3 times) until no more starting material was observed by LCMS.

1.8.1.15. Amino Acid Coupling to Hindered Amines under Microwave Condtions

A solution of Fmoc-Xaa (4 equiv), COMU (4 equiv), and DIPEA (6 equiv) in DMF was allowed to pre-react for 5 min. This solution was added to the deprotected peptide on-resin and allowed to react for 45 min at 50 °C under microwave heating. The solution was drained and resin was washed 3 times with DMF and 3 times with DCM. The reaction was monitored by LCMS and repeated until starting material was no longer observed.

1.8.1.16. Peptide Cleavage

Complete linear peptides were cleaved off resin in 5 resin volumes of 2.5% TFA in DCM for 4 minutes three times with a 5 resin volume DCM wash in between each step.

Solvent was removed under N_2 followed by dissolution in acetone or DCM and evaporation under reduced pressure. For solution phase cyclizations residual TFA was removed *in vacuo* overnight.

1.8.1.17. Cyclization with COMU

Linear peptides were dissolved in 20 mL of dry acetonitrile with DIPEA (4 equiv) and added (to a final concentration 1 mg crude peptide per mL) dropwise to a solution of 1:1 THF/ACN containing COMU (2 equiv). Reactions were stirred from 2 to 24 h until complete cyclization was achieved as monitored by LCMS.

1.8.1.18. Removal of Acid Labile Side Chain Protecting Groups

Peptides were dissolved in 25 mL of 1:1 TFA/DCM and allowed to react for 30 minutes. Solvent was removed under N_2 followed by dissolution in MeOH and evaporation under reduced pressure.

1.8.1.19. N-O Acyl shift

Pure **1** was transferred to a clean scintillation vial and suspended in 1 M ethanolic HCl at 1 mg/mL and sealed with a PTFE lined lid. The reaction was allowed to proceed at 50 °C for 15 h. Alternative conditions include 0.1 M HCl at 30 ° C for 15 h. Solvent was removed under a stream of dry N_2 yielding **2** as an HCl salt in quantitative yield.

Procedure was repeated as above with the conditions noted in the text when testing the reactivity series.

1.8.1.20. Coupling of 'tails'

A film of **2** was prepared in a dry scintillation vial. A stock solution was made with the molar ratio of carboxylic acid (3 equiv), DIC (3 equiv), and lutidine (2 equiv) in DCM and was allowed to pre-react for 5 min. An appropriate amount of this solution for a final equivalence of 3, 3, 2, of carboxylic acid, DIC, and lutidine, respectively, was transferred to the scintillation vial containing **2**, this reaction was allowed to proceed for 15 h at 30 °C and monitored by LCMS. If the reaction was incomplete it was allowed to react for up to 24 h.

1.8.1.21. Purification of Peptides

COMU by-products were removed after solution phase cyclization on a Biotage Isolera Prime system equipped with a KP-C18-HS 12g column eluting with H-2O/Acetonitrile modified with 0.1% TFA. Peptides were purified after global deprotection on a Waters mass-directed prep system equipped with an XBridge BEH130 5µm 19x150 C18 column eluting with H_2O/Acetonitrile modified with 0.1% formic acid or 0.1% TFA.

1.8.2. RRCK Cell Permeability

Cell permeability was determined using RRCK cells (Pfizer, Inc. Groton, CT)[31]. RRCK cells were generated in house as a subclone of Madin-Darby Canine Kidney wild-type (MDCK-WT) cells that displayed low expression of endogenous p-glycoprotein (~ 1–2% of MDCK-WT cells, based on mRNA level). Cells were cultured in minimal essential medium α with supplements and passaged when 70–80% confluent. Cell monolayer flux studies were conducted five days after seeding in 24-well transwell inserts (RRCK in 1.0 μm pore size, Becton Dickinson, Cowley, UK) at 4.2 x 10^4 cells/cm^2. Donor and acceptor solutions were prepared from HBSS containing HEPES at 20 mM, pH 7.4. Stock solutions of test compounds, prepared at 10 mM in DMSO, were used to prepare donor solutions of 2 μM compound in 0.05% (v/v) DMSO. Apparent permeability (P_{app}) was determined in apical to basolateral (AB) direction in triplicate by incubating with compound for 2 h at 37 °C. Samples of the medium were analyzed by liquid-chromatography tandem mass spectrometry (LC-MS/MS). *P*app values were calculated according to the equation P_{app} = (Q/t) x $1/C_0$ x 1/A, where Q is the sampled concentration in the acceptor compartment, t is the incubation time, C_0 is the initial concentration in the donor compartment and A is the area of the filter of the transwell plate.

1.8.3. X-ray Crystal Structure of 1

Compound **1** was crystallized via vapor diffusion between benzene and cyclohexane. The crystal cell contained one benzene molecule.

Table 1-3 X-ray measurements, solution and refinement of structure **1**

Empirical formula	$C_{45}H_{62}N_6O_8$
Formula weight/g. mol^{-1}	815.01
Crystal color, shape	Colorless, block
Crystal size/mm^3	0.20 X 0.15 X 0.12
Crystal system	Orthorhombic
Space group	P4 (1)
a/Å b/Å c/Å	16.8989 (18) 16.8989 (18) 16.5857 (18)
a/° b/° g/°	90 90 90
V/Å^3	4736.4 (9)
Z	4
ρ_{calc}/mg.m^{-3}	1.143
$\mu(Mo_{k\alpha})$/mm^{-1}	0.079
2θ/°	4.20 – 54.96
Reflections measured	47190
Independent reflections	10327
R(int)	0.0984
Parameters	485
Restraints	1
$R_1(I > 2\sigma(I))$	0.0814
wR_2 $(I > 2\sigma(I))$	0.1863
GooF	0.902

1.8.3.1. Details of the Single-Crystal Data Collection, Structure solution and Refinement

Data were collected on a Bruker APEX II single crystal X-ray diffractometer with graphite monochromated Mo Kα radiation (λ = 0.71073 Å) by ω scan technique. Structure solution was realized by direct method. The structure was refined by a Full matrix least squares procedure on F^2. All non-hydrogen atoms were refined anisotropically. All hydrogen atoms were included in calculated positions. Calculations were performed using the SHELXTL V 6.14 program package.

CCDC deposition number: CCDC 1016001

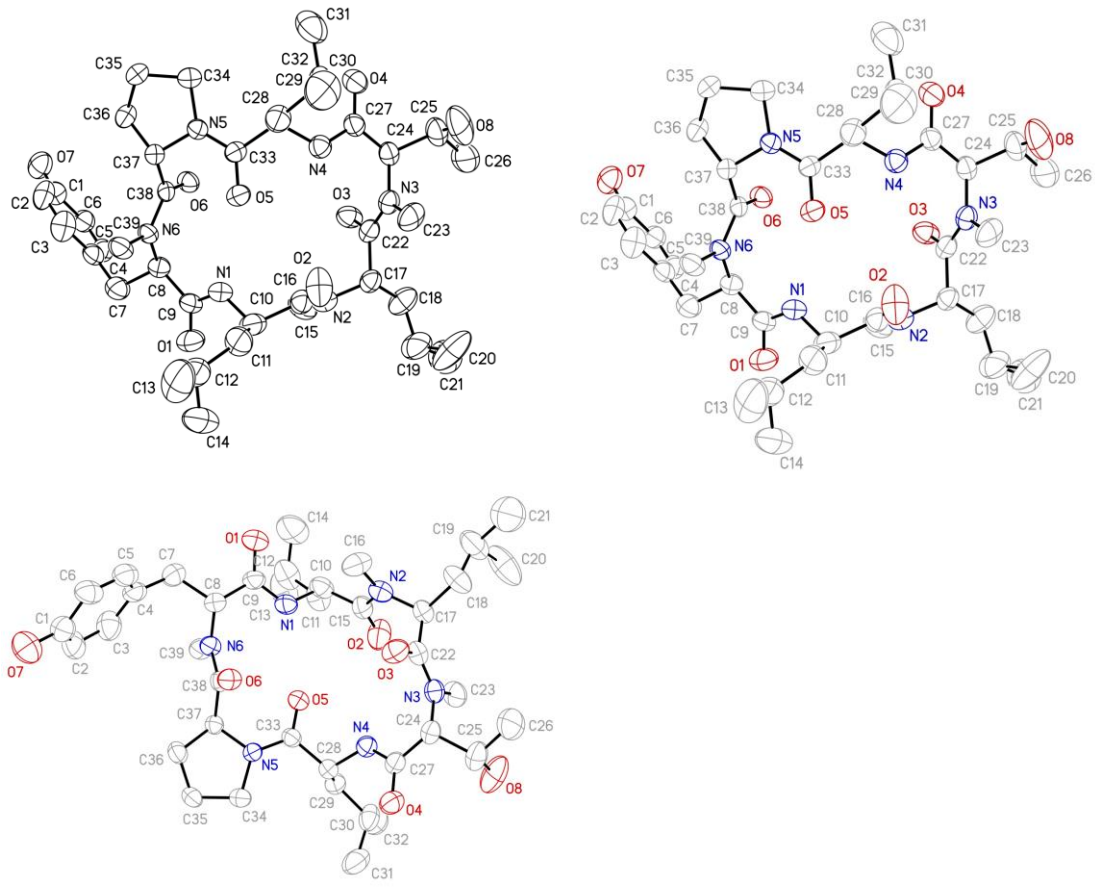

Figure 1-7 ORTEP Images of 1

1.8.4. NMR Analysis and Assignment

1.8.4.1. Acquisition Parameters

All 2D spectra were acquired on a Varian/Agilent 600 MHz NMR with a Unity Inova console with a 5 mm triple resonances cold probe. Additional spectra, ^{1}H spectra of compounds synthesized along with temperature coefficient experiments, were acquired on a Agilent/Varian 500 MHz NMR with Unity Plus console and a 5 mm broadband probe or a 5 mm HX indirect detection probe. All spectra were acquired at 15 °C (600 MHz) or 25 °C (500 MHz) unless otherwise noted. For peak assignment of **1** and **3** HSQC, HMBC, TOCSY, COSY, ^{13}C, and ^{1}H spectra were acquired using the pulse sequences supplied with Varian CHEMPack.

NOESY build up curves were generated for **1** showing maximum signal intensity at 600 ms mixing time. The NOESY spectrum used in conformational analysis was gathered then for **1** at a mixing time of 600 ms with a d1=1.5 at 15 °C. NOESY spectra for **3** at 15 °C displayed peaks with a mixture of phases showing a correlation time in the intermediate regime preventing NOE analysis at that temperature. Upon cooling to 4 °C the peaks became in phase with the diagonal and the NOESY spectrum used in conformational analysis was acquired at 4 °C with a d1=2.0 and a 600 ms mixing time.

1.8.4.1. Temperature Coefficients

^{1}H spectra were acquired at 25 °C, 30 °C, 35 °C, 40 °C, 45 °C with between 32 and 64 transients. Spectra were referenced to $CDCl_3$ at 7.26ppm and processed without apodization.

Table 1-4 Temperature coefficients for **1** and **3**.

Compound	Amide	Δppb/K
1	Leu1	-1.2
1	Leu4	-0.7
3	Leu1	-2.2
3	Leu4	-0.4

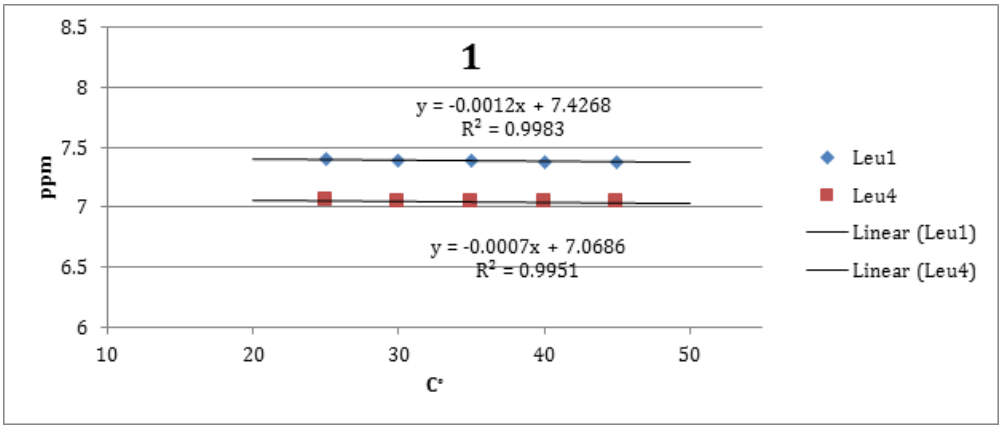

Figure 1-8 Temperature dependence of the amide protons of compound **1**

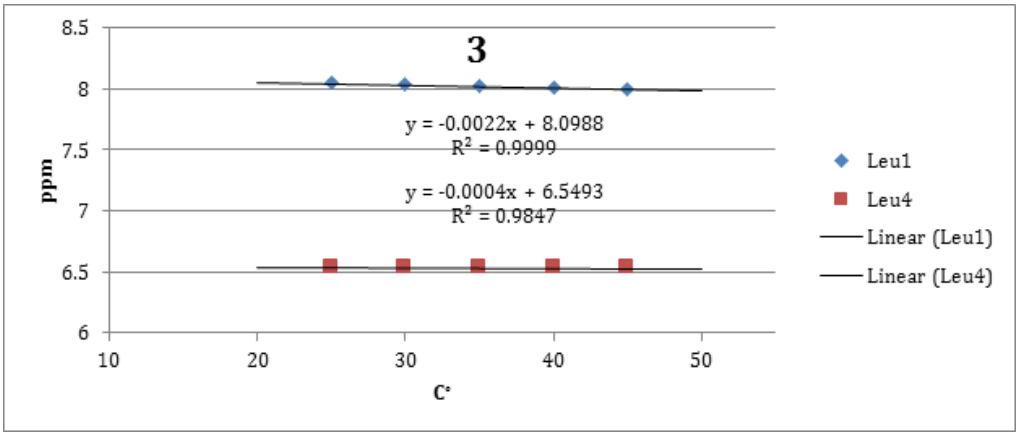

Figure 1-9 Temperature dependence of the amide protons of compound **3**

1.8.4.2. Spectral Assignment

Table 1-5 NMR Assignment of Compound **1**

Leu1	^{1}H ppm	^{13}C ppm
Hα	5.1	47.81
Hβ	1.68	41.88
Hβ'	1.81	
Hγ	1.53	25.06
Hδ	~0.95	~23
Hδ'	~0.95	~23
NH	7.4	

Leu2	^{1}H ppm	^{13}C ppm
Hα	4.99	52.15
Hβ	1.47	37.75
Hβ'	1.87	
Hγ	1.58	25.44
Hδ	1.01	23.38
Hδ'	~0.95	~23
Nme	3.2	31.49

Thr3	^{1}H ppm	^{13}C ppm
Hα	5.23	60.74
Hβ	4.64	66.81
OH	n.d.	
Me	1.09	18.01
Nme	3.31	33.67

Pro5	^{1}H ppm	^{13}C ppm
Hα	4.41	56.01
Hβ	1.48	28.1
Hβ'	1.75	
Hγ	1.77	25.64
Hγ'	2.06	
Hδ	3.78	47.58
Hδ'	3.55	

Leu4	^{1}H ppm	^{13}C ppm
Hα	4.91	48.69
Hβ	1.65	41.79
Hβ'	1.74	
Hγ	1.56	25.1
Hδ	~0.95	~23
Hδ'	~0.95	~23
NH	7.05	

Tyr6	^{1}H ppm	^{13}C ppm
Hα	5.64	57.53
Hβ	3.5	32.7
Hβ'	2.75	
Hδ	6.96	129.66
Hε	6.68	115.29
Nme	2.95	31.44
OH	n.d.	

Tertiary Carbons	
Leu1 CO	173.8
Leu2 CO	175.04
Thr3 CO	169.12
Leu4 CO	170.51
Pro5 CO	173.63
Tyr6 CO	169.04
Tyr6 Cγ	128.46
Tyr6 Cζ	155.36

Table 1-6 NMR Assignment of Compound **3**

Leu1	^{1}H ppm	^{13}C ppm
Hα	5.02	47.91
Hβ	2.02	41.98
Hβ'	1.49	
Hγ	1.51	25.03
Hδ	~0.95	~23
Hδ'	~0.95	~23
NH	8.06	

Leu2	^{1}H ppm	^{13}C ppm
Hα	5.35	53.95
Hβ	1.69	35.66
Hβ'	1.69	
Hγ	1.43	24.83
Hδ	0.88	21.85
Hδ'	~0.95	~23
Nme	2.86	30.13

Thr3	^{1}H ppm	^{13}C ppm
Hα	5.33	59.16
Hβ	5.04	70.76
Me	1.23	16.93
Nme	3.03	34.57
AcMe	2.14	21.73
OH	n.d.	

Pro5	^{1}H ppm	^{13}C ppm
Hα	4.43	56.04
Hβ	1.51	27.91
Hβ'	1.78	
Hγ	1.8	25.81
Hγ'	2.05	
Hδ	3.67	47.85
Hδ'	3.97	

Leu4	^{1}H ppm	^{13}C ppm
Hα	4.98	48.18
Hβ	1.7	40.86
Hβ'	1.7	
Hγ	1.55	24.96
Hδ	~0.95	~23
Hδ'	~0.95	~23
NH	6.56	

Tyr6	^{1}H ppm	^{13}C ppm
Hα	5.61	57.65
Hβ	2.8	32.83
Hβ'	3.51	
Hδ	6.97	129.7
Hε	6.6	115.25
Nme	2.98	31.73
OH	n.d.	

Tertiary Carbons	
Leu1 CO	171
Leu2 CO	169.42
Thr3 CO	167.5
Thr3 AcCO	171.76
Leu4 CO	170.86
Pro5 CO	173.82
Tyr6 CO	169.13
Tyr6 Cγ	128.53
Tyr6 Cζ	155.16

1.8.4.3. Conformation Generation and DISCON Analysis

To obtain starting conformations for input into DISCON, the NAMD[32] molecular dynamics (MD) protocol was used, beginning with an arbitrary conformation, to generate a diverse family of minimized conformers. We used the CHARMM forcefield with MMFF94 partial charge estimation for the MD simulation, which was carried out for 1 ns at 1000 ˚K with a 1 fs time step. Snapshots were saved every 5 ps, leading to an ensemble of 200 snapshots. The resulting high temperature snapshots were energy minimized using the generalized Born implicit solvent model with a dielectric of 4. The 200 snapshots were taken forward into the DISCON calculations. We have found that these MD parameters adequately sample conformational space in cyclic hexapeptides with multiple N-methyl groups and are able to recapitulate the independently calculated NMR solution structures of well-studied cyclic peptides such as **1NMe3**[13], including the ability to sample all N-Me and Pro cis-trans rotamers. The resulting energy-minimized conformers were used as input into the DISCON protocol using the NOESY crosspeak volumes to provide experimental distances, for 5000 iterations at a cluster level of 20.

Compound **3** showed a mixture of four different conformations with the major constituting 54% of the ensemble. The second and third (29% and 10%) most abundant conformations when visually inspected contained a similar backbone motif to each other, primarily differing by the orientation about the Pro5 to Tyr6 N-methyl amide bond and positioning of the N-Acetyl threonine group.

Table 1-7 NOE correlations **1**

DISCON	Res 1	Atom 1	Res 2	Atom 2	|Norm Int.|	|Diag.|	Int/Diag	Calc. dist. Å
y	Pro5	HA	Tyr6	Nme	36.55	536.05	0.06818	2.06
y	Leu2	HA	Thr3	Nme	28.74	524.34	0.05481	2.13
y	Leu4	HA	Pro5	HD	25.84	545.91	0.04733	2.19
y	Leu4	HA	Pro5	HD	20.08	545.91	0.03678	2.28
y	Leu1	HA	Leu2	Nme	16.32	554.09	0.02945	2.37
y	Leu4	HN	Thr3	Nme	13.19	502.08	0.02627	2.41
y	Leu1	HN	Tyr6	Nme	9.68	446.61	0.02167	2.49
y	Leu1	HN	Tyr6	HA	7.56	446.61	0.01693	2.59
y	Leu1	HN	Leu4	NH	3.08	446.61	0.00690	3.01
y	Leu4	HN	Thr3	HA	3.34	502.08	0.00665	3.03
y	Leu4	HN	Leu2	HA	1.82	502.08	0.00362	3.35
y	Tyr6	HA	Leu2	Nme	1.72	541.32	0.00318	3.43
y	Leu1	HN	Leu2	Nme	1.26	446.61	0.00282	3.50
y	Leu1	HN	Pro5	HA	1.19	446.61	0.00266	3.53
y	Leu4	HA	Pro5	HG	1.35	545.91	0.00247	3.57
y	Tyr6	HA	Leu1	HA	0.79	541.32	0.00146	3.90
y	Leu4	HA	Thr3	Nme	0.73	545.91	0.00134	3.96
y	Leu1	HA	Tyr6	Nme	0.68	554.09	0.00123	4.02
y	Leu4	HA	Pro5	HA	0.63	545.91	0.00115	4.06
y	Tyr6	HE	Leu2	Nme	1.28	1203.91	0.00106	4.11
y	Tyr6	HA	Pro5	HA	0.28	541.32	0.00052	4.64
y	Leu4	HN	Thr3	HB	0.24	502.08	0.00048	4.70
ref	Tyr6	HB	Tyr6	HB	72.71	364.94	0.19924	1.72

Table 1-8 NOE correlations **3**

DISCON	Res 1	Atom 1	Res 2	Atom 2	|Norm Int.|	|Diag.|	Int/Diag	Calc. dist. Å
y	Leu4	NH	Pro5	HD	0.1	198.68	0.000503	4.72
y	Tyr6	HA	Pro5	HA	0.15	202.96	0.000739	4.43
y	Leu4	NH	Leu2	Nme	0.18	198.68	0.000906	4.28
y	Pro5	HD	Tyr6	Nme	0.15	118.55	0.001265	4.05
y	Leu1	NH	Leu2	HA	0.21	152.71	0.001375	3.99
y	Leu1	NH	Tyr6	HB	0.25	152.71	0.001637	3.88
y	Leu1	NH	Pro5	HA	0.51	152.71	0.00334	3.44
y	Leu1	NH	Thr3	HG	0.57	152.71	0.003733	3.38
y	Leu4	NH	Tyr6	Nme	0.81	198.68	0.004077	3.33
y	Leu4	HA	Pro5	HA	0.95	219.8933	0.00432	3.30
y	Leu1	NH	Leu4	NH	0.93	152.71	0.00609	3.11
y	Leu1	NH	Leu2	Nme	1	152.71	0.006548	3.08
y	Tyr6	HA	Thr3	HG	1.59	202.96	0.007834	2.99
y	Leu4	NH	Thr3	HG	2.58	198.68	0.012986	2.75
y	Leu1	NH	Tyr6	HA	3.27	152.71	0.021413	2.53
y	Leu4	NH	Thr3	HA	4.97	198.68	0.025015	2.46
y	Leu1	NH	Tyr6	Nme	4.2	152.71	0.027503	2.42
y	Leu4	HA	Pro5	HD	10.59	219.8933	0.04816	2.21
y	Thr3	HB	Leu2	Nme	10.68	219.8933	0.048569	2.20
y	Pro5	HA	Tyr6	Nme	10.39	188.1	0.055237	2.16
ref	Tyr6	HB	Tyr6	HB	28.24	131.46	0.214818	1.72

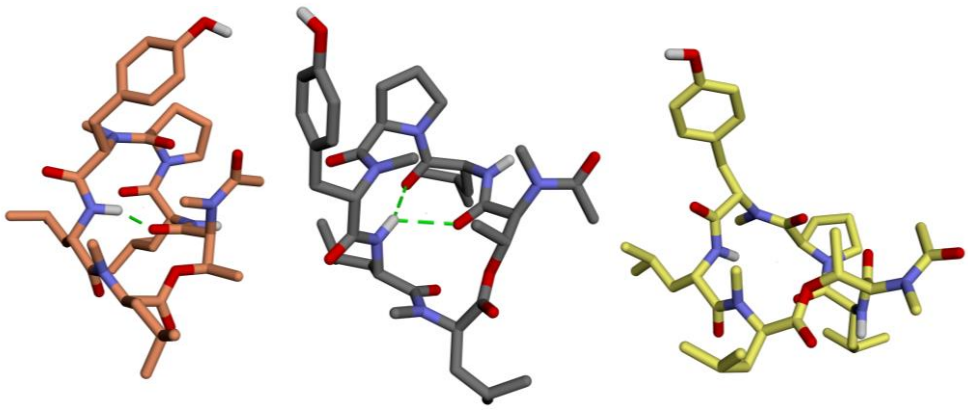

29.1% 10.3% 6.6%

Figure 1-10 Minor conformations of **3** as determined by DISCON with their respective contribution to the ensemble listed below.

1.8.5. Molecular Dynamics of the N-to-O Acyl Rearrangement

To assess the likelihood of **1** and **9** of accessing the conformation necessary for rearrangement the NAMD[32] molecular dynamics (MD) protocol was used. We used the CHARMM forcefield with MMFF94 partial charge estimation. The simulation was carried out for 10 ns with a 1 fs time step at 500 ˚K. At this simulation temperature, diverse rotamers and backbone conformations are sampled while not enabling cis-trans peptide bond isomerization. Since previous investigations showed that side-chain substitutions within the **1NMe3**[13] scaffold did not yield a significantly different backbone conformation the starting conformations of each simulation contained only *trans* peptide bonds, the configuration of **1NMe3**. Snapshots were saved every 5 ps, generating an ensemble of 2000 conformations. The distance of Thr-OH oxygen to the carbonyl carbon of the i – 1 residue and the angle between the Thr-OH, the i - 1 carbonyl carbon, and the i – 1carbonyl oxygen[23] were extracted for all snapshots.

1.8.6. Compound structures and synthetic considerations

Compound **1**

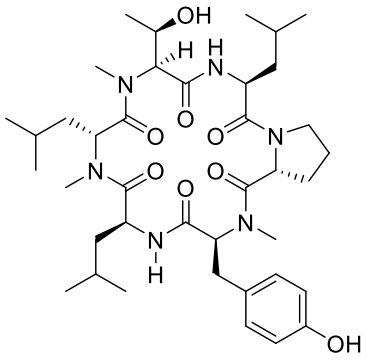

Chemical Formula: $C_{39}H_{62}N_6O_8$
Exact Mass: 742.4629
Molecular Weight: 742.9590

Compound **1** was prepared with on-resin cyclization and selective methylation. ESI cacld. for C39H62N6O8[M+H]+ m/z = 743.46; found 743.55. 1H NMR (600 MHz, Chloroform-d) δ 7.40 (d, *J* = 9.4 Hz, 1H), 7.05 (d, *J* = 9.0 Hz, 1H), 6.98 (d, *J* = 8.4 Hz, 2H), 6.68 (d, *J* = 8.4 Hz, 2H), 5.67 (dd, *J* = 12.1, 4.8 Hz, 1H), 5.24 (d, *J* = 3.6 Hz, 1H), 5.10 (m, 1H), 5.02 (dd, *J* = 9.9, 5.5 Hz, 1H), 4.90 (m, 1H), 4.63 (m, 1H), 4.41 (m, 1H), 3.78 (dt, *J* = 9.9, 7.3 Hz, 1H), 3.56 (m, 1H), 3.49 (dd, *J* = 15.4, 4.8 Hz, 1H), 3.30 (s, 3H), 3.21 (s, 3H), 2.94 (s, 3H), 2.76 (dd, *J* = 15.4, 12.2 Hz, 1H), 2.05 (m, 1H), 1.87 (ddd, *J* = 15.2, 10.2, 5.4 Hz, 1H), 1.84 – 1.62 (m, integrated together for 6H), 1.61 – 1.51 (m, integrated together for 3H), 1.51 – 1.43 (m, integrated together for 2H), .09 (d, *J* = 6.5 Hz, 3H), 1.01 (d, *J* = 6.6 Hz, 3H), 0.98 – 0.93 (m, integrated together for 15H).

Compound **2**

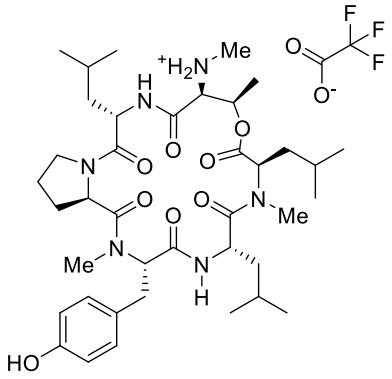

Chemical Formula: $C_{41}H_{63}F_3N_6O_{10}$
Exact Mass: 856.46
Molecular Weight: 856.98

Compound **2** was prepared via treatment of pure **1** with 0.1 M ethanolic HCl at 30 °C or 1 M ethanolic HCl at 50 °C, solvent was removed under a stream of nitrogen. The free amine was isolated as a TFA salt via reverse phase chromatography. ESI cacld. for $C_{39}H_{62}N_6O_8[M+H]^+$ *m/*z = 743.46; found 743.55. ^{1}H NMR (600 MHz, DMSO-d_6) δ 9.16 – 9.09 (m, 1H), 7.87 (d, *J* = 9.7 Hz, 1H), 7.05 – 6.94 (m, 1H), 6.94 – 6.88 (m, 2H), 6.62 – 6.57 (br, 2H), 6.56 – 6.53 (br, 1H), 5.47 (dd, *J* = 11.4, 4.6 Hz, 1H), 5.30 (dd, *J* = 11.7, 4.7 Hz, 1H), 5.10 (dt, *J* = 8.2, 5.8 Hz, 1H), 4.83 (ddd, *J* = 9.5, 7.9, 6.3 Hz, 1H), 4.72 (q, *J* = 7.7 Hz, 1H), 4.50 (t, *J* = 7.0 Hz, 1H), 3.92 (m, integrated together for 2H), 3.62 (ddd, *J* = 9.7, 7.3, 5.0 Hz, 1H), 3.20 (dd, *J* = 15.1, 4.6 Hz, 1H), 2.88 (s, 3H), 2.75 (dd, *J* = 15.1, 11.7 Hz, 1H), 2.69 (s, 3H), 2.51 (s, 3H), 1.98 (tdd, *J* = 12.2, 6.6, 4.8 Hz, 1H), 1.92 – 1.79 (m, integrated together for 3H), 1.74 – 1.66 (m, integrated together for 2H), 1.64 – 1.45 (m, integrated together for 4H), 1.42 – 1.30 (m, integrated together for 3H), 1.06 (d, *J* = 6.6 Hz, 3H), 0.95 – 0.85 (m, integrated together for 15H), 0.84 (d, *J* = 6.5 Hz, 3H).

Compound **3**

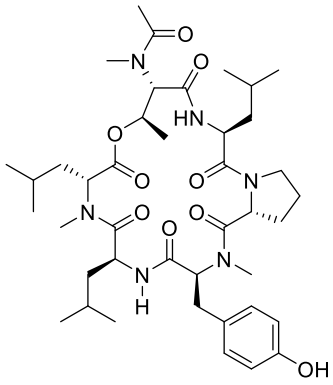

Chemical Formula: $C_{41}H_{64}N_6O_9$
Exact Mass: 784.47
Molecular Weight: 785.00

Compound **3** was prepared via treatment of the pure acyl rearranged compound **2** with 1% acetic anhydride in DCM at 50°C overnight and isolated after RP-HPLC purification in 62% yield. **ESI** cacld. for $C_{39}H_{62}N_6O_8[M+H]^+$ *m/z* = 785.47; found 785.43. Compoud **3** existed as a mixture of two conformers 0.85 : 0.15. Full assignment of the major conformer is included in Methods Table 1-6.

Compound **4**

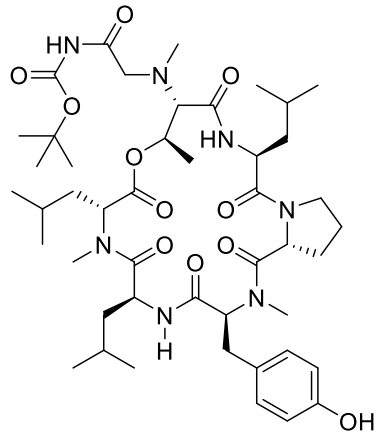

Chemical Formula: $C_{46}H_{73}N_7O_{11}$
Exact Mass: 899.53
Molecular Weight: 900.12

Compound **4** was synthesized in two steps from **1**. Following treatment of **1** in 1M ethanolic HCl at 30 °C overnight the solution was dried under a stream of nitrogen. The tail was coupled on as described in 1.8.1 General Synthetic and Procedures. After RP-HPLC purification the title compound was isolated as a white powder in 41% yield over 2 steps. ^{1}H spectra showed a mixture of 2 conformers in intermediate/slow exchange. For brevity, peak list is not included, spectra shown in 1.8.8 Selected NMR Spectra. ESI cacld. for $C_{46}H_{73}N_7O_{11}[M+H]^+$ *m/*z = 900.54; found 900.76.

Compound **5**

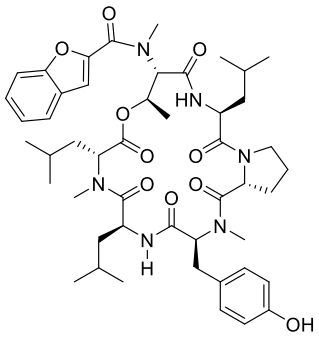

Chemical Formula: $C_{48}H_{66}N_6O_{10}$
Exact Mass: 886.48
Molecular Weight: 887.08

Compound **5** was synthesized in two steps from **1**. Following treatment of **1** in 1M ethanolic HCl at 30 °C overnight the solution was dried under a stream of nitrogen. The tail was coupled on as described on in 1.8.1 General Synthetic and Procedures. After RP-HPLC purification the title compound was isolated as a white powder in 56% yield over 2 steps. Room temperature ^{1}H NMR showed multiple conformers in slow and intermediate exchange. Increasing temperature to 45°C yielded a single conformer with some broad peaks. ^{1}H NMR (500 MHz, Acetone-d_6) δ 7.94 (d, J = 9.7 Hz, 1H), 7.73 (d, J = 7.9 Hz, 1H), 7.58 (d, J = 7.9 Hz, 1H), 7.45 (t, J = 7.8 Hz, 1H), 7.33 (m, 1H), 7.02 (d, J = 8.1 Hz, 2H), 6.72 (d, J = 8.2 Hz, 1H), 6.68 (d, J = 9.9 Hz, 1H), 5.58 (dd, J = 11.6, 4.8 Hz, 1H), 5.35 (m, 1H), 5.26 – 5.20 (m, 1H), 5.12 – 4.99 (m, 2H), 4.67 (t, J = 6.8 Hz, 1H), 3.95 (m, 1H), 3.74 (m, 1H), 3.42 (dd, J = 15.4, 4.7 Hz, 1H), 3.39 – 3.25 (m, 4H), 3.06 (s, 3H), 2.92 (s, 3H), 2.83 (dd, J = 15.4, 11.7 Hz, 1H), 2.14 (m, 1H), 1.93 (m, 2H), 1.86 – 1.70 (m, 2H), 1.60 (m, 5H), 1.45 (d, J = 6.7 Hz, 3H), 1.31 (s, 3H), 0.94 (m, 16H), 0.89 – 0.80 (m, 11H). ESI cacld. for $C_{48}H_{66}N_6O_{10}[M+H]^+$ m/z = 887.48 found 887.57.

Compound **6**

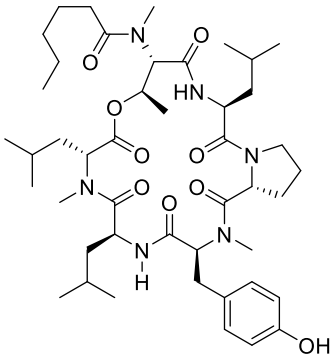

Chemical Formula: $C_{45}H_{72}N_6O_9$
Exact Mass: 840.54
Molecular Weight: 841.10

Compound **6** was synthesized in two steps from **1**. Following treatment of **1** in 1M ethanolic HCl at 30 °C overnight the solution was dried under a stream of nitrogen. The tail was coupled on as described in 1.8.1 General Synthetic and Procedures. After RP-HPLC purification the title compound was isolated as a white powder in 43% yield over 2 steps. ^{1}H spectra showed a mixture of 2 conformers in intermediate/slow exchange. For brevity, peak list is not included, spectra shown in 1.8.8 Selected NMR Spectra. ESI cacld. for $C_{45}H_{72}N_6O_9[M+H]^+$ *m/*z = 841.54; found 841.71.

Compound **7**

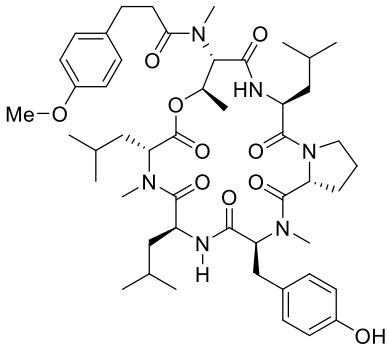

Chemical Formula: $C_{49}H_{72}N_6O_{10}$
Exact Mass: 904.53
Molecular Weight: 905.14

Compound **7** was synthesized in two steps from **1**. Following treatment of **1** in 1 M ethanolic HCl at 30 °C overnight the solution was dried under a stream of nitrogen. The tail was coupled on as described in 1.8.1 General Synthetic and Procedures. After RP-HPLC purification the title compound was isolated as a white powder in 43% yield over 2 steps. Proton NMR revealed a mixture of two isomers, peaks were integrated together when possible. ^{1}H NMR (500 MHz, Acetonitrile-d_3) δ 7.68 – 7.49 (m, 1H), 7.20 – 7.09 (m, 2H), 6.98 (m, 2H), 6.86 – 6.79 (m, 2H), 6.71 – 6.64 (m, 2H), 6.53 (d, J = 8.9 Hz, 1H), 5.44 (dd, J = 11.8, 4.7 Hz, 1H), 5.33 (br, 1H), 5.23 (s, 1H), 5.09 – 4.99 (m, 1H), 4.98 – 4.84 (m, 1H), 4.78 (m, 1H), 4.52 (m, 1H), 3.74 (s, 3H), 3.74 – 3.68 (m, 1H), 3.66 – 3.57 (m, 1H), 3.35 (dd, J = 15.1, 4.3 Hz, 1H), 2.95 (s, 3H), 2.88 (s, 3H), 2.82 (s, 3H), 2.81 – 2.74 (m, 1H), 2.68 – 2.57 (m, 2H), 2.41 (dt, J = 15.8, 7.7 Hz, 1H), 2.00 (dd, J = 12.2, 6.6 Hz, 1H), 1.91 – 1.41 (m, 11H), 1.36 (dd, J = 12.1, 6.4 Hz, 1H), 1.31 – 1.24 (m, 2H), 1.19 (d, J = 6.6 Hz, 2H), 0.97 – 0.81 (m, 18H). ESI cacld. for $C_{49}H_{72}N_6O_{10}[M+H]^+$ m/z = 905.53; found 905.74.

Compound **8**

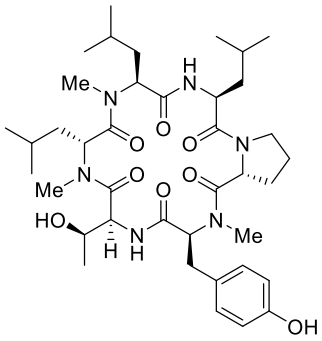

Chemical Formula: $C_{39}H_{62}N_6O_8$
Exact Mass: 742.46
Molecular Weight: 742.96

Compound **8** was prepared with on-resin cyclization and selective methylation. ESI cacld. for $C_{39}H_{62}N_6O_8[M+H]^+$ *m/*z = 743.46; found 743.66. Compound **8** was observed as a mixture of two rotamers, and peaks were integrated together when possible and reported as 'm, integrated together for'. ^{1}H NMR (500 MHz, Chloroform-*d*) δ 7.97 (m, integrated together for 1H), 7.02 – 6.95 (m, integrated together for 2H), 6.88 (d, *J* = 8.3 Hz, 0H), 6.70 (d, *J* = 7.9 Hz, 2H), 6.63 (d, *J* = 8.6 Hz, 1H), 5.72 (m integrated together for 1H), 5.29 (dd, *J* = 11.7, 4.0 Hz, 1H), 5.07 (dd, *J* = 9.7, 5.6 Hz, 1H), 4.94 (m, integrated together for 1H), 4.89 – 4.82 (m, 1H), 4.41 (dt, *J* = 14.0, 6.8 Hz, 1H), 4.22 (q, *J* = 6.5 Hz, 1H), 3.78 – 3.65 (m, 1H), 3.53 (dt, *J* = 15.3, 3.4 Hz, 2H), 3.17 (s, 3H), 3.07 (s, 3H), 3.00 (m, integrated together for 3H), 2.80 (m, integrated together for 1H), 2.18 – 2.02 (m, integrated together for 1H), 1.99 (m, integrated together for 1H), 1.91 – 1.75 (m, integrated together for 3H), 1.65 – 1.41 (m, integrated together for 8H), 1.41 – 1.32 (m, integrated together for 1H), 1.17 (m, integrated together for 3H), 1.02 (d, *J* = 6.5 Hz, 3H), 0.99 – 0.89 (m, integrated together for 15H), 0.87 (m integrated together for 3H).

Compound **9**

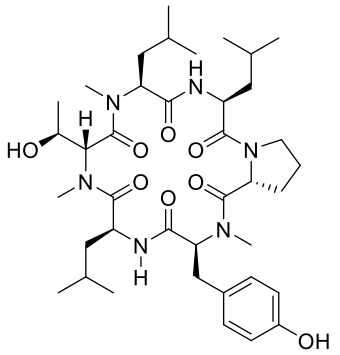

Chemical Formula: $C_{39}H_{62}N_6O_8$
Exact Mass: 742.4629
Molecular Weight: 742.9590

Compound **9** was prepared with on-resin cyclization and selective methylation. ESI cacld. for $C_{39}H_{62}N_6O_8[M+H]^+$ *m/*z = 743.46; found 743.66. ^{1}H NMR (500 MHz, Chloroform-*d*) δ 7.60 (d, *J* = 9.7 Hz, 1H), 6.95 (d, *J* = 8.1 Hz, 2H), 6.84 (d, *J* = 9.0 Hz, 1H), 6.69 (d, *J* = 8.0 Hz, 2H), 5.64 (dd, *J* = 11.6, 4.9 Hz, 1H), 5.35 (dd, *J* = 11.7, 4.0 Hz, 1H), 5.06 (dt, *J* = 9.6, 7.2 Hz, 1H), 4.88 (q, *J* = 7.5 Hz, 1H), 4.76 (d, *J* = 9.2 Hz, 1H), 4.37 (t, *J* = 7.0 Hz, 1H), 4.29 (dt, *J* = 12.5, 6.6 Hz, 1H), 3.78 (dt, *J* = 9.8, 7.2 Hz, 1H), 3.57 – 3.50 (m, 1H), 3.47 (dd, *J* = 15.3, 4.8 Hz, 1H), 3.30 (s, 3H), 3.15 (s, 3H), 2.93 (s, 3H), 2.76 (dd, *J* = 15.3, 12.1 Hz, 1H), 2.00 (m, integrated together for 2H), 1.85 – 1.64 (m, integrated together for 5H), 1.56 (m, integrated together for 5H), 1.35 (m, 1H), 1.28 (d, *J* = 6.2 Hz, 3H), 0.93 (m, integrated together for 15H), 0.87 (d, *J* = 6.4 Hz, 3H).

Compound **10**

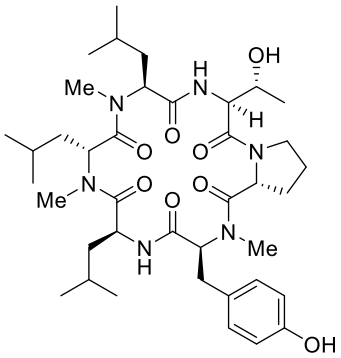

Chemical Formula: $C_{39}H_{62}N_6O_8$
Exact Mass: 742.4629
Molecular Weight: 742.9590

Compound **10** was prepared with on-resin cyclization and selective methylation. ESI cacld. for $C_{39}H_{62}N_6O_8[M+H]^+$ *m/*z = 743.46; found 743.66. ^{1}H NMR (500 MHz, Chloroform-*d*) δ 7.25 – 7.19 (m, integrated together for 2H), 6.98 (d, *J* = 8.0 Hz, 2H), 6.71 (d, *J* = 7.9 Hz, 2H), 5.66 (dd, *J* = 12.4, 4.7 Hz, 1H), 5.37 (dd, *J* = 11.8, 4.0 Hz, 1H), 5.13 (m, 1H), 4.87 (dd, *J* = 10.5, 4.9 Hz, 1H), 4.82 (m, 1H), 4.42 (m, 1H), 4.11 (m, 1H), 3.79 (m, 1H), 3.61 (m, 1H), 3.53 (dd, *J* = 15.6, 4.9 Hz, 1H), 3.20 (s, 4H), 3.11 (s, 4H), 2.93 (s, 3H), 2.78 (m, 1H), 2.18 – 2.07 (m, 1H), 1.99 (ddd, *J* = 14.7, 10.7, 4.0 Hz, 1H), 1.94 – 1.47 (m, integrated together for 10H), 1.37 (m, 1H), 1.14 (d, *J* = 6.2 Hz, 3H), 1.01 (d, *J* = 6.5 Hz, 4H), 1.00 – 0.89 (m, integrated together for 15H), 0.87 – 0.84 (m, 3H).

Compound **11**

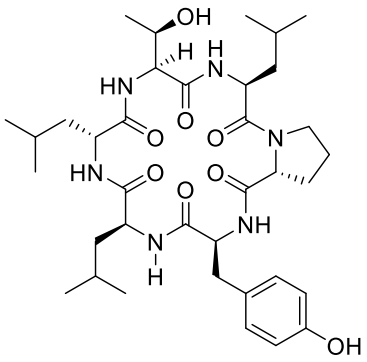

Chemical Formula: $C_{36}H_{56}N_6O_8$
Exact Mass: 700.4160
Molecular Weight: 700.8780

Compound **11** was prepared with on-resin cyclization. ESI cacld. for $C_{36}H_{56}N_6O_8[M+H]^+$ *m/z* = 701.46; found 701.50. ^{1}H NMR (500 MHz, DMSO-d_6) δ 9.19 (s, 1H), 8.63 (d, *J* = 8.0 Hz, 1H), 8.13 (d, *J* = 8.2 Hz, 1H), 8.09 (d, *J* = 7.0 Hz, 1H), 7.58 (d, *J* = 7.9 Hz, 1H), 7.01 (d, *J* = 8.4 Hz, 2H), 6.64 (d, *J* = 8.4 Hz, 2H), 6.58 (br s, 1H), 4.78 (d, *J* = 5.9 Hz, 1H), 4.70 (td, *J* = 8.5, 5.1 Hz, 1H), 4.41 (m, integrated together for 2H), 4.19 (td, *J* = 6.1, 2.7 Hz, 1H), 4.16 – 4.08 (m, integrated together for 2H), 3.94 (dd, *J* = 8.3, 2.7 Hz, 1H), 3.55 – 3.45 (m, integrated together for 2H), 3.11 (dd, *J* = 14.2, 3.2 Hz, 1H), 2.65 (dd, *J* = 14.3, 11.1 Hz, 1H), 1.96 (dt, *J* = 11.1, 6.9 Hz, 1H), 1.91 – 1.77 (m, integrated together for 2H), 1.63 – 1.33 (m, integrated together for 13H), 1.05 (d, *J* = 6.4 Hz, 3H), 0.94 – 0.80 (m, integrated together for 21H).

Compound **12**

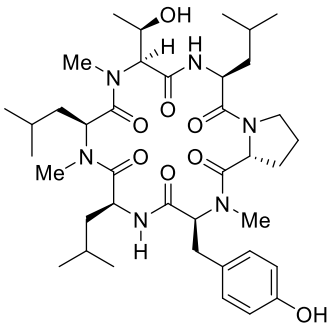

Chemical Formula: $C_{39}H_{62}N_6O_8$
Exact Mass: 742.4629
Molecular Weight: 742.9590

Compound **12** was prepared with in-sequence methylations followed by solution-phase cyclization. ESI cacld. for $C_{39}H_{62}N_6O_8[M+H]^+$ *m/*z = 743.46; found 743.54. ^{1}H NMR (500 MHz, DMSO-d_6) δ 9.13 (s, 1H), 7.81 (d, *J* = 5.9 Hz, 1H), 7.59 (d, *J* = 9.1 Hz, 1H), 6.94 (d, *J* = 8.2 Hz, 2H), 6.62 (d, *J* = 8.2 Hz, 2H), 5.34 (dd, *J* = 11.7, 4.6 Hz, 1H), 5.27 – 5.21 (m, 1H), 4.97 (m, 1H), 4.83 (m, 1H), 4.67 – 4.60 (m, 2H), 4.52 (m, 1H), 3.94 (m, 1H), 3.61 (dt, *J* = 9.6, 6.8 Hz, 1H), 3.53 (dt, *J* = 9.7, 6.5 Hz, 1H), 3.22 (dd, *J* = 15.2, 4.7 Hz, 1H), 3.02 (s, 3H), 2.96 (s, 3H), 2.77 (dd, *J* = 15.2, 11.7 Hz, 1H), 2.56 (s, 3H), 2.14 – 2.04 (m, 1H), 1.94-1.80 (m, integrated together for 3H), 1.78 – 1.62 (m, integrated together for 2H), 1.53-1.38 (m, integrated together for 6H), 1.29 – 1.17 (m, integrated together for 4H), 1.14 (d, *J* = 5.9 Hz, 3H), 0.97 (d, *J* = 6.4 Hz, 3H), 0.91 (d, *J* = 5.9 Hz, 3H), 0.89 – 0.80 (m, integrated together for 12H).

Compound **13**

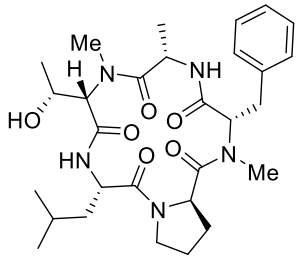

Chemical Formula: $C_{29}H_{43}N_5O_6$
Exact Mass: 557.32
Molecular Weight: 557.69

Compound **13** was prepared with in-sequence methylation or installation of *N*-Me Fmoc amino acids followed by solution-phase cyclization. ESI cacld. for $C_{29}H_{43}N_5O_6[M+H]^+$ *m/*z = 558.32; found 558.36. ^{1}H NMR (500 MHz, Chloroform-*d*) δ 8.04 (s, 1H), 7.76 (d, *J* = 8.7 Hz, 1H), 7.49 (d, *J* = 9.2 Hz, 1H), 7.25 – 7.22 (m, 2H), 7.20 – 7.16 (m, 1H), 7.16 – 7.11 (m, 2H), 5.74 (dd, *J* = 12.5, 4.6 Hz, 1H), 4.94 (dq, *J* = 8.4, 6.4 Hz, 1H), 4.76 (dq, *J* = 7.9, 6.2 Hz, 1H), 4.67 (ddd, *J* = 11.0, 9.2, 3.9 Hz, 1H), 4.45 (dd, *J* = 7.8, 5.7 Hz, 1H), 3.89 (dt, *J* = 9.6, 7.2 Hz, 1H), 3.76 (dd, *J* = 15.8, 4.7 Hz, 1H), 3.47 (m, *J* = 9.7, 7.2, 4.4 Hz, 1H), 3.36 (d, *J* = 8.0 Hz, 1H), 2.98 (2 s, integrated together for 6H), 2.89 (dd, *J* = 15.9, 12.4 Hz, 1H), 2.33 – 2.24 (m, 1H), 1.95 – 1.79 (m, 2H), 1.70 (m, *J* = 7.5, 5.9, 5.3 Hz, 2H), 1.57 (ddd, *J* = 13.7, 11.1, 4.6 Hz, 1H), 1.37 (d, *J* = 6.4 Hz, 3H), 1.31 (td, *J* = 9.4, 4.6 Hz, 1H), 1.21 (d, *J* = 6.1 Hz, 3H), 0.94 (2 d, integrated together for 6H).

Compound **14**

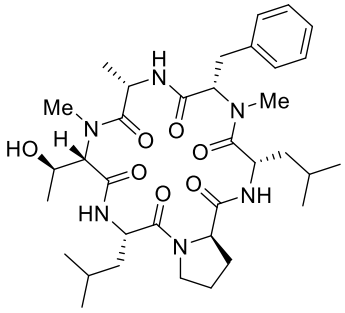

Chemical Formula: $C_{35}H_{54}N_6O_7$
Exact Mass: 670.41
Molecular Weight: 670.85

Compound **14** was prepared with in-sequence methylation or installation of *N*-Me Fmoc amino acids followed by solution-phase cyclization. ESI cacld. for $C_{35}H_{54}N_6O_7[M+H]^+$ *m/*z = 671.41; found 671.50. JLT6 was observed as a mixture of 3 rotamers (2 major, 1 minor) and for brevity peak list is not included, spectra shown in 1.8.8 Selected NMR Spectra.

Compound **15**

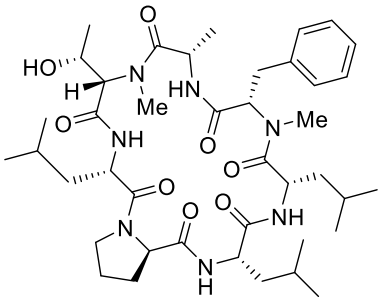

Chemical Formula: $C_{41}H_{65}N_7O_8$
Exact Mass: 783.49
Molecular Weight: 784.01

Compound **15** was prepared with in-sequence methylation or installation of *N*-Me Fmoc amino acids followed by solution-phase cyclization. ESI cacld. for $C_{41}H_{65}N_7O_8[M+H]^+$ *m/*z = 784.49; found 784.58. ^{1}H NMR (500 MHz, Chloroform-*d*) δ 8.31 (d br, 1H), 8.14 (d, *J* = 7.8 Hz, 1H), 7.47 (d, *J* = 7.8 Hz, 1H), 7.30 (t, *J* = 7.5 Hz, 2H), 7.25 – 7.21 (m, 1H), 7.18 – 7.14 (m, 2H), 6.13 (d, *J* = 7.1 Hz, 1H), 5.02 (m, integrated together for 2H), 4.87 – 4.76 (m, 1H), 4.56 (d, *J* = 7.8 Hz, 1H), 4.43 (p, *J* = 6.2 Hz, 1H), 4.35 (ddd, *J* = 11.2, 7.2, 3.8 Hz, 1H), 4.17 (q, *J* = 7.5 Hz, 1H), 3.83 – 3.76 (m, 1H), 3.67 (d, *J* = 4.8 Hz, 1H), 3.40 (m, 1H), 3.28 (s, 3H), 3.09 (m integrated together for 2H), 2.91 (s, 3H), 2.45 (dd, *J* = 12.4, 6.0 Hz, 1H), 1.93 (m, integrated together for 2H), 1.80 (m, 1H), 1.65 (m ,integrated together for 4H), 1.41 (m, integrated together for 4H), 1.31 (d, *J* = 6.6 Hz, 3H), 1.21 (d, *J* = 6.4 Hz, 3H), 0.99 (d, *J* = 6.4 Hz, 3H), 0.94 (d, *J* = 6.6 Hz, 3H), 0.91 (d, *J* = 6.4 Hz, 3H), 0.86 (d, *J* = 6.3 Hz, 3H), 0.70 (d, *J* = 6.6 Hz, 3H), 0.56 (d, *J* = 6.5 Hz, 3H), -0.07 (m, 1H).

1.8.7. HPLC MS data for compounds 1-15

HPLC-MS of Compound **1**

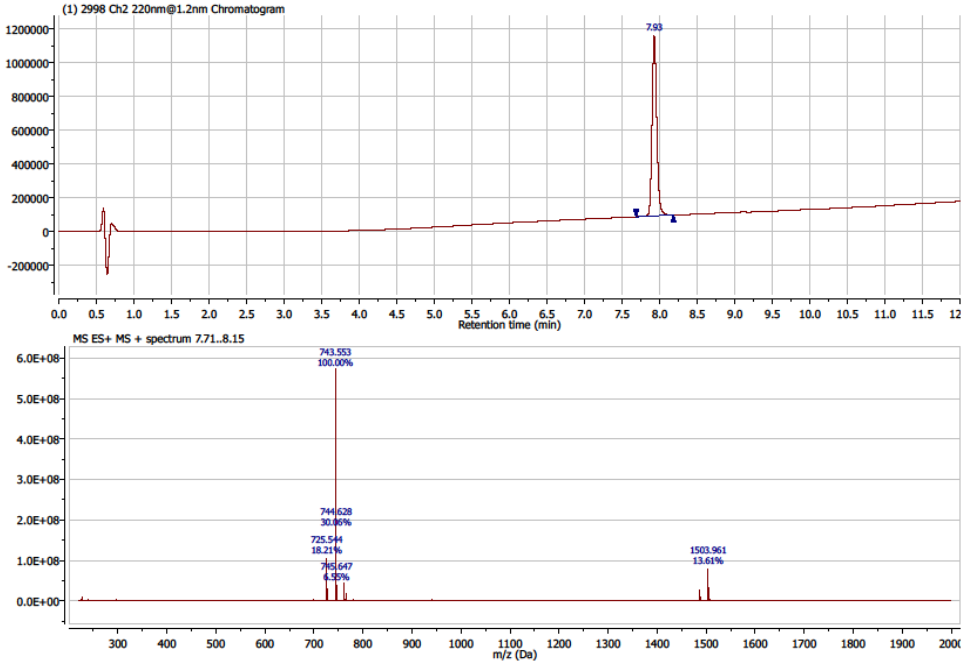

HPLC-MS of Compound **2**

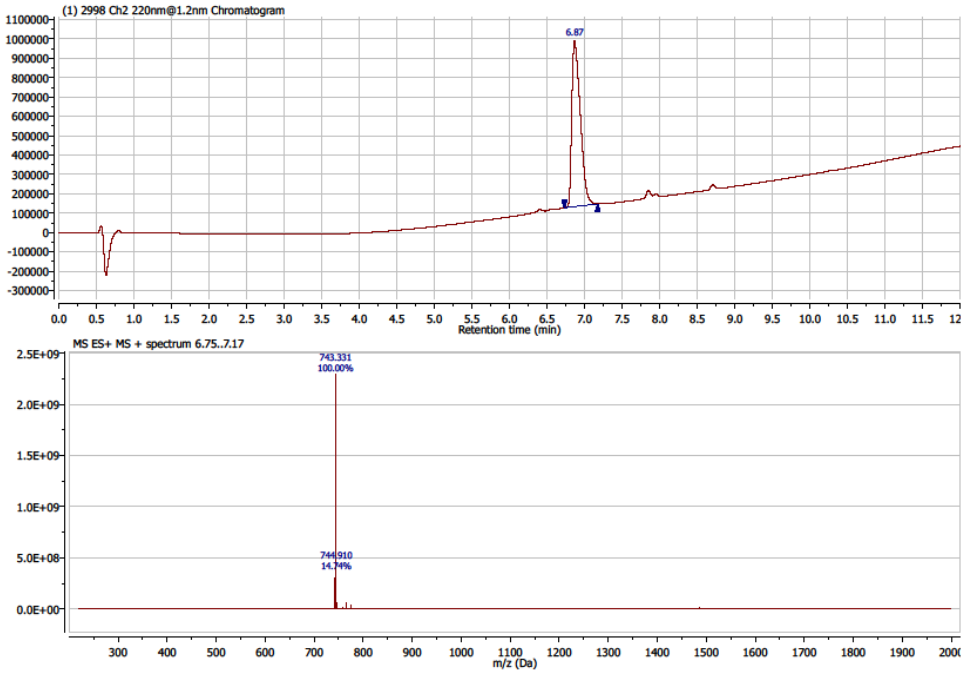

HPLC-MS of Compound **3**

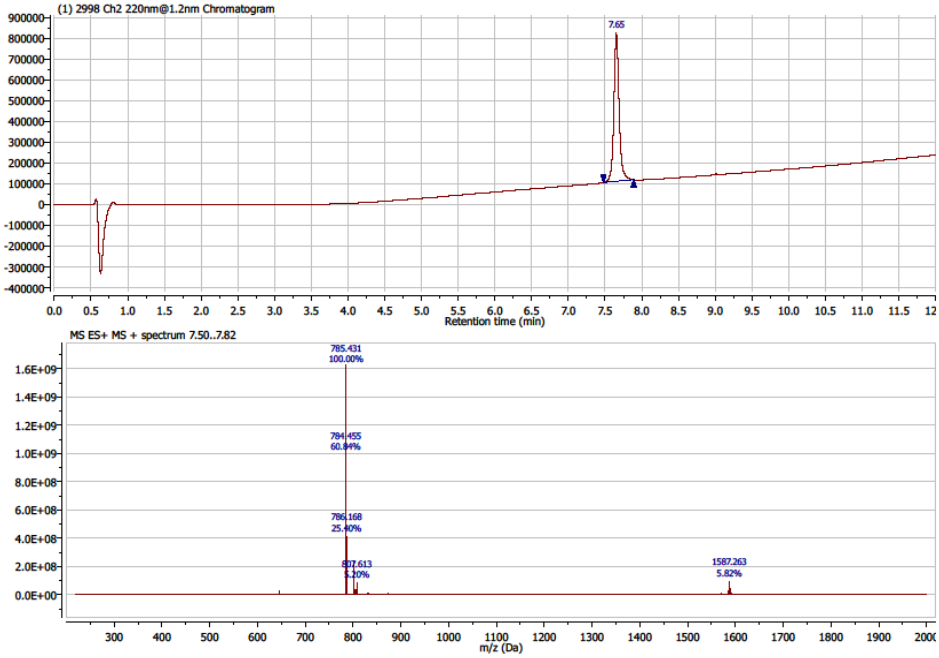

HPLC-MS of Compound **4**

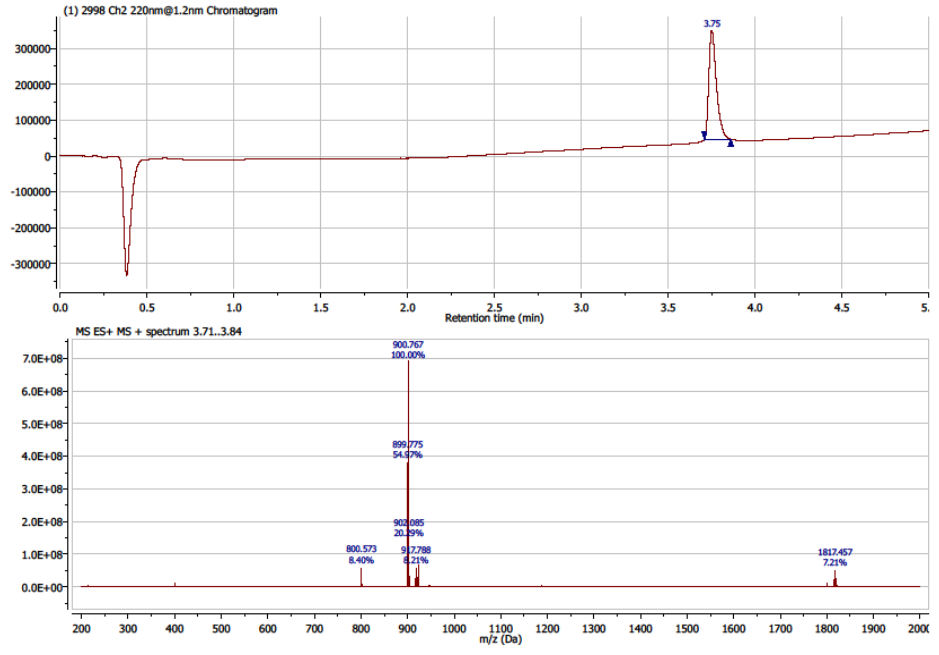

HPLC-MS of Compound **5**

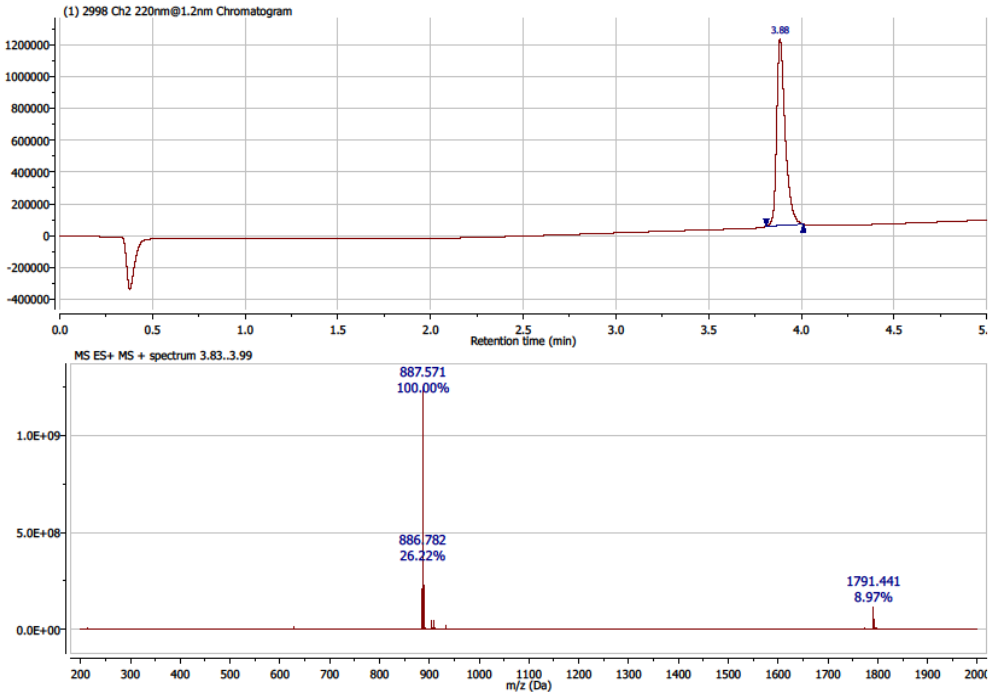

HPLC-MS of Compound **6**

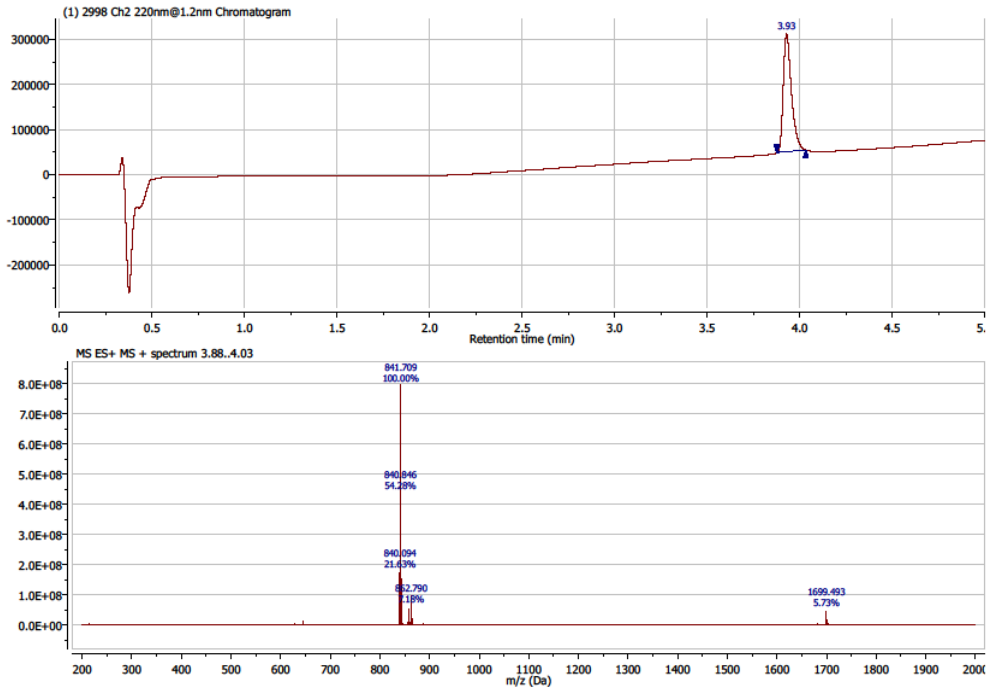

HPLC-MS of Compound **7**

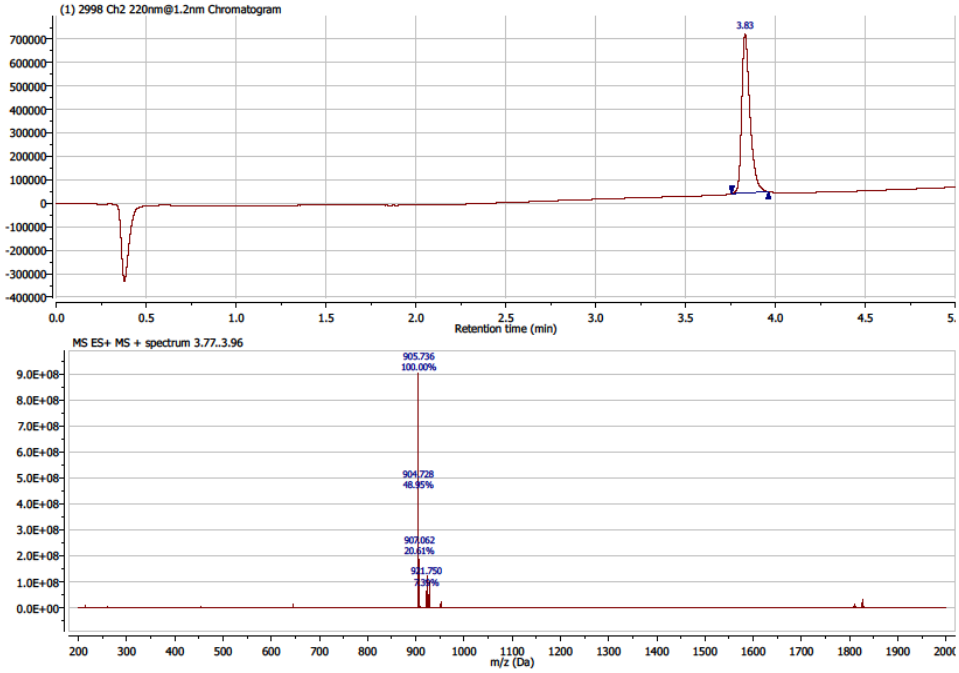

HPLC-MS of Compound **8**

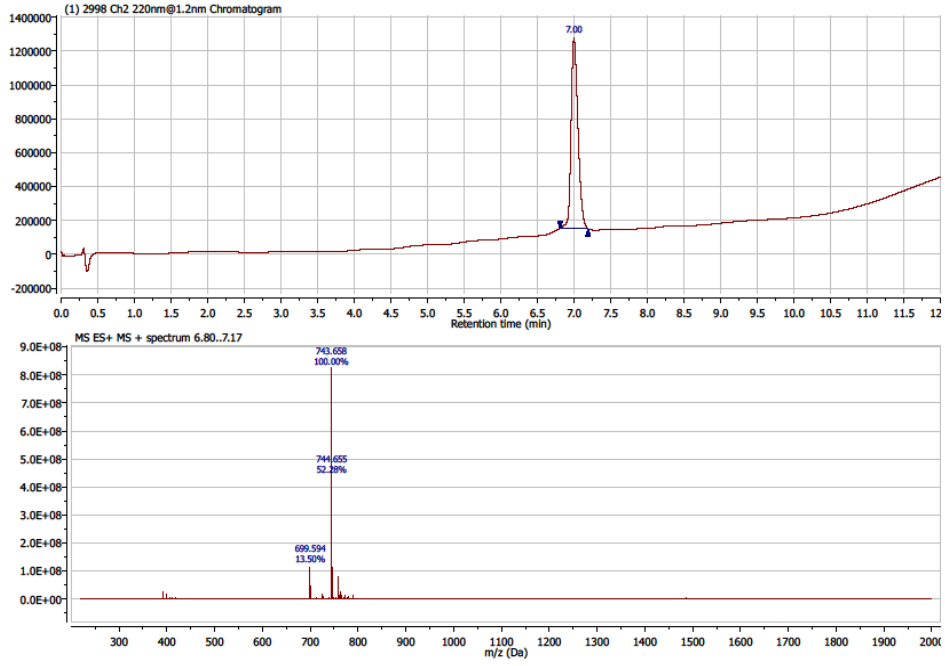

HPLC-MS of Compound **9**

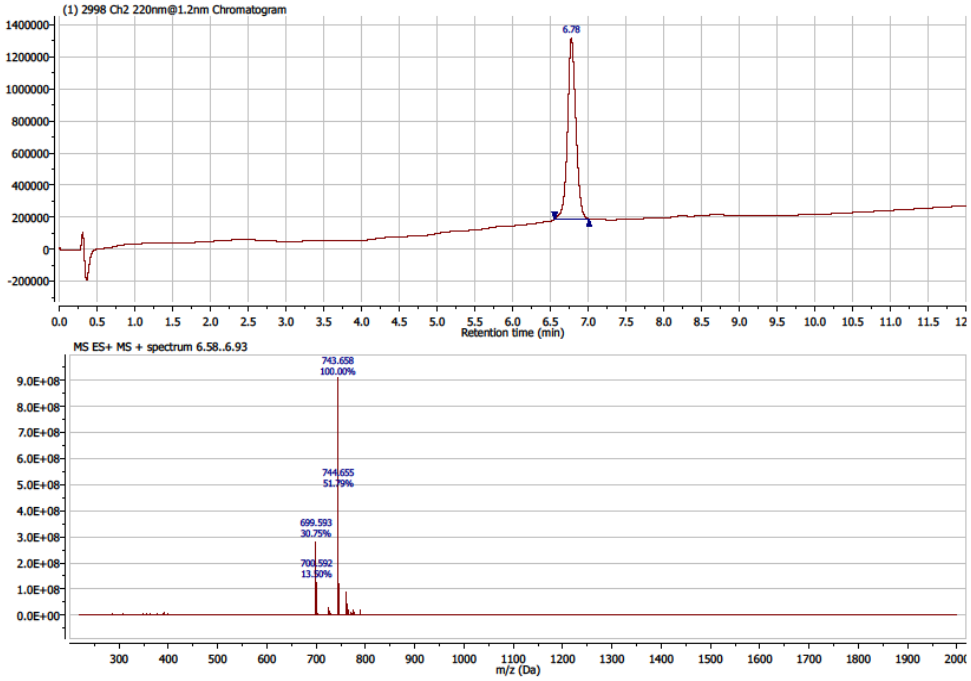

HPLC-MS of Compound **10**

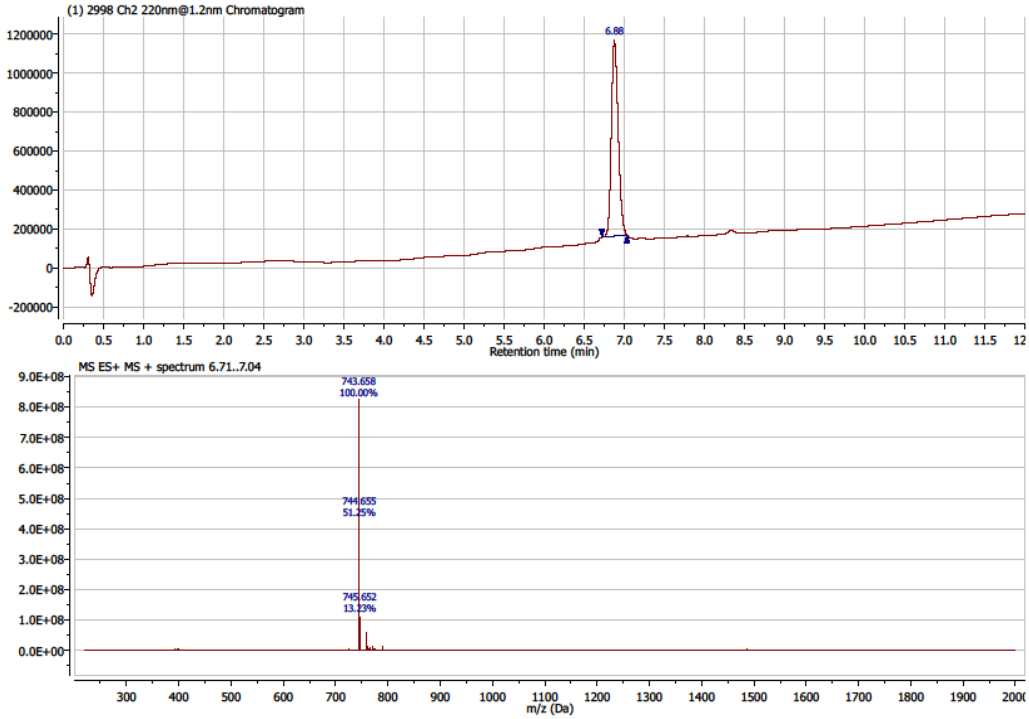

HPLC-MS of Compound **11**

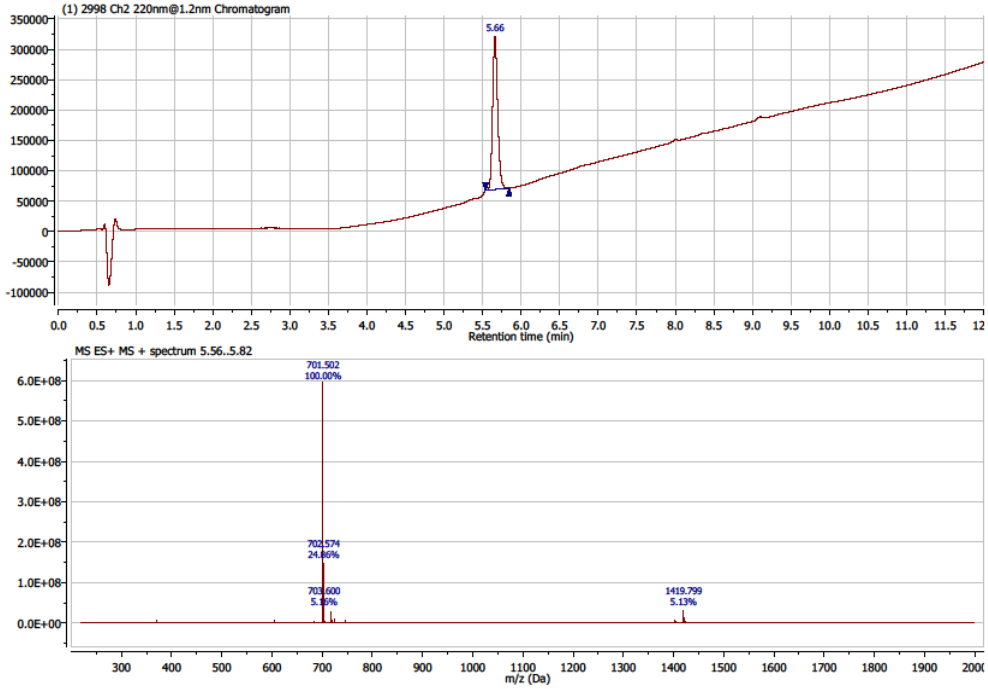

HPLC-MS of Compound **12**

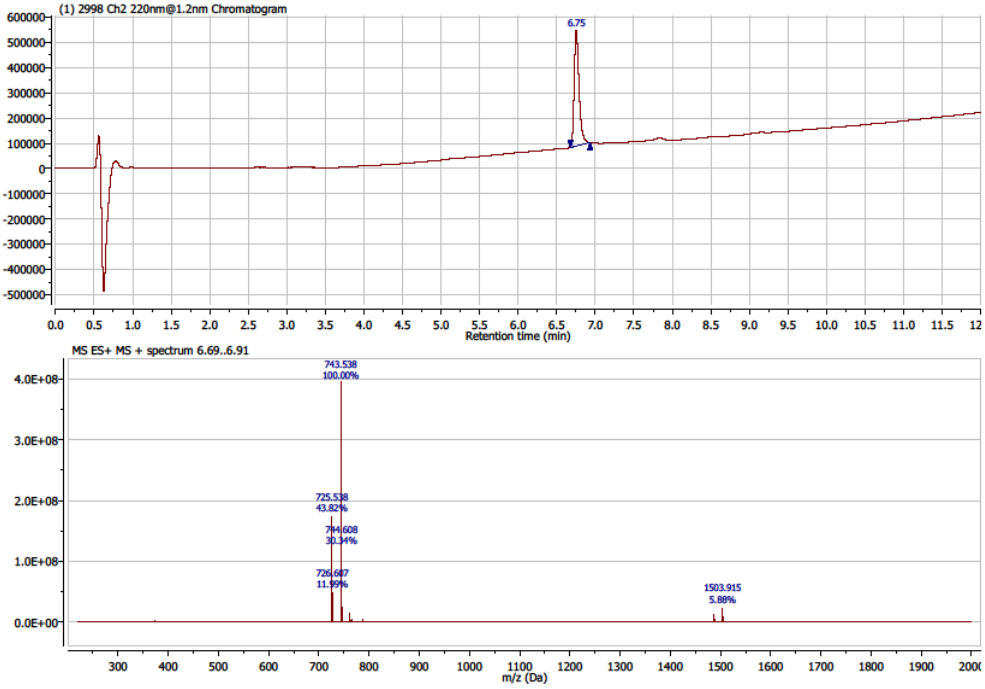

HPLC-MS of Compound **13**

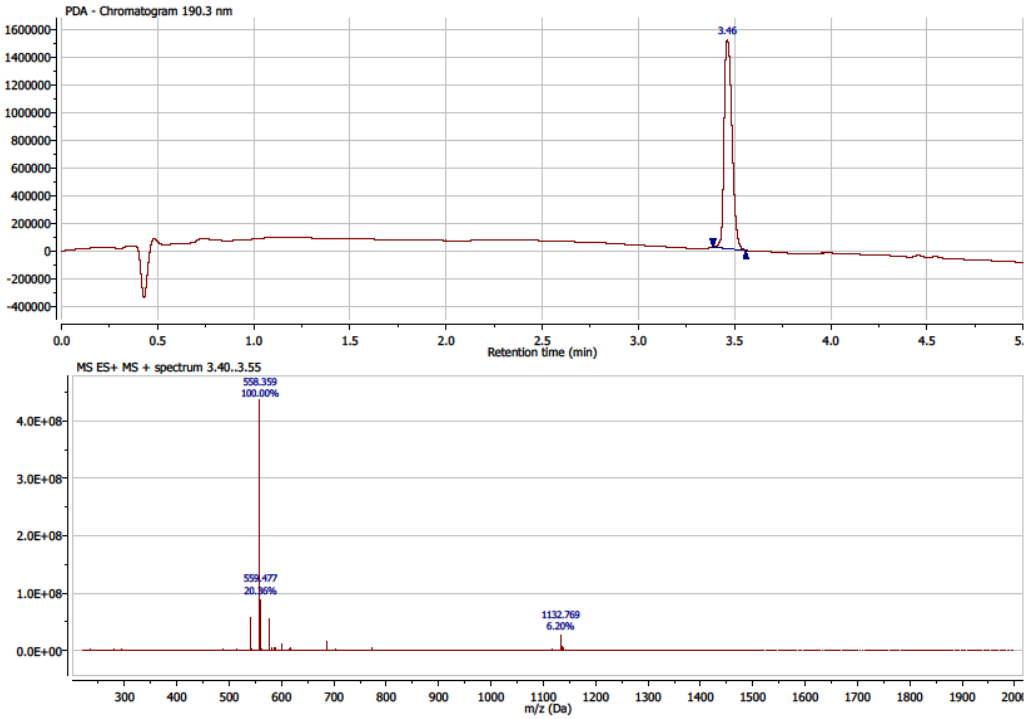

HPLC-MS of Compound **14**

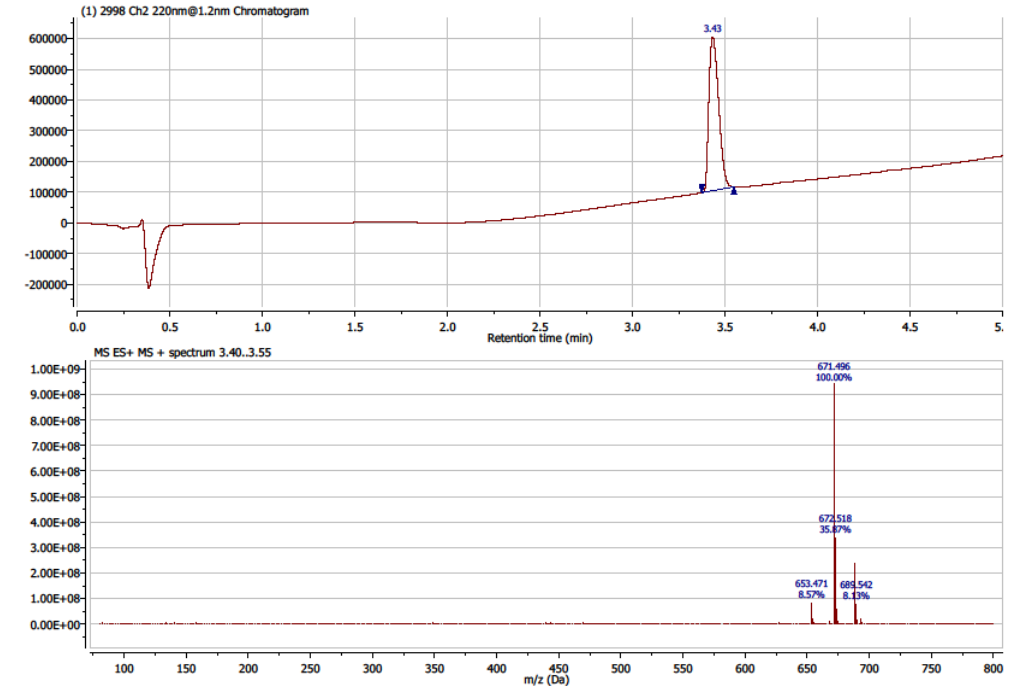

HPLC-MS of Compound **15**

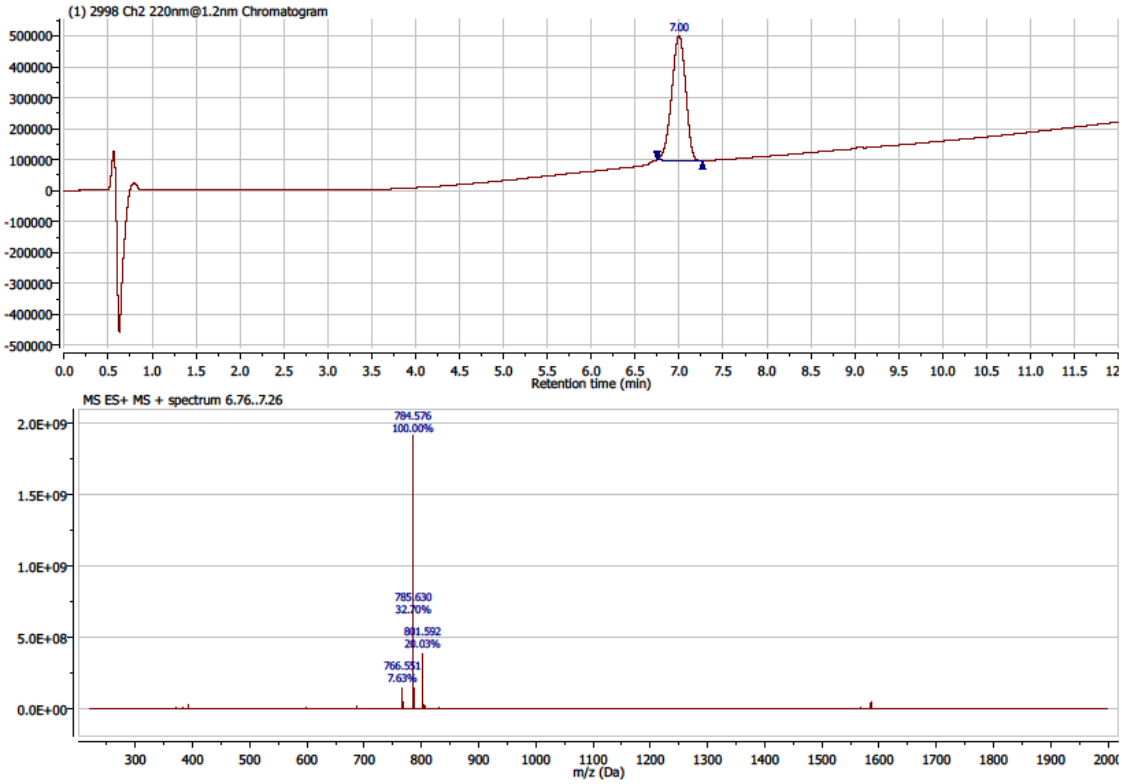

1.8.8. Selected NMR Spectra

1 ^{1}H $CDCl_3$

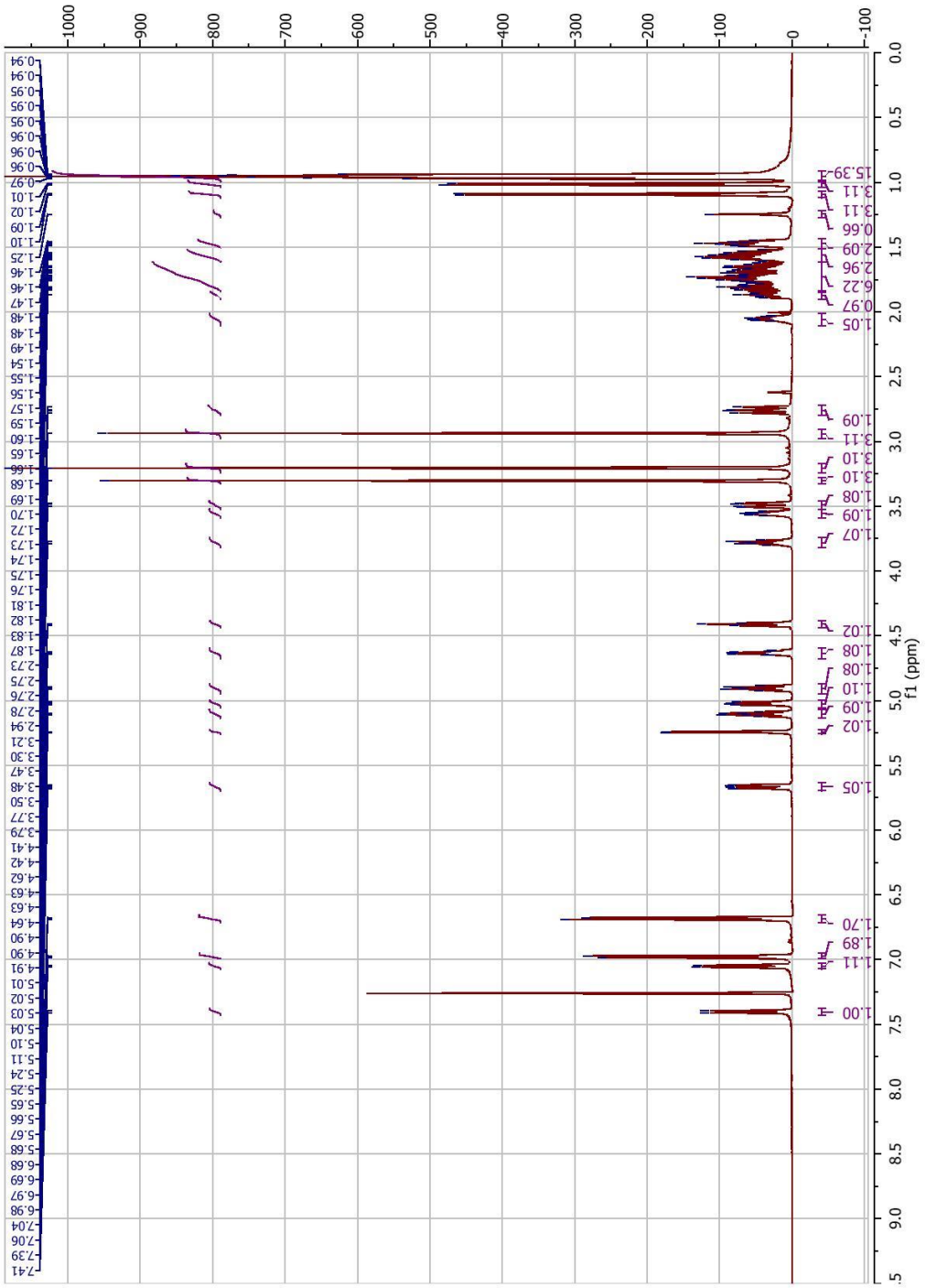

1 ^{13}C $CDCl_3$

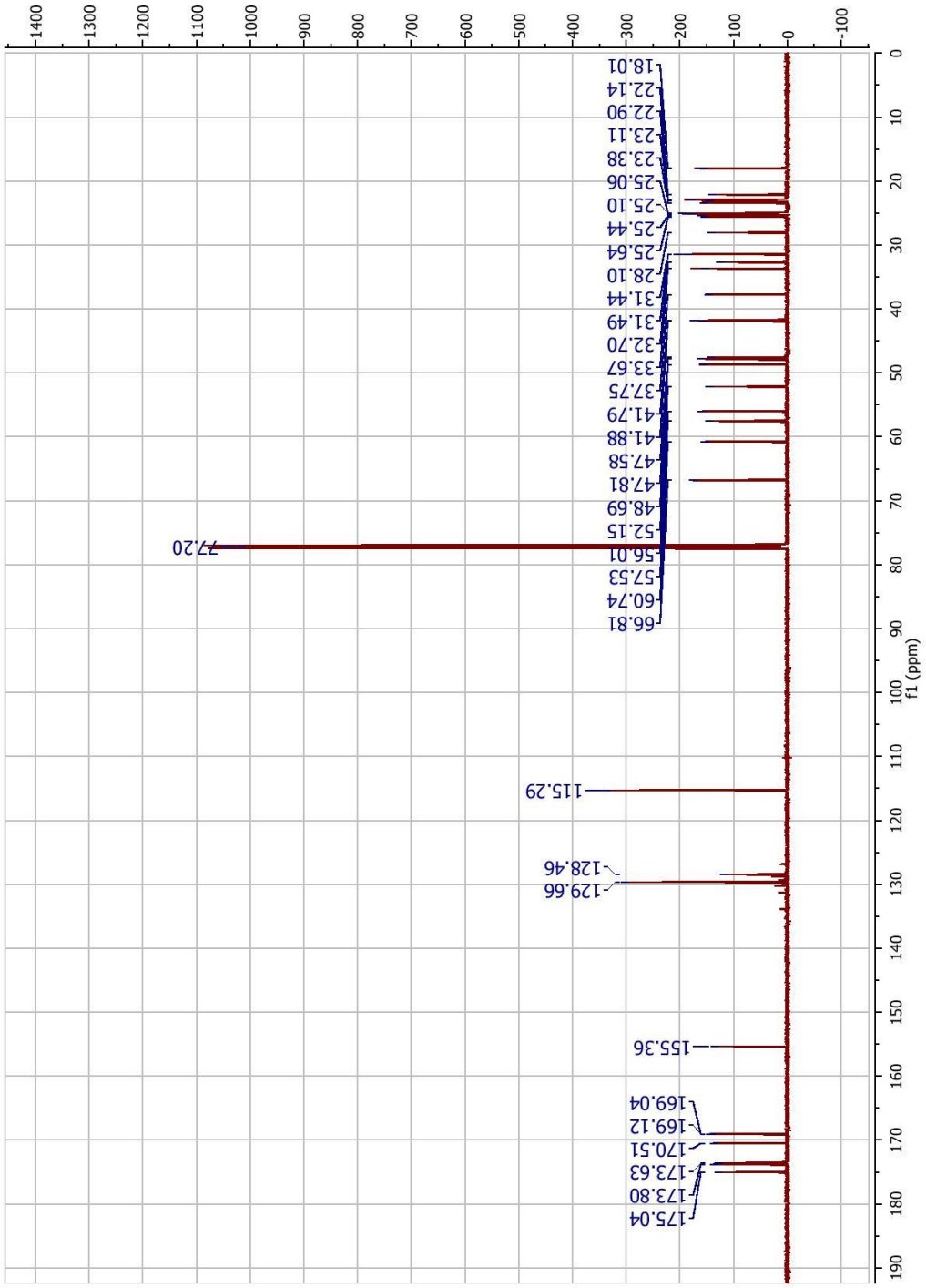
18.01
22.14
22.90
23.11
23.38
25.06
25.10
25.44
25.64
28.10
31.44
31.49
32.70
33.67
37.75
41.79
41.88
47.58
47.81
48.69
52.15
56.01
57.53
60.74
66.81
77.20
115.29
128.46
129.66
155.36
169.04
169.12
170.51
173.63
173.80
175.04
f1 (ppm)

1 COSY

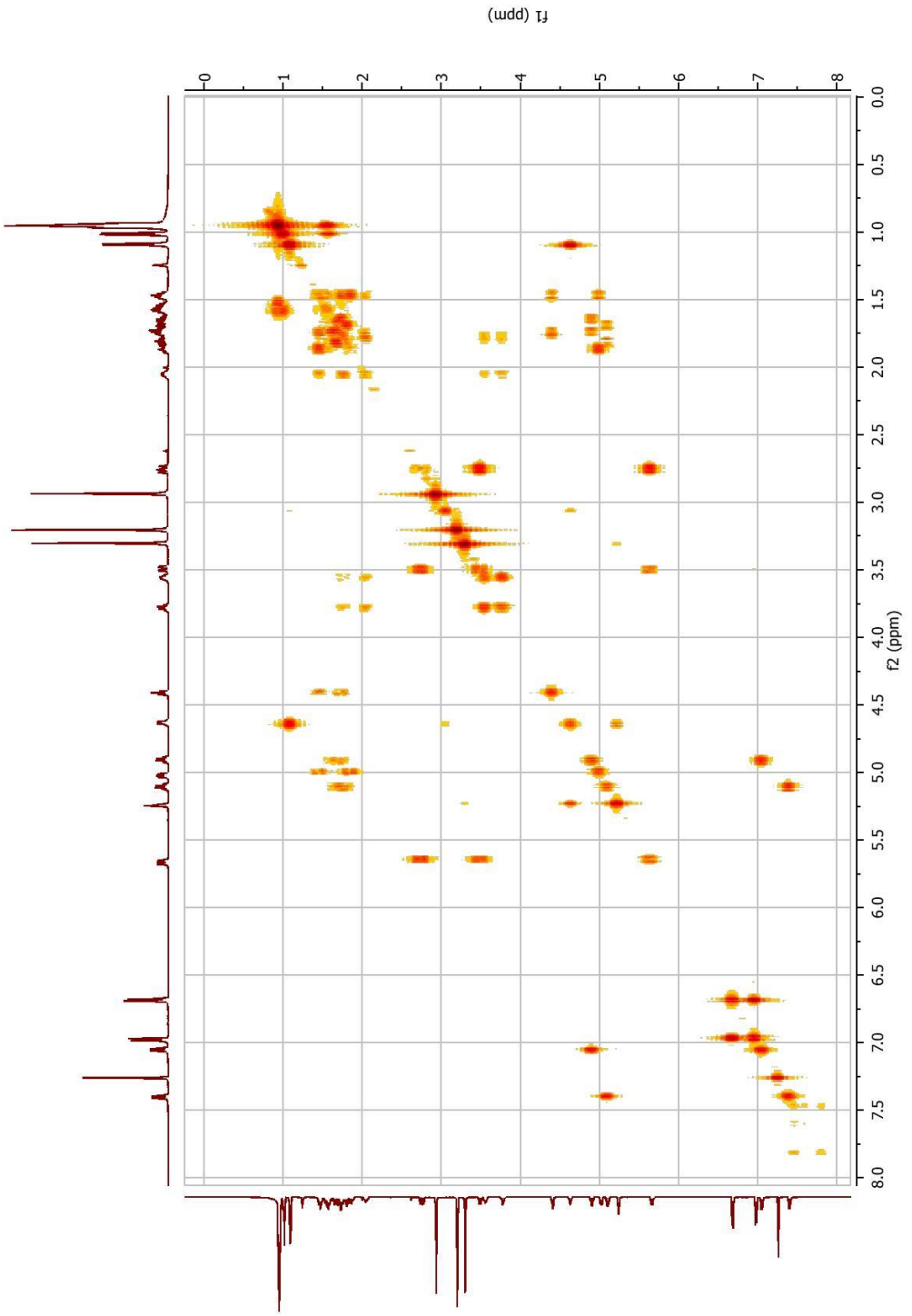

1 TOCSY

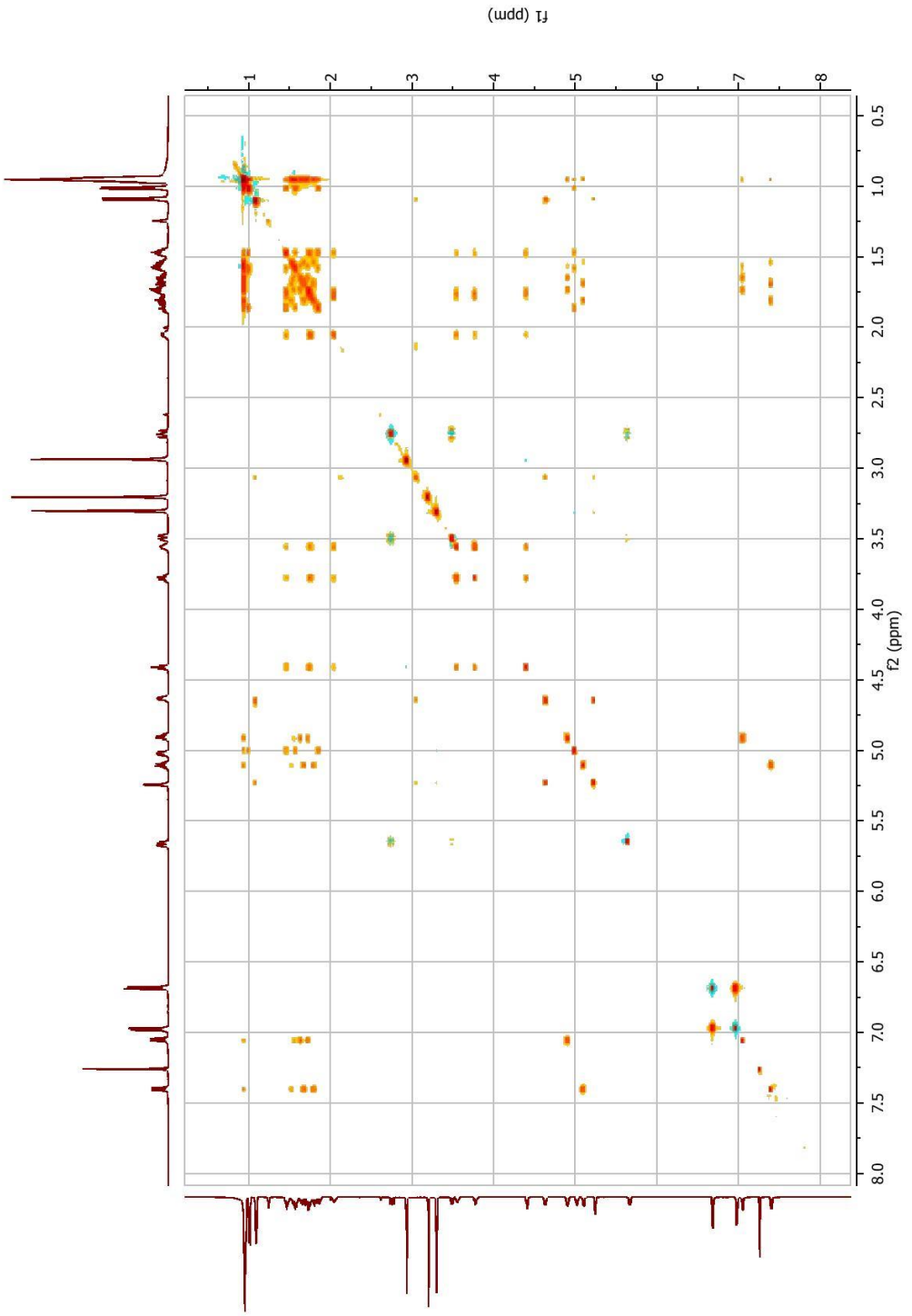

1 HSQC

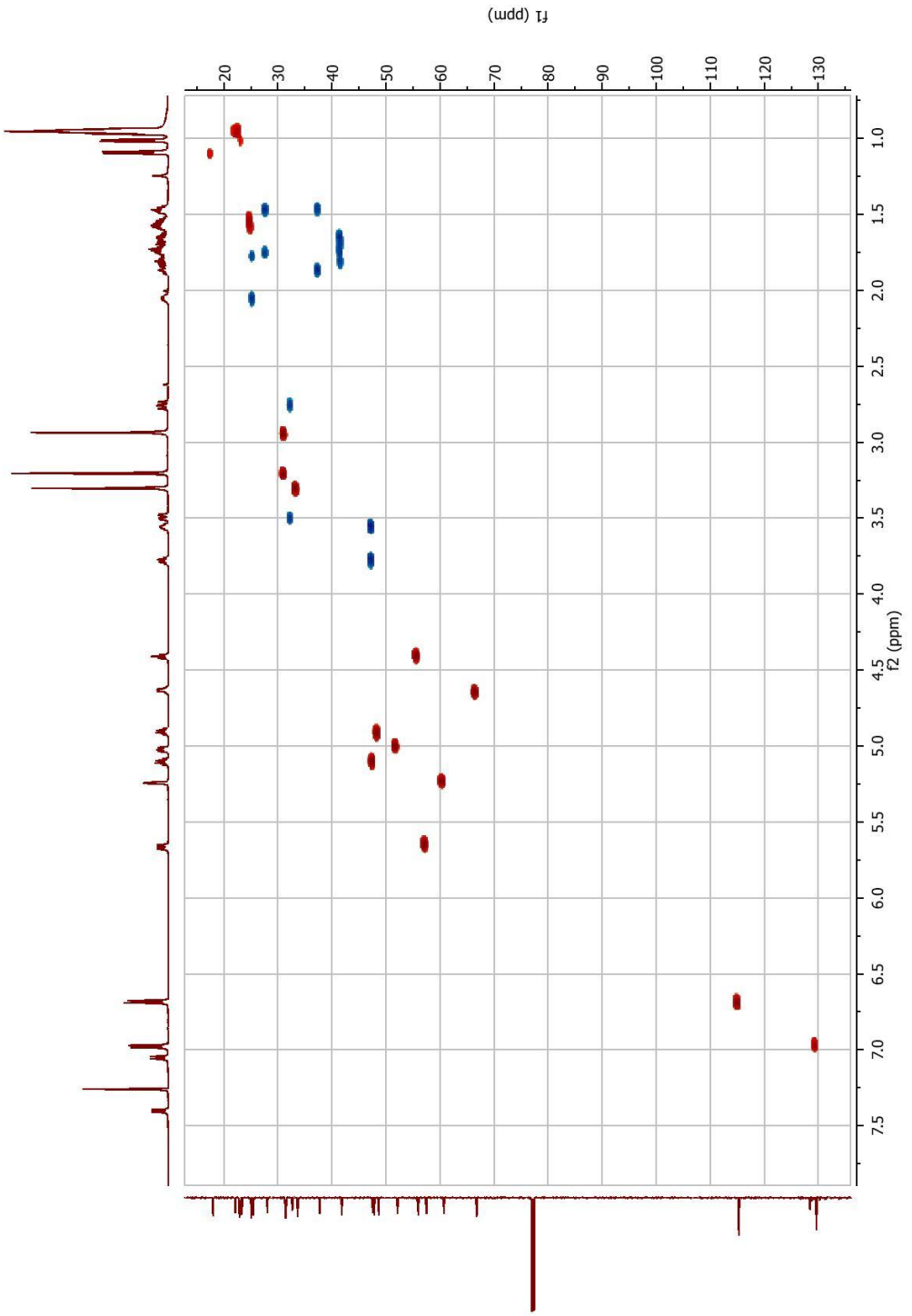
f1 (ppm)
20
30
40
50
60
70
80
90
100
110
120
130
f2 (ppm)
1.0
1.5
2.0
2.5
3.0
3.5
4.0
4.5
5.0
5.5
6.0
6.5
7.0
7.5

1 HMBC

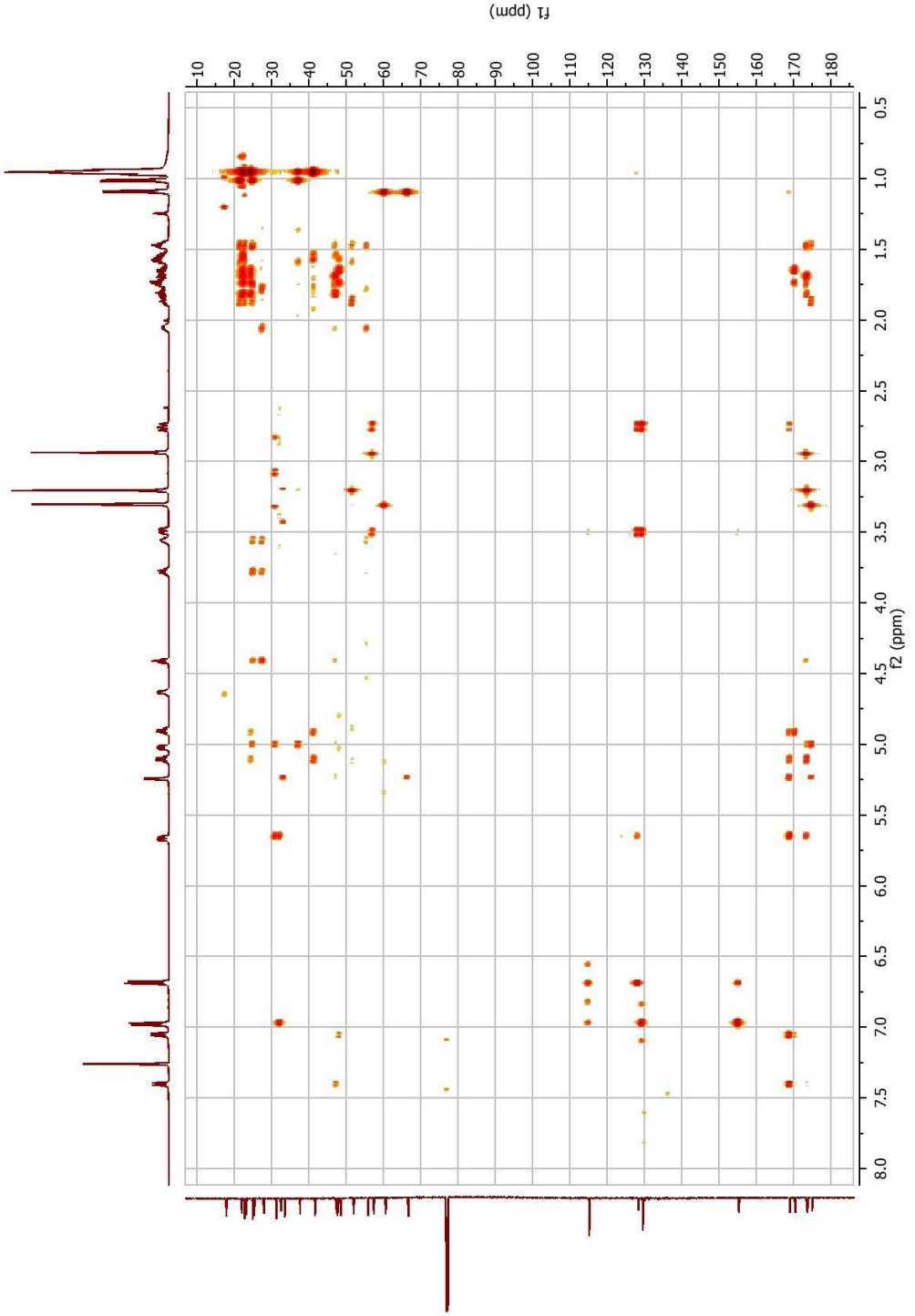

1 NOESY 600 ms 15°C

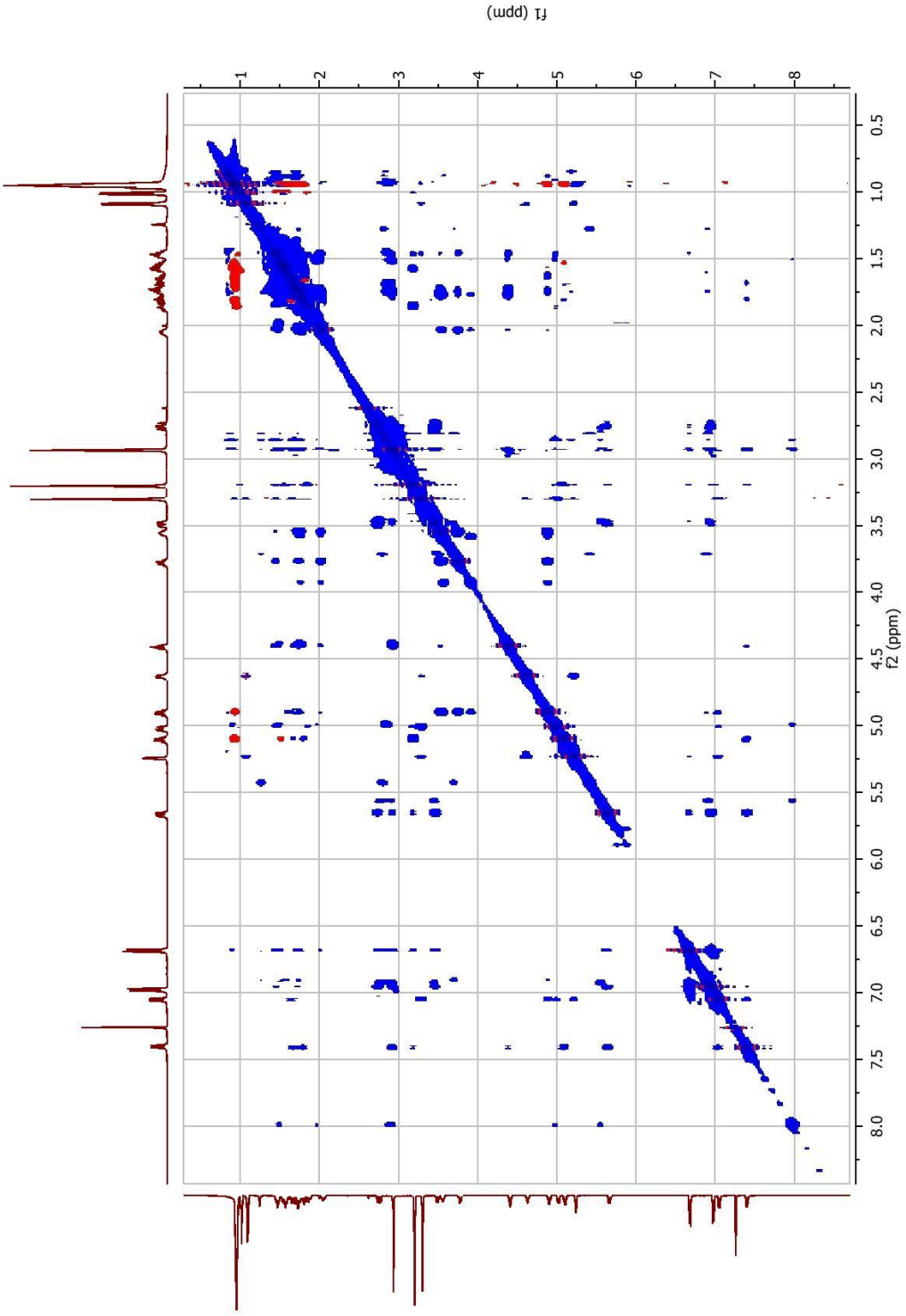

3 ^{1}H $CDCl_3$

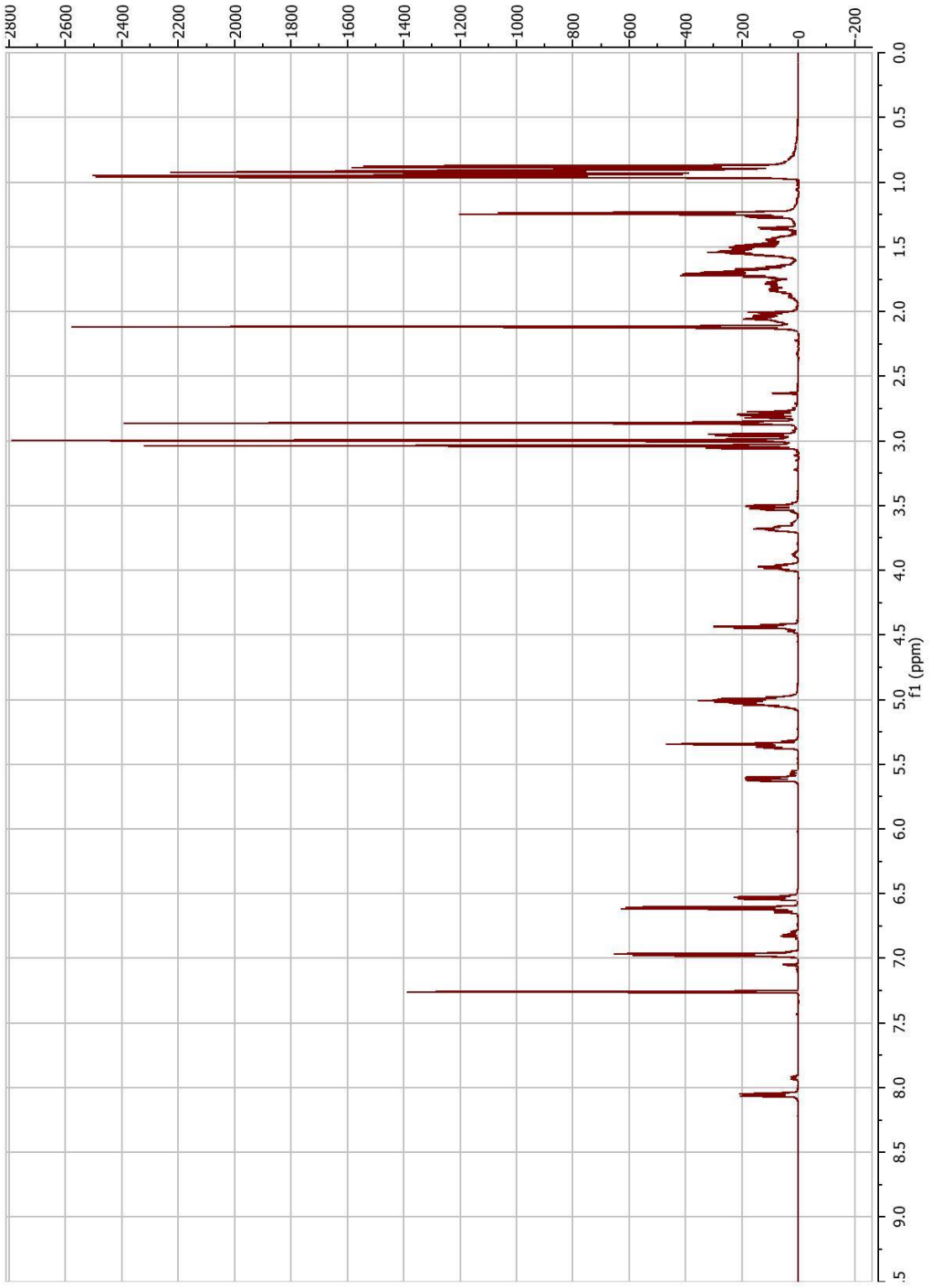

3 ^{13}C $CDCl_3$

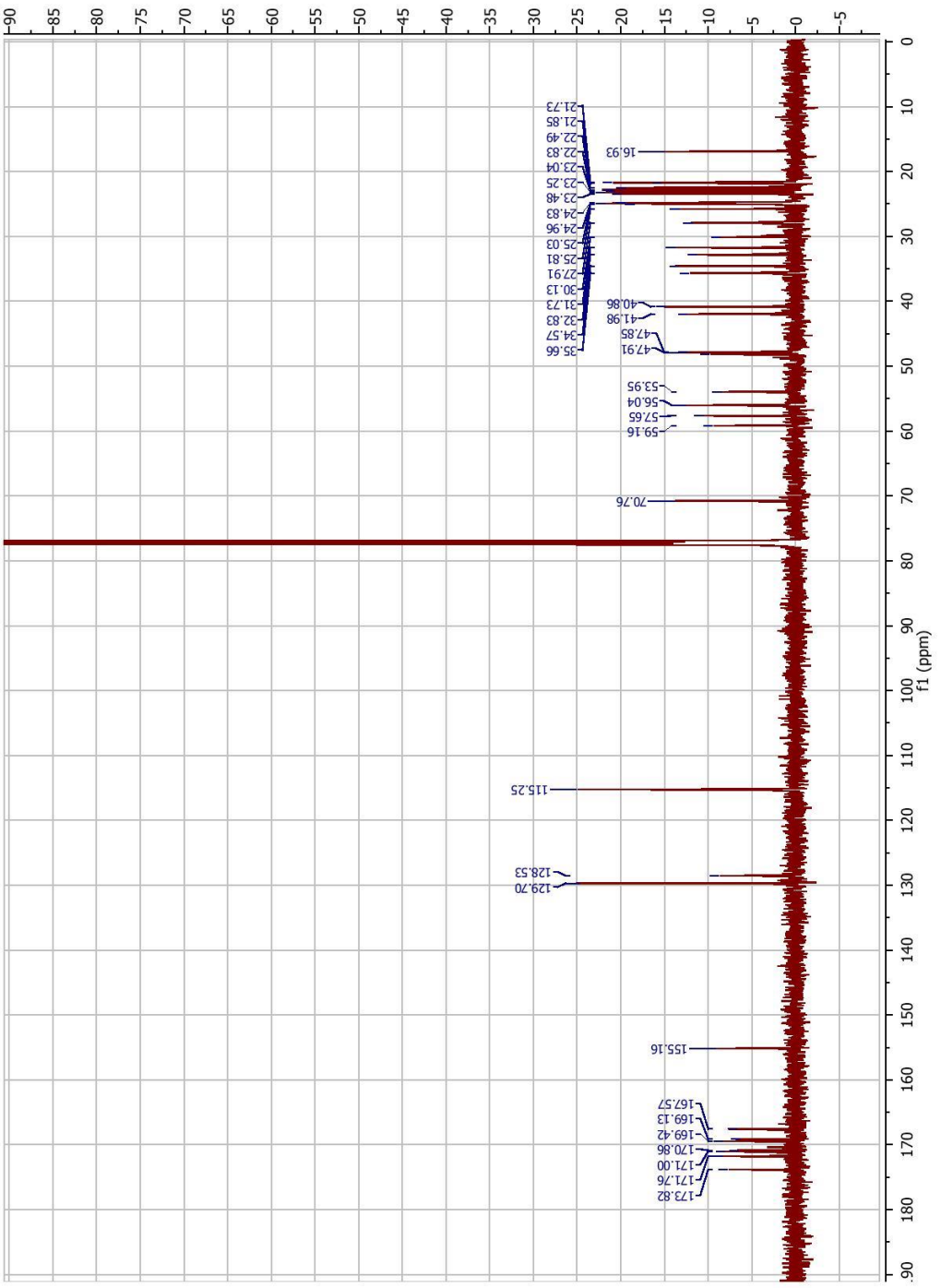
f1 (ppm)
173.82
171.76
171.00
170.86
169.42
169.13
167.57
155.16
129.70
128.53
115.25
70.76
59.16
57.65
56.04
53.95
47.91
47.85
41.98
40.86
35.66
34.57
32.83
31.73
30.13
27.91
25.81
25.03
24.96
24.83
23.48
23.25
23.04
22.83
22.49
21.85
21.73
16.93

3 COSY

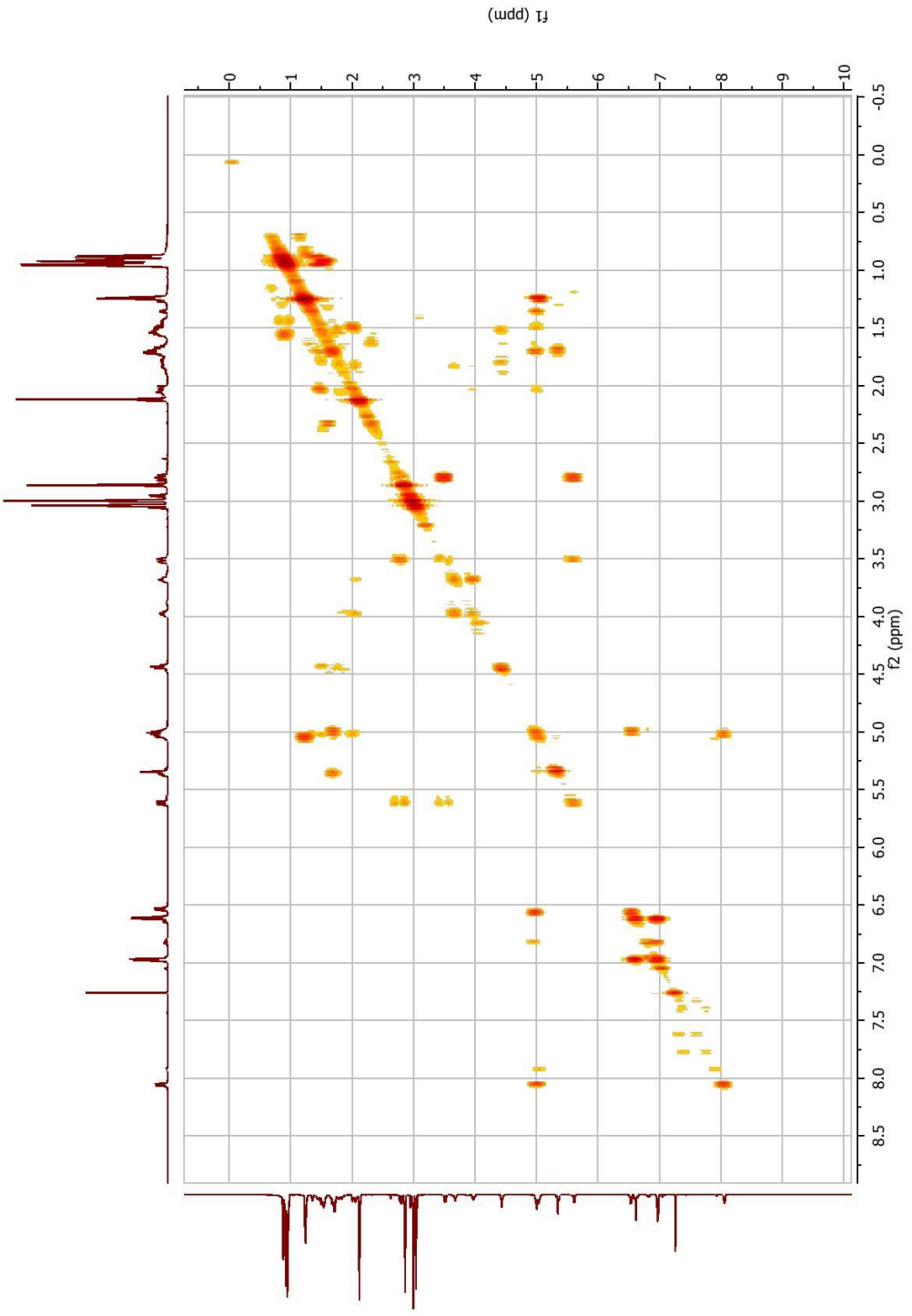

3TOCSY

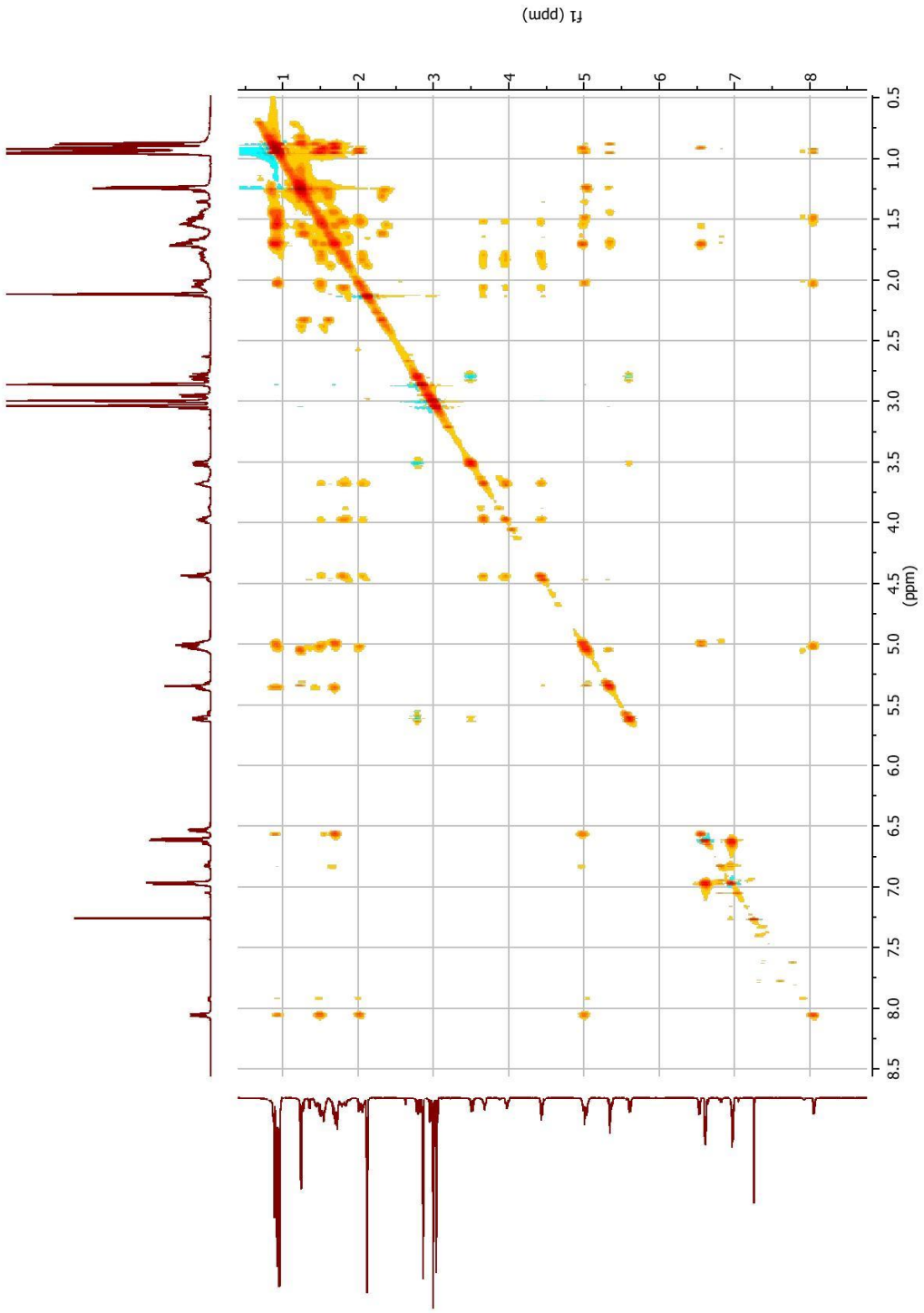
f1 (ppm)
1
2
3
4
5
6
7
8
0.5
1.0
1.5
2.0
2.5
3.0
3.5
4.0
4.5
5.0
5.5
6.0
6.5
7.0
7.5
8.0
8.5
(ppm)

3 HSQC

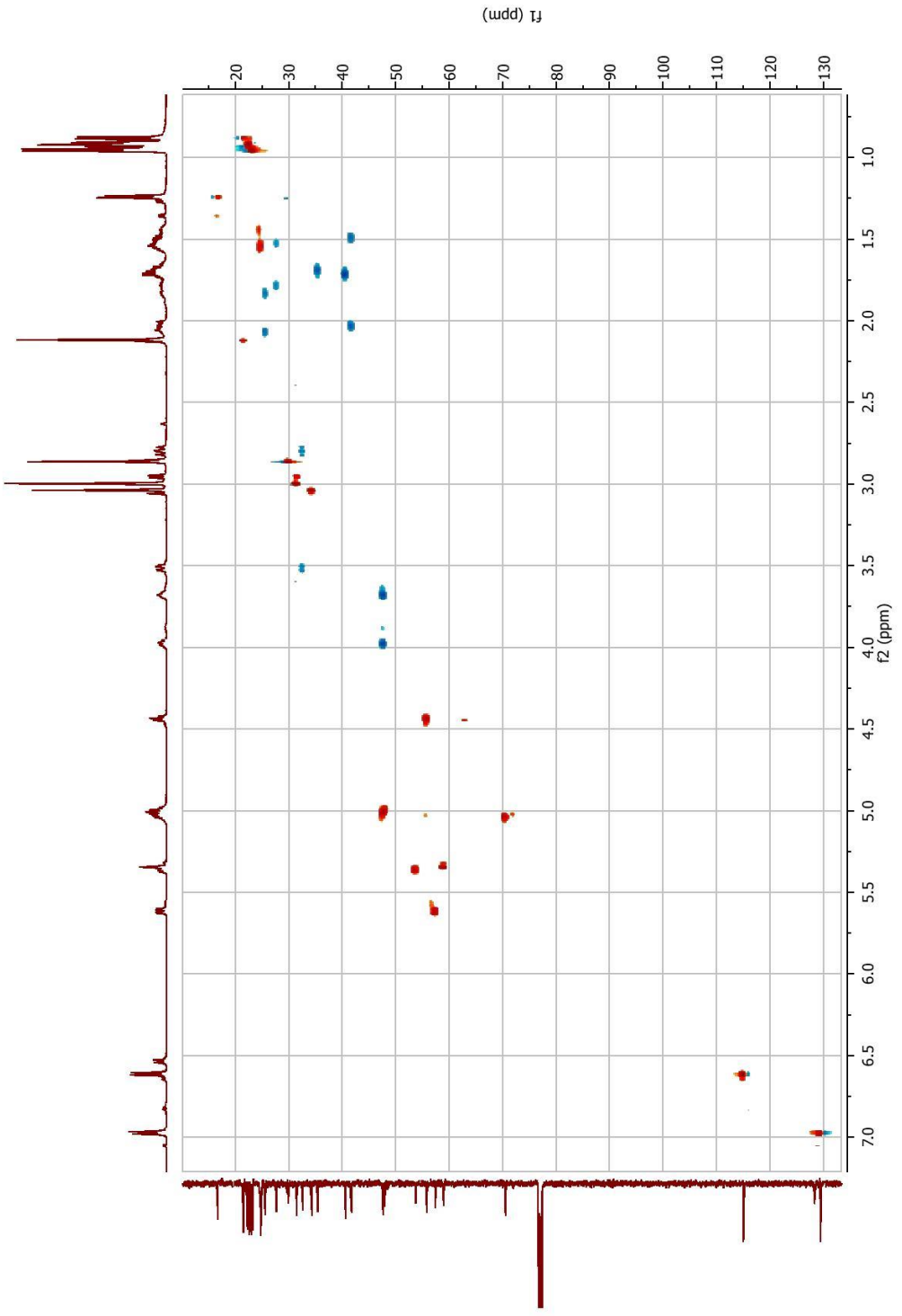
f1 (ppm)
20
30
40
50
60
70
80
90
100
110
120
130
1.0
1.5
2.0
2.5
3.0
3.5
4.0
4.5
5.0
5.5
6.0
6.5
7.0
f2 (ppm)

3 HMBC

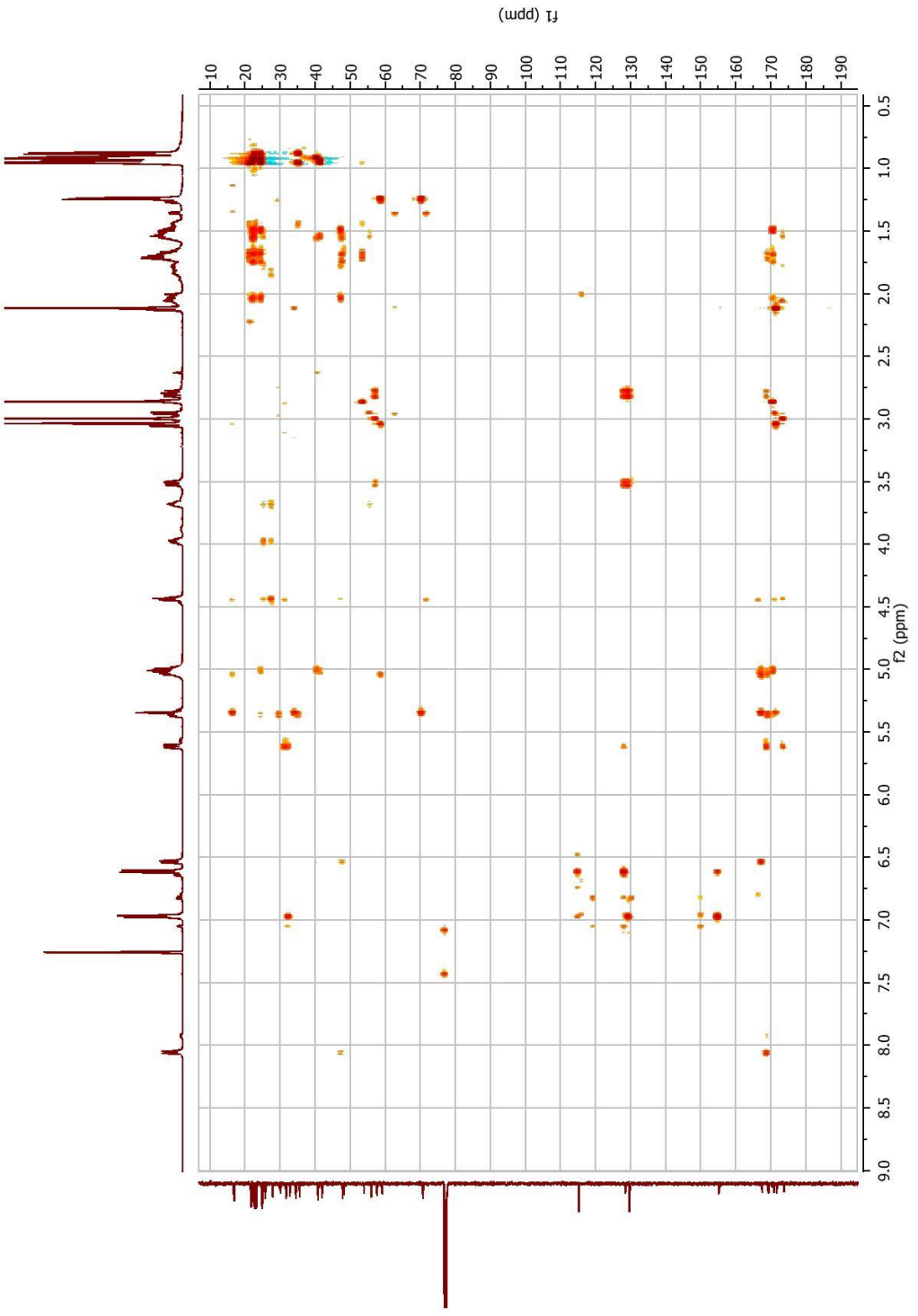

3 NOESY 600 ms 4°C

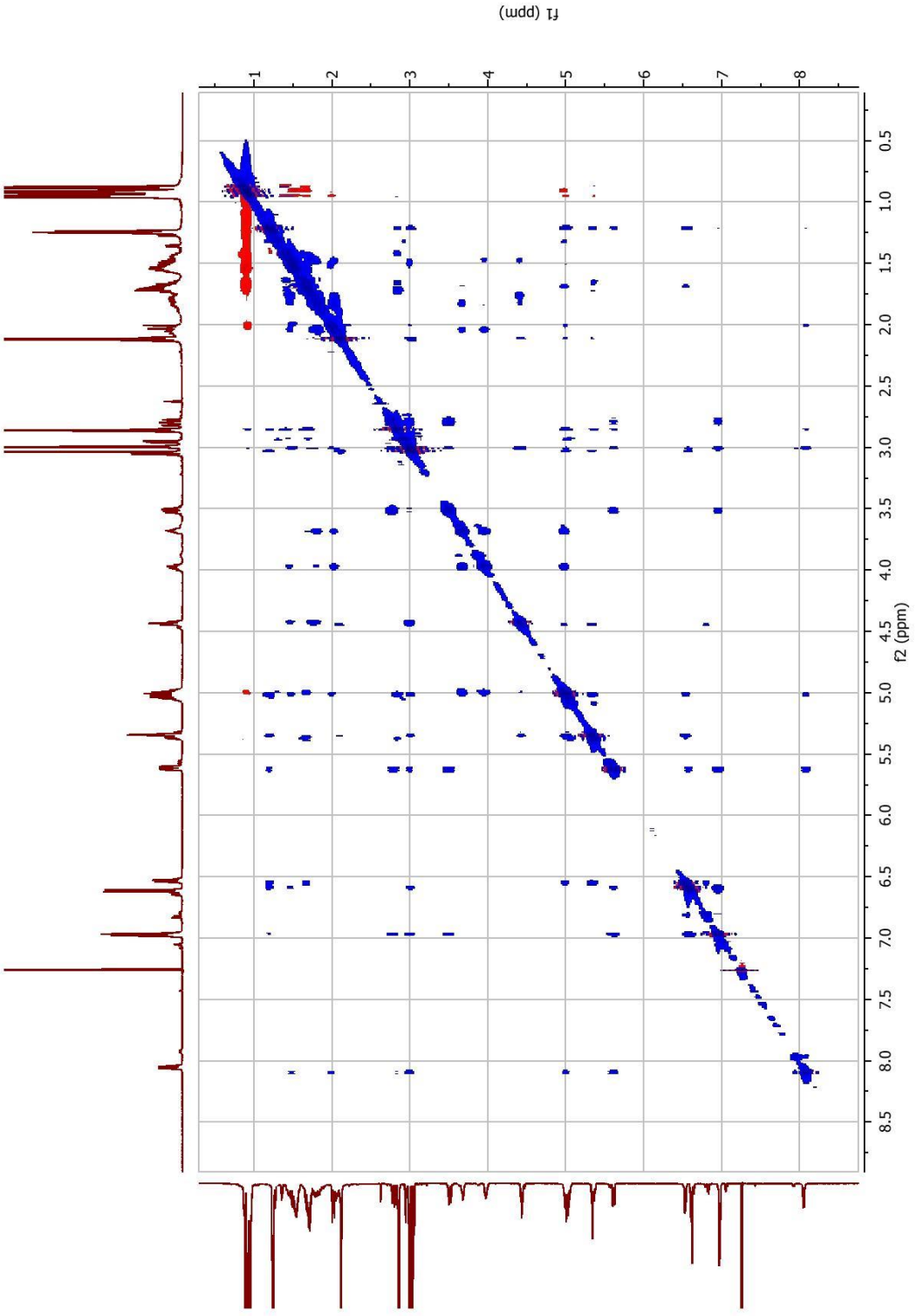

4 ^{1}H $CDCl_3$

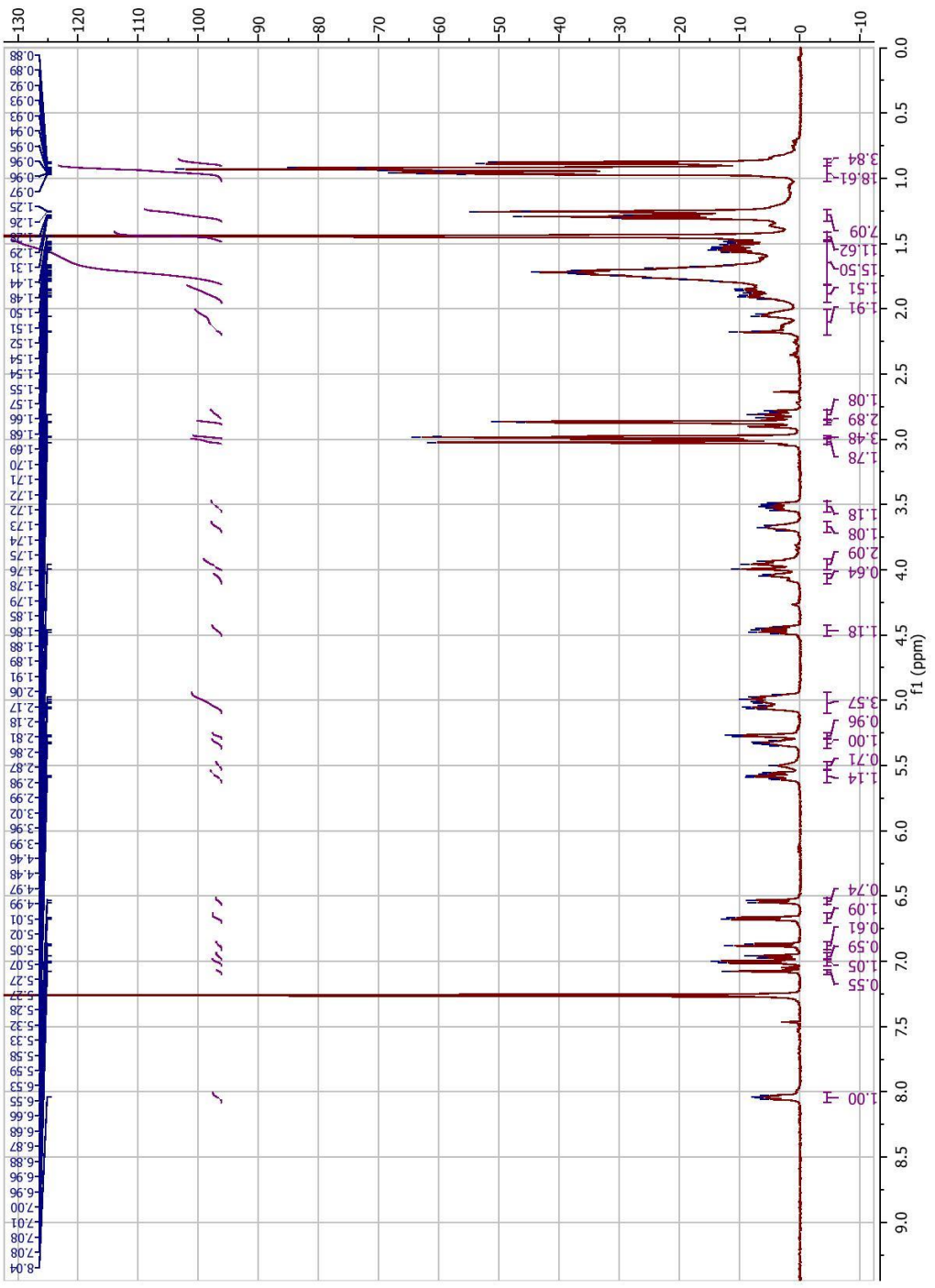

5 ^{1}H *d*6 Acetone 45°C

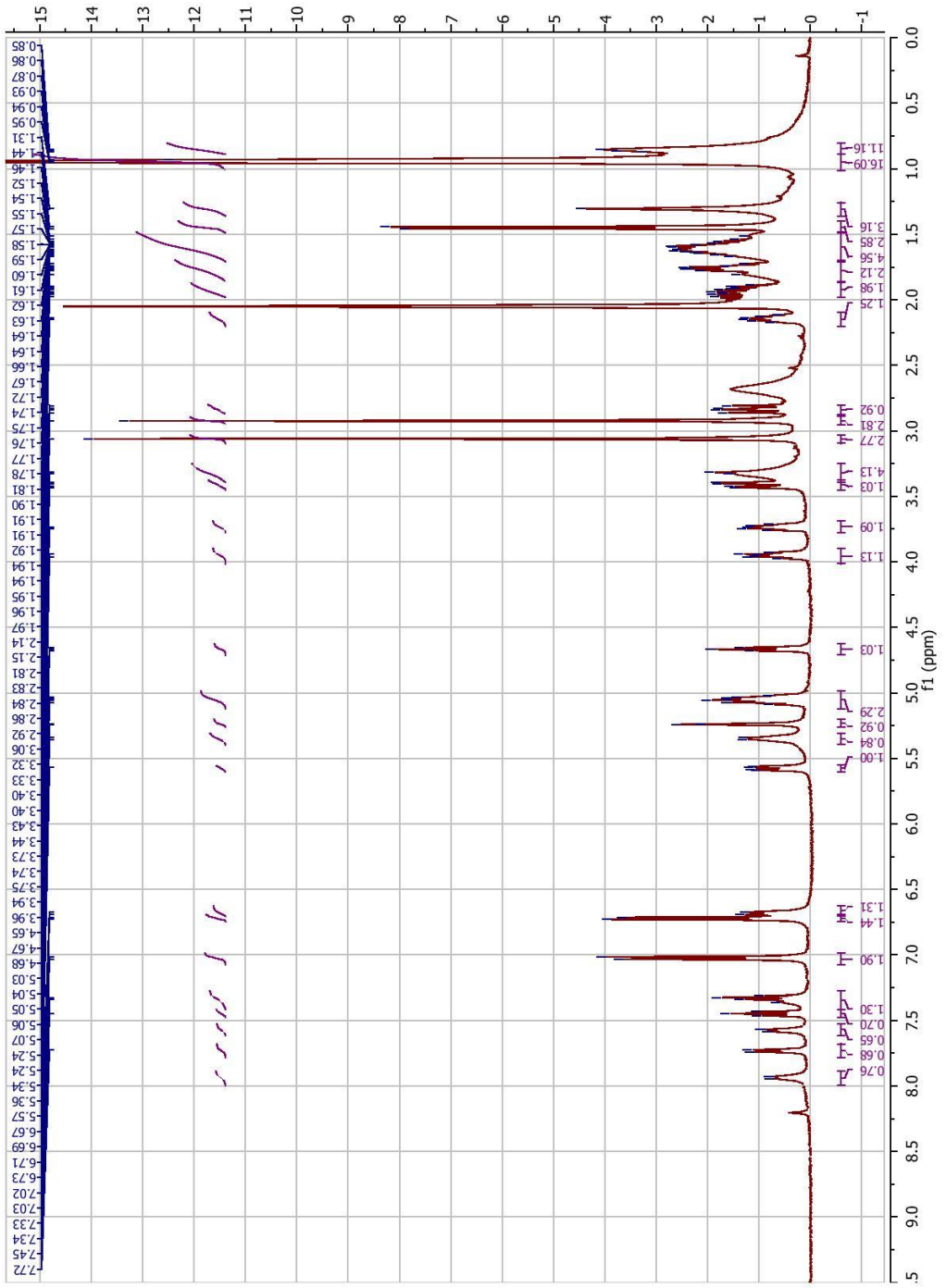

6 ^{1}H $CDCl_3$

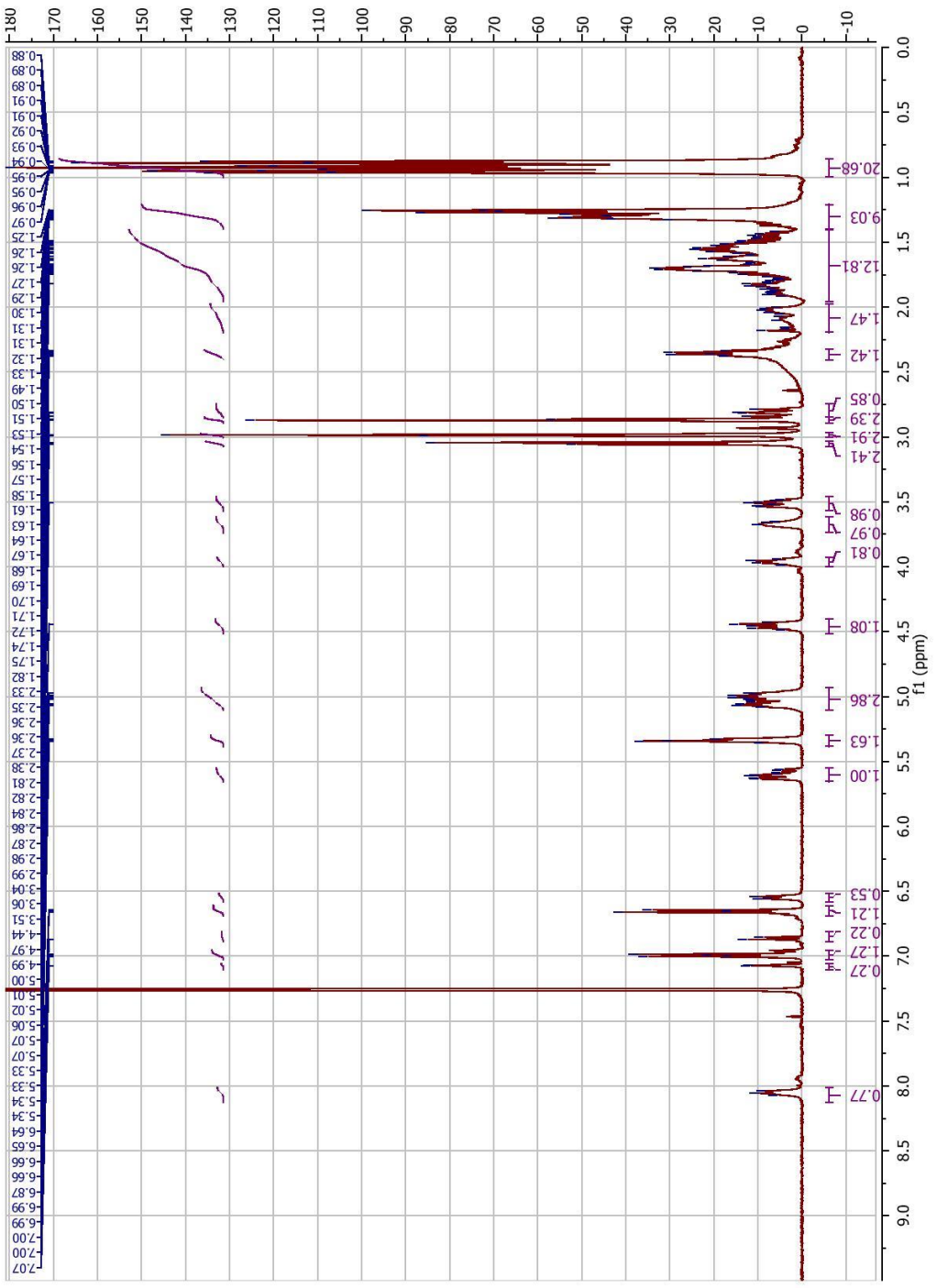

7 ^{1}H *d*3 Acetonitrile

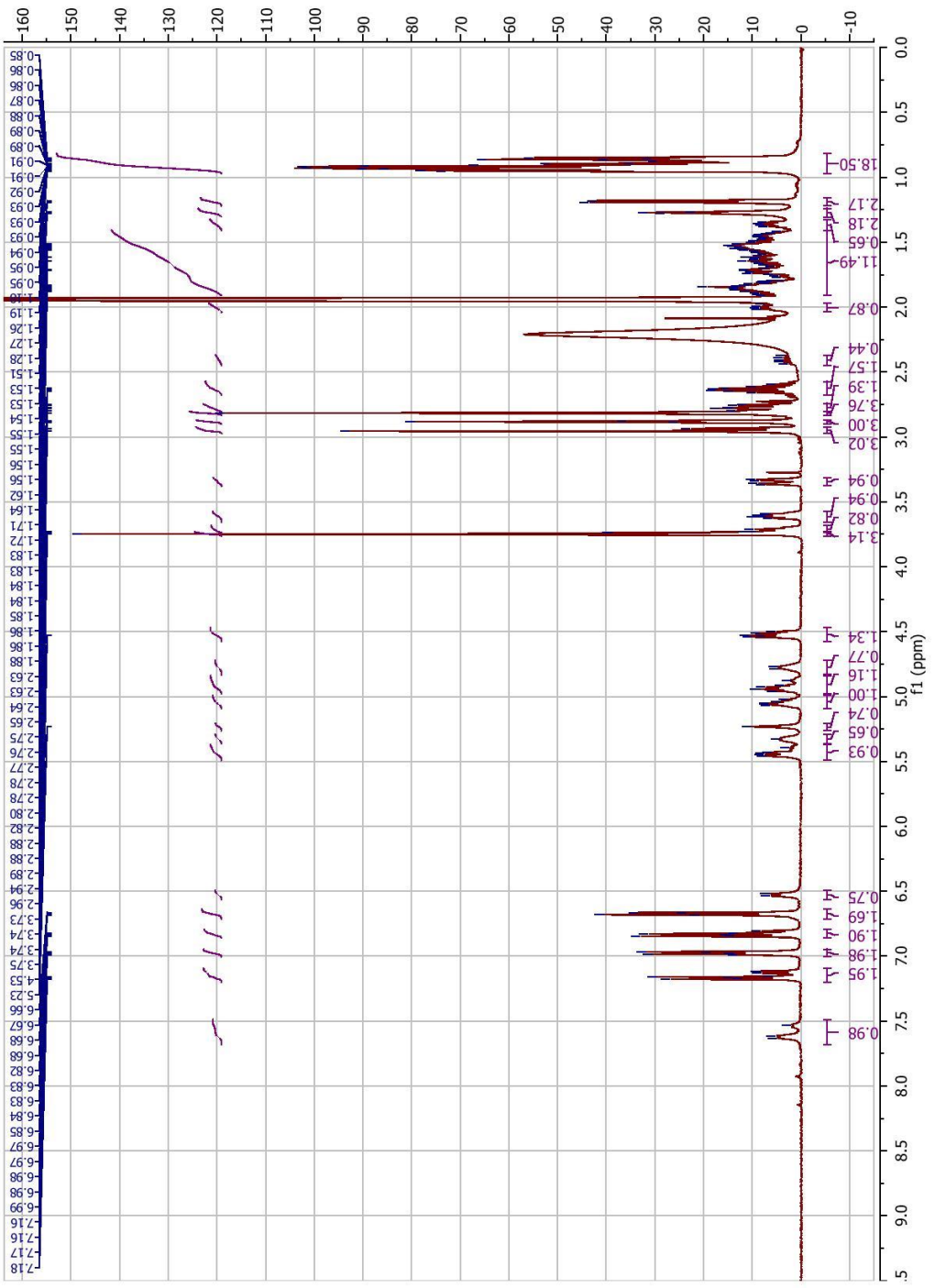

8 ^{1}H $CDCl_3$

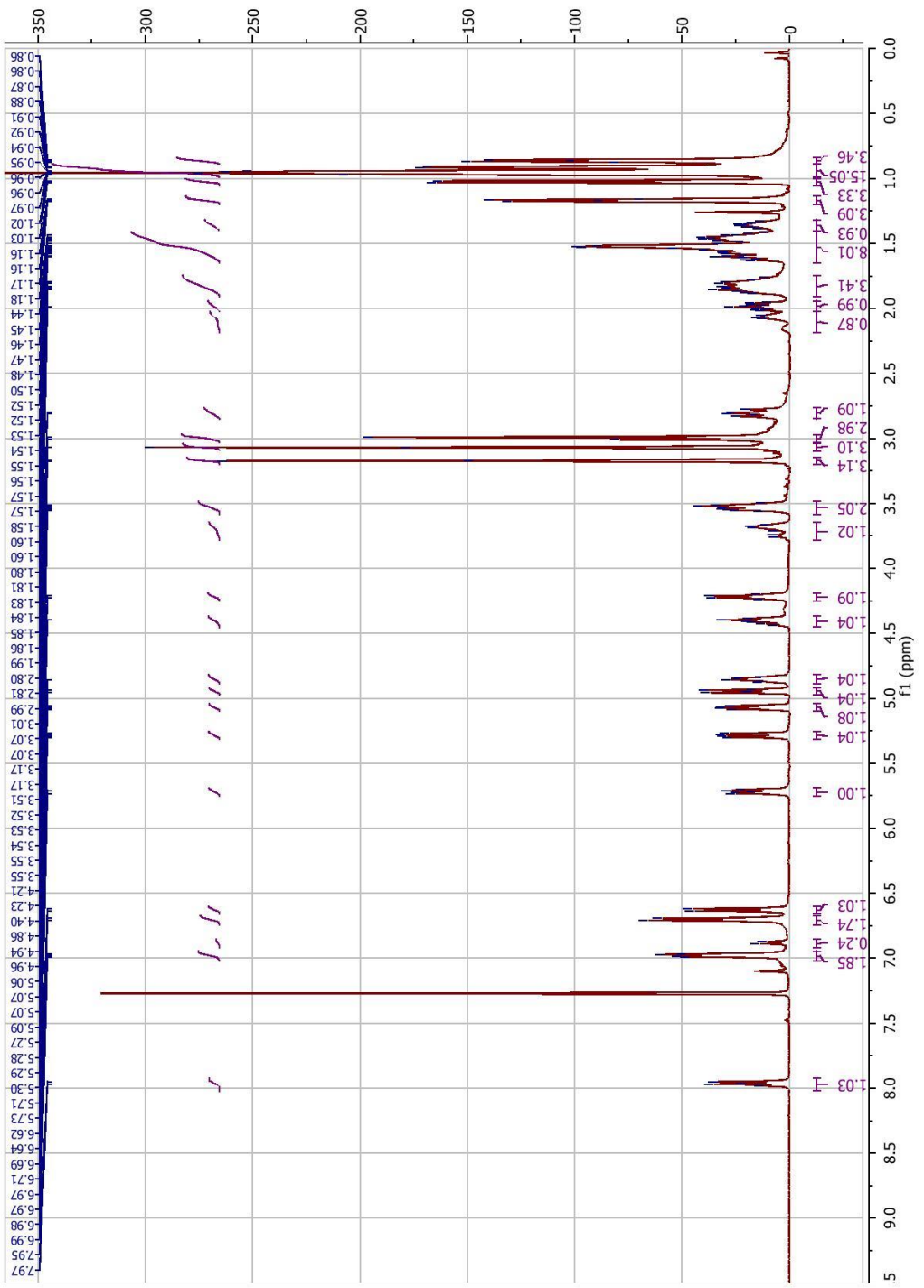

9 ^{1}H $CDCl_3$

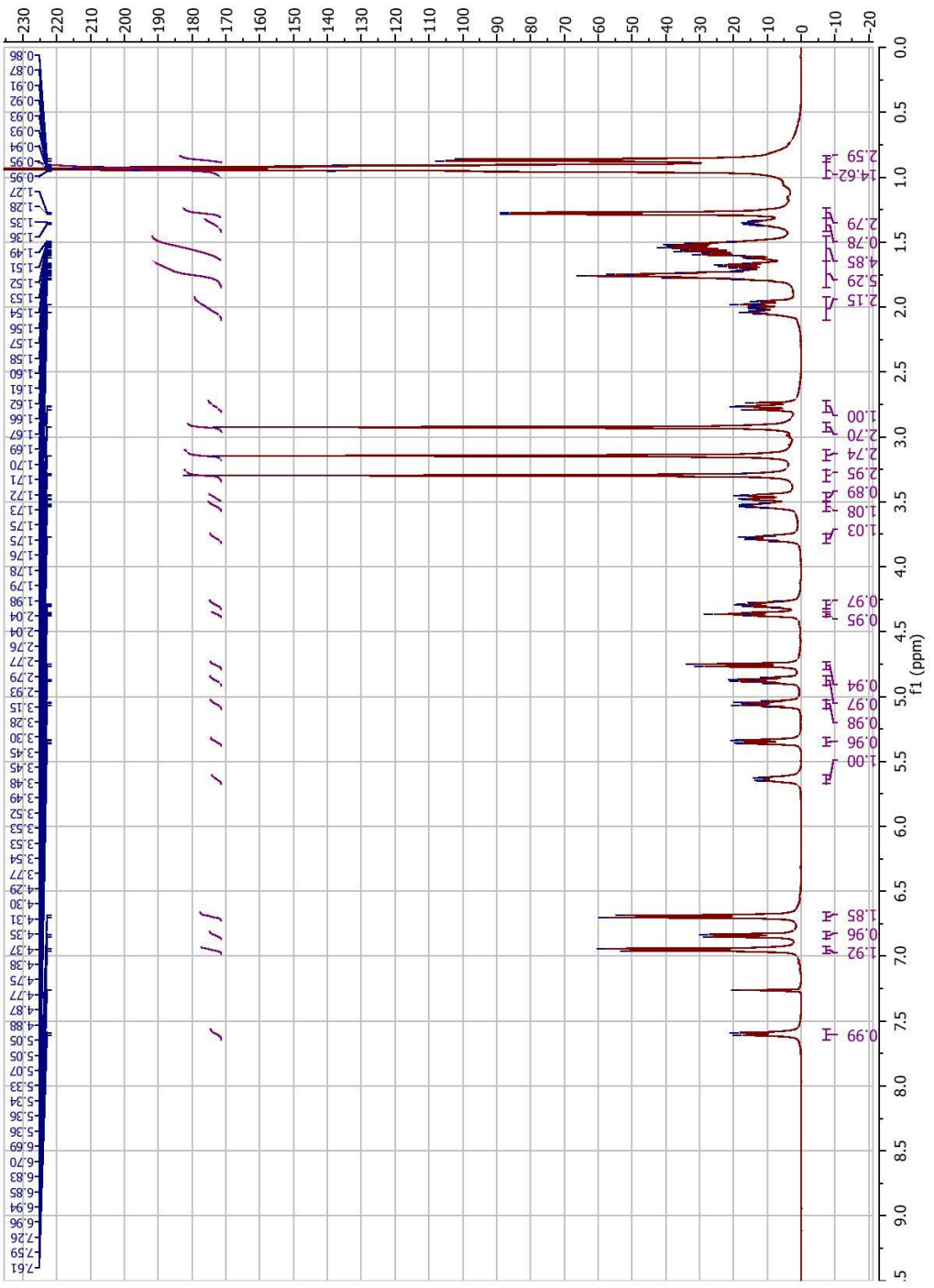

10 ^{1}H $CDCl_3$

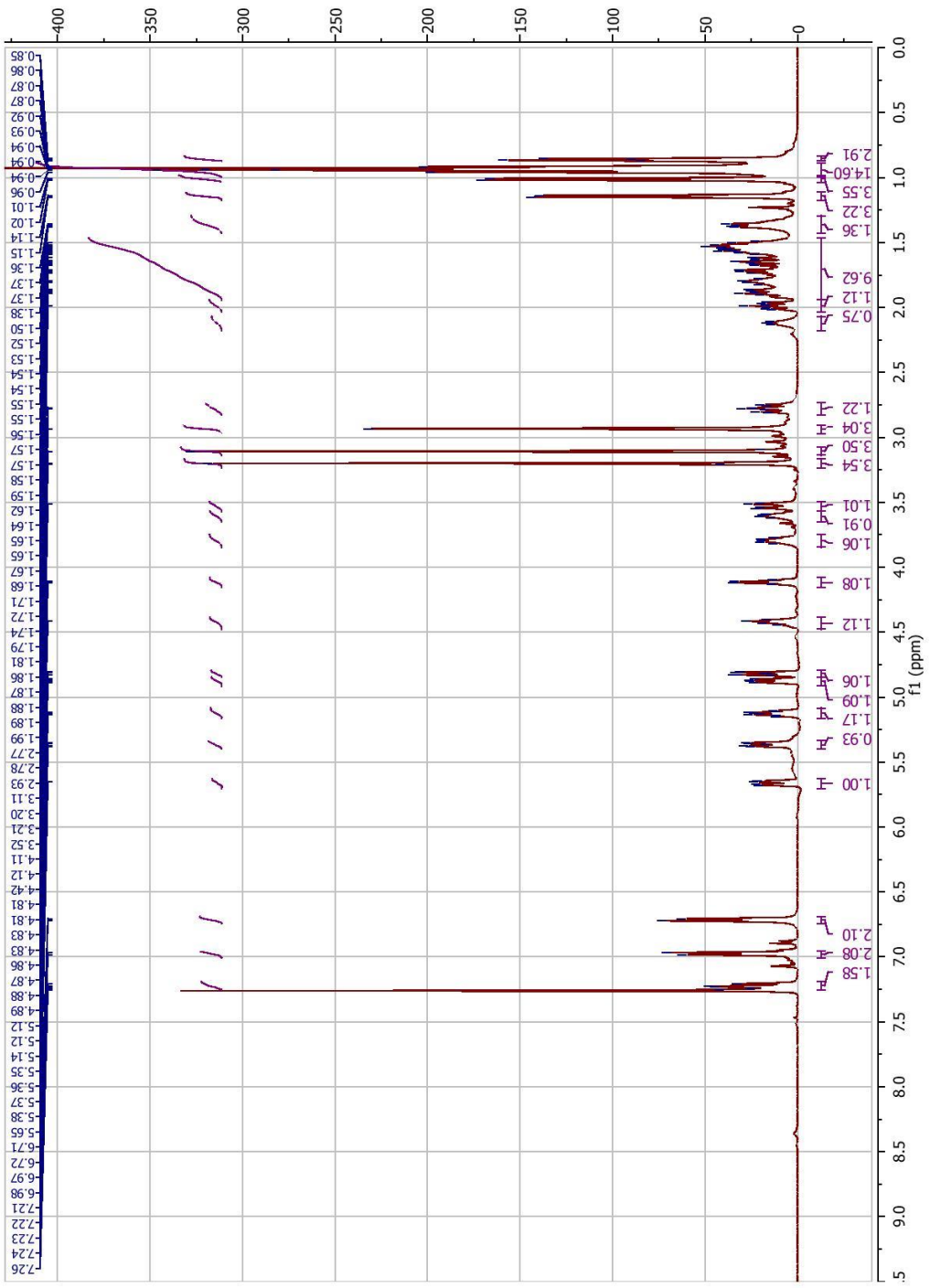

11 ^{1}H *d*6 DMSO

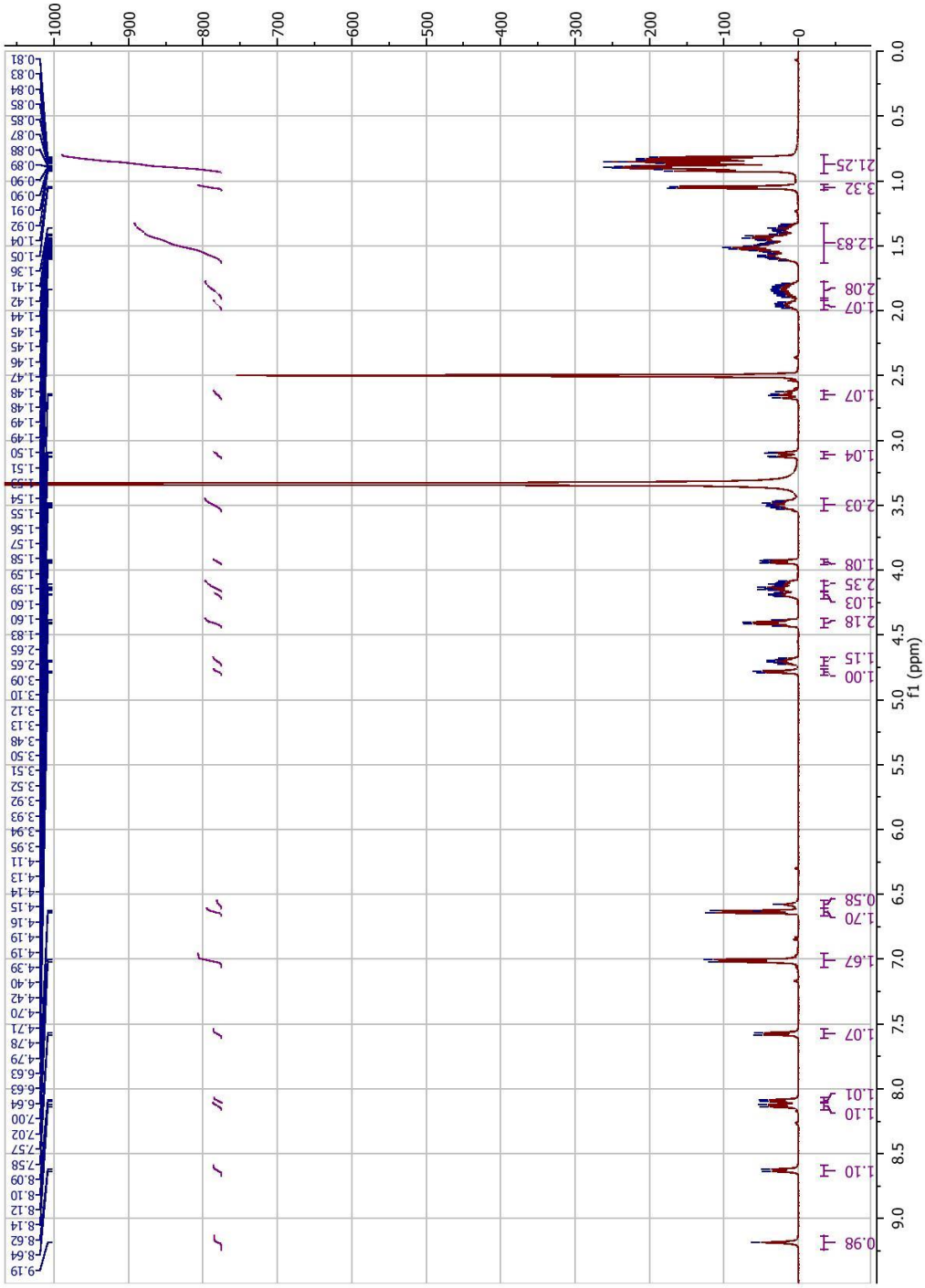

12 ^{1}H *d*6 DMSO

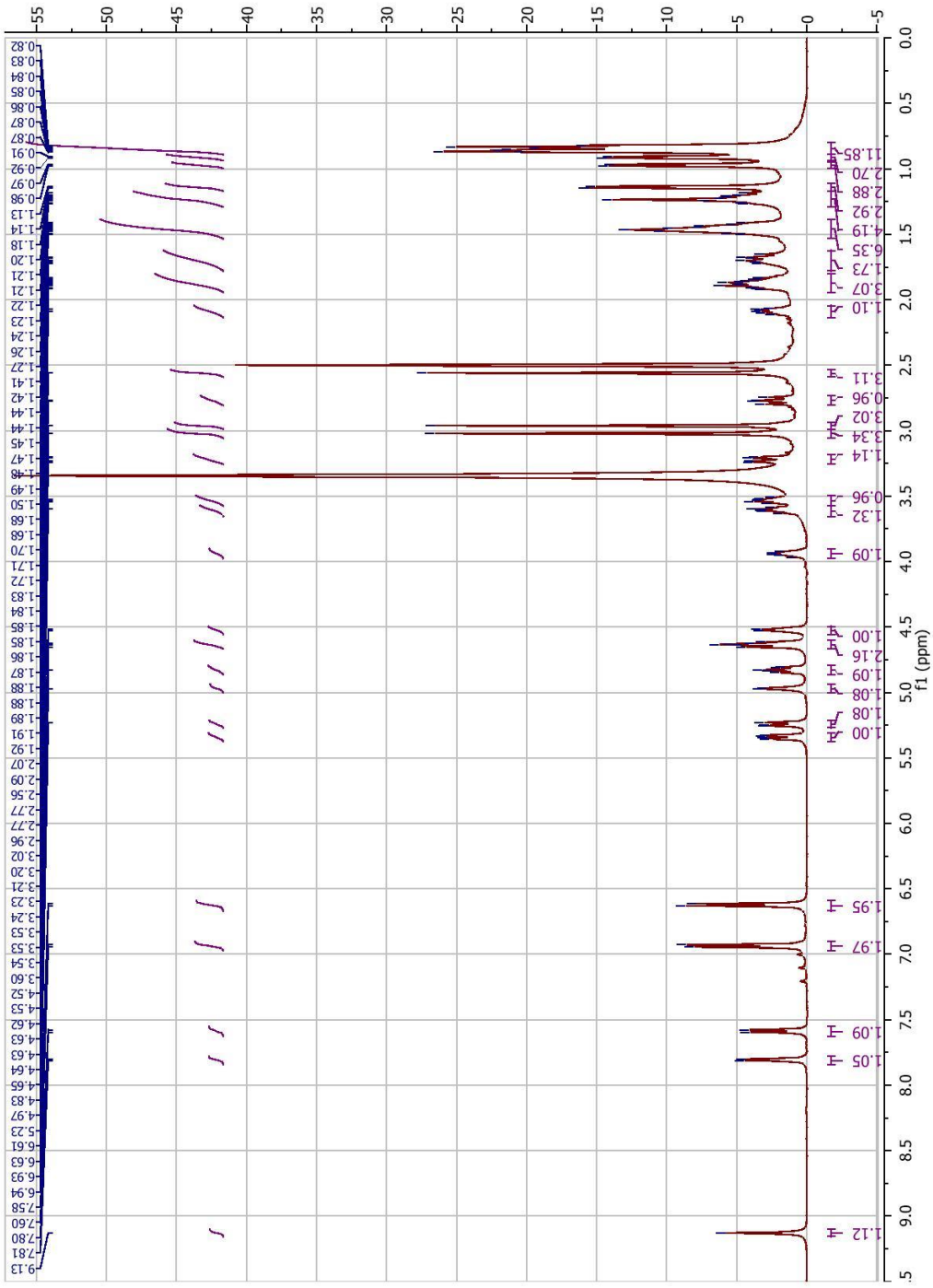

13 ^{1}H $CDCl_3$

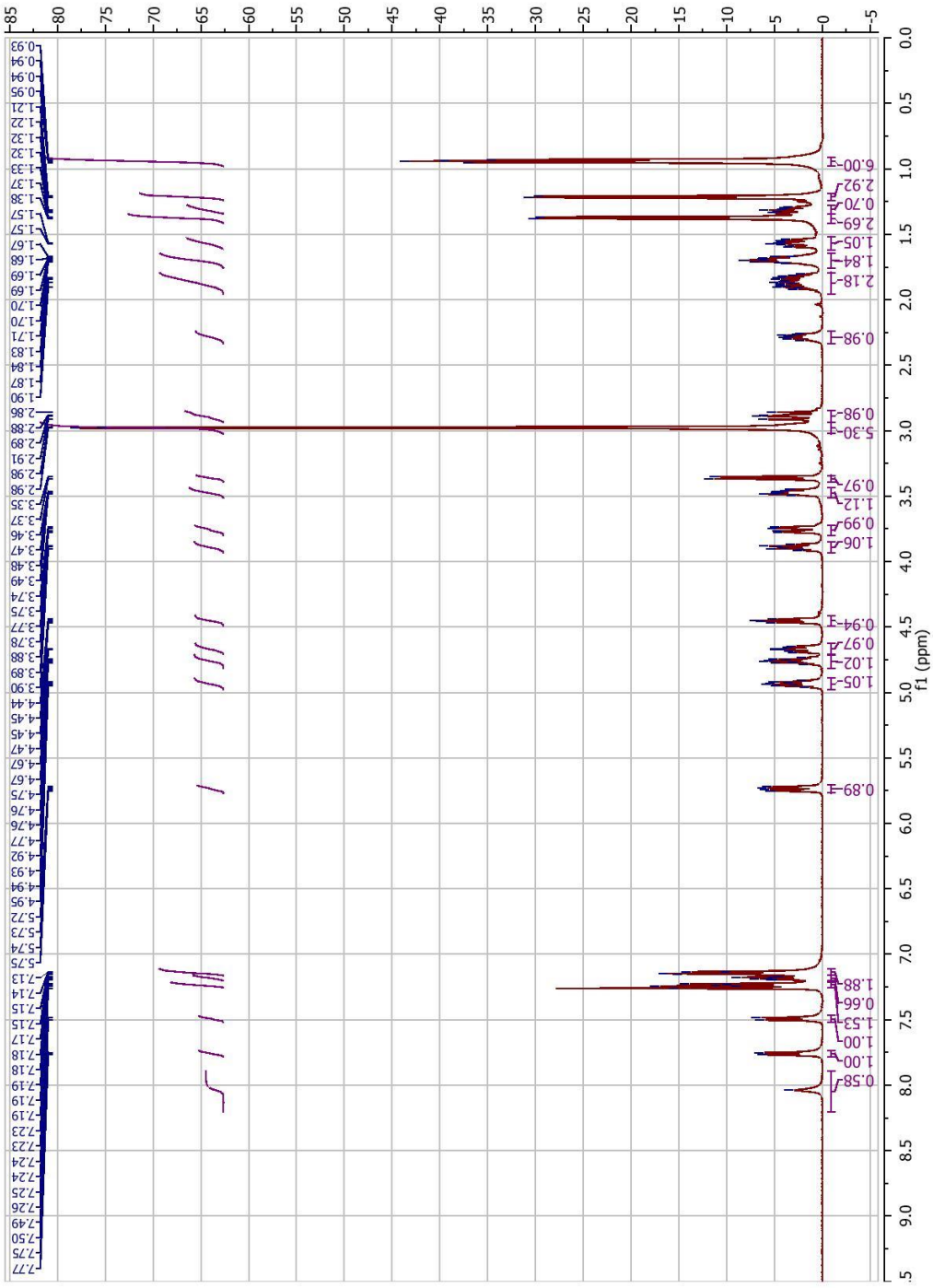

14 ^{1}H *d*6 acetonitrile

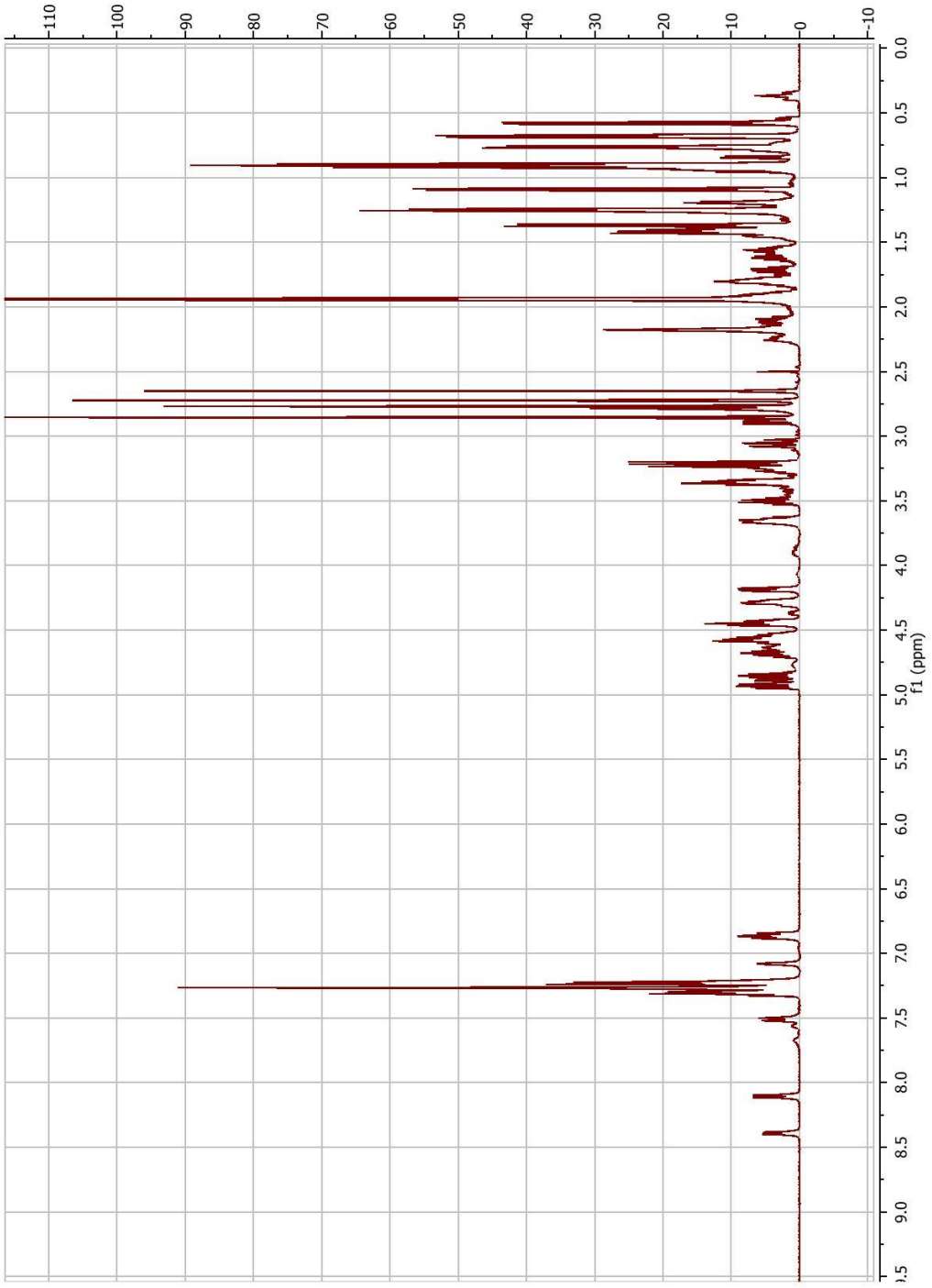

15 ^{1}H $CDCl_3$

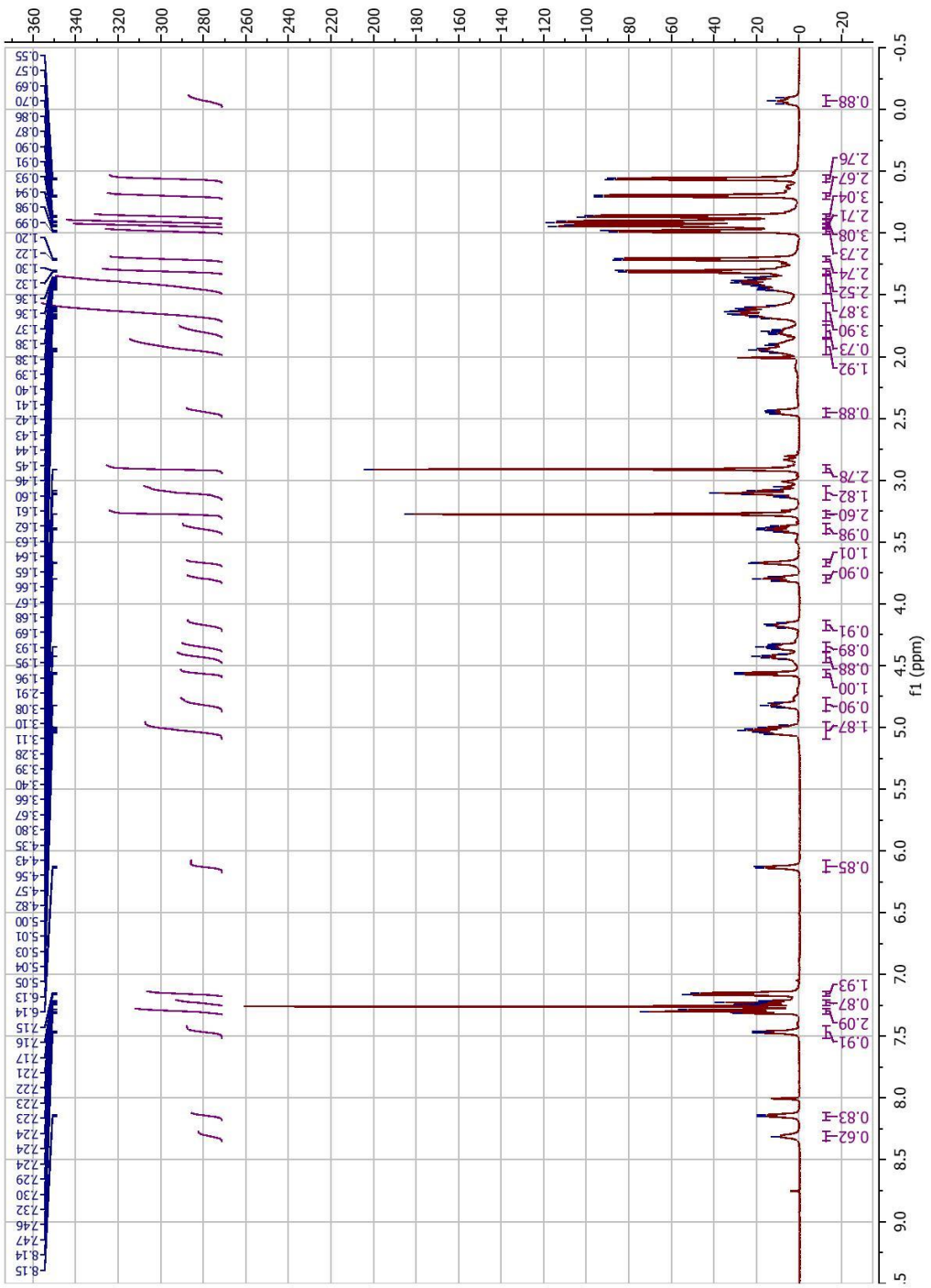

1.9. References

(1) Munoz-Alonso, M. J.; Gonzalez-Santiago, L.; Martinez, T.; Losada, A.; Galmarini, C. M.; Munoz, A. The Mechanism of Action of Plitidepsin. *Curr. Opin. Investig. Drugs* **2009**, *10* (6), 536–542.

(2) Wei, D. G.; Chiang, V.; Fyne, E.; Balakrishnan, M.; Barnes, T.; Graupe, M.; Hesselgesser, J.; Irrinki, A.; Murry, J. P.; Stepan, G.; Stray, K. M.; Tsai, A.; Yu, H.; Spindler, J.; Kearney, M.; Spina, C. A.; McMahon, D.; Lalezari, J.; Sloan, D.; Mellors, J.; Geleziunas, R.; Cihlar, T. Histone Deacetylase Inhibitor Romidepsin Induces HIV Expression in CD4 T Cells from Patients on Suppressive Antiretroviral Therapy at Concentrations Achieved by Clinical Dosing. *Plos Pathog.* **2014**, *10* (4).

(3) Tan, H. W.; Tay, S. T. The Inhibitory Effects of Aureobasidin A on Candida Planktonic and Biofilm Cells. *Mycoses* **2013**, *56* (2), 150–156.

(4) Westendorf, C.; Schmidt, A.; Coin, I.; Furkert, J.; Ridelis, I.; Zampatis, D.; Rutz, C.; Wiesner, B.; Rosenthal, W.; Beyermann, M.; Schuelein, R. Inhibition of Biosynthesis of Human Endothelin B Receptor by the Cyclodepsipeptide Cotransin. *J. Biol. Chem.* **2011**, *286* (41), 35588–35600.

(5) Jimenez, J. C.; Lopez-Macia, A.; Gracia, C.; Varon, S.; Carrascal, M.; Caba, J. M.; Royo, M.; Francesch, A. M.; Cuevas, C.; Giralt, E.; Albericio, F. Structure-Activity Relationship of Kahalalide F Synthetic Analogues. *J. Med. Chem.* **2008**, *51* (16), 4920–4931.

(6) Grundmann, F.; Kaiser, M.; Kurz, M.; Schiell, M.; Batzer, A.; Bode, H. B.

Structure Determination of the Bioactive Depsipeptide Xenobactin from Xenorhabdus Sp PB30.3. *Rsc Adv.* **2013**, *3* (44), 22072–22077.

(7) Capon, R. J.; Skene, C.; Stewart, M.; Ford, J.; O'Hair, R. A. J.; Williams, L.; Lacey, E.; Gill, J. H.; Heiland, K.; Friedel, T. Aspergillicins A-E: Five Novel Depsipeptides from the Marine-Derived Fungus Aspergillus Carneus. *Org. Biomol. Chem.* **2003**, *1* (11), 1856–1862.

(8) Okino, T.; Murakami, M.; Haraguchi, R.; Munekata, H.; Matsuda, H.; Yamaguchi, K. Micropeptins A and B, Plasmin and Trypsin Inhibitors from the Blue-Green Alga Microcystis Aeruginosa. *Tetrahedron Lett.* **1993**, *34* (50), 8131–8134.

(9) Pelay-Gimeno, M.; Tulla-Puche, J.; Albericio, F. "Head-to-Side-Chain" Cyclodepsipeptides of Marine Origin. *Mar. Drugs* **2013**, *11* (5), 1693–1717.

(10) Biron, E.; Chatterjee, J.; Ovadia, O.; Langenegger, D.; Brueggen, J.; Hoyer, D.; Schmid, H. A.; Jelinek, R.; Gilon, C.; Hoffman, A.; Kessler, H. Improving Oral Bioavailability of Peptides by Multiple N-Methylation: Somatostatin Analogues. *Angew. Chemie-International Ed.* **2008**, *47* (14), 2595–2599.

(11) Chatterjee, J.; Gilon, C.; Hoffman, A.; Kessler, H. N-Methylation of Peptides: A New Perspective in Medicinal Chemistry. *Acc. Chem. Res.* **2008**, *41* (10), 1331–1342.

(12) Chatterjee, J.; Mierke, D. F.; Kessler, H. Conformational Preference and Potential Templates of N-Methylated Cyclic Pentaalanine Peptides. *Chem. Eur. J.* **2008**, *14* (5), 1508–1517.

(13) White, T. R.; Renzelman, C. M.; Rand, A. C.; Rezai, T.; McEwen, C. M.; Gelev, V. M.; Turner, R. A.; Linington, R. G.; Leung, S. S. F.; Kalgutkar, A. S.; Bauman, J. N.; Zhang, Y.; Liras, S.; Price, D. A.; Mathiowetz, A. M.; Jacobson, M. P.; Lokey, R. S. On-Resin N-Methylation of Cyclic Peptides for Discovery of Orally Bioavailable Scaffolds. *Nat. Chem. Biol.* **2011**, *7* (11).

(14) Rand, A. C.; Leung, S. S. F.; Eng, H.; Rotter, C. J.; Sharma, R.; Kalgutkar, A. S.; Zhang, Y.; Varma, M. V; Farley, K. A.; Khunte, B.; Limberakis, C.; Price, D. A.; Liras, S.; Mathiowetz, A. M.; Jacobson, M. P.; Lokey, R. S. Optimizing PK Properties of Cyclic Peptides: The Effect of Side Chain Substitutions on Permeability and Clearance. *Medchemcomm* **2012**, *3* (10), 1282–1289.

(15) Raiford, L. C.; Couturn, J. R. The Migration of Acyl from Nitrogen to Oxygen. *J. Am. Chem. Soc.* **1922**, *44*, 1792–1798.

(16) Carpino, L. A.; Krause, E.; Sferdean, C. D.; Bienert, M.; Beyermann, M. Dramatically Enhanced N→O Acyl Migration during the Trifluoroacetic Acid-Based Deprotection Step in Solid Phase Peptide Synthesis. *Tetrahedron Lett.* **2005**, *46* (8), 1361–1364.

(17) Skwarczynski, M.; Kiso, Y. Application of the O-N Intramolecular Acyl Migration Reaction in Medicinal Chemistry. *Curr Med Chem* **2007**, *14* (26), 2813–2823.

(18) Oliyai, R.; Stella, V. J. Kinetics and Mechanism of Isomerization of Cyclosporin A. *Pharm Res* **1992**, *9* (5), 617–622.

(19) Driggers, E. M.; Hale, S. P.; Lee, J.; Terrett, N. K. The Exploration of

Macrocycles for Drug Discovery - an Underexploited Structural Class. *Nat. Rev. Drug Discov.* **2008**, *7* (7), 608–624.

(20) Peypoux, F.; Bonmatin, J. M.; Wallach, J. Recent Trends in the Biochemistry of Surfactin. *Appl. Microbiol. Biotechnol.* **1999**, *51* (5), 553–563.

(21) Turner, R. A.; Hauksson, N. E.; Gipe, J. H.; Lokey, R. S. Selective, On-Resin N-Methylation of Peptide N-Trifluoroacetamides. *Org. Lett.* **2013**, *15* (19), 5012–5015.

(22) Biron, E.; Kessler, H. Convenient Synthesis of N-Methylamino Acids Compatible with Fmoc Solid-Phase Peptide Synthesis. *J. Org. Chem.* **2005**, *70* (13), 5183–5189.

(23) Burgi, H. B.; Dunitz, J. D.; Lehn, J. M.; Wipff, G. Stereochemistry of Reaction Paths at Carbonyl Centres. *Tetrahedron* **1974**, *30* (12), 1563–1572.

(24) Cicero, D. O.; Barbato, G.; Bazzo, R. Nmr Analysis of Molecular Flexibility in Solution - a New Method for the Study of Complex Distributions of Rapidly Exchanging Conformations - Application to a 13-Residue Peptide with an 8-Residue Loop. *J. Am. Chem. Soc.* **1995**, *117* (3), 1027–1033.

(25) Atasoylu, O.; Furst, G.; Risatti, C.; Smith III, A. B. The Solution Structure of (+)-Spongistatin 1 in DMSO. *Org. Lett.* **2010**, *12* (8), 1788–1791.

(26) Evans, D. A.; Bodkin, M. J.; Baker, S. R.; Sharman, G. J. Janocchio - a Java Applet for Viewing 3D Structures and Calculating NMR Couplings and NOEs. *Magn. Reson. Chem.* **2007**, *45* (7), 595–600.

(27) Knipp, G. T.; Vander Velde, D. G.; Siahaan, T. J.; Borchardt, R. T. The Effect

of Beta-Turn Structure on the Passive Diffusion of Peptides across Caco-2 Cell Monolayers. *Pharm. Res.* **1997**, *14*, 1332–1340.

(28) Goetz, G. H.; Philippe, L.; Shapiro, M. J. EPSA: A Novel Supercritical Fluid Chromatography Technique Enabling the Design of Permeable Cyclic Peptides. *ACS Med. Chem. Lett.* **2014**, *5* (10), 1167–1172.

(29) Guimaraes, C. R. W.; Mathiowetz, A. M.; Shalaeva, M.; Goetz, G.; Liras, S. Use of 3D Properties to Characterize Beyond Rule-of-5 Property Space for Passive Permeation. *J. Chem. Inf. Model.* **2012**, *52* (4), 882–890.

(30) Mauger, A. B.; Stuart, O. A. Synthesis of an Actinomycin-Related Peptide Lactone from the Corresponding Cyclic Pentapeptide by N,O-Acyl Shift. *Int. J. Pept. Protein Res.* **1989**, *34* (3), 196–199.

(31) Callegari, E.; Malhotra, B.; Bungay, P. J.; Webster, R.; Fenner, K. S.; Kempshall, S.; LaPerle, J. L.; Michel, M. C.; Kay, G. G. A Comprehensive Non-Clinical Evaluation of the CNS Penetration Potential of Antimuscarinic Agents for the Treatment of Overactive Bladder. *Br. J. Clin. Pharmacol.* **2011**, *72* (2), 235–246.

(32) Phillips, J. C.; Braun, R.; Wang, W.; Gumbart, J.; Tajkhorshid, E.; Villa, E.; Chipot, C.; Skeel, R. D.; Kale, L.; Schulten, K. Scalable Molecular Dynamics with NAMD. *J. Comput. Chem.* **2005**, *26* (16), 1781–1802.

2. INVESTIGATION OF PEPTOID SUBSTITUTIONS IN 1NME3: ADME AND CONFORMATIONAL CONSEQUENCES

2.1. Foreword

This chapter contains text and figures from the following manuscript.

Schwochert, J.; Turner, R.; Thang, M.; Berkeley, R. F.; Ponkey, A. R.; Rodriguez, K. M.; Leung, S. S. F.; Khunte, B.; Goetz, G.; Limberakis, C.; Kalgutkar, A. S.; Eng, H.; Shapiro, M. J.; Mathiowetz, A. M.; Price, D. A.; Liras, S.; Jacobson, M. P.; Lokey, R. S. Peptide to Peptoid Substitutions Increase Cell Permeability in Cyclic Hexapeptides. *Org. Lett.* **2015**, 17 (12), 2928–2931.

The work was completed as a collaboration between all authors, though I prepared the manuscript, performed most the spectroscopic analysis, and synthesized some compounds. Rushia Turner initially conceived of the project and performed or oversaw most the synthesis. The undergraduates Melissa Thang, Ray Berkeley, Alexandra Ponkey, and Kelsie Rodriguez helped with synthesis. The team at Pfizer conducted ADME assays and helped with analysis.

2.2. Introduction

2.2.1. Preamble

As drug discovery efforts increasingly focus on challenging intracellular targets such as protein-protein interactions (PPIs) and other types of relatively “flat” binding sites,

finding highly potent inhibitors among classically drug-like molecules has become increasingly challenging[1,2]. Macrocycles occupy a middle ground in chemical space between biologics and typical small molecule drugs, with the complexity (and potential for binding flat surfaces) approaching that of the former, and the potential for cell permeability and oral bioavailability of the latter.[3–7] Their modular synthesis, combined with the favorable impact of macrocyclization on metabolic stability and cell permeability, make cyclic peptides ideal macrocyclic scaffolds for exploring this "middle chemical space". Furthermore, one-bead-one-compound (OBOC), DNA-encoded and DNA-programmed synthesis methodologies allow large (10^5) to very large (10^{12}) libraries of cyclic peptides to be generated and screened[8–10], while structural diversity and complexity can be achieved by permuting backbone elements such as stereochemistry[11] and backbone N-methylation[12], variables that can be modulated at the monomer level. Although solid phase peptide synthesis (SPPS) has been thoroughly developed since its first implementation over 50 years ago[13], achieving side chain diversity in peptide libraries requires access to diverse amino acid building blocks, of which relatively few are commercially available.

2.2.2. Peptoids as Modular Building Blocks

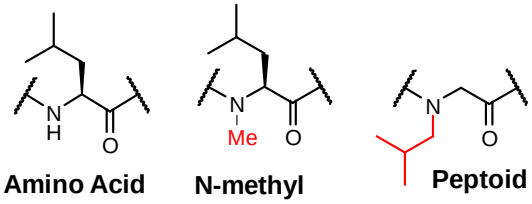

Figure 2-1 Structural Elements of Peptoids

Oligomers of N-substituted glycine units ("peptoids", Figure 2-1) were originally conceived as synthetic peptide derivatives that possess the modularity and protein binding characteristics of peptides, but avoid the pitfalls associated with the notoriously poor metabolic stability of peptides. Since then, peptoids have found a number of uses including metal chelation[14], *in vitro* gene delivery[15], and antifouling coatings[16]. Unlike peptides, which are generated (both chemically and biosynthetically) by coupling amino acids sequentially to a growing peptide chain, peptoids can be generated by the "submonomer method" in which the terminal amine is capped with a chloro- or bromoacetamide followed by introduction of the peptoid side chain by S_N2 substitution with an incoming primary amine, Figure 2-2.[17] In contrast to the relatively small pool of commercially available amino acids, the pool of commercially available primary amines numbers in the thousands.

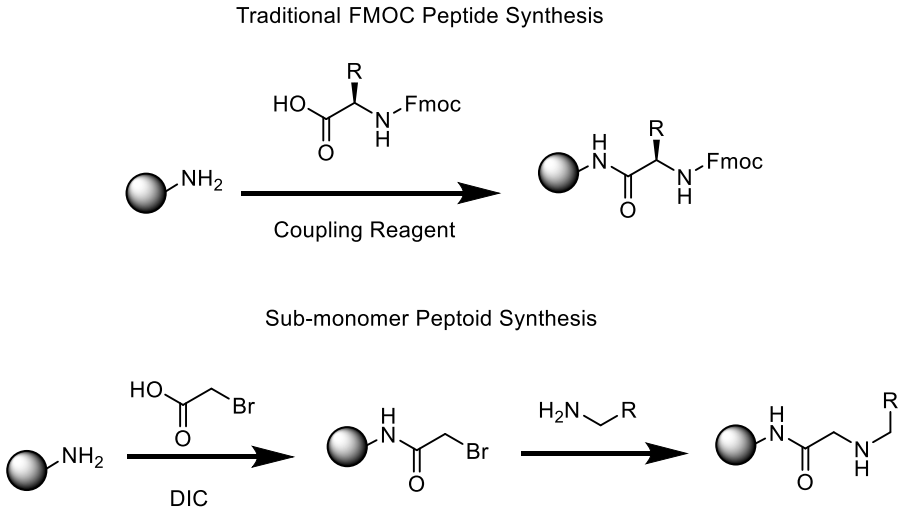

Figure 2-2 FMOC SPPS versus Peptoid Synthesis

2.2.3. Peptoids in Drug Discovery

Large peptoid libraries have yielded potent hits in phenotypic screens[18,19] and against a variety of protein targets, including VEGF[20,21], the proteasome[22], p53-MDM2[23], and MMP14[24], among others[25]. Kodakek *et al.* recently reported that libraries of cyclic peptoids generated more high affinity hits over their linear counterparts[26] while Ovadia *et al.* found peptide to peptoid substitutions in a cyclic melanocortin agonist improved both metabolic stability and paracellular permeability.[27] A number of studies have evaluated the effect of peptide to peptoid substitution on the potency of bioactive cyclic peptides[28–31], and their conformational preferences have been extensively investigated.[32,33] There is evidence that peptoids are more membrane permeable than peptides[27,34]; however, most of the peptoid ligands discovered to date have either been directed at extracellular targets[35,36] or have shown modest activity when directed against intracellular targets.[22,37] To date there has been no direct comparison between cyclic peptides and peptide-peptoid hybrids with respect to passive transcelluar permeability.

2.3. Previous Results and Experimental Design

Previously our laboratories investigated the influence of backbone stereochemistry and N-methylation on the permeability and metabolic stability of cyclic hexapeptides. One permeable scaffold identified by our laboratory, cyclo[Leu1–D(NMe)Leu2–(NMe)Leu3–Leu4–DPro5–(NMe)Tyr6] (**1NMe3**)[38] Figure 2-3, has been featured prominently as a model cyclic peptide in recent publications from our group and other.[39–43] This compound's defining structural characteristics are a double type II' β-

turn structure, engaging both non-N-methylated amide protons in intramolecular hydrogen bonds. The mimicry of β-turns may represent an accessible pharmacological niche for small cyclic peptides, as a number of protein-protein interactions are mediated by loops containing this structural motif.[44] Because of its favorable ADME/PK properties, double β-turn structure, and multiple N-alkylated residues, **1NMe3** provided a model system for the systematic investigation of the physiochemical properties imparted by N-methyl amino acid-to-peptoid substitutions. To this end, we systematically replaced every N-methylated residue of **1NMe3** with the equivalent N-substituted glycine (peptoid) residue Figure 2-3. In addition, the Leu at position 1 was replaced with N-isobutyl glycine (**1**) and all residues but Pro were replaced with peptoid residues (**9**). Peptoid residues were accessed through the introduction of bromoacetic acid followed by nucleophilic displacement with the desired amine[17].

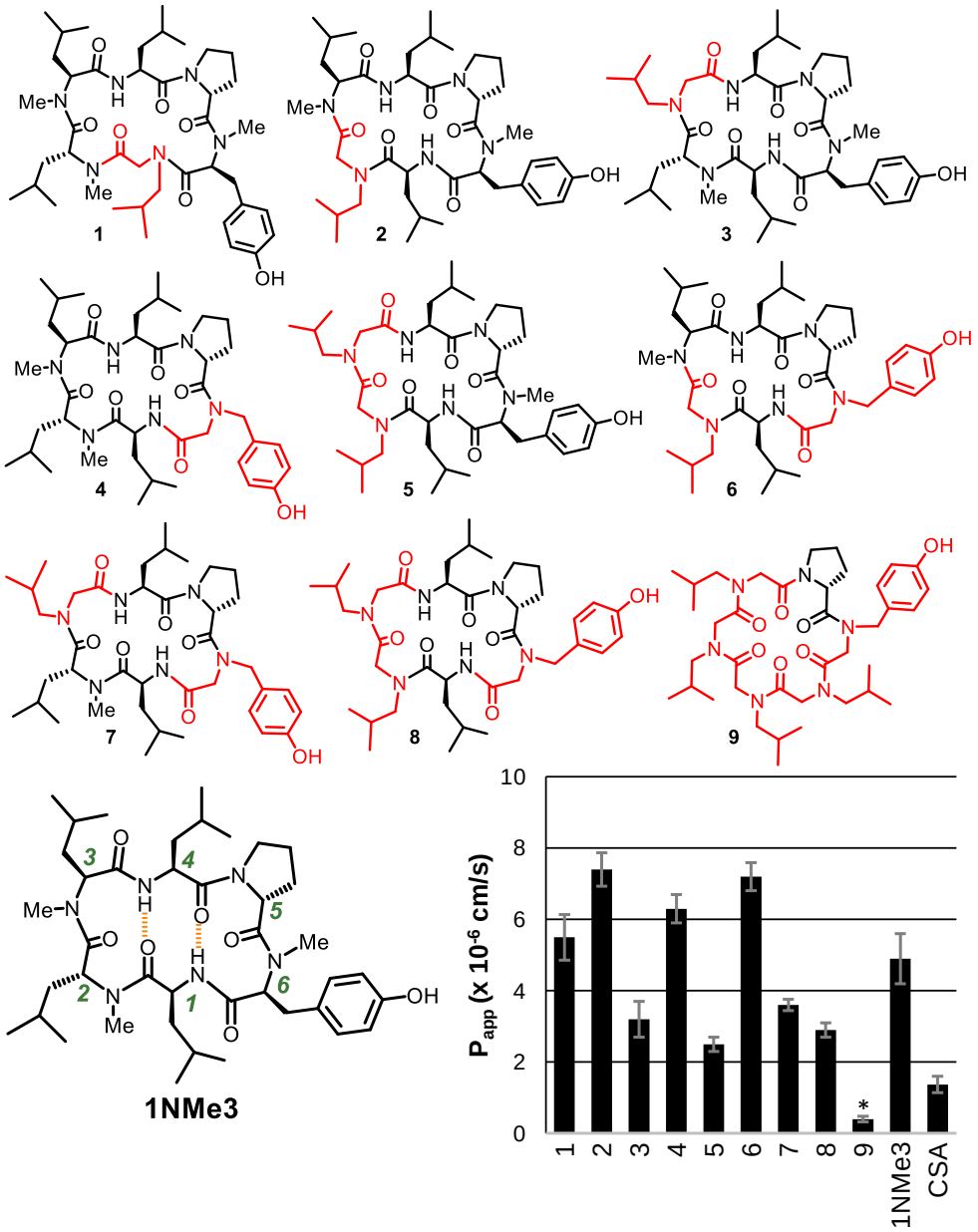

Figure 2-3 Peptoid Series and MDCK-LE Apparent Cell Permeability (average of 3 replicates, * denotes 2 replicates only)

2.4. ADME Properties of Peptoid Analogs of 1NMe3

Interestingly, a number of these compounds, notably **1** and **9,** displayed mixtures on the NMR and even chromatographic time scales highlighting the propensity for N-

substituted glycine residues to adopt the *cis*-amide conformation.[45] To further explore the properties imparted by these peptoid substitutions, this small series was subjected to the MDCK-LE[46] (Madin-Darby Canine Kidney epithelial cells – Low Efflux) trans-well assay, an *in vitro* assessment of compound permeation across a monolayer of epithelial cells selected for low efflux pump expression with results reported as a 1 dimensional diffusion rate (x 10^{-6} cm/s) across the cell monolayer (Figure 2-3).

Peptoid substitutions generally maintained the cell permeability of the parent compound. The single peptoid substitutions at Leu2 and Tyr6 (**2** and **4**, respectively) led to a nearly 50% increase in cellular permeability. The bis-substiution Leu2, Tyr6 (**6**) exhibited a similar increase in cell permeability. The exception to this trend was the pentapeptoid substitution **9**, which showed drastically reduced permeability. Notably, all compounds containing a Leu3-to-peptoid (**3**; **5**; **7**; **8**; and **9**) substitution exhibited lower cell permeability than the parent, while all compounds in which Leu3 remained an N-methyl amino acid (**1, 2**, **4**, and **6**) exhibited increased cell permeability. Since Leu2 and Leu3 represent *i + 1* and *i + 2* positions of a β-turn hypothesized that positionally-dependent modulation of this key structural element was the source of the augmented cellular permeability between the peptide-peptoid hybrids in this series.

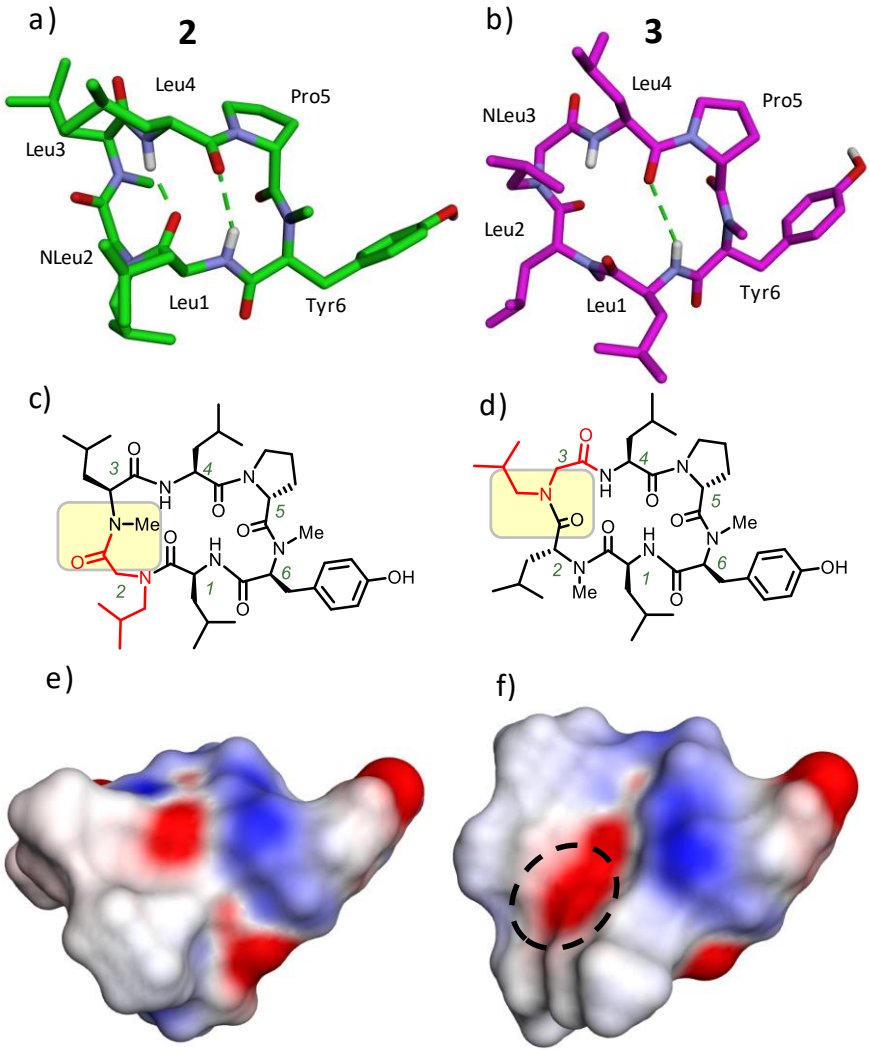

Figure 2-4 a,b) NMR restrained solution conformations of **L2N** and **L3N**, respectively. c,d) 2D representation of the conformations of **L2N** and **L3N**, respectively, with the amide between positions 2 and 3 highlighted in yellow, peptoid residues highlighted in red. e, f) Electrostatic surfaces of the **L2N** and **L3N**, with the solvent exposed carbonyl of Leucine 1 highlighted with a dashed circle.

2.5. Structural Analysis of L2N and L3N

In order to understand the relationship between peptoid position and cell permeability we sought to investigate and compare the low dielectric solution structures of **2** and **3**. NMR experiments were conducted in $CDCl_3$, which approximates the internal

dielectric of a phospholipid bilayer[47]. Peak assignments were made using COSY, TOCSY, HSQC, and HMBC experiments, and ROESY-derived inter-proton distances were calculated based on crosspeak volumes. ^{3}JH-H couplings were also used to provide dihedral information where available. Conformers were generated using molecular dynamics (MD) simulations and ensembles were fit to the distance and dihedral restraints using the program DISCON[48,49].

Of particular interest is how the β-turn is affected by the introduction of a peptoid residue in a cyclic system, a topic explored previously in linear di-and-tetrapeptide model systems.[50,51] In the structure of **1NMe3**, both the dLeu2-Leu3 and dPro5-Tyr6 β-turns adopt a type II' β-turn, enforced by the D-residue at the *i* + 1 position.[38] Both **2** and **3** also adopt a double β-turn structure. Interestingly, the β-turn encompassing positions 2 and 3 in compound **2** has inverted to a type II β-turn, likely due to the loss of D chirality at the *i* + 1 position. **3** maintains the chirality at position 2 but, in contrast to the parent **1NMe3**, fails to achieve a tight β-turn about positions 2 and 3 with H-O hydrogen bond distances of 3.9 Å and 1.9 Å respectively. This is likely due to the steric constraints imposed by the increased size of the N-alkyl group leading to increased solvent exposure of the carbonyl of Leu1 in the more expanded structure of **L3N** Figure 2-4. Using the aforementioned NMR structures the expanded conformation of **L3N** has a higher computationally-derived solvent exposed polar surface area (101 Å^2) than either **L2N** (78 Å^2) or **1NMe3** (87.2 Å^2) employing the method developed by Ertl *et al.*[52] and used extensively by Guimaraes *et al.*[53] to analyze a large library of permeable macrocycles. However, both L2N and L3N have minor conformations that are stable

on the NMR time scale (most likely cis-trans rotamers about the peptoid and/or N-Me amide bonds). Therefore, the observed difference in permeability between these compounds cannot be attributed solely to differences in solvent exposure between the major conformers alone. Future NMR studies should provide insight into the contribution of minor conformers to the permeability of the ensemble.

2.6. Diversification of the Y6 Position

Finally, since a benefit of introducing peptoid residues is the potential for facile diversification, we sought to test whether the favorable cell permeability properties of **4** tolerated the introduction of more diverse chemical functionality. To this end, we synthesized a small series of cyclic peptide peptoid hybrids encompassing chemical space not easily accessible by traditional amino acids (non-natural heterocycles, trifluoromethylation, and ether linkages) and subjected these to the same MDCK-LE assay as compounds **1** – **9**.

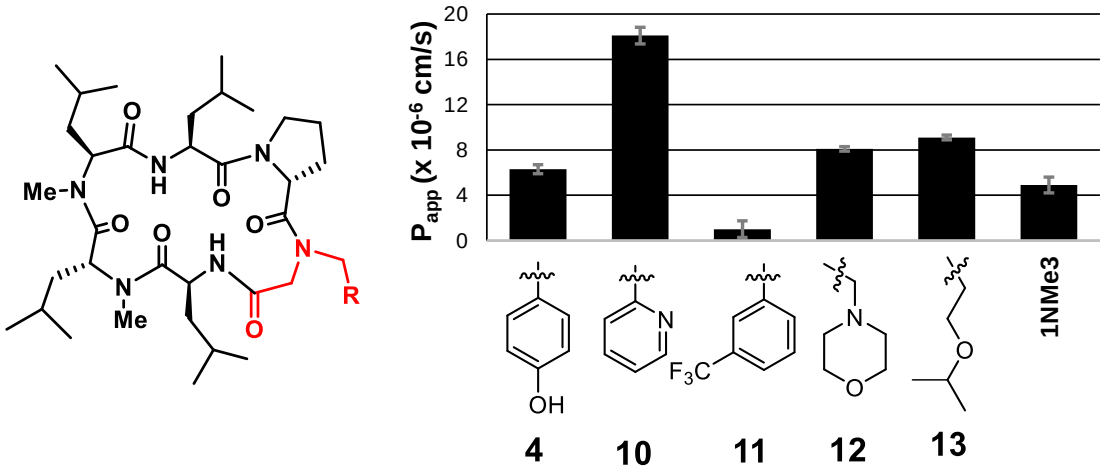

Figure 2-5 Peptoid Series and MDCK-LE Apparent Cell Permeability (average of 3 replicates)

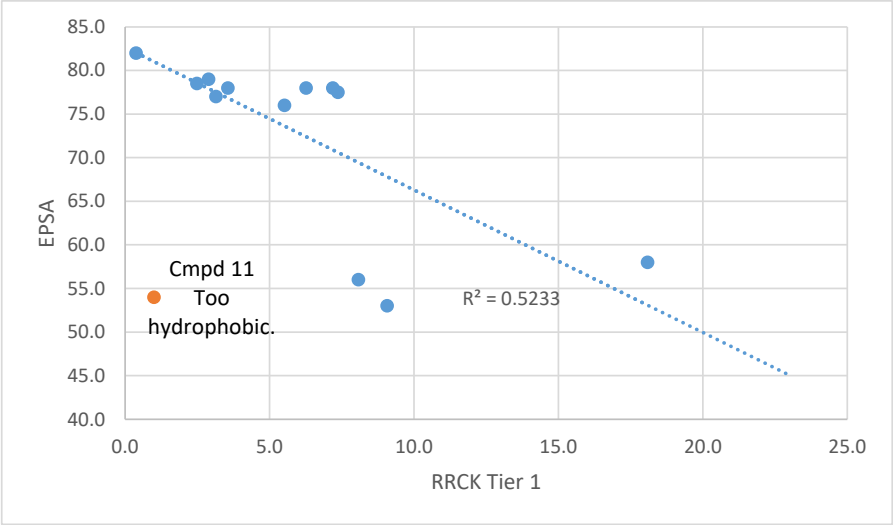

Figure 2-6 EPSA values (compared to RRCK) as caclulated in Goetz et al.[54]

Compound **10** exhibited increased permeability over **1-9** while **12** and **13** showed a modest increase (Figure 2-5). The increased permeability of **10, 12,** and **13** over **4** may be due to the removal of the hydrogen bond donating phenolic –OH. Despite the mild basicity of **12** (pKa ~7.4), it shows comparable permeability to the parent compound. The low permeability of compound **11** is likely due to low recovery (40.5%) in the MDCK-LE assay, which is not surprising given its exceedingly high lipophilicity. Compounds **4**, **10**, **12**, and **13** have calculated (2D) ALogP[55] values of < 4.0 while **11** has an ALogP of 5.2. Additionally, the replacement of the phenolic sidechain (present in compounds **1-9**) with one lacking a hydrogen bond donor (**10-13**) greatly decreased the experimental polar surface area[54] (EPSA) for those peptides: 76-82 Å^2 versus 53-58 Å^2 respectively,

Figure 2-6 and **Error! Reference source not found.**. The EPSA value is determined through a chromatographic technique designed to experimentally asses the

polar surface area of a molecule in a low dielectric environment. This highlights the permeability penalty incurred by the presence of unsatisfied hydrogen bond donors in the side chains.

2.7. Conclusions

The series of compounds **1-13** demonstrate promise for designing peptide-peptoid hybrid macrocyles with favorable ADME properties. Interestingly, **1** exhibits permeability in the top 50% of those observed in our study, higher than that of **1NMe3**. The replacement of the amide hydrogen of L1 with an isobutyl would completely prevent any beta turn about this position due to the removal of a hydrogen bond donor and the increased steric bulk. A complex mixture on the NMR time scale in chloroform, Methods Table 2-6, prevents a solution structure from being obtained, but it has likely found another or multiple lipophilic conformations other than the double beta-turned structure.

In the cases of **2** and 3 the use of NMR and molecular dynamics offers a potential explanation into the source of their observed differences in permeability. These results suggest that cyclic peptide peptoid hybrids combine the chemical diversity achievable using amine-derived peptoids with the stereochemical complexity and intramolecular hydrogen bonding of peptides to allow access to novel, versatile, and cell permeable macrocycles.

2.7.1. Abbreviations

ACN, acetonitrile; COMU, (1-Cyano-2-ethoxy-2-oxoethylidenaminooxy)dimethylamino-morpholino-carbenium hexafluorophosphate; DBU, 1,8- Diazabicyclo[5.4.0]undec-7-ene; DCM, dichloromethane; DIAD, diisopropyl azodicarboxylate; DMF, N,N-dimethylformamide; DIC, diisopropylcarbodiimide; DIPEA, diisopropylethylamine, DMSO, dimethylsulfoxide; DVB, divinylbenzene; EtOH, ethanol; Fmoc, 9-fluorenylmethoxycarbonyl; HBTU, N,N,N',N'-Tetramethyl-O-(1H-benzotriazol-1-yl)-uronium hexafluorophosphate; HOAt, 1-hydroxy-7-azabenzotriazole; IR, infrared; LCMS, liquid chromatography mass spectrometry; MeOH, methanol; N2, nitrogen; NMP, 1-methyl-2-pyrrolidinone; PTFE, Polytetrafluoroethylene; PyBOP, (benzotriazol-1-yloxy)tripyrrolidinophosphonium hexafluorophosphate; RP, reverse phase; SPPS, solid phase peptide synthesis; TFA, trifluoroacetic acid; THF, tetrahydrofuran

2.8. Methods

2.8.1. General Synthetic Prodcedures

2.8.1.1. Compound Specific Considerations

Peptides were prepared with the following procedures; **1**, **2**, **3**, **5**, **6**, **7**, **8**, and **9** were prepared using room temperature peptide couplings with in-sequence *N*-methylation (TFA strategy) or installation of pre-*N*-methylated Fmoc-amino acids followed by solution phase cyclization with EDC/HOAt. **4**, **10**, **11**, **12**, and **13**, were prepared using microwave assisted peptide couplings with installation of pre-methylated amino acids followed by solution phase cyclization with COMU.

2.8.1.2. Microwave Reaction Conditions

Microwave assisted reactions were done in a CEM Discover microwave reactor with an open reaction vessel. Reactions were heated to 50 °C with 12 watts of power while temperature was monitored with an IR probe from within the reaction vessel.

2.8.1.3. Loading of 2-Chlorotrityl resin

Loading Fmoc-Xaa-OH onto 2-chlorotrityl chloride resin: Fmoc-Xaa-OH (3 g) was dried under vacuum for 24 h. A bottle of 2-chlorotrityl chloride resin (5 g , 200-400 mesh; 1% DVB) was stored in a dessicator under vacuum prior to use. Anhydrous DCM was added to the Fmoc-Xaa-OH, followed by of dry DIPEA (4 equiv, 5.6 mL). This solution was transferred by syringe to a flame-dried round bottom flask containing 5.0

g of resin and a stir bar. The resin and solution were stirred gently at room temperature for 3 h. After 3 h, the resin and solution were transferred to a polypropylene synthesis vial containing a fritted disk and fitted with a Teflon stopcock. The resin was drained and rinsed with DCM (3x30 mL), DMF (3x30 mL), and again with DCM (3x30 mL) then treated with a solution of DCM, methanol, and DIPEA (17:2:1 respectively, 2x30 min), in order to cap any unreacted linker. Resin loading value was calculated by mass difference.

2.8.1.4. Room Temperature Amino Acid Coupling

Fmoc-Xaa (4 equiv), DIPEA (5 equiv), and HBTU (4 equiv) were added to the resin in DMF. The reaction was agitated via shaking for 45 min then drained. The resin was washed with DMF (3 x 3 mL) and DCM (3 x 3 mL). The reaction was monitored by LCMS and repeated until starting material was no longer observed.

2.8.1.5. Room Temperature Amino Acid Coupling onto Secondary Amines

Fmoc-Xaa (2 equiv), DIPEA (4 equiv), and COMU (2 equiv) were added to the resin in DMF. The reaction was agitated via shaking for 30 min then drained. The resin was washed with DMF (3 x 3 mL) and DCM (3 x 3 mL). The reaction was monitored by LCMS and repeated until starting material was no longer observed.

2.8.1.6. Amino Acid Coupling under Microwave Condtions

A solution of Fmoc-Xaa (4 equiv), HBTU (4 equiv), and HoAT (4 equiv), and DIPEA (6 equiv) in DMF was allowed to pre-react for 5 min. This solution was added to the deprotected peptide on-resin and allowed to react for 10 min at 50 °C under microwave heating. The solution was drained and resin was washed 3 times with DMF (3 x 3 mL) and DCM (3 x 3 mL). The reaction was monitored by LCMS and repeated until starting material was no longer observed.

2.8.1.7. Amino Acid Coupling onto N-Methylated Amino Acids under Microwave Conditions

A solution of Fmoc-Xaa (4 equiv), HATU (4 equiv), and DIPEA (6 equiv) in DMF was allowed to pre-react for 5 min. This solution was added to the deprotected peptide on-resin and allowed to react for 30 min at 50 °C under microwave heating. The solution was drained and resin was washed DMF (3 x 3 mL) and DCM (3 x 3 mL). The reaction was monitored by LCMS and repeated until starting material was no longer observed.

2.8.1.8. Coupling of Bromoacetic acid at Room Temperature

A solution of BrAcOH (3 equiv) and DIC (3 equiv) in DMF was allowed to pre-react for 10 min. This solution was added to the deprotected peptide on-resin. The reaction was agitated via shaking for 45 min then drained. The resin was washed with

DMF (3 x 3 mL) and DCM (3 x 3 mL). The reaction was monitored by LCMS and repeated until starting material was no longer observed.

2.8.1.9. Coupling of Bromoacetic acid Under Microwave Conditions

A solution of BrAcOH (4 equiv) and DIC (4 equiv) in DMF was allowed to pre-react for 10 min. This solution was added to the deprotected peptide on-resin. This solution was added to the deprotected peptide on-resin and allowed to react for 10 min at 50 °C under microwave heating. The solution was drained and resin was washed 3 times with DMF (3 x 3 mL) and DCM (3 x 3 mL). The reaction was monitored by LCMS and repeated until starting material was no longer observed.

2.8.1.10. Installation of Peptoid Sidechain

A solution of the desired amine (5-10 equiv) was prepared in a minimum volume of DMF. The resin containing the BrAc-peptide was swollen with DCM for 5 min prior to reaction. The amine was added the reaction was agitated vigorously for 45 min. The solution was drained and resin was washed 3 times with DMF (3 x 3 mL) and DCM (3 x 3 mL). The reaction was monitored by LCMS and repeated until starting material was no longer observed.

2.8.1.11. Removal of the N-Fmoc Protecting Group at Room Tempearture

A solution of 2% piperidine and 2% DBU in DMF was added to the resin. The reaction was agitated via shaking for 20 min then drained. The resin was washed with DMF (3 x 3 mL) and DCM (3 x 3 mL).

2.8.1.12. Removal of the N-Fmoc Protecting Group Under Microwave Conditions

A solution of 2% piperidine and 2% DBU in DMF was added to the resin. The reaction was allowed to react for 5 min at 50 °C under microwave heating then drained. The resin was washed with DMF (3 x 3 mL) and DCM (3 x 3 mL).

2.8.1.13. On-Resin Installation of the TFA protecting group

A solution of ethyltrifluoroacetate (10 equiv) and DBU (12 equiv) in THF was added to the deprotected amino acid on resin. The reaction was heated in a microwave reactor for 10 min at 50 °C. The solution was drained and resin was washed DMF (3 x 3 mL) and DCM (3 x 3 mL).

2.8.1.14. N-Alkylation under Mitsunobu Conditions

The resin was washed 3 times with dry THF, 5 mL. Triphenylphosphine (5 equiv) was dissolved in a minimum volume of dry THF and MeOH (10 equiv, stored over molecular sieves) was added. This mixture was added to the resin and vortexed while

DIAD (5 equiv, stored over molecular sieves) was added dropwise. The reaction was sealed and allowed to proceed for 10 min at rt under gentle rocking. The resin was washed once with dry THF and the procedure was repeated (2-5 times) until no more starting material was observed by LCMS. Prior to the removal of the TFA or *o*-Ns group the resin was washed DMF (3 x 3 mL) and DCM (3 x 3 mL).

2.8.1.15. On-Resin TFA Deprotection

A 1:1 solution of dry THF and dry EtOH was added to the resin. A large excess of sodium borohydride (10-40 eq) was added and the reaction was allowed to proceed at room temperature for one hour. This procedure was repeated (1-3 times) until no more starting material was observed by LCMS. The resin was washed with MeOH (3 x 3 mL) DMF (3 x 3 mL) and DCM (3 x 3 mL)

2.8.1.16. Peptide Cleavage

Complete linear peptides were cleaved off resin in 5 resin volumes of 2.5% TFA in DCM for 4 minutes three times with a 5 resin volume DCM wash in between each step. Solvent was removed under N_2 followed by dissolution in acetone or DCM and evaporation under reduced pressure. Residual TFA was removed *in vacuo* overnight.

2.8.1.17. Cyclization with EDC and HOAt

Linear peptides were dissolved in 20 mL of dry acetonitrile with DIPEA (4 equiv) and added dropwise to a solution of (final concentration 1 mg crude peptide per mL) 1:1 THF/ACN containing EDC (4 equiv) and HOAt (4 equiv). Reactions were stirred from 2 to 24 h until complete cyclization was achieved as monitored by LCMS. The reaction was reduced *in vacuo*, redissolved in ethyl acetate (100 mL), and was washed with 0.5 M HCl (50 mL x 3). The combined aqueous layers were back extracted with ethyl acetate (50 mL). The combined organic layers were washed with brine (50 mL) and dried over sodium sulfate and reduced *in vacuo* for purification via HPLC.

2.8.1.18. Cyclization with COMU

Linear peptides were dissolved in 20 mL of dry acetonitrile with DIPEA (4 equiv) and added dropwise to a solution of (final concentration 1 mg crude peptide per mL) 1:1 THF/ACN containing COMU (2 equiv). Reactions were stirred from 0.5 to 24 h until complete cyclization was achieved as monitored by LCMS. The reaction was reduced *in vacuo* for purification via HPLC.

2.8.1.19. Removal of Acid Labile Side Chain Protecting Groups

Peptides were dissolved in 25 mL of 1:1 TFA/DCM and allowed to react for 30 minutes. Solvent was removed under N_2 followed by dissolution in MeOH and evaporation under reduced pressure.

2.8.1.20. Purification of Peptides

COMU by-products were removed after solution phase cyclization on a Biotage Isolera Prime system equipped with a KP-C18-HS 12g column eluting with H_2O/Acetonitrile modified with 0.1% TFA. Peptides were purified after global deprotection on a Waters mass-directed prep system equipped with an XBridge BEH130 5µm 19x150 C18 column eluting with H_2O/Acetonitrile modified with 0.1% formic acid or 0.1% TFA.

2.8.2. RRCK Permeability

Cell permeability was determined using RRCK (MDCK-LE) cells (Pfizer, Inc. Groton, CT)[56]. RRCK cells were generated in house as a subclone of Madin-Darby Canine Kidney wild-type (MDCK-WT) cells that displayed low expression of endogenous p-glycoprotein (~ 1–2% of MDCK-WT cells, based on mRNA level). Cells were cultured in minimal essential medium α with supplements and passaged when 70–80% confluent. Cell monolayer flux studies were conducted five days after seeding in 24-well transwell inserts (RRCK in 1.0 μm pore size, Becton Dickinson, Cowley, UK) at 4.2 x 10^4 cells/cm^2. Donor and acceptor solutions were prepared from HBSS containing HEPES at 20 mM, pH 7.4. Stock solutions of test compounds, prepared at 10 mM in DMSO, were used to prepare donor solutions of 2 μM compound in 0.05% (v/v) DMSO. Apparent permeability (P_{app}) was determined in apical to basolateral (AB) direction in triplicate by incubating with compound for 2 h at 37 °C. Samples of the medium were analyzed by liquid-chromatography tandem mass spectrometry (LC-MS/MS). *P*app values were calculated according to the equation P_{app} = (Q/t) x 1/C_0 x 1/A, where Q is the sampled concentration in the acceptor compartment, t is the incubation time, C_0 is the initial concentration in the donor compartment and A is the area of the filter of the transwell plate.

2.8.3. NMR Analysis and Assignment

All 2D spectra were acquired on a Varian/Agilent 600 MHz NMR with a Unity Inova console with a 5 mm triple resonances cold probe. Additional spectra, 1H spectra of compounds synthesized were acquired on a Agilent/Varian 500 MHz NMR with Unity Plus console and a 5 mm broadband probe or a 5 mm HX indirect detection probe. All spectra were acquired at 25 °C (600 MHz) or 15 °C (500 MHz) unless otherwise noted. For peak assignment of 2 and 3 HSQC, HMBC, TOCSY, COSY, 13C, and 1H spectra were acquired using the pulse sequences supplied with Varian CHEMPack. Our lab has found that a ROESY mixing time of 200 ms is optimal for peptides of this size (unpublished work). The ROESY spectrum for the conformational analysis of 2 and 3 was acquired with a mixing time of 200 ms, a d1=1.0, and 16 scans.

Table 2-1 Compound **2** Assignment

Leu1	^{1}H	^{13}C
Hα	5.11	46.07
Hβ	1.89	41.27
Hβ'	1.59	
Hγ	1.55	24.63
Hδ	0.96	23.37
Hδ'	0.96	22.42
NH	7.47	NA

Pep2	^{1}H	^{13}C
Hα	4.48	48.29
Hα	3.19	
Hβ	3.95	57.73
Hβ'	3.23	
Hγ	1.85	28.63
Hδ	0.97	20.04
Hδ'	0.97	19.76

Leu 3	^{1}H	^{13}C
Hα	5.38	55.4
Hβ	1.99	36.07
Hβ'	1.58	
Hγ	1.4	24.97
Hδ	0.91	23.52
Hδ'	0.86	21.28
Nme	3.02	31.29

Leu4	^{1}H	^{13}C
Hα	4.93	48.21
Hβ	1.79	41.17
Hβ'	1.61	
Hγ	1.51	24.86
Hδ	0.92	22.77
Hδ'	0.92	22.86
NH	7.2	NA

Pro5	^{1}H	^{13}C
Hα	4.4	55.61
Hβ	1.72	27.97
Hβ'	1.49	
Hγ	2.06	25.46
Hγ'	1.72	
Hδ	3.83	47.46
Hδ'	3.56	

Tyr6	^{1}H	^{13}C
Hα	5.69	57.43
Hβ	3.54	32.4
Hβ'	2.73	
Hδ	6.96	129.3
Hε	6.69	115.2
Nme	2.95	31.25
OH	ND	NA

Tertiary	^{13}C
Leu1 CO	172.83
Pep2 CO	170.48
Leu3 CO	169.85
Leu4 CO	170.34
Pro5 CO	173.61
Tyr6 CO	168.96
Tyr6 Cγ	128.05
Tyr6 Cζ	155.32

Table 2-2 Compound **3** Assignment

Leu1	^{1}H	^{13}C
Hα	5.01	47.99
Hβ	1.74	41.27
Hβ'	1.74	
Hγ	1.55	24.64
Hδ	0.96	22.6
Hδ'	0.96	22.61
NH	7.6	NA

Leu 2	^{1}H	^{13}C
Hα	4.93	51.88
Hβ	2.04	37.22
Hβ'	1.24	
Hγ	1.59	25.38
Hδ	0.9	23.53
Hδ'	0.98	20.84
Nme	3.12	30.96

Pep3	^{1}H	^{13}C
Hα	4.88	50.5
Hα	3.32	
Hβ	4	56.47
Hβ'	2.79	
Hγ	1.95	28.73
Hδ	0.98	20.33
Hδ'	0.92	20.18

Leu4	^{1}H	^{13}C
Hα	4.92	48.03
Hβ	1.64	42.32
Hβ'	1.55	
Hγ	1.53	24.81
Hδ	0.97	22.96
Hδ'	0.91	22.89
NH	6.75	NA

Pro5	^{1}H	^{13}C
Hα	4.34	55.7
Hβ	1.77	28.14
Hβ'	1.52	
Hγ	2.06	25.43
Hγ'	1.77	
Hδ	3.84	47.61
Hδ'	3.52	

Tyr6	^{1}H	^{13}C
Hα	5.67	56.97
Hβ	3.5	32.45
Hβ'	2.78	
Hδ	6.96	129.5
Hε	6.71	115.2
OH	ND	NA
Nme	2.91	31.32

Tertiary	^{13}C
Leu1 CO	173.12
Leu2 CO	174.18
Pep3 CO	167.44
Leu4 CO	170.33
Pro5 CO	173.04
Tyr6 CO	169.13
Tyr6 Cγ	128.05
Tyr6 Cζ	155.27

Table 2-3 Compound **2** Minor Conformer Assignment

Leu1	^{1}H	^{13}C
Hα	5.01	47.92
Hβ	1.69	41.87
Hβ'	1.42	
Hγ	1.69	25.01
Hδ	1.06	20-25
Hδ'	0.94	20-25
NH	7.51	NA

Pep2	^{1}H	^{13}C
Hα	4.61	46.91
Hα	3.13	
Hβ	3.47	57.07
Hβ'	3.32	
Hγ	1.93	28.05
Hδ	~0.96	20-25
Hδ'	~0.96	20-25

Leu 3	^{1}H	^{13}C
Hα	4.94	59.56
Hβ	1.89	37.32
Hβ'	1.5	
Hγ	1.44	24.44
Hδ	~0.92	20-25
Hδ'	~0.92	20-25
Nme	2.7	29.22

Leu4	^{1}H	^{13}C
Hα	4.73	50.16
Hβ	1.51	43.43
Hβ'	1.48	
Hγ	1.55	24.62
Hδ	~0.92	20-25
Hδ'	~0.92	20-25
NH	8.44	NA

Pro5	^{1}H	^{13}C
Hα	4.5	55.71
Hβ	1.76	28.12
Hβ'	1.52	
Hγ	2.14	25.46
Hγ'	1.79	
Hδ	3.8	47.32
Hδ'	3.52	

Tyr6	^{1}H	^{13}C
Hα	5.66	57.87
Hβ	3.55	32.45
Hβ'	2.78	
Hδ	6.96	129.32
Hε	6.72	115.17
Nme	3.02	31.29
OH	ND	NA

Tertiary	^{13}C
Leu1 CO	172.87
Pep2 CO	170.04
Leu3 CO	169.18
Leu4 CO	170.41
Pro5 CO	174.37
Tyr6 CO	169.27
Tyr6 Cγ	128.41
Tyr6 Cζ	155.18

2.8.4. DISCON Analysis:

To obtain starting conformations for input into DISCON, the NAMD[57] molecular dynamics (MD) protocol was used, beginning with an arbitrary conformation, to generate a diverse family of minimized conformers. We used the CHARMM forcefield with MMFF94 partial charge estimation for the MD simulation, which was carried out for 5 ns at 2000˚ K with a 1 fs time step. Snapshots were saved every 20 ps, leading to an ensemble of 250 snapshots. The resulting high temperature snapshots were energy minimized using the generalized Born implicit solvent model with a dielectric of 4. The 250 snapshots (plus 5 from an initial dynamics cascade) were taken forward into the DISCON calculations. We have found that these MD parameters adequately sample conformational space in cyclic hexapeptides with multiple N-methyl groups and are able to recapitulate the independently calculated NMR solution structures of well-studied cyclic peptides such as **1NMe3**[38], including the ability to sample all N-Me and Pro cis-trans rotamers. The resulting energy-minimized conformers were used as input into the DISCON protocol using the ROESY crosspeak volumes and the two HN-HA ^{3}J couplings to provide experimental distances, for 5000 iterations at a cluster level of 20.

Both **2** and **3** showed a dominant cluster representing >94% of the DISCON ensemble.

Table 2-4 ROE correlations **2**

DISCON	Res 1	Atom 1	Res 2	Atom 2	Norm Int.	|Diagonal|	Int/Diag	Distance
y	L1	NH	Y6	Nme	10.38	907	0.01144	2.66
y	L1	NH	Y6	HA	6.33	907	0.00698	2.89
y	L1	NH	P5	HA	1.2	907	0.00132	3.81
y	L1	NH	Pep2	HB	0.89	907	0.00098	4.01
y	L1	NH	L4	HB	0.46	907	0.00051	4.47
y	L4	NH	L3	HA	4.1	831	0.00493	3.06
y	L4	NH	Pep2	HA	1.63	831	0.00196	3.57
y	L4	NH	Pep2	HA	0.17	831	0.00020	5.20
y	L4	NH	P5	HG	0.75	831	0.00090	4.06
y	L4	NH	L1	HB	0.38	831	0.00046	4.55
y	L4	NH	L3	Nme	10.64	831	0.01280	2.61
y	Y6	HA	Pep2	HB	0.86	1066	0.00081	4.14
y	Y6	HA	L1	HA	0.55	1066	0.00052	4.46
y	L3	HA	P5	HD	0.53	526	0.00101	3.99
y	L1	HA	Pep2	HB	67.28	1094	0.06150	2.01
y	L4	HA	P5	HD	24.54	1019	0.02408	2.35
y	P5	HA	Y6	Nme	48.44	948	0.05110	2.07
y	L1	NH	L4	NH	1.48	907	0.00163	3.68
ref	Pep3	HB	Pep3	HB	122.05	1022	0.11942	1.80

Table 2-5 ROE correlations **3**

DISCON	Residue	Atom	Residue2	Atom2	Absolute	|Diagonal|	Int/Diag	I
y	L1	NH	Y	HA	7.73	789	0.009797	
y	L1	NH	L4	NH	2.11	789	0.002674	
y	L1	NH	L2	Nme	2.26	789	0.002864	
y	L1	NH	P5	HA	1.24	789	0.001572	
y	L1	HA	L2	NME	46.34	1202	0.038552	
y	L1	HA	Y6	NME	0.61	1202	0.000507	
y	L1	HA	Pep3	HG	0.54	1202	0.000449	
y	L1	NH	Y6	Nme	10.41	789	0.013194	
y	L2	HA	L1	HB	0.68	1019	0.000667	
y	L2	HA	Pep3	HB	73.85	1019	0.072473	
y	L2	HA	Pep3	HB'	5.24	1019	0.005142	
y	L4	NH	Pep3	HB	9.1	1004	0.009064	
y	L4	NH	Pep3	HA	1.31	1004	0.001305	
y	L4	NH	Pep3	HB'	5.55	1004	0.005528	
y	L4	NH	Pep3	HG	0.58	1004	0.000578	
y	P5	HA	Y6	NME	53.06	1047	0.050678	
y	Pep3	HA	Pep3	HG	14.08	1019	0.013817	
y	Y6	HA	L2	NME	3.32	1073	0.003094	
y	Y6	HE	P5	HG	0.64	2140	0.000299	
y	Y6	HA	P5	HA	0.67	1073	0.000624	
y	Y6	HE	P5	HD	0.79	2140	0.000369	
ref	Pep3	HB	Pep3	HB	141.62	901	0.157181	

Table 2-6 Conformer Contribution NMR Spectra

Compd.	Major	Minor1	Minor2	Minor3
1	43	30	17	10
2	66	34		
3	87	13		
4	90	10		
5	97	3		
6	58	38	4	
7	81	17	2	
8	93	7		
9	~35	many others		
10	95	5		
11	93	7		
12	92	8		
13	98	2		

Integration of ^{1}H spectra was performed where sufficiently resolved protons were available, NH or Cα, in the case of **1** the NMe region was used. All spectra were acquired in $CDCl_3$.

2.8.5. Characterization of Compounds

1

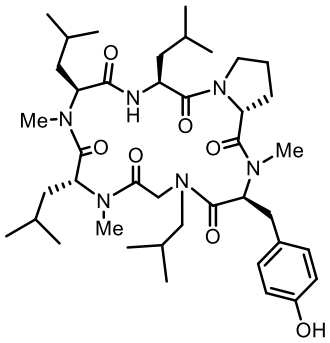

Chemical Formula: $C_{41}H_{66}N_6O_7$
Exact Mass: 754.50
Molecular Weight: 755.01

ESI cacld. for $C_{41}H_{66}N_6O_7[M+H]^+$ *m/*z = 755.50; found 755.39.

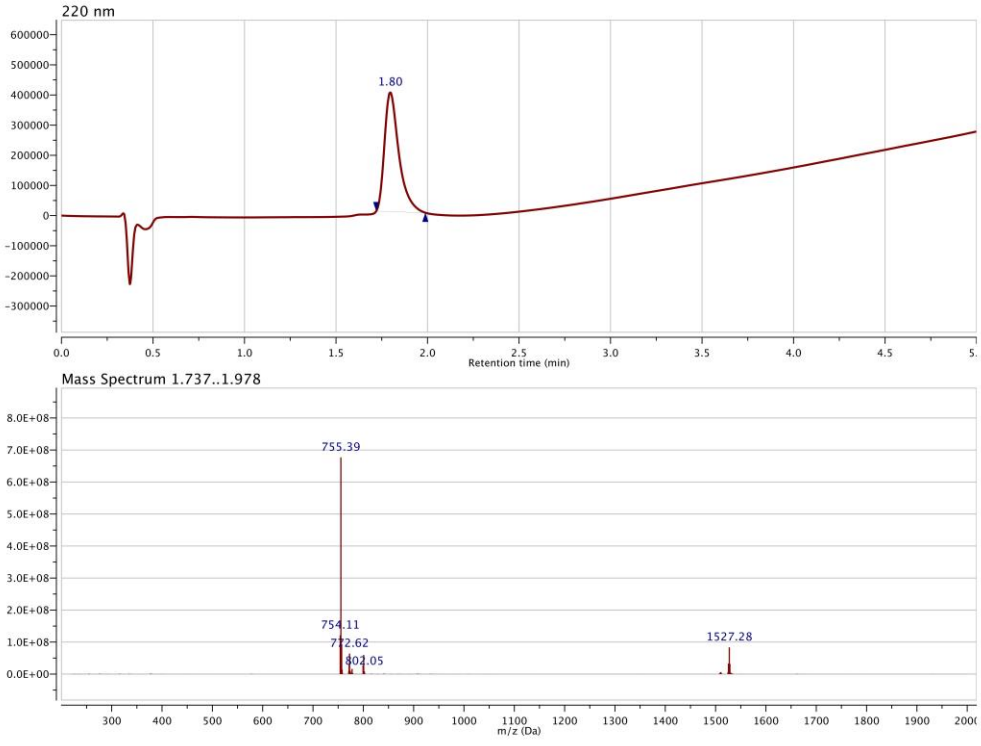

2

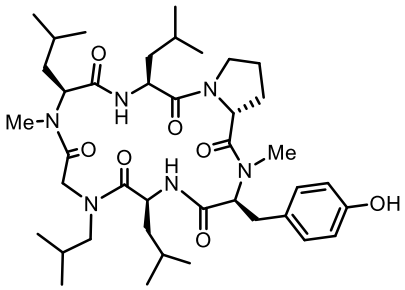

Chemical Formula: $C_{40}H_{64}N_6O_7$
Exact Mass: 740.48
Molecular Weight: 740.99

ESI cacld. for $C_{40}H_{64}N_6O_7[M+H]^+$ *m/*z = 741.48; found 741.95.

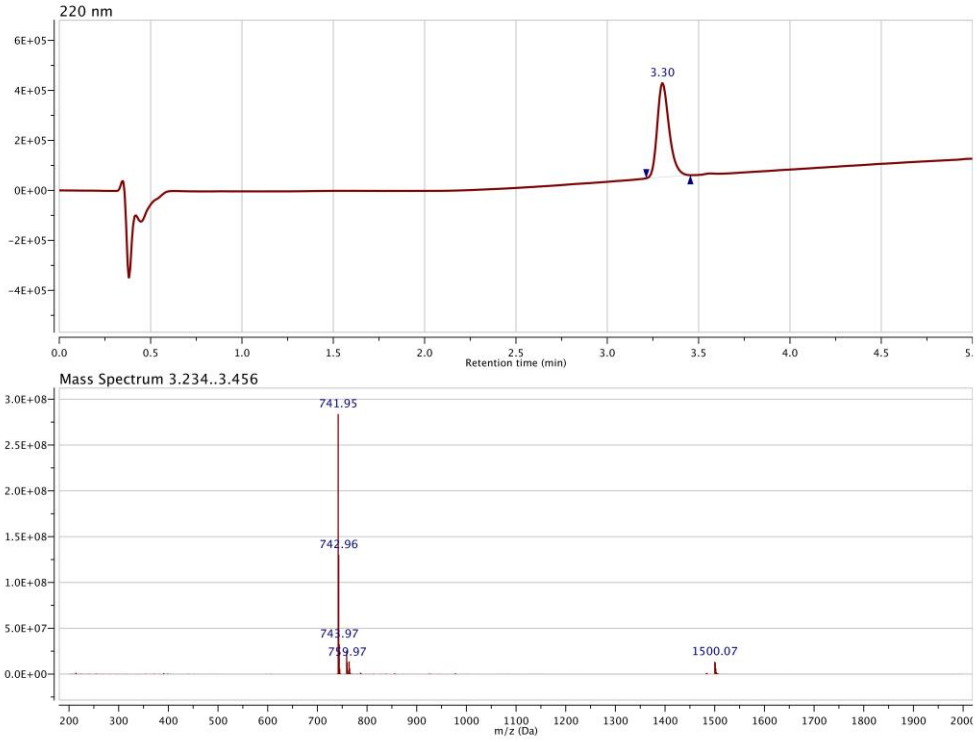

3

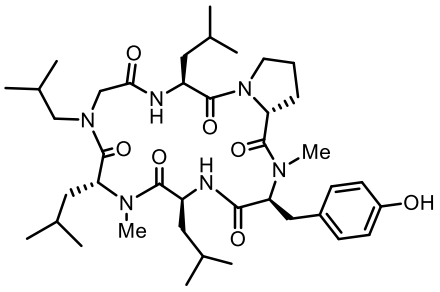

Chemical Formula: $C_{40}H_{64}N_6O_7$
Exact Mass: 740.48
Molecular Weight: 740.99

ESI cacld. for $C_{40}H_{64}N_6O_7[M+H]^+$ *m/*z = 741.48; found 741.95.

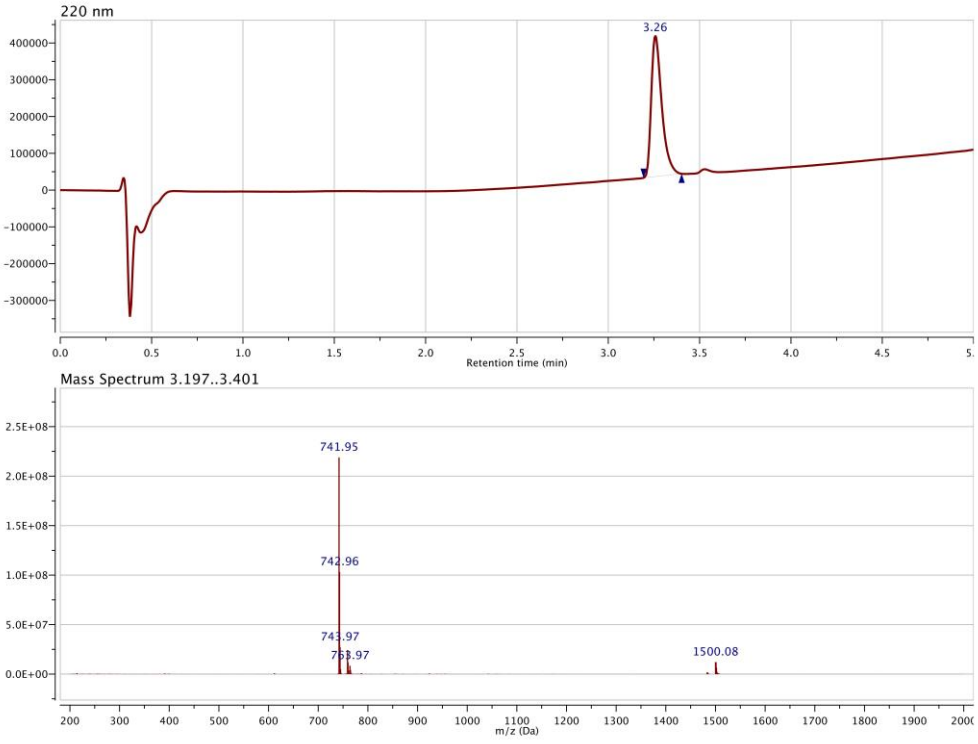

4

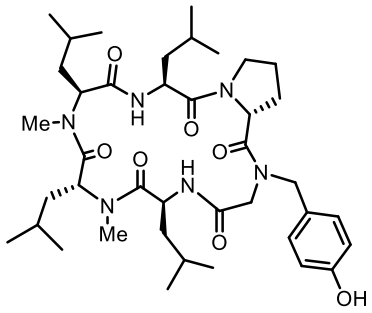

Chemical Formula: $C_{40}H_{64}N_6O_7$
Exact Mass: 740.48
Molecular Weight: 740.99

ESI cacld. for $C_{40}H_{64}N_6O_7[M+H]^+$ *m/*z = 741.48; found 741.95.

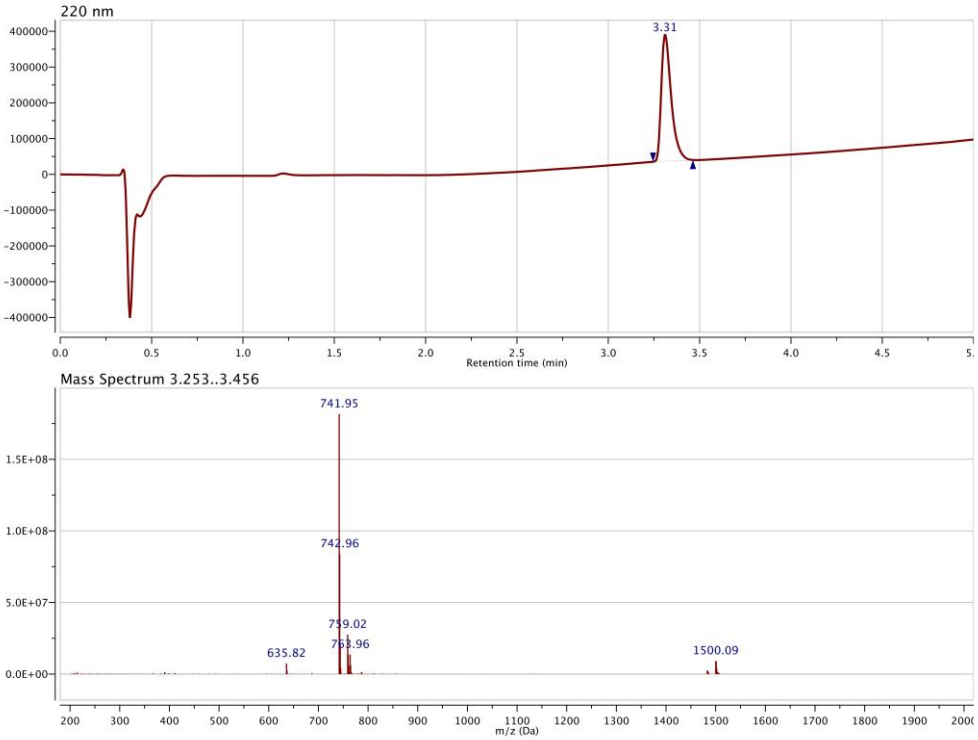

5

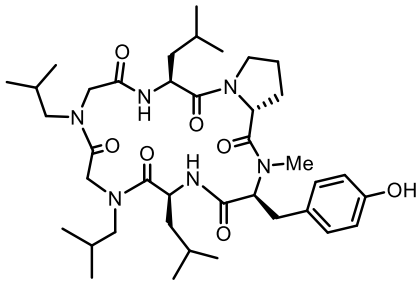

Chemical Formula: $C_{39}H_{62}N_6O_7$
Exact Mass: 726.47
Molecular Weight: 726.96

ESI cacld. for $C_{39}H_{62}N_6O_7[M+H]^+$ *m/*z = 727.47; found 727.97.

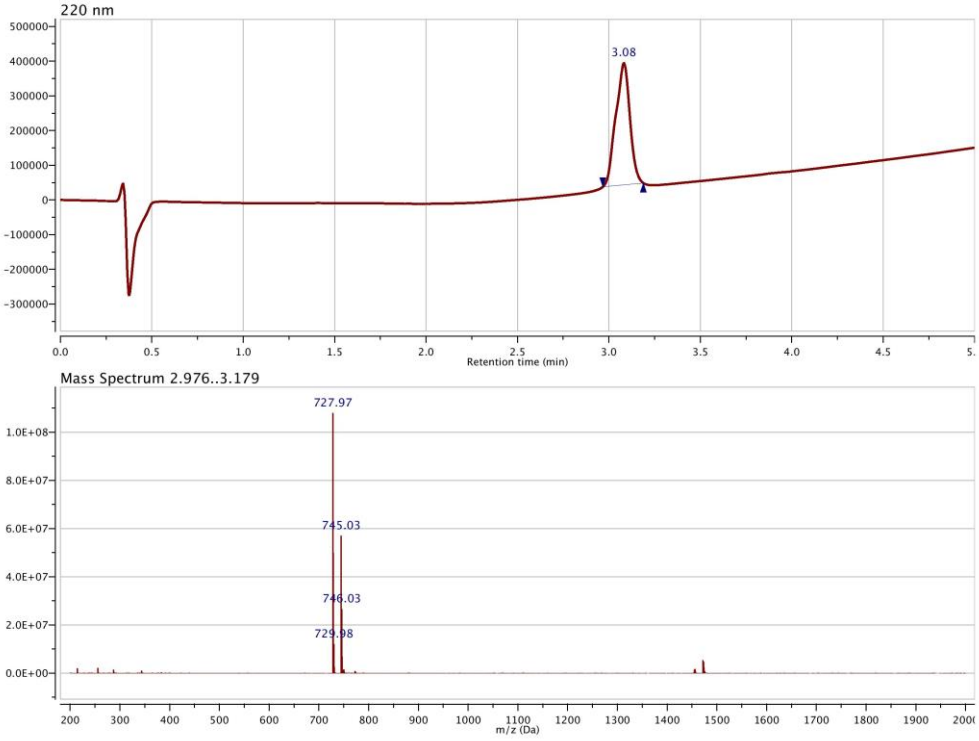

6

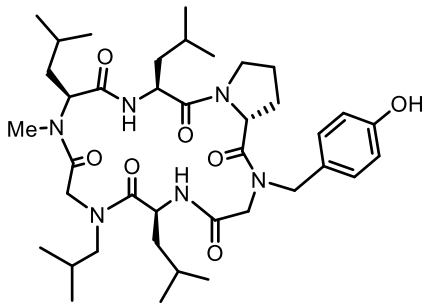

Chemical Formula: $C_{39}H_{62}N_6O_7$
Exact Mass: 726.47
Molecular Weight: 726.96

ESI cacld. for $C_{39}H_{62}N_6O_7[M+H]^+$ *m/*z = 727.47; found 727.60.

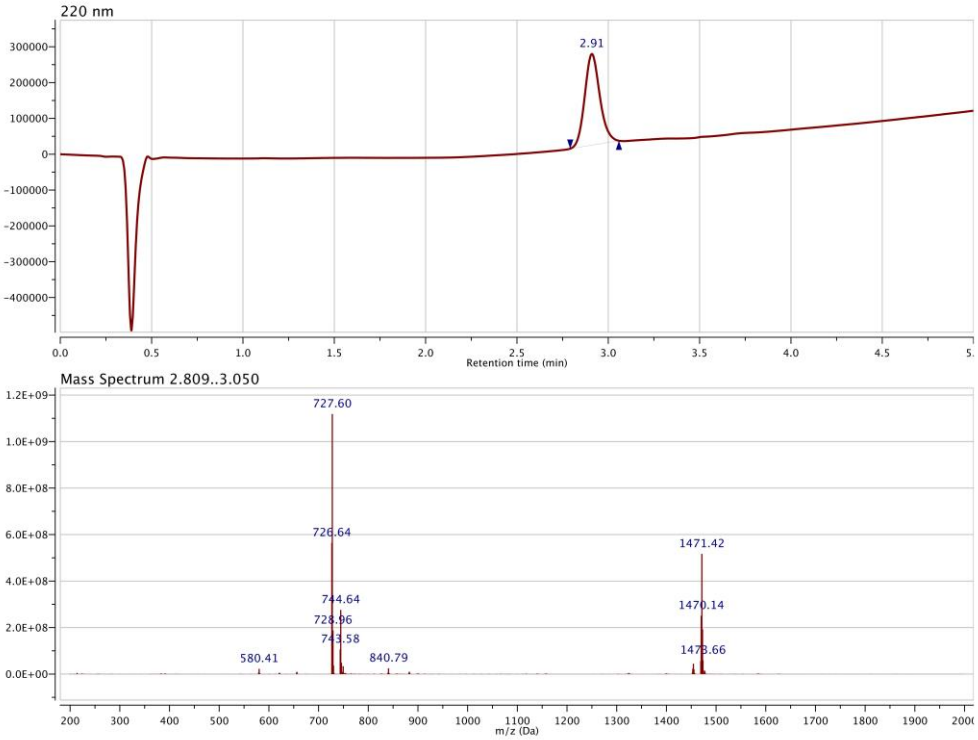

7

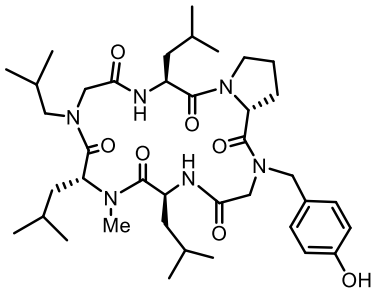

Chemical Formula: $C_{39}H_{62}N_6O_7$
Exact Mass: 726.47
Molecular Weight: 726.96

ESI cacld. for $C_{39}H_{62}N_6O_7[M+H]^+$ *m/*z = 727.47; found 727.97.

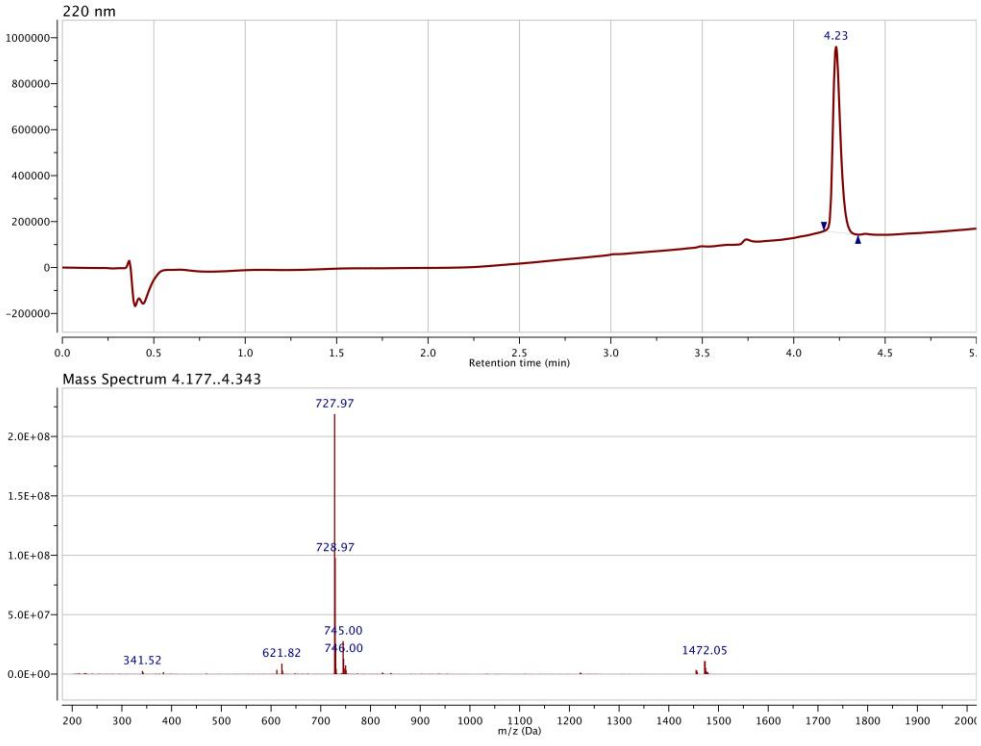

8

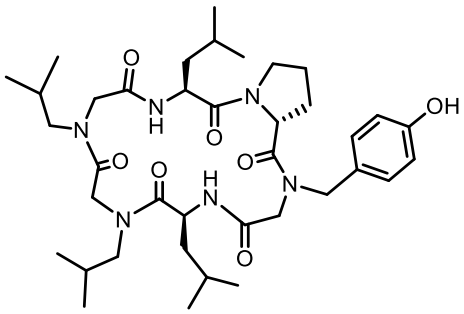

Chemical Formula: $C_{38}H_{60}N_6O_7$
Exact Mass: 712.45
Molecular Weight: 712.93

ESI cacld. for $C_{38}H_{60}N_6O_7[M+H]^+$ *m/*z = 713.45; found 713.87.

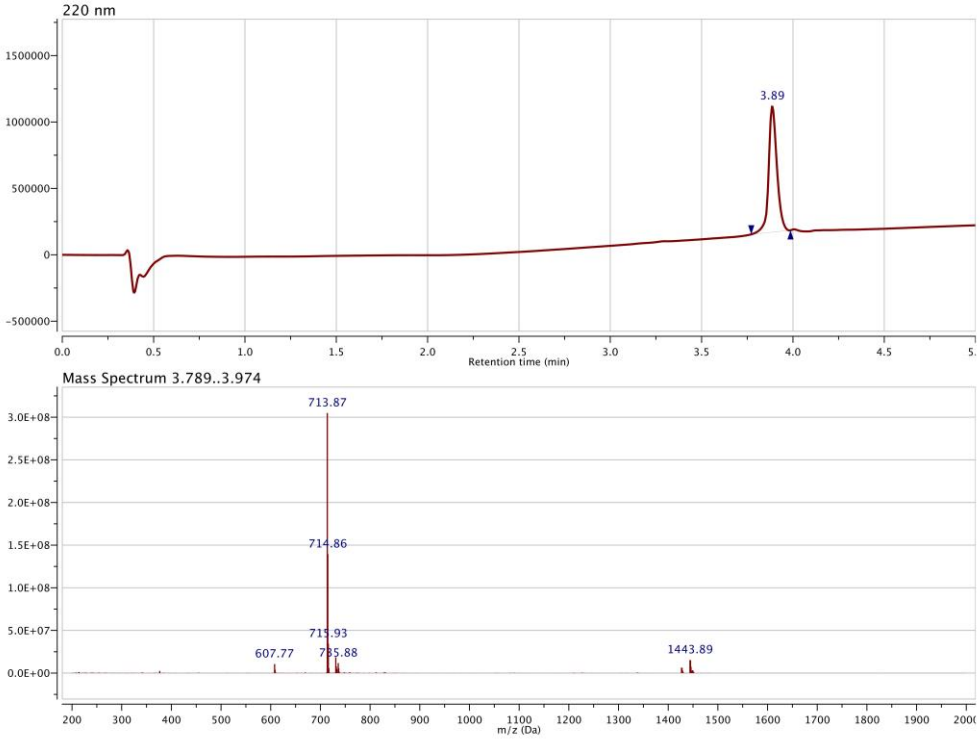

9

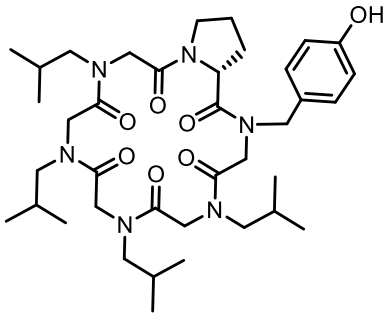

Chemical Formula: $C_{38}H_{60}N_6O_7$
Exact Mass: 712.45
Molecular Weight: 712.93

Compound **9** exhibited 2 conformations on the chromatographic timescale, showing a double humped peak. Below are the following traces in order: 220 nm UV spectra; mass spectrum encompassing the peak above; EIC spectra 713.9; EIC spectra 607.7. The EIC shows that the mass 607.7 is in fact a fragment of the parent mass and not an impurity. ESI cacld. for C38H60N6O7[M+H]+ m/z = 713.45; found 713.92.

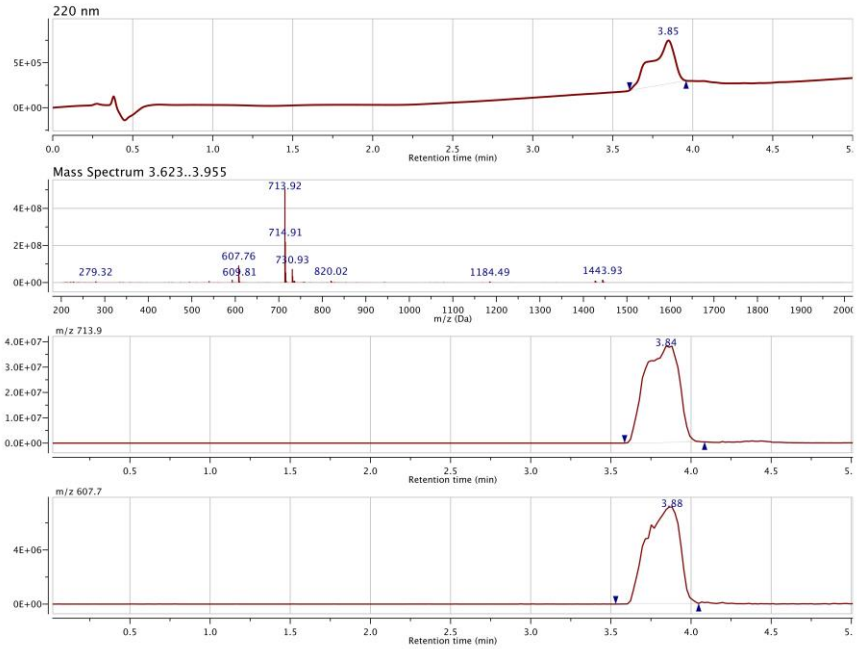

10

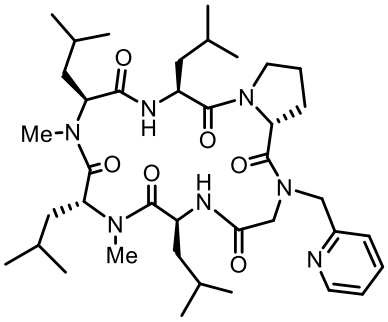

Chemical Formula: $C_{39}H_{63}N_7O_6$
Exact Mass: 725.48
Molecular Weight: 725.98

ESI cacld. for $C_{39}H_{63}N_7O_6[M+H]^+$ *m/*z = 726.48; found 726.96.

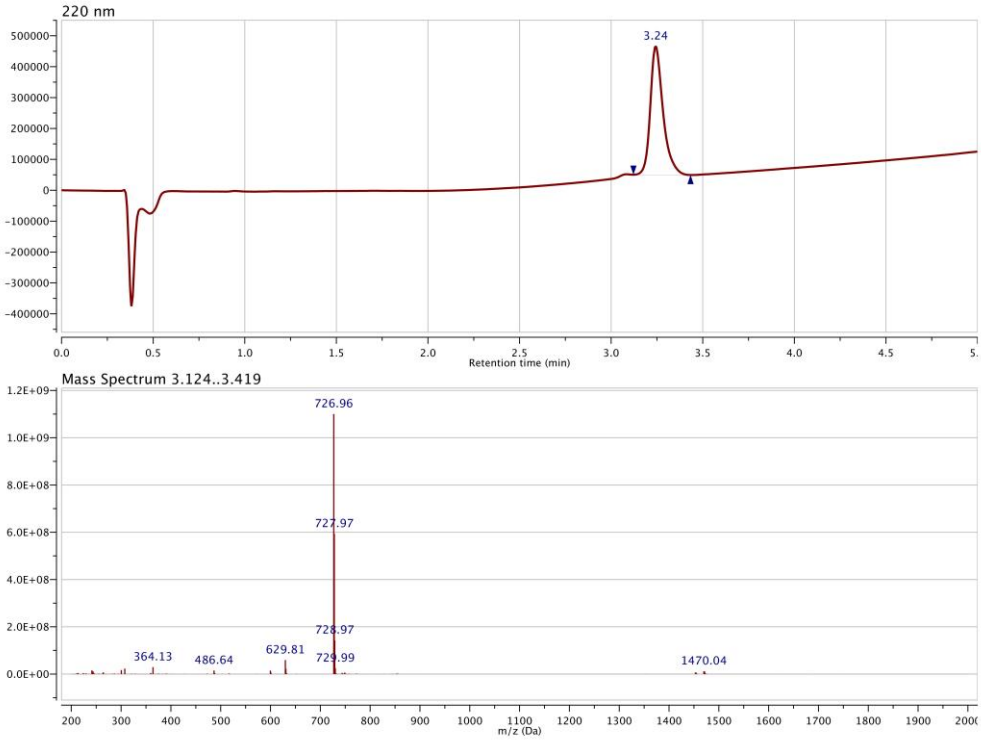

11

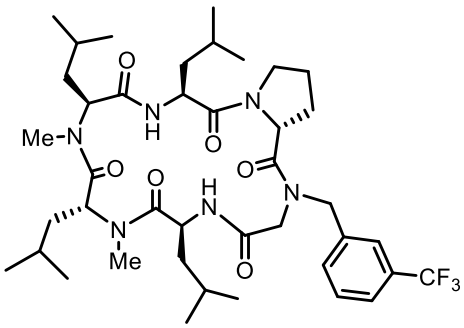

Chemical Formula: $C_{41}H_{63}F_3N_6O_6$
Exact Mass: 792.48
Molecular Weight: 792.99

ESI cacld. for $C_{41}H_{63}F_3N_6O_6[M+H]^+$ *m/*z = 793.48; found 794.02.

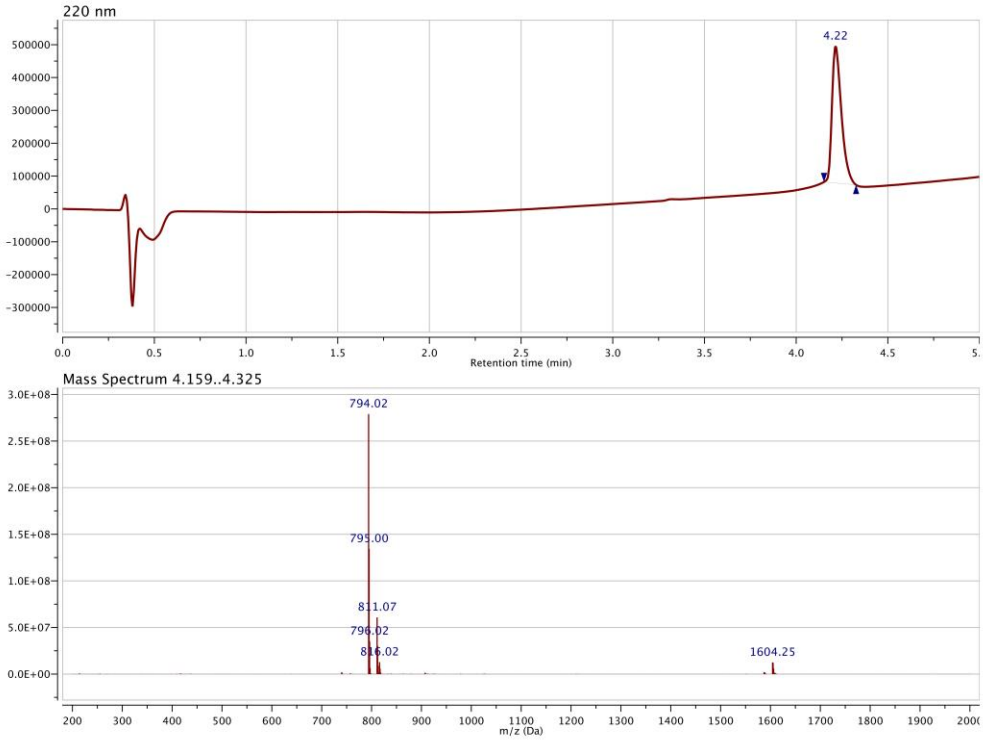

12

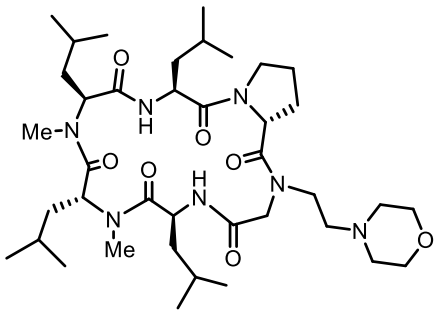

Chemical Formula: $C_{39}H_{69}N_7O_7$
Exact Mass: 747.53
Molecular Weight: 748.02

ESI cacld. for $C_{39}H_{69}N_7O7[M+H]^+$ *m/z* = 748.53; found 749.01.

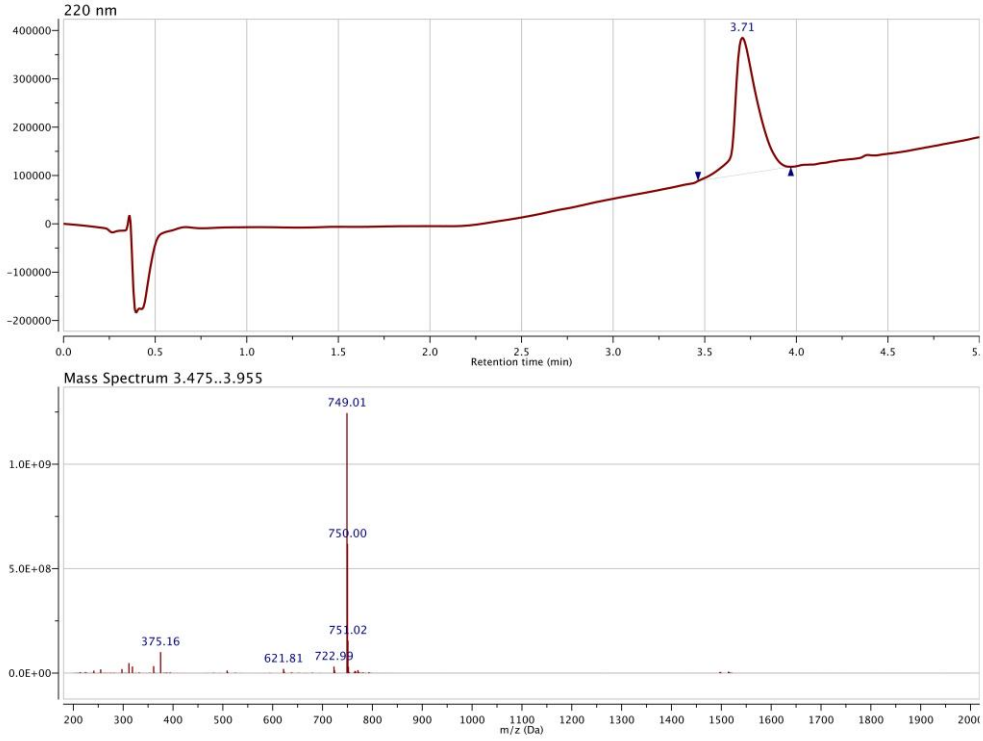

13

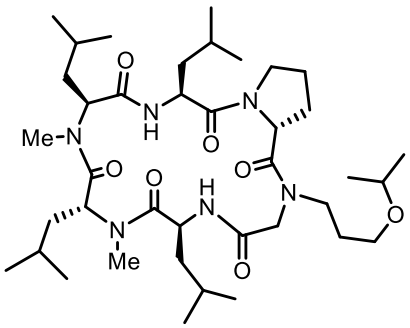

Chemical Formula: $C_{39}H_{70}N_6O_7$
Exact Mass: 734.53
Molecular Weight: 735.02

ESI cacld. for $C_{39}H_{70}N_6O_7[M+H]^+$ *m/*z = 735.53; found 736.03.

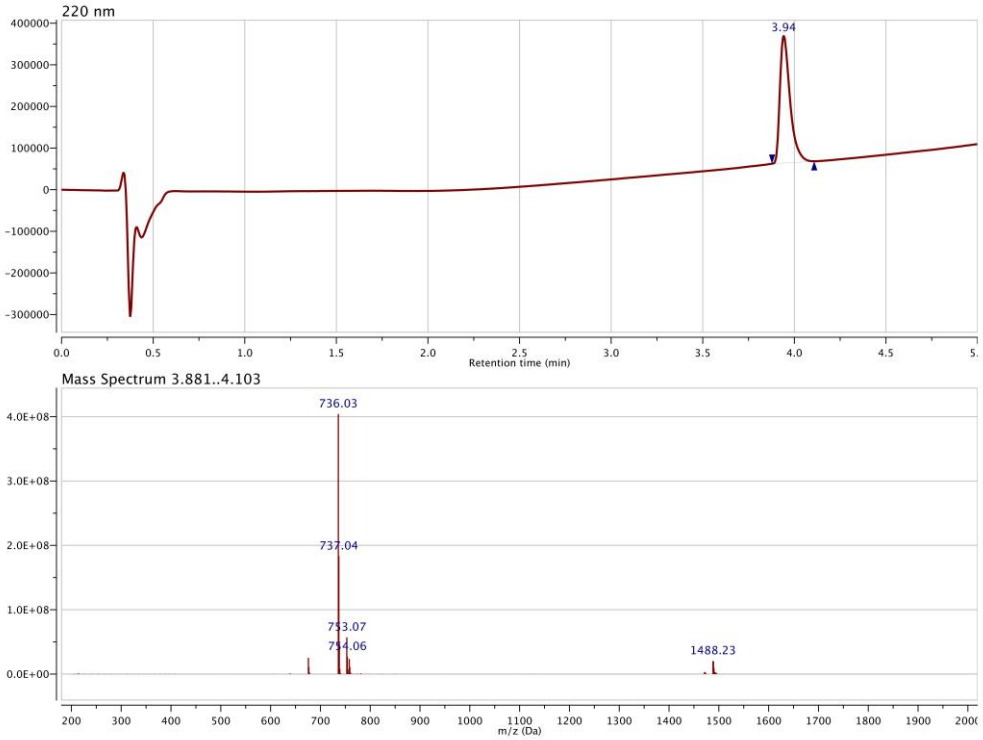

2.8.6. Selected NMR Spectra

2 ^{1}H $CDCl_3$

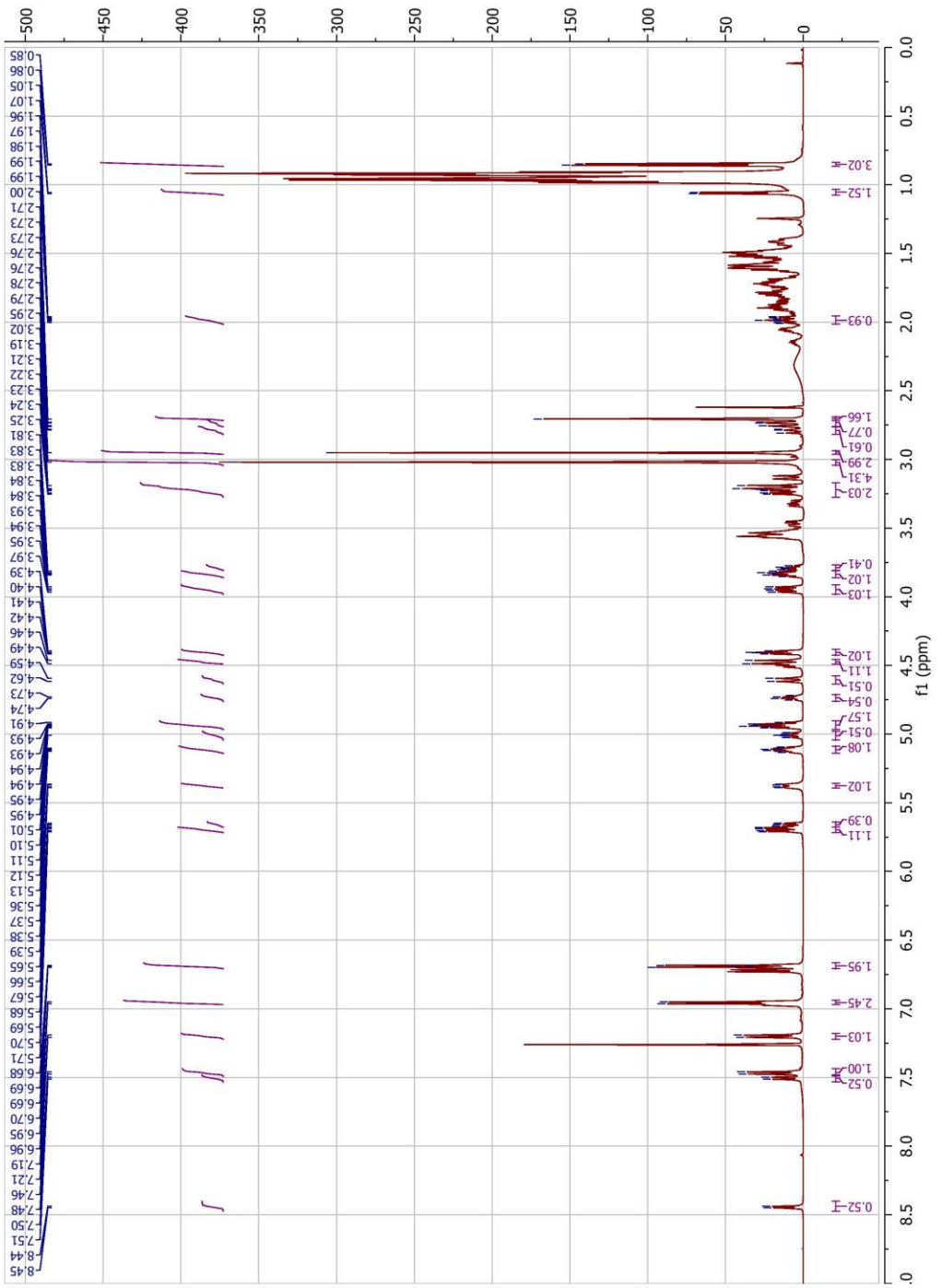

2 ^{13}C $CDCl_3$

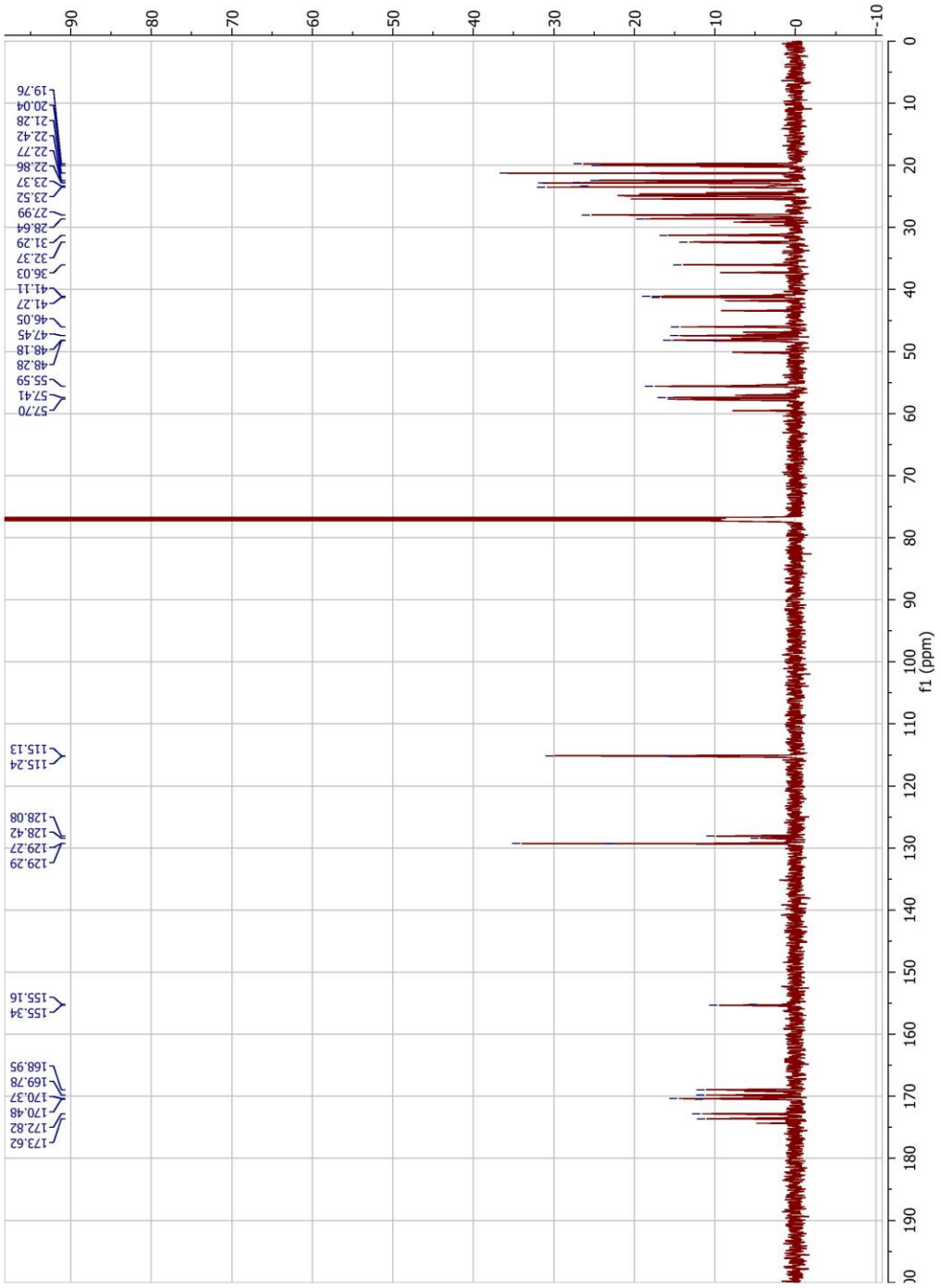
19.76
20.04
21.28
22.42
22.77
22.86
23.37
23.52
27.99
28.64
31.29
32.37
36.03
41.11
41.27
46.05
47.45
48.18
48.28
55.59
57.41
57.70
115.13
115.24
128.08
128.42
129.27
129.29
155.16
155.34
168.95
169.78
170.37
170.48
172.82
173.62
f1 (ppm)

2 COSY

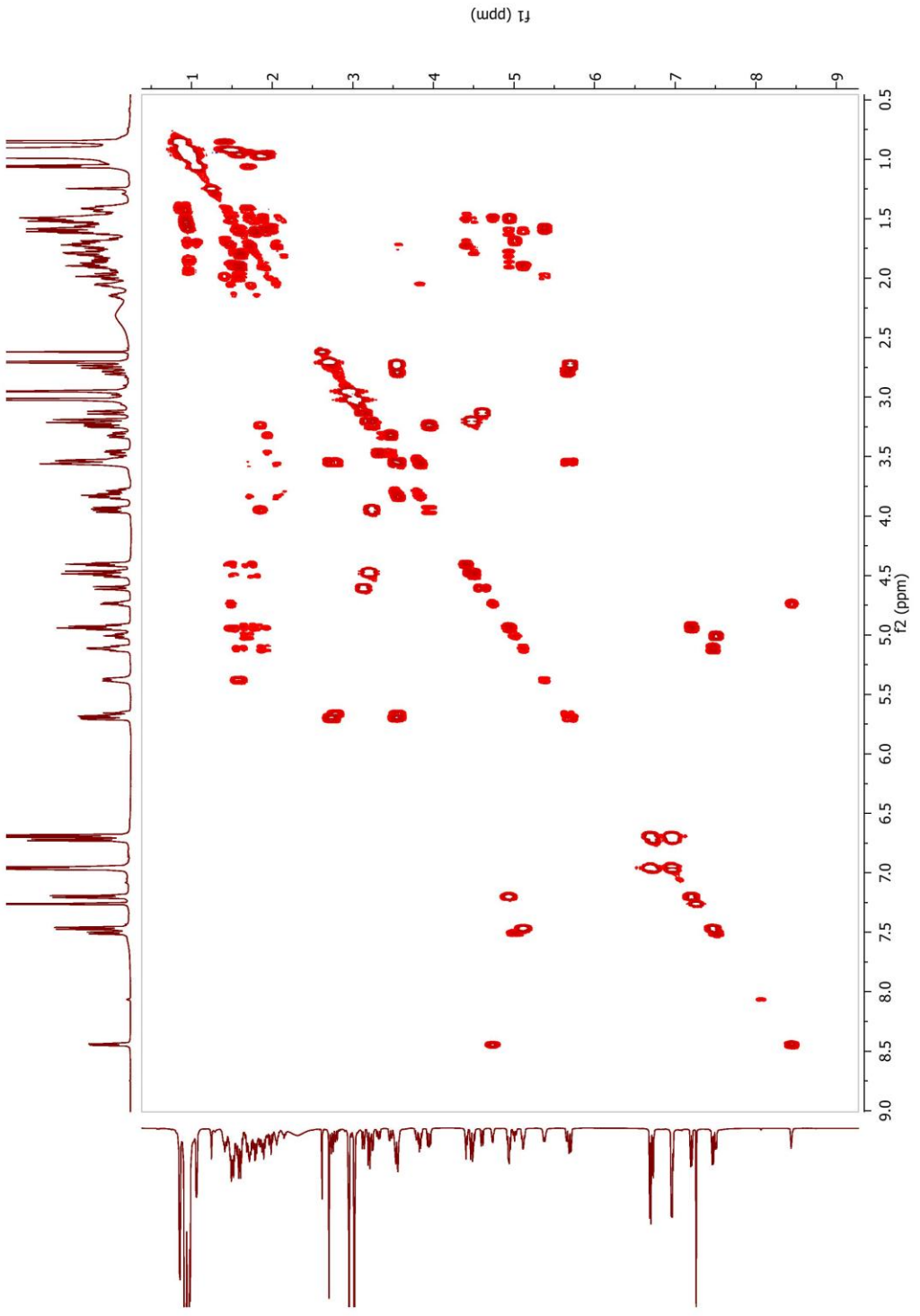

2 TOCSY

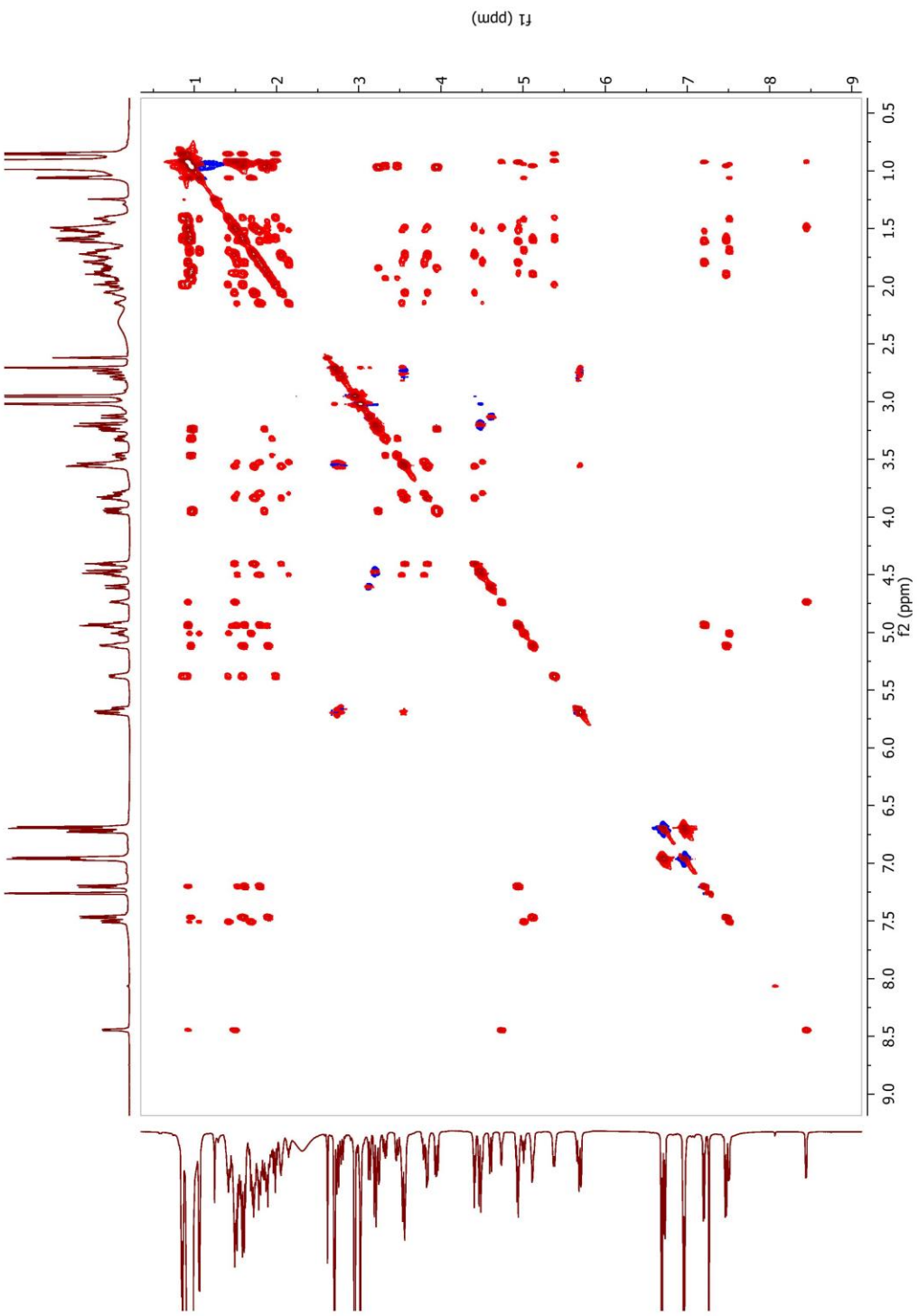
f1 (ppm)
f2 (ppm)

2 HSQC

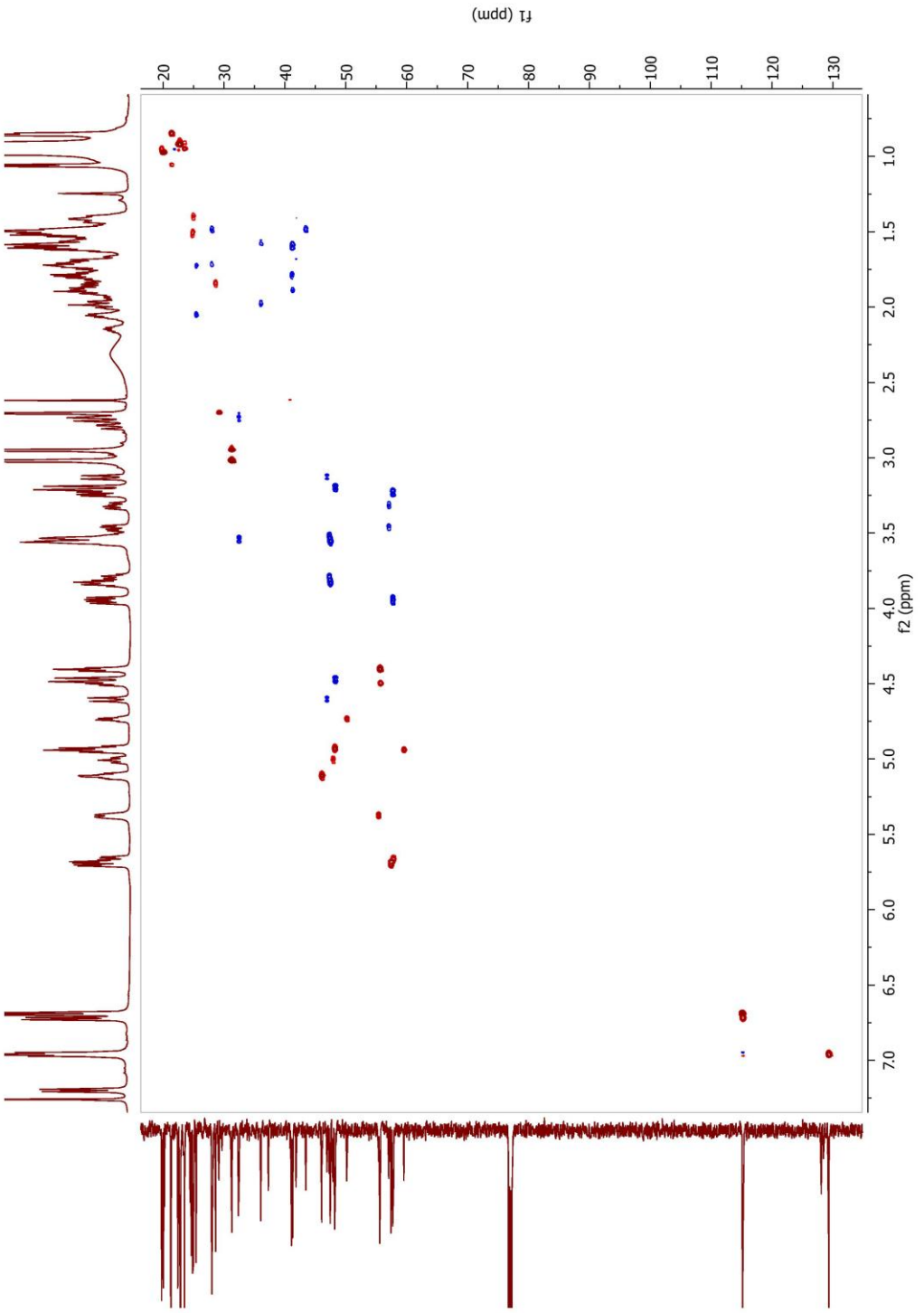
f1 (ppm)
20
30
40
50
60
70
80
90
100
110
120
130
f2 (ppm)
1.0
1.5
2.0
2.5
3.0
3.5
4.0
4.5
5.0
5.5
6.0
6.5
7.0

2 HMBC

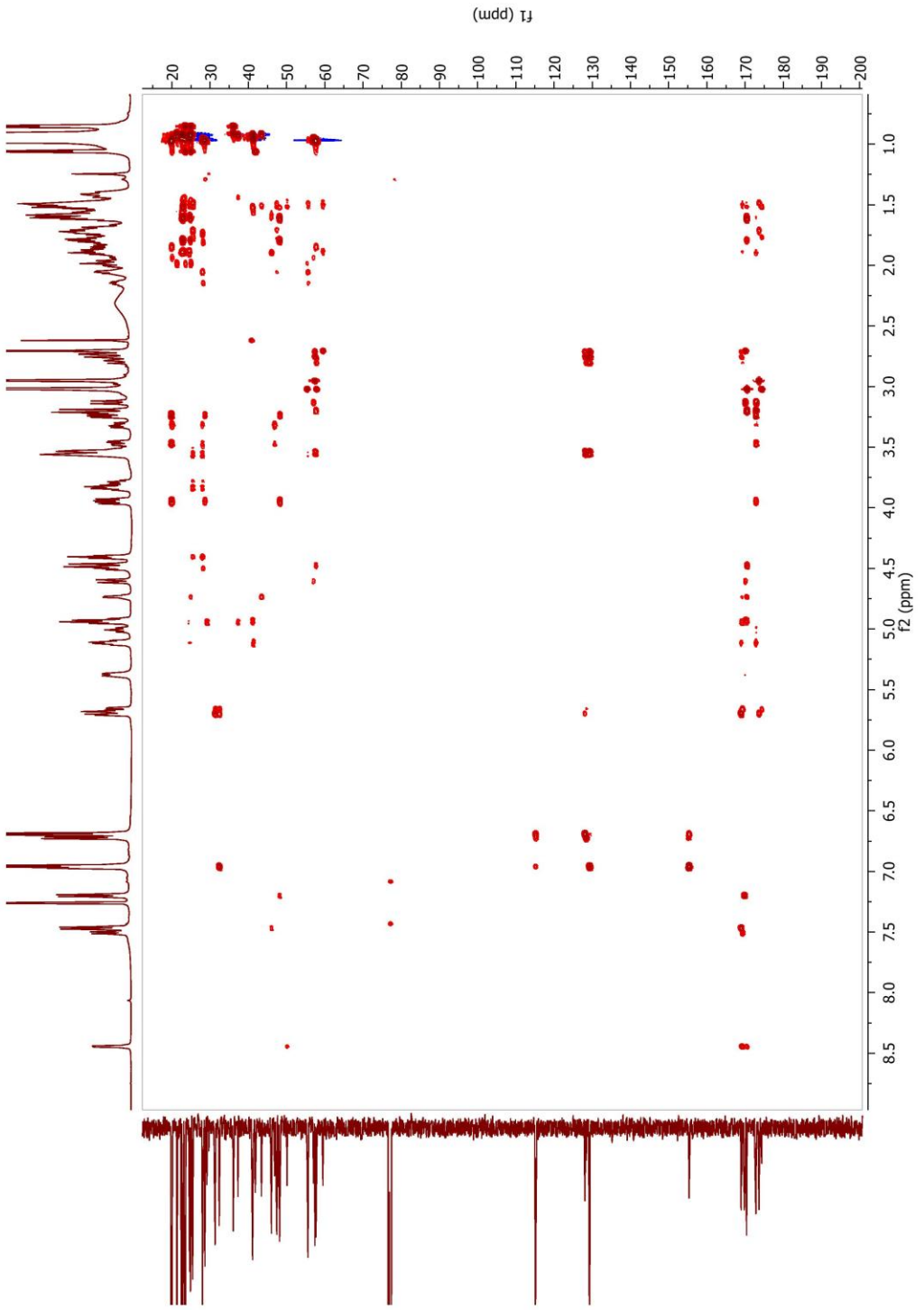

2 ROESY 200 ms

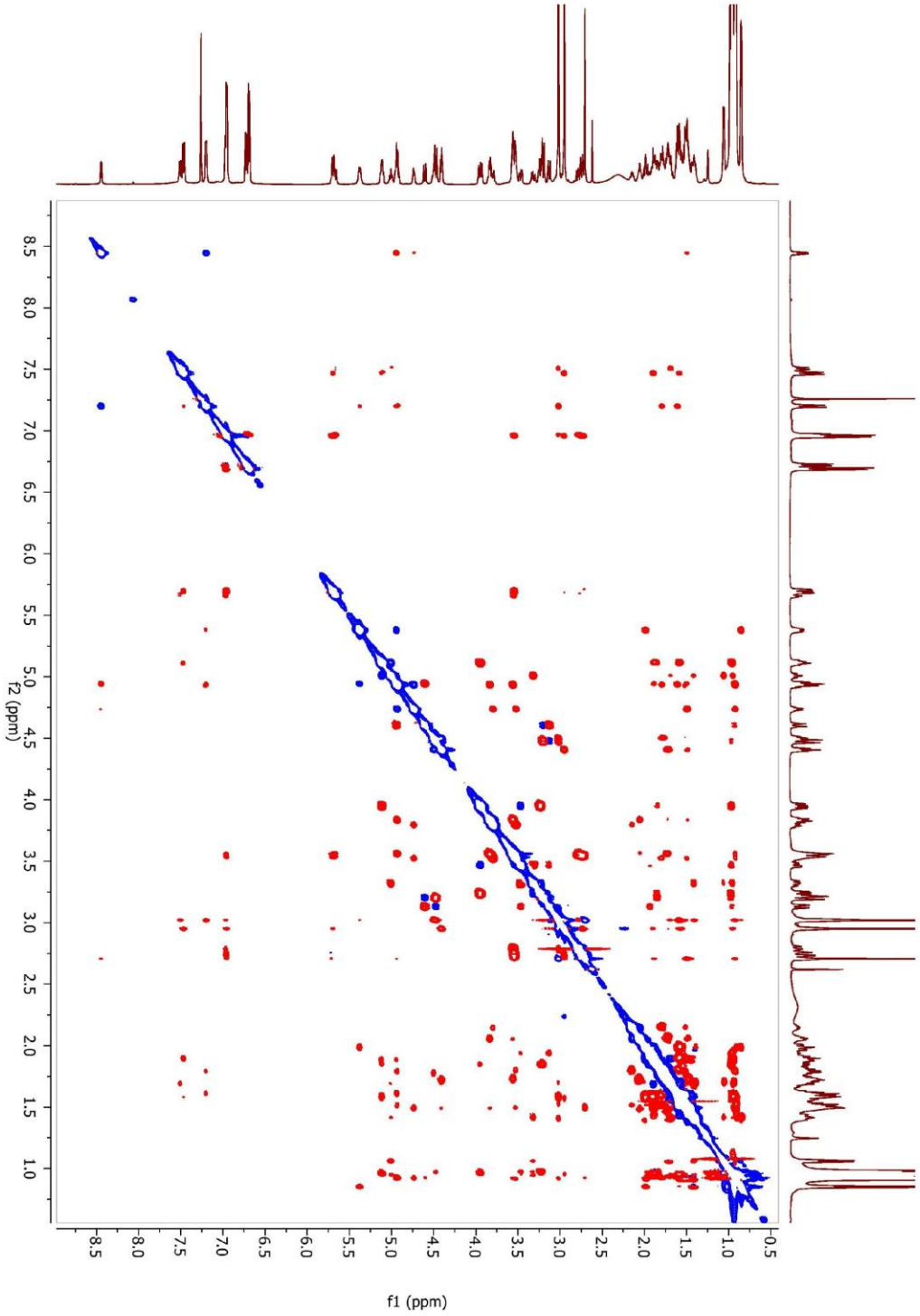

3 ^{1}H $CDCl_3$

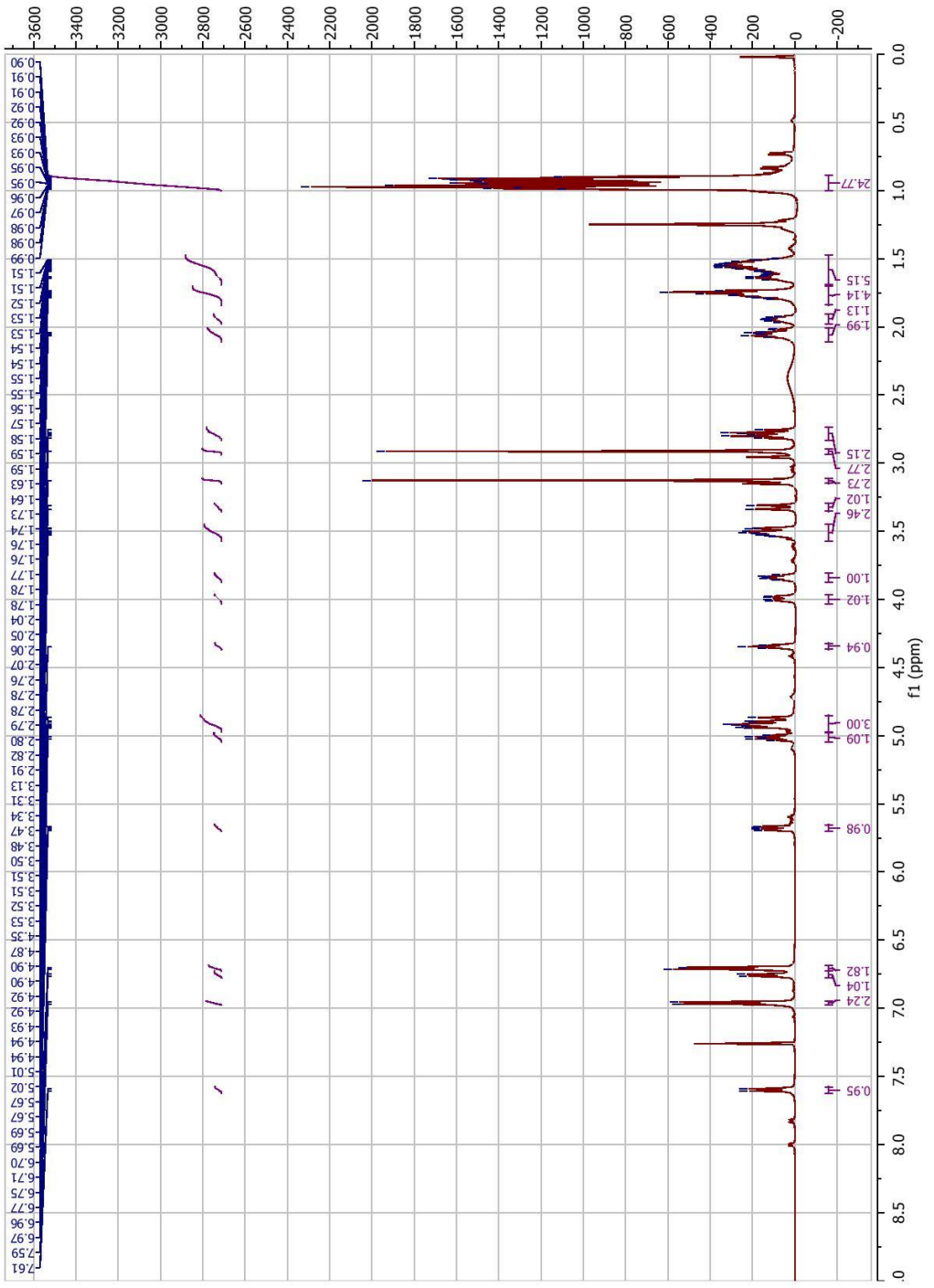

3 ^{13}C $CDCl_3$

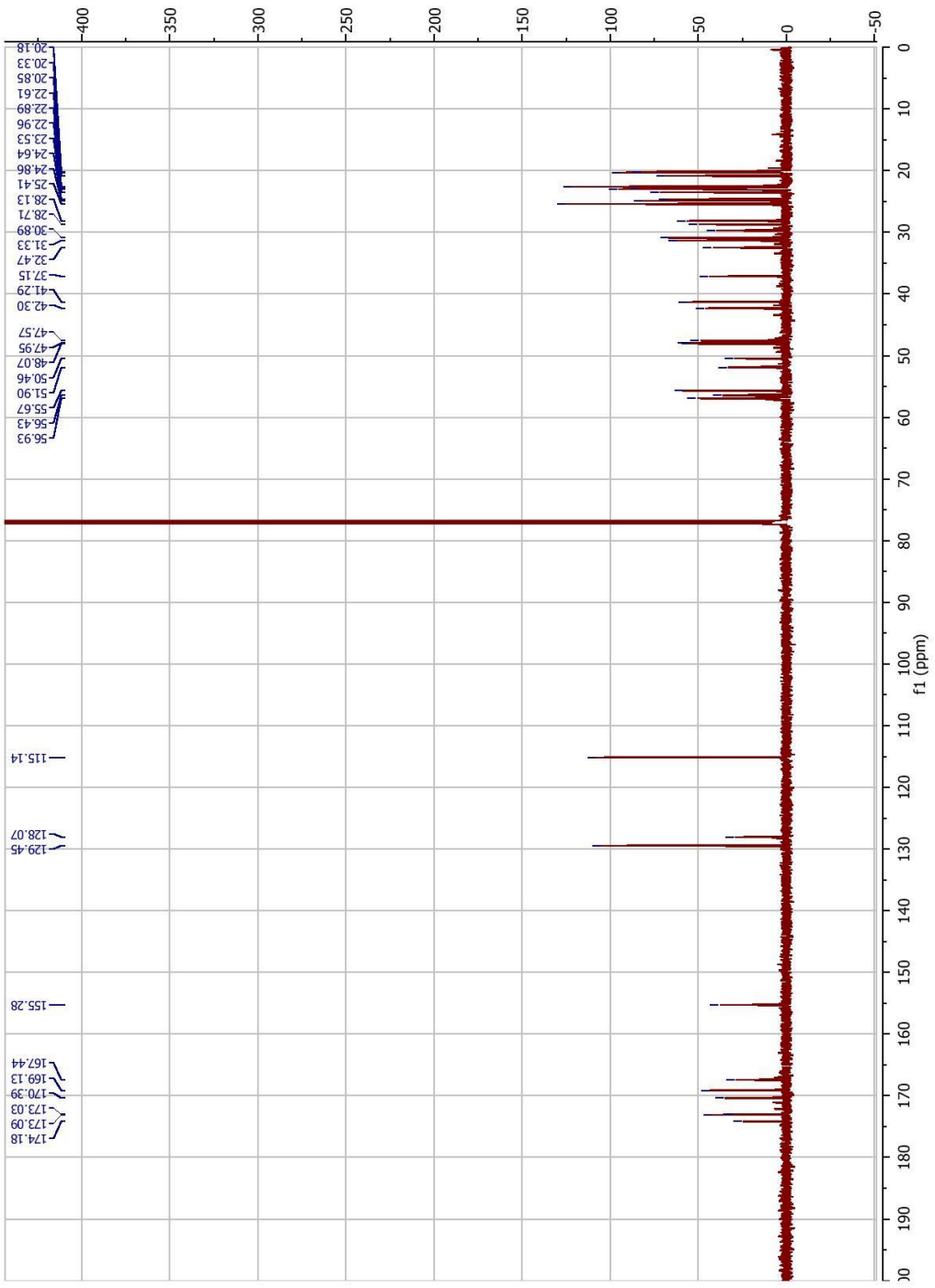
20.18
20.33
20.85
22.61
22.89
22.96
23.53
24.64
24.86
25.41
28.13
28.71
30.89
31.33
32.47
37.15
41.29
42.30
47.57
47.95
48.07
50.46
51.90
55.67
56.43
56.93
115.14
128.07
129.45
155.28
167.44
169.13
170.39
173.03
173.09
174.18
f1 (ppm)

3 COSY

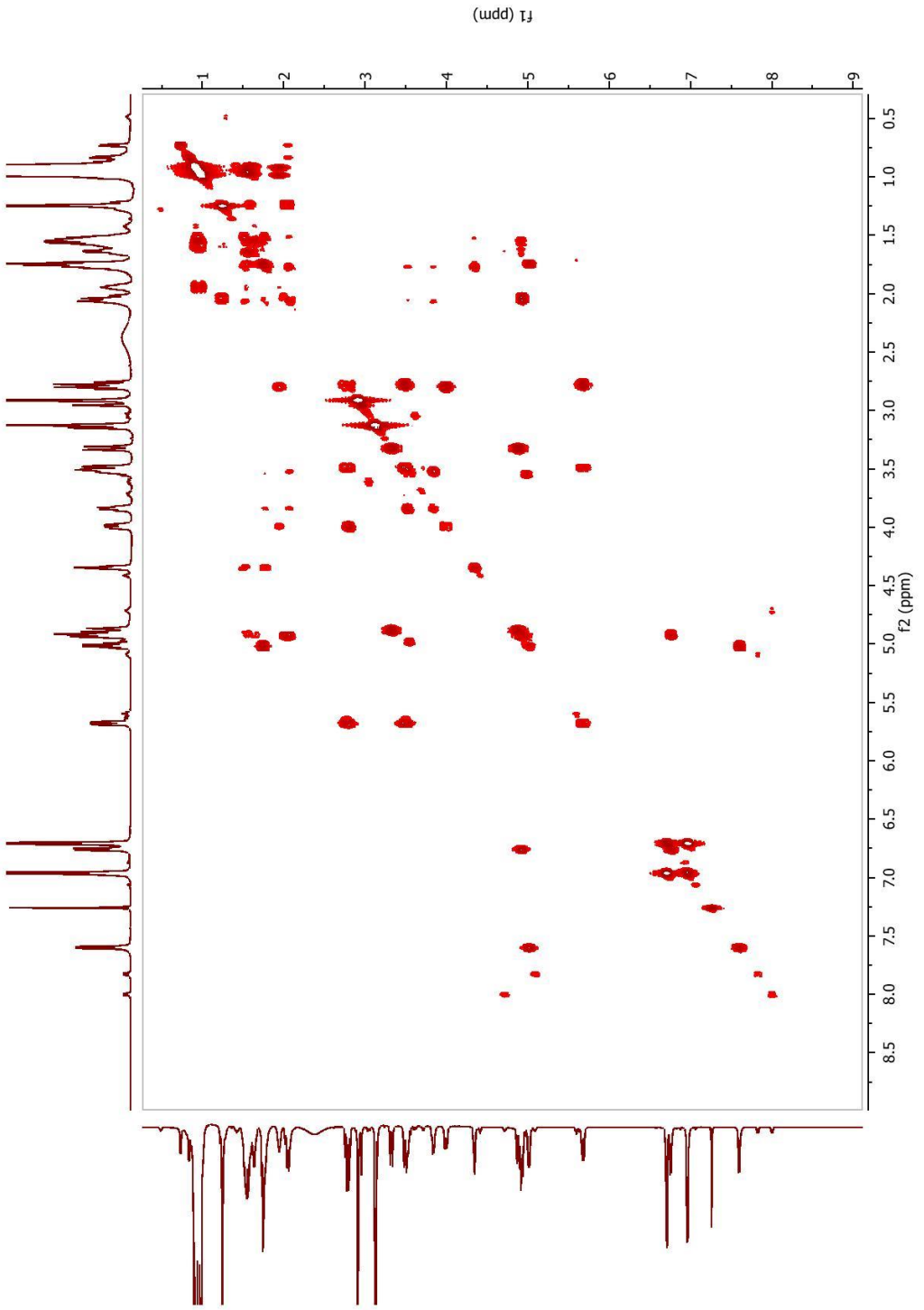

3TOCSY

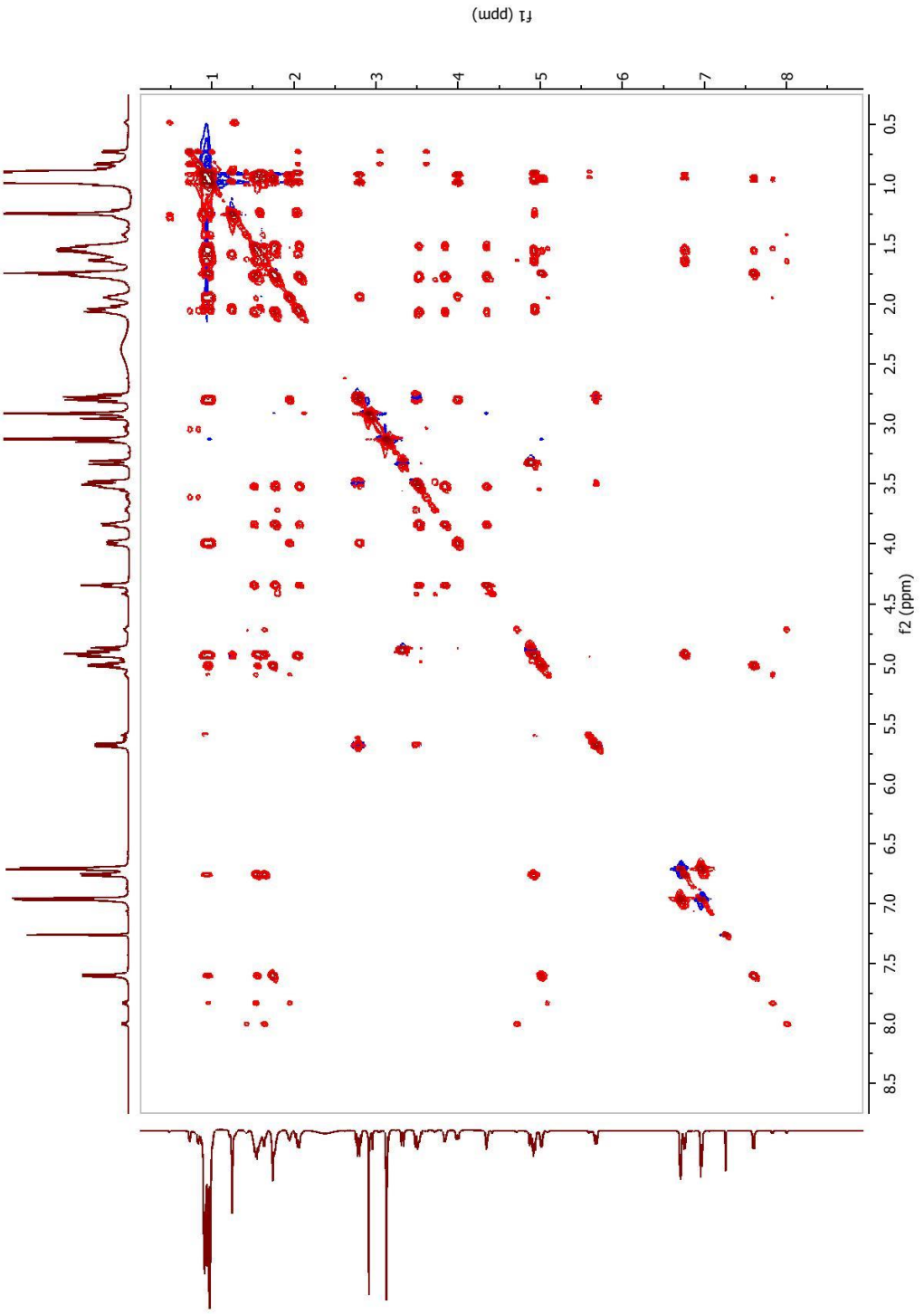

3 HSQC

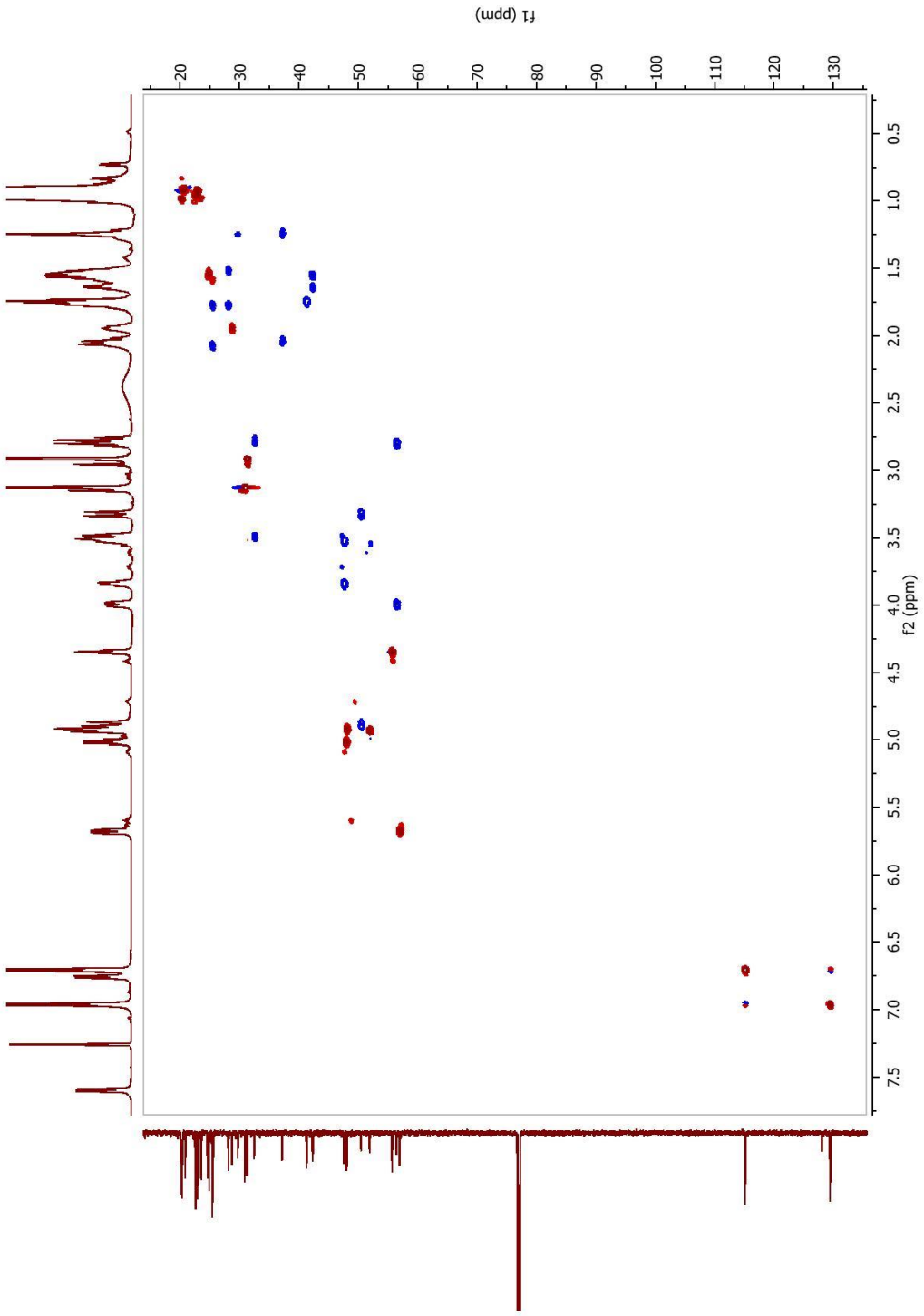
f1 (ppm)
20
30
40
50
60
70
80
90
100
110
120
130
0.5
1.0
1.5
2.0
2.5
3.0
3.5
4.0
4.5
5.0
5.5
6.0
6.5
7.0
7.5
f2 (ppm)

3 HMBC

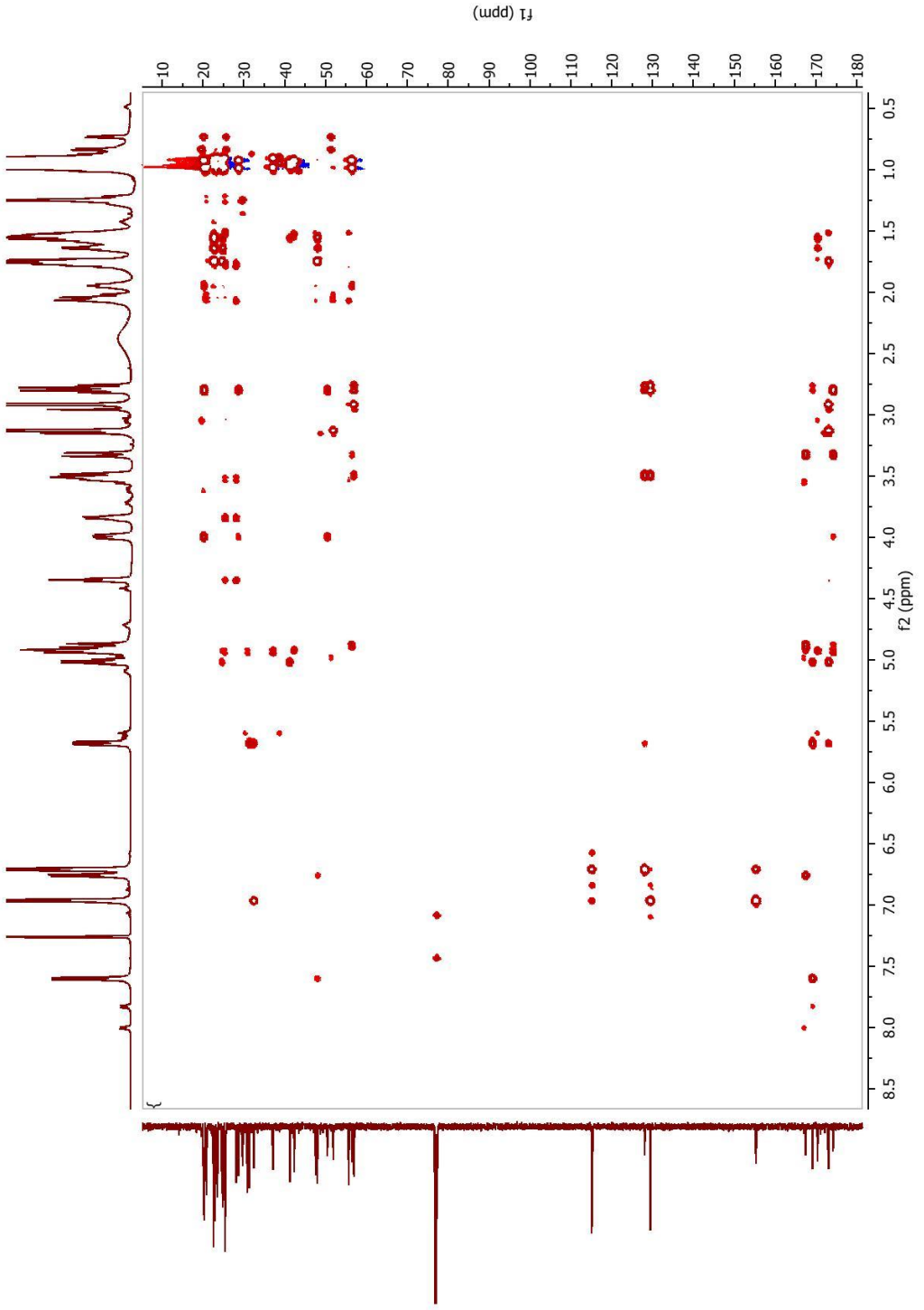

3 ROESY 200 ms

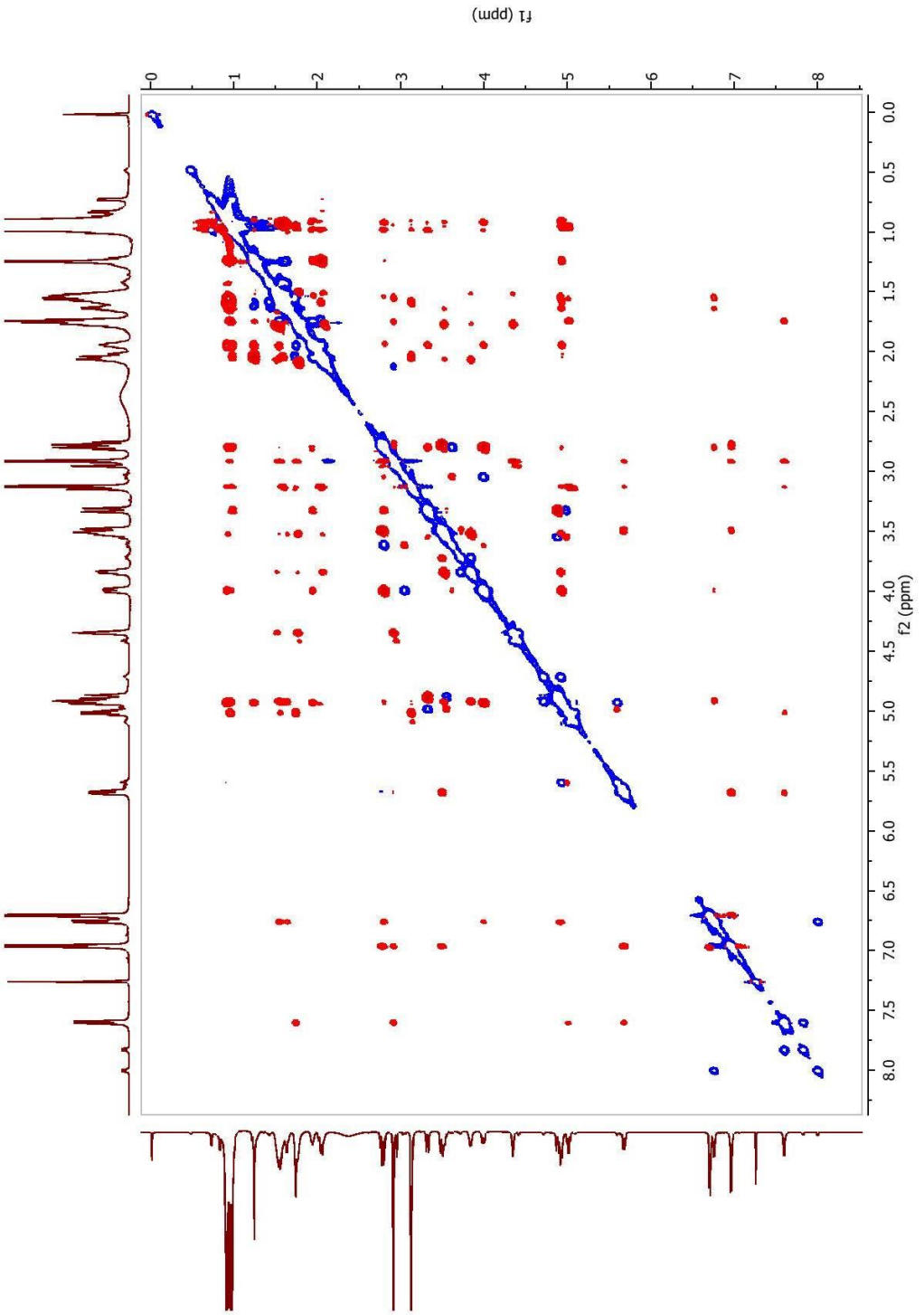

1 ^{1}H $CDCl_3$

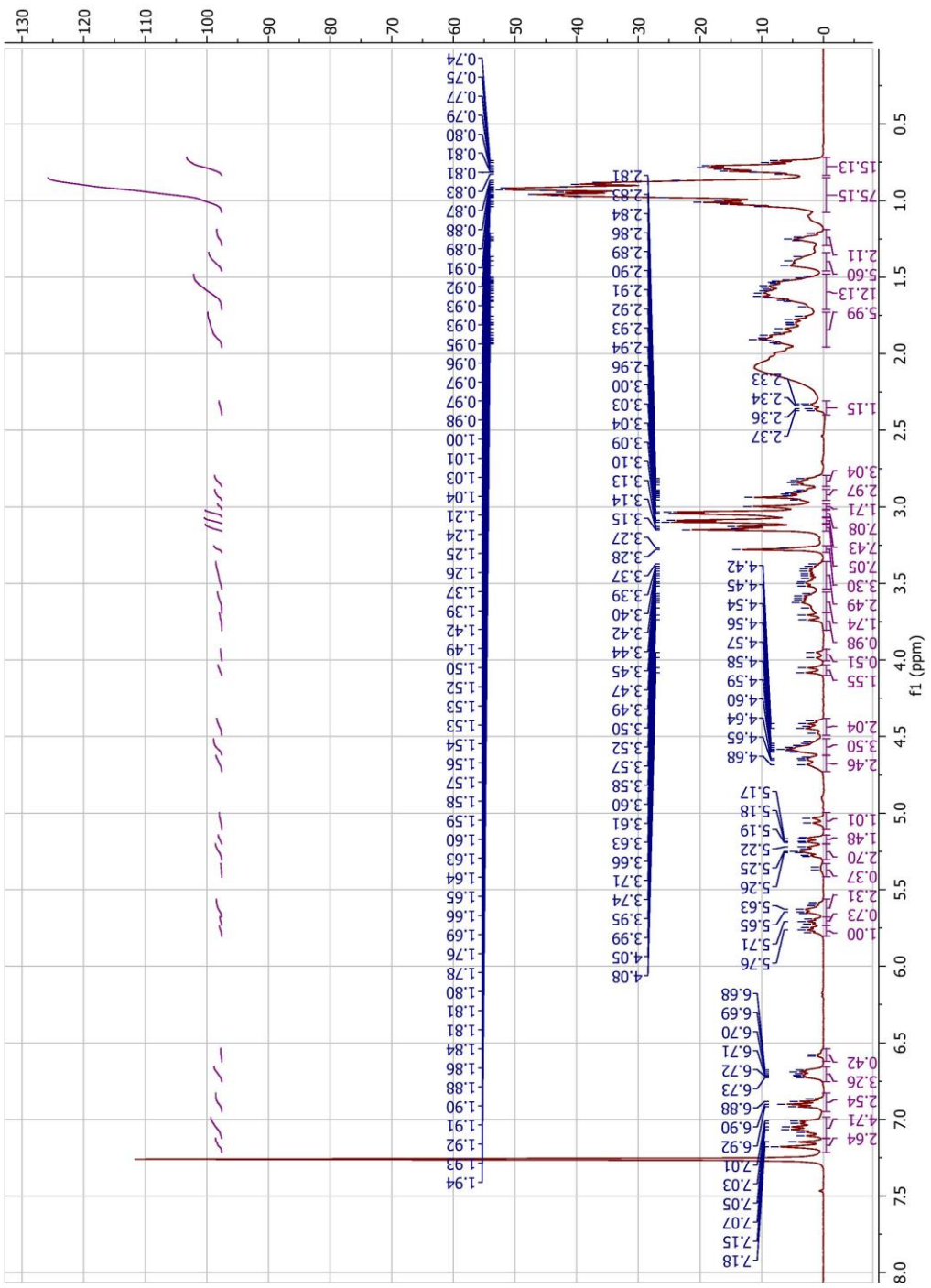

4 ^{1}H $CDCl_3$

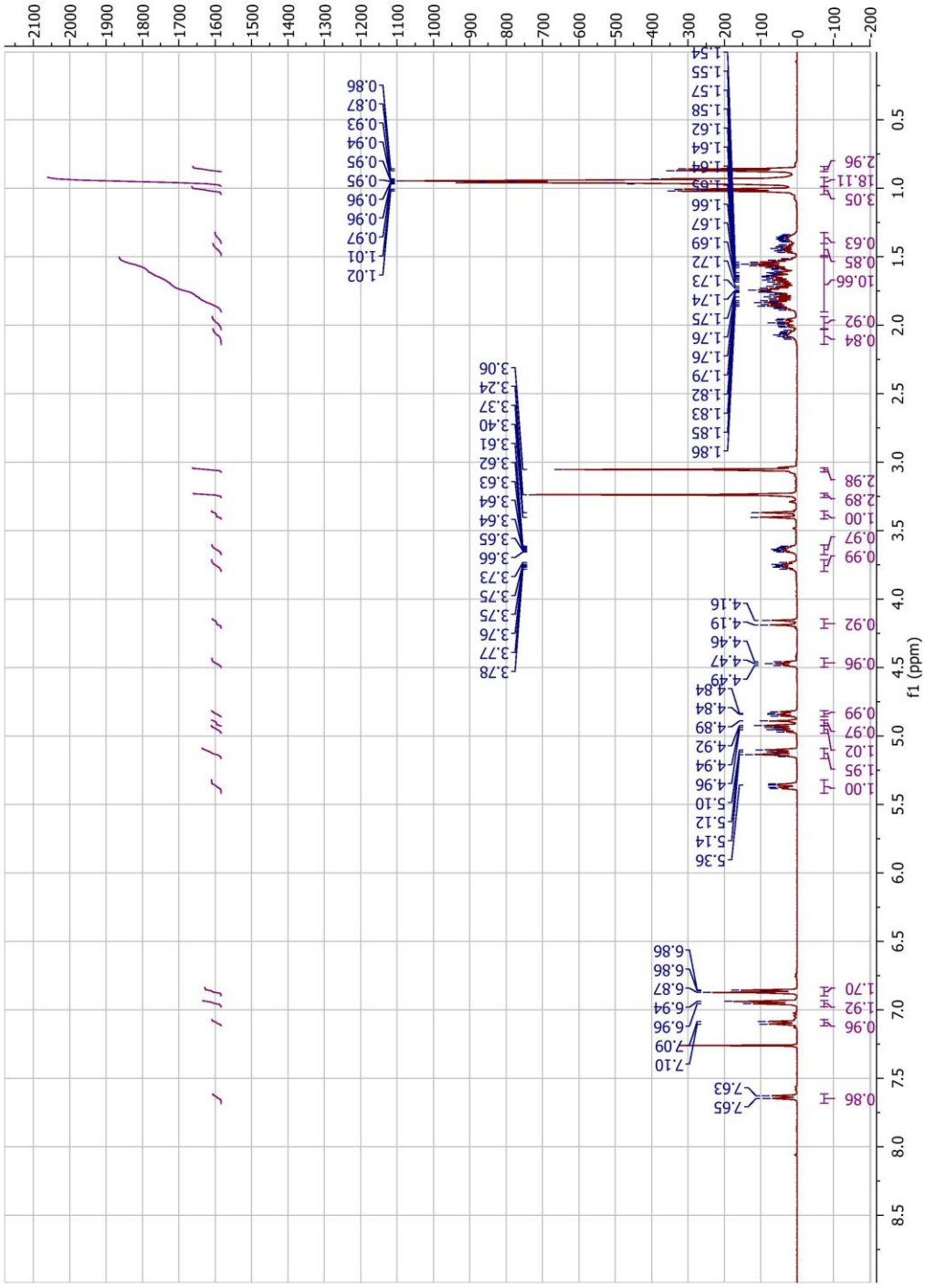

5 ^{1}H *d*3 Acetonitrile

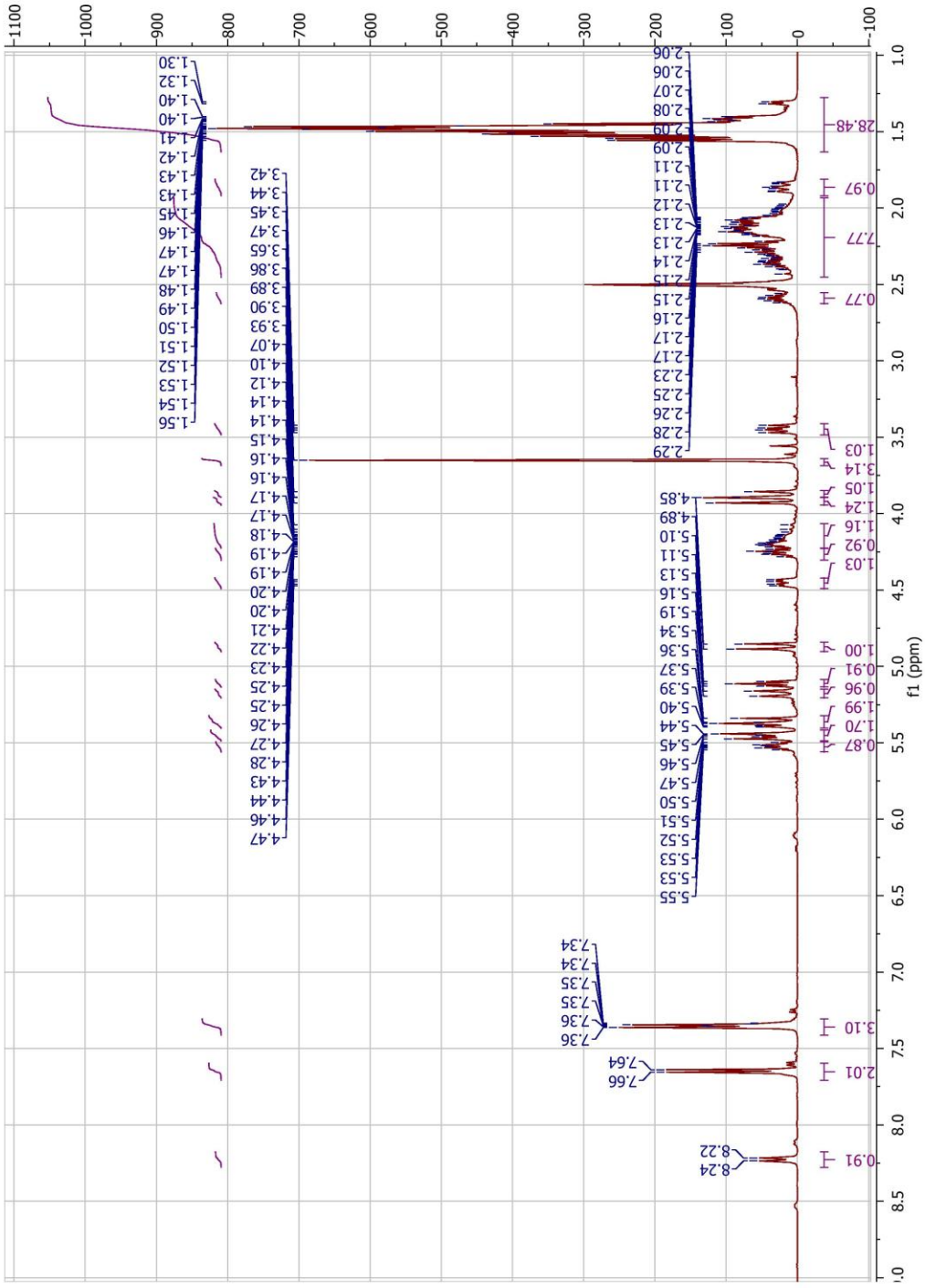

6 ^{1}H *d*3 Acetonitrile

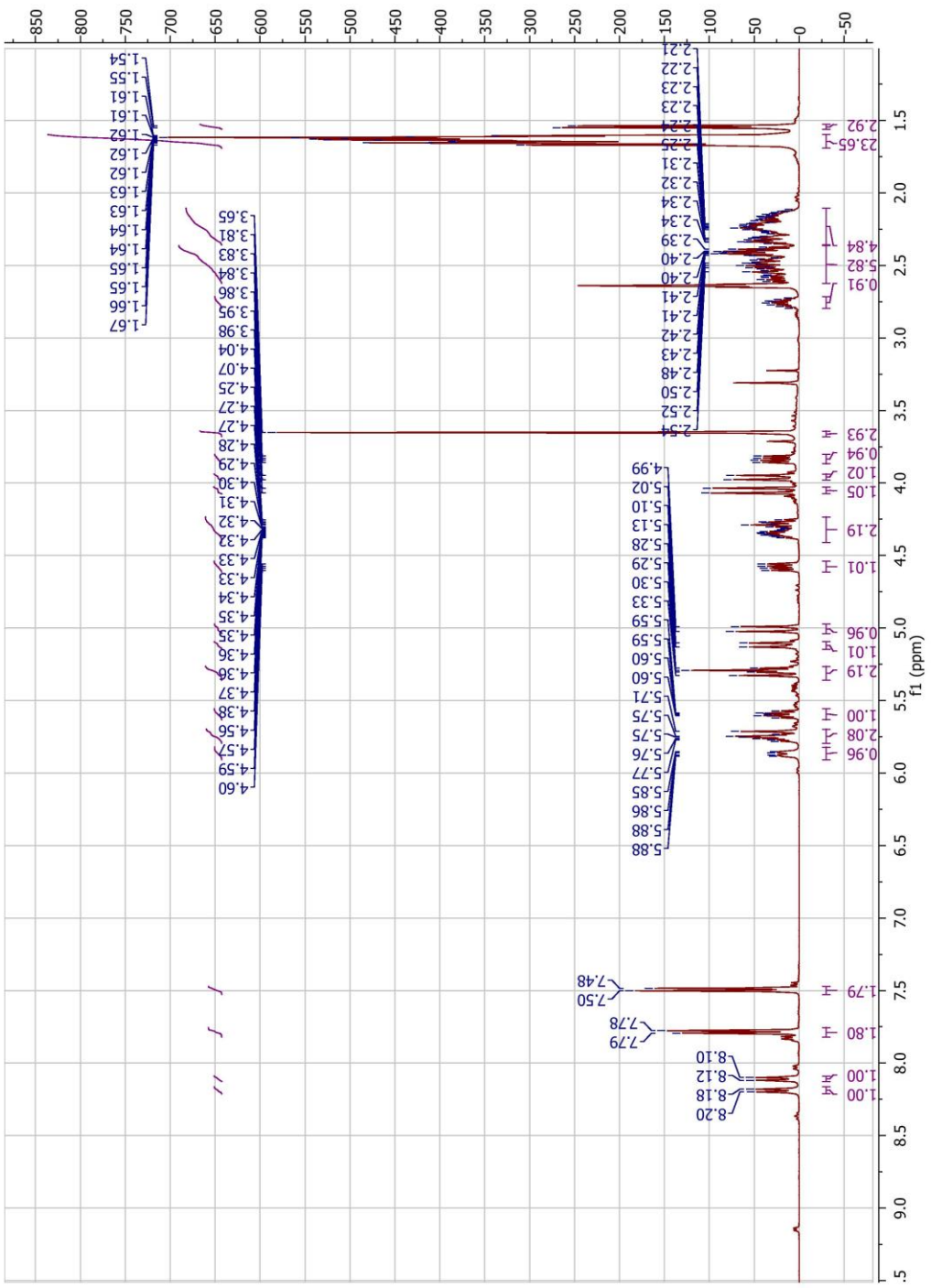

7 ^{1}H *d*3 Acetonitrile

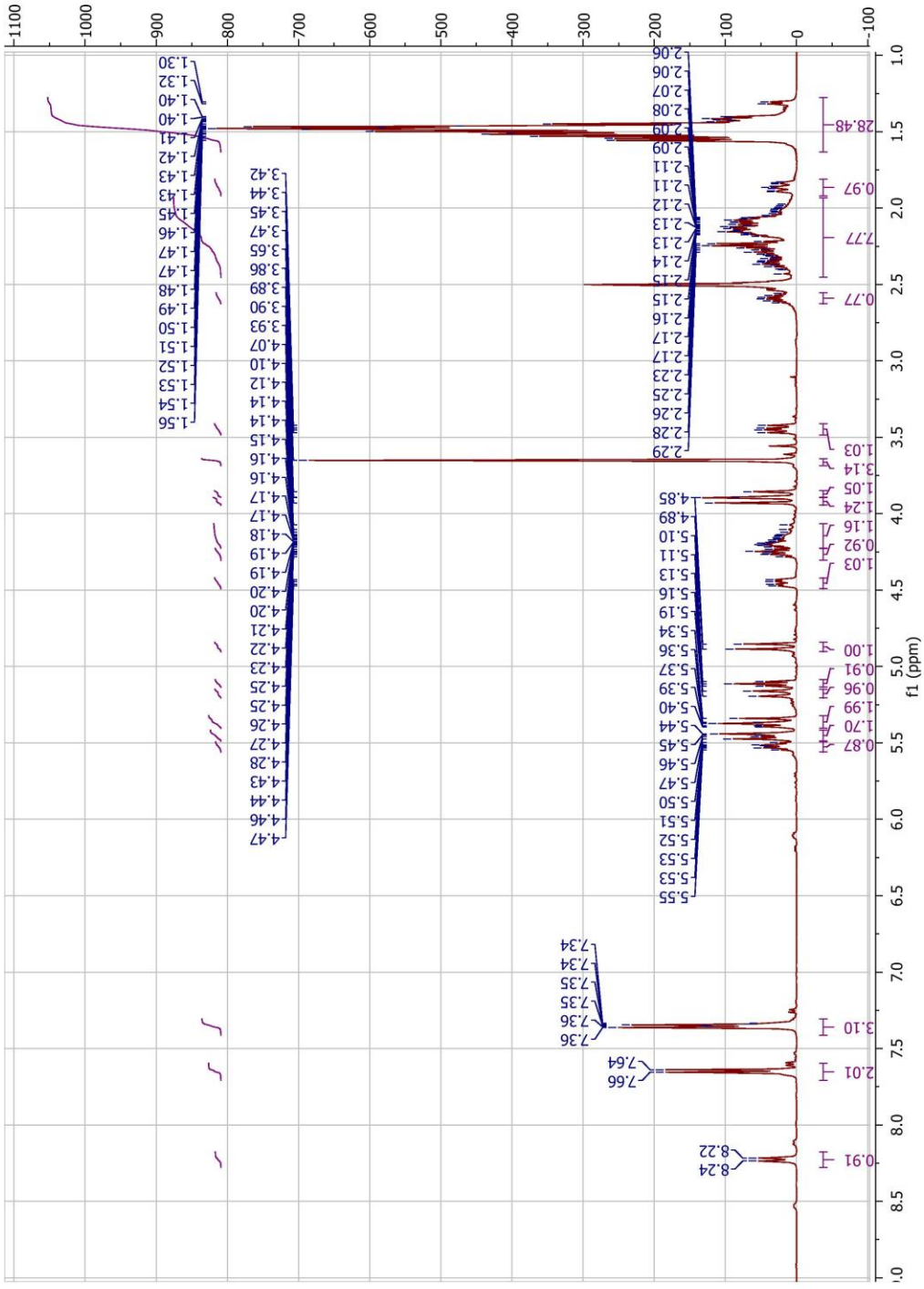

8 ^{1}H $CDCl_3$

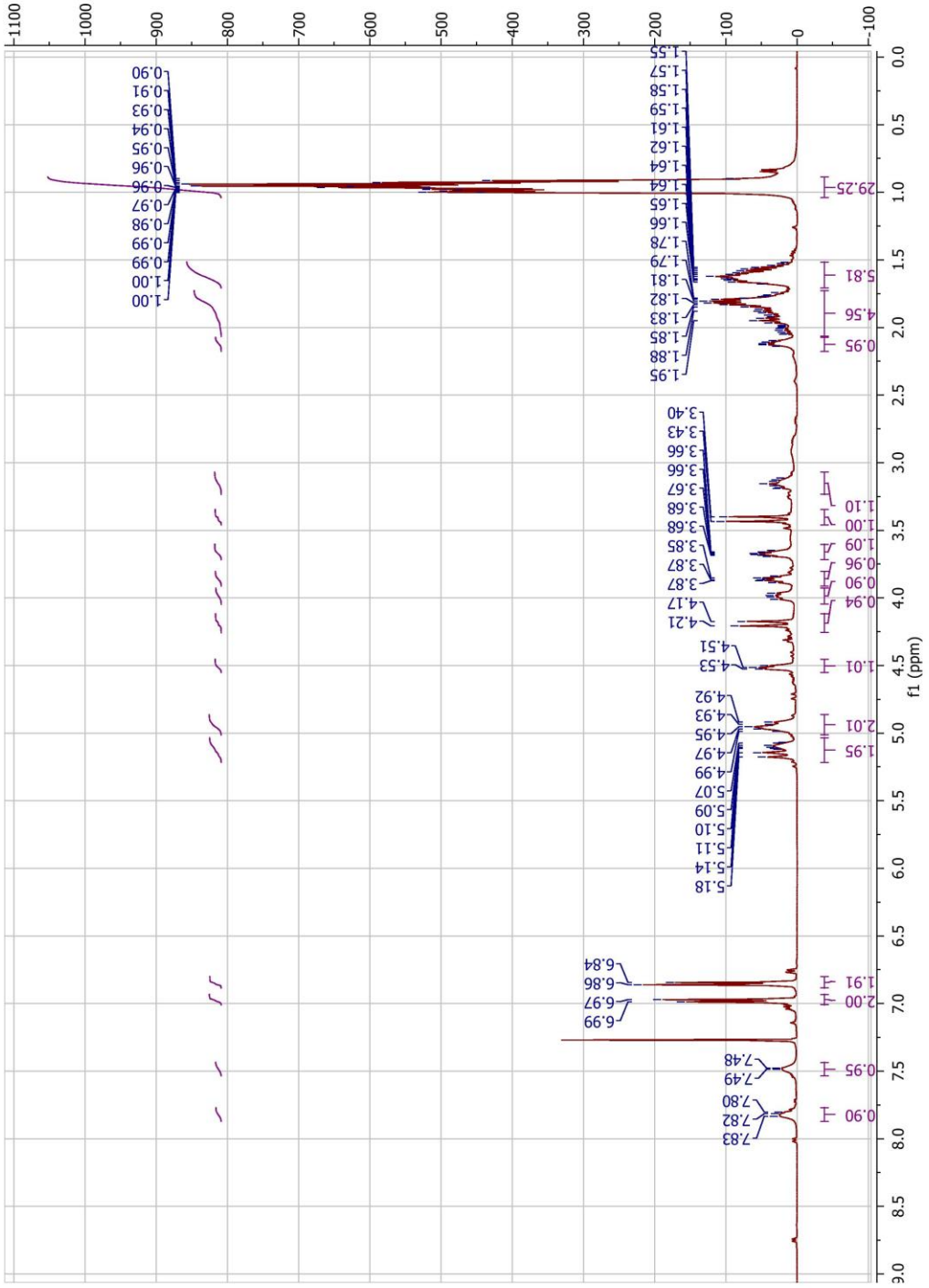

9 ^{1}H $CDCl_3$

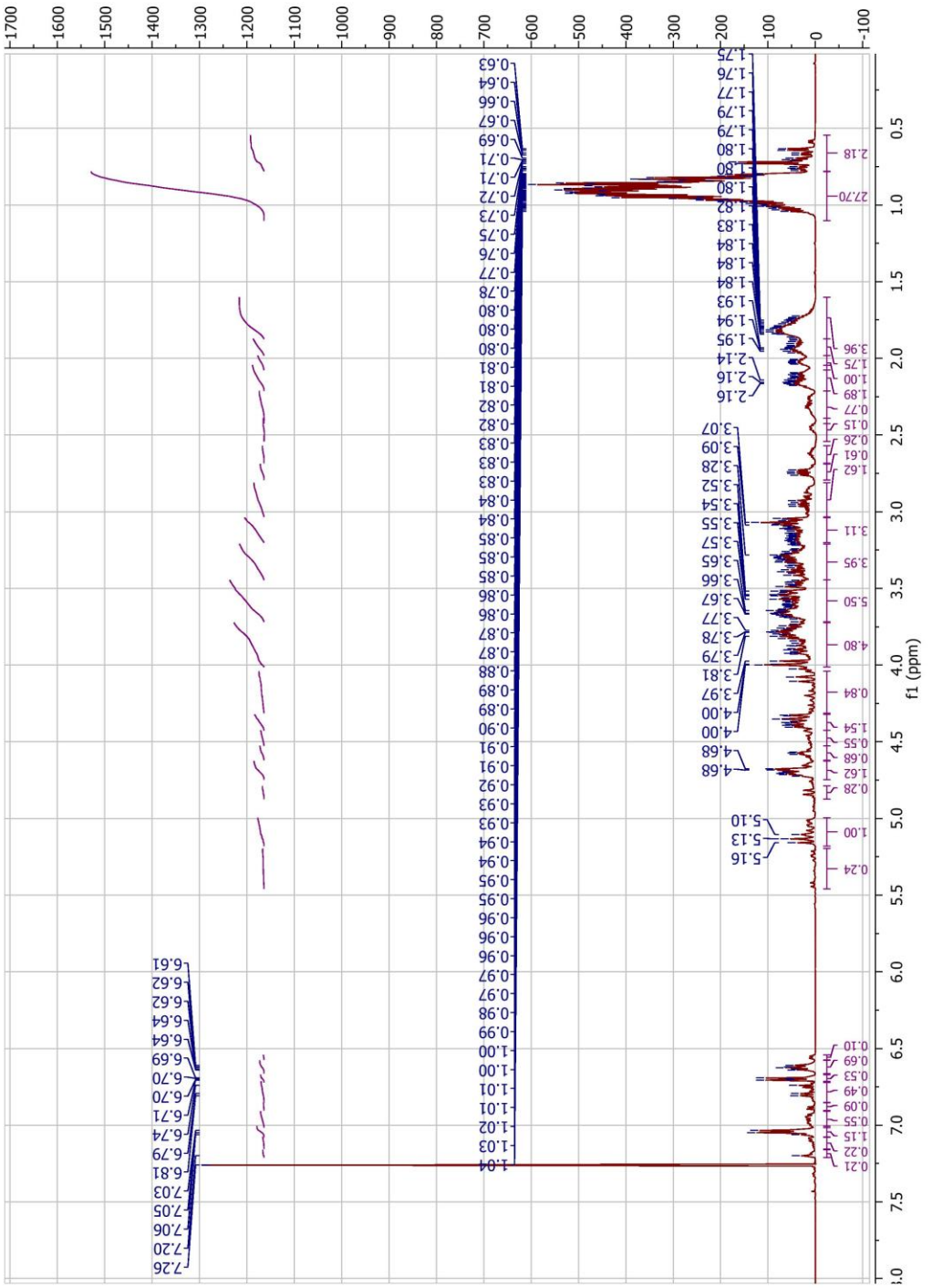

10 ^{1}H $CDCl_3$

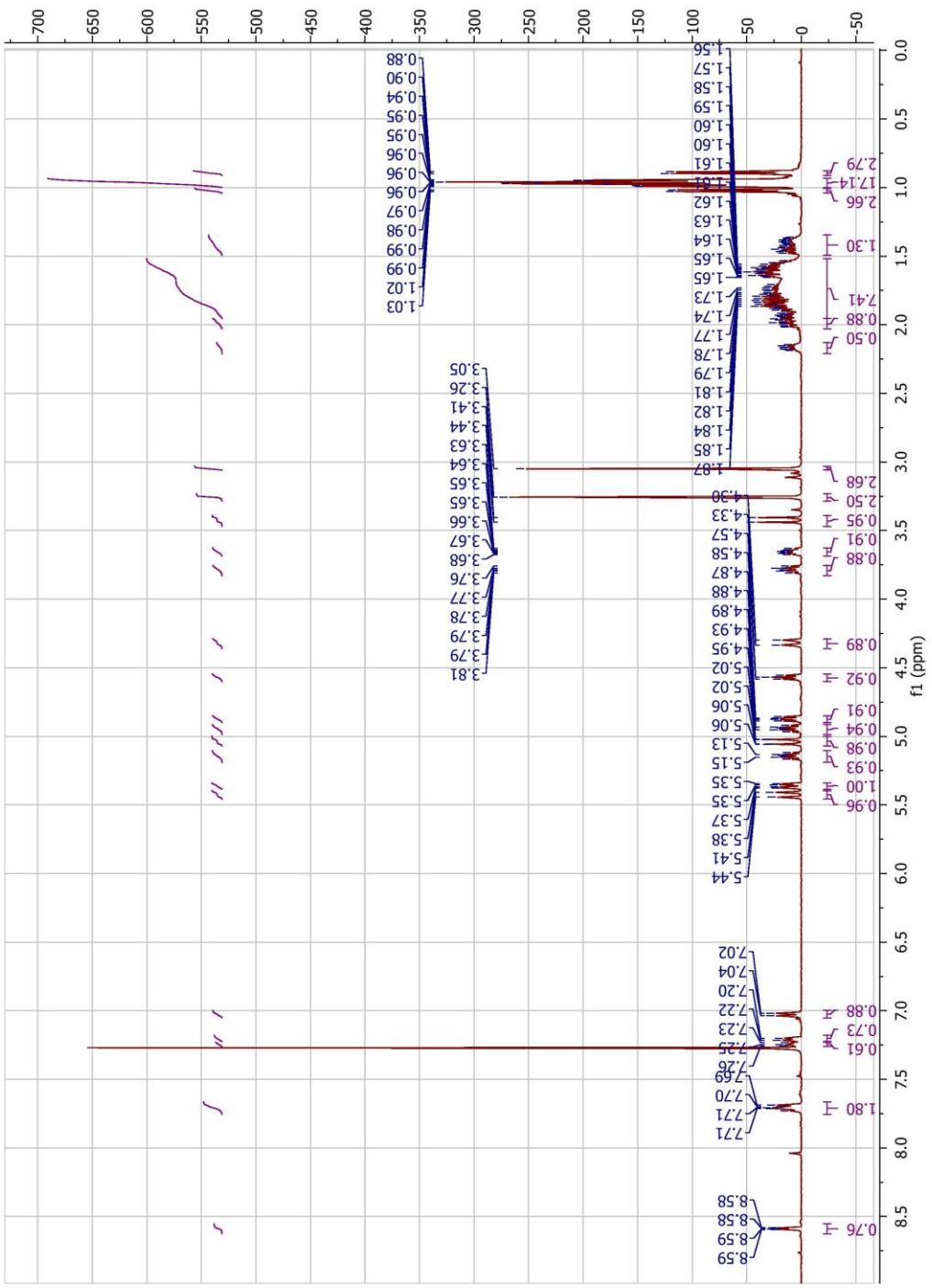

11 ^{1}H $CDCl_3$

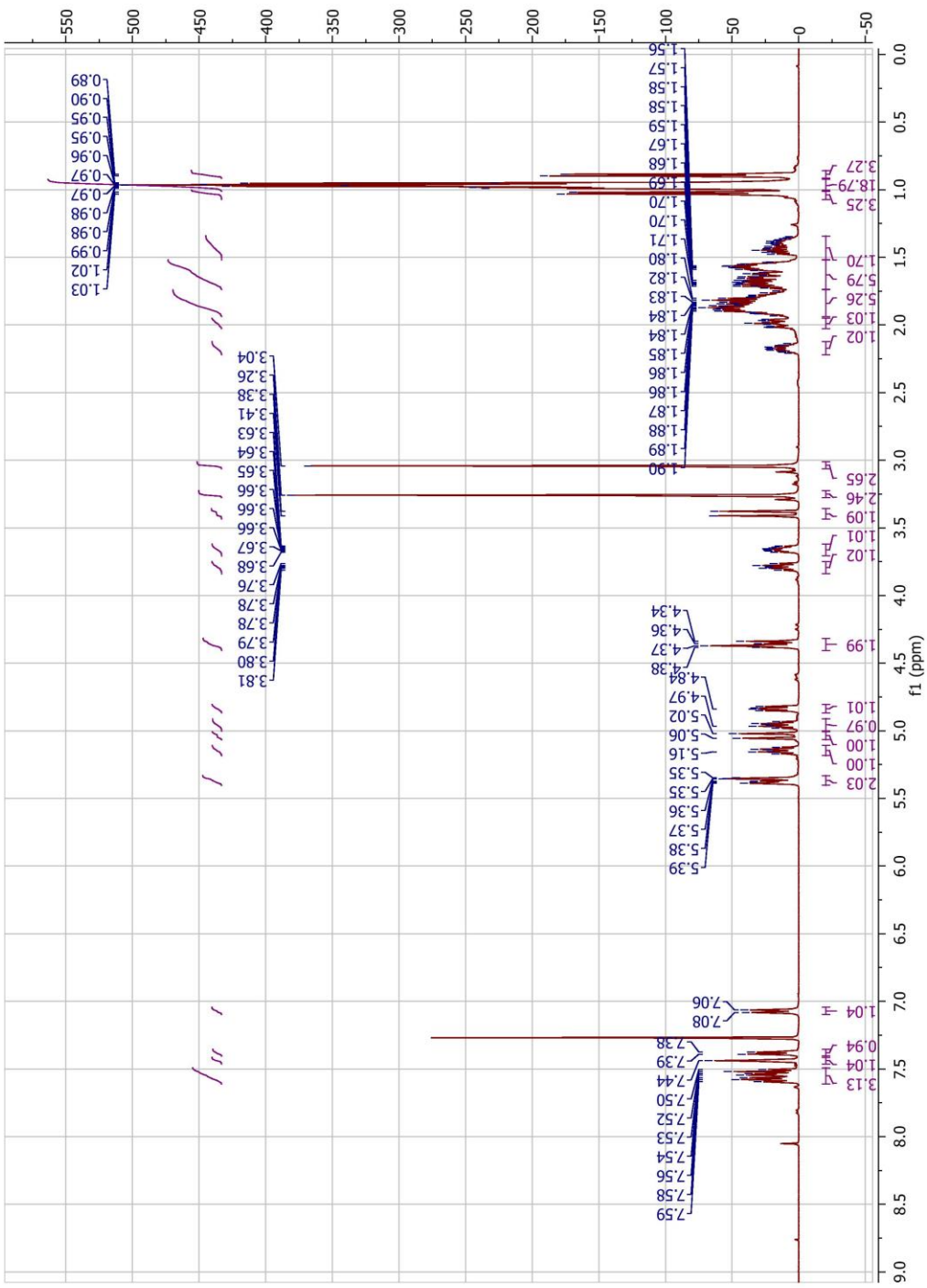

12 ^{1}H *d3* acetonitrile

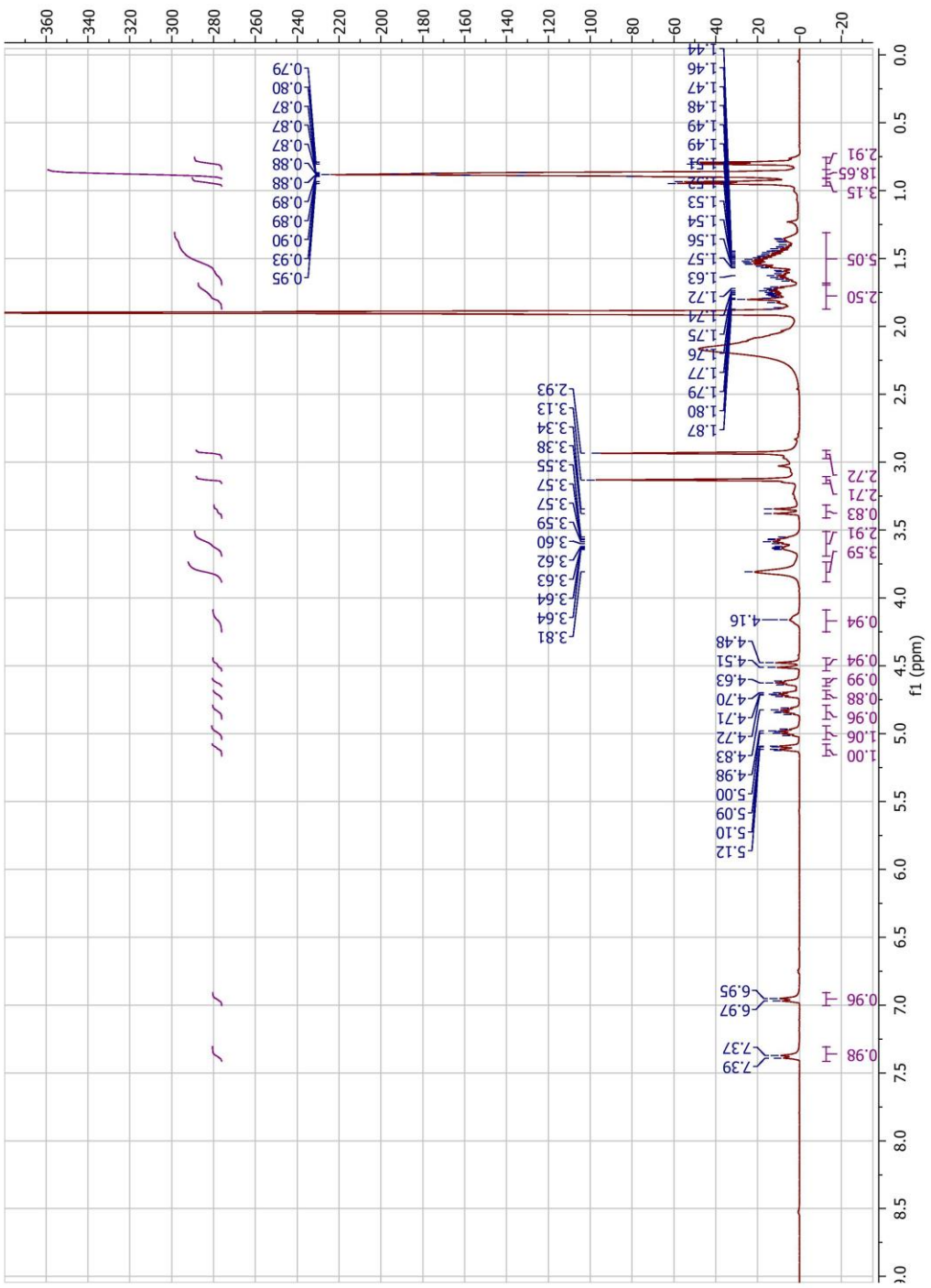

13 ^{1}H $CDCl_3$

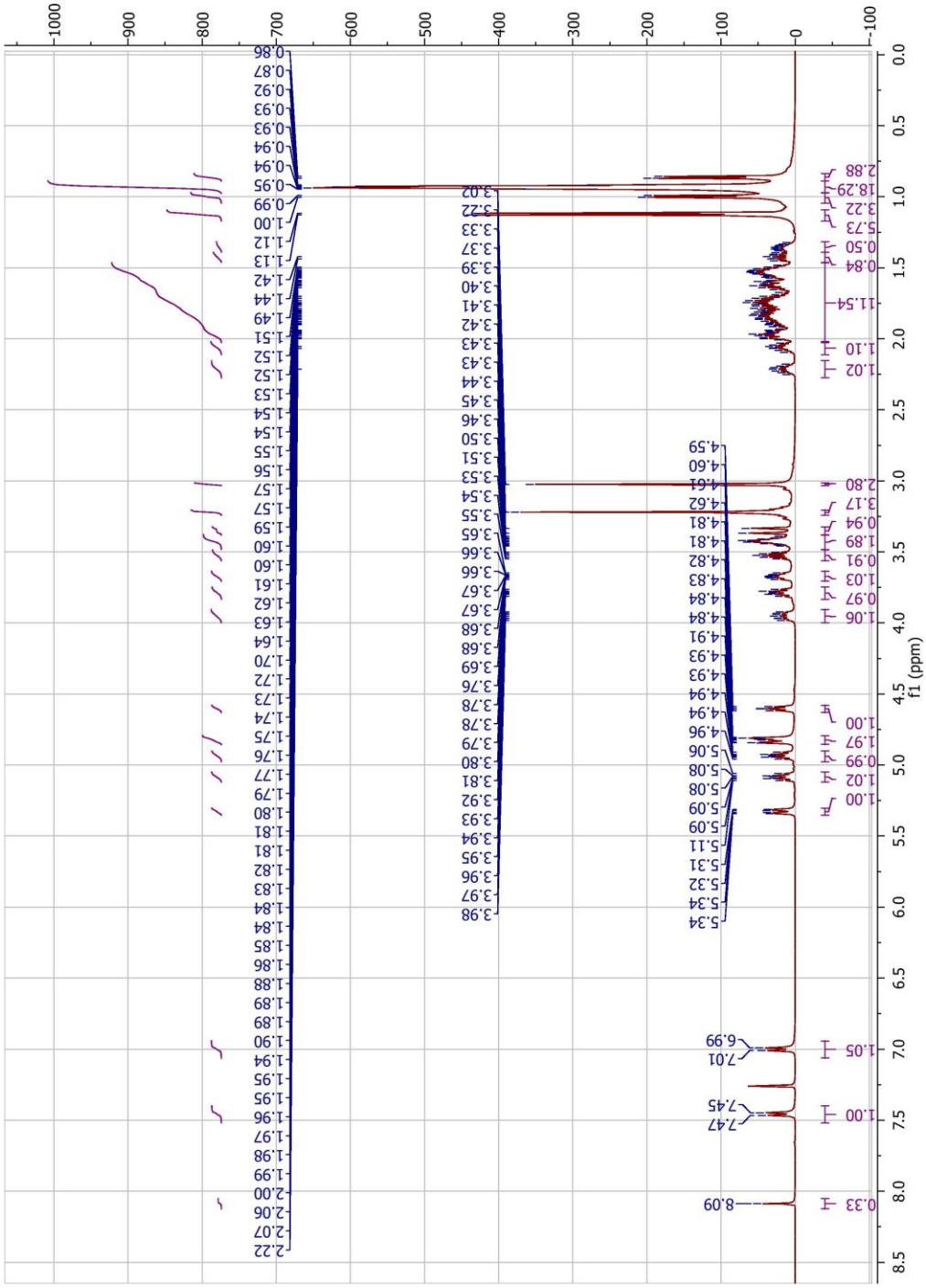

2.9. References

(1) Hopkins, A. L.; Groom, C. R. The Druggable Genome. *Nat. Rev. Drug Discov.* **2002**, *1* (9), 727–730.

(2) Raj, M.; Bullock, B. N.; Arora, P. S. Plucking the High Hanging Fruit: A Systematic Approach for Targeting Protein-Protein Interactions. *Bioorg. Med. Chem.* **2013**, *21* (14), 4051–4057.

(3) Driggers, E. M.; Hale, S. P.; Lee, J.; Terrett, N. K. The Exploration of Macrocycles for Drug Discovery--an Underexploited Structural Class. *Nat. Rev. Drug Discov.* **2008**, *7* (7), 608–624.

(4) Villar, E. A.; Beglov, D.; Chennamadhavuni, S.; Porco, J. A.; Kozakov, D.; Vajda, S.; Whitty, A. How Proteins Bind Macrocycles. *Nat. Chem. Biol.* **2014**, *10* (9), 723–731.

(5) Biron, E.; Chatterjee, J.; Ovadia, O.; Langenegger, D.; Brueggen, J.; Hoyer, D.; Schmid, H. A.; Jelinek, R.; Gilon, C.; Hoffman, A.; Kessler, H. Improving Oral Bioavailability of Peptides by Multiple N-Methylation: Somatostatin Analogues. *Angew. Chem. Int. Ed. Engl.* **2008**, *47* (14), 2595–2599.

(6) Beck, J. G.; Chatterjee, J.; Laufer, B.; Kiran, M. U.; Frank, A. O.; Neubauer, S.; Ovadia, O.; Greenberg, S.; Gilon, C.; Hoffman, A.; Kessler, H. Intestinal Permeability of Cyclic Peptides: Common Key Backbone Motifs Identified. *J. Am. Chem. Soc.* **2012**, *134* (29), 12125–12133.

(7) Nielsen, D. S.; Hoang, H. N.; Lohman, R.-J.; Diness, F.; Fairlie, D. P. Total Synthesis, Structure, and Oral Absorption of a Thiazole Cyclic Peptide,

Sanguinamide A. *Org. Lett.* **2012**, *14* (22), 5720–5723.

(8) Liu, T.; Joo, S. H.; Voorhees, J. L.; Brooks, C. L.; Pei, D. Synthesis and Screening of a Cyclic Peptide Library: Discovery of Small-Molecule Ligands against Human Prolactin Receptor. *Bioorg. Med. Chem.* **2009**, *17* (3), 1026–1033.

(9) Georghiou, G.; Kleiner, R. E.; Pulkoski-Gross, M.; Liu, D. R.; Seeliger, M. A. Highly Specific, Bisubstrate-Competitive Src Inhibitors from DNA-Templated Macrocycles. *Nat. Chem. Biol.* **2012**, *8* (4), 366–374.

(10) Yamagishi, Y.; Shoji, I.; Miyagawa, S.; Kawakami, T.; Katoh, T.; Goto, Y.; Suga, H. Natural Product-like Macrocyclic N-Methyl-Peptide Inhibitors against a Ubiquitin Ligase Uncovered from a Ribosome-Expressed de Novo Library. *Chem. Biol.* **2011**, *18* (12), 1562–1570.

(11) Rezai, T.; Bock, J. E.; Zhou, M. V.; Kalyanaraman, C.; Lokey, R. S.; Jacobson, M. P. Conformational Flexibility, Internal Hydrogen Bonding, and Passive Membrane Permeability: Successful in Silico Prediction of the Relative Permeabilities of Cyclic Peptides. *J. Am. Chem. Soc.* **2006**, *128*, 14073–14080.

(12) Chatterjee, J.; Mierke, D. F.; Kessler, H. Conformational Preference and Potential Templates of N-Methylated Cyclic Pentaalanine Peptides. *Chem. Eur. J.* **2008**, *14* (5), 1508–1517.

(13) Merrifield, R. B. Solid Phase Peptide Synthesis. I. The Synthesis of a Tetrapeptide. *J. Am. Chem. Soc.* **1963**, *85* (14), 2149–2154.

(14) Knight, A. S.; Zhou, E. Y.; Pelton, J. G.; Francis, M. B. Selective

chromium(VI) Ligands Identified Using Combinatorial Peptoid Libraries. *J. Am. Chem. Soc.* **2013**, *135* (46), 17488–17493.

(15) Murphy, J. E.; Uno, T.; Hamer, J. D.; Cohen, F. E.; Dwarki, V.; Zuckermann, R. N. A Combinatorial Approach to the Discovery of Efficient Cationic Peptoid Reagents for Gene Delivery. *Proc. Natl. Acad. Sci.* **1998**, *95* (4), 1517–1522.

(16) van Zoelen, W.; Buss, H. G.; Ellebracht, N. C.; Lynd, N. A.; Fischer, D. A.; Finlay, J.; Hill, S.; Callow, M. E.; Callow, J. A.; Kramer, E. J.; Zuckermann, R. N.; Segalman, R. A. Sequence of Hydrophobic and Hydrophilic Residues in Amphiphilic Polymer Coatings Affects Surface Structure and Marine Antifouling/Fouling Release Properties. *ACS Macro Lett.* **2014**, *3* (4), 364–368.

(17) Zuckermann, R. N.; Kerr, J. M.; Kent, S. B. H.; Moos, W. H. Efficient Method for the Preparation of Peptoids [oligo(N-Substituted Glycines)] by Submonomer Solid-Phase Synthesis. *J. Am. Chem. Soc.* **1992**, *114* (26), 10646–10647.

(18) Montoliu, C.; Humet, M.; Canales, J.-J.; Burda, J.; Planells-Cases, R.; Sánchez-Baeza, F.; Carbonell, T.; Pérez-Payá, E.; Messeguer, A.; Ferrer-Montiel, A.; Felipo, V. Prevention of in Vivo Excitotoxicity by a Family of Trialkylglycines, a Novel Class of Neuroprotectants. *J. Pharmacol. Exp. Ther.* **2002**, *301*, 29–36.

(19) Mas-Moruno, C.; Cruz, L. J.; Mora, P.; Francesch, A.; Messeguer, A.; Pérez-

Payá, E.; Albericio, F. Smallest Peptoids with Antiproliferative Activity on Human Neoplastic Cells. *J. Med. Chem.* **2007**, *50*, 2443–2449.

(20) De León-Rodríguez, L. M.; Lubag, A.; Udugamasooriya, D. G.; Proneth, B.; Brekken, R. A.; Sun, X.; Kodadek, T.; Dean Sherry, A. MRI Detection of VEGFR2 in Vivo Using a Low Molecular Weight Peptoid-(Gd)8-Dendron for Targeting. *J. Am. Chem. Soc.* **2010**, *132*, 12829–12831.

(21) Lynn, K. D.; Udugamasooriya, D. G.; Roland, C. L.; Castrillon, D. H.; Kodadek, T. J.; Brekken, R. A. GU81, a VEGFR2 Antagonist Peptoid, Enhances the Anti-Tumor Activity of Doxorubicin in the Murine MMTV-PyMT Transgenic Model of Breast Cancer. *BMC Cancer* **2010**, *10*, 397.

(22) Lim, H.-S.; Archer, C. T.; Kim, Y.-C.; Hutchens, T.; Kodadek, T. Rapid Identification of the Pharmacophore in a Peptoid Inhibitor of the Proteasome Regulatory Particle. *Chem. Commun. (Camb).* **2008**, No. 9, 1064–1066.

(23) Hara, T.; Durell, S. R.; Myers, M. C.; Appella, D. H. Probing the Structural Requirements of Peptoids That Inhibit HDM2-p53 Interactions. *J. Am. Chem. Soc.* **2006**, *128*, 1995–2004.

(24) Gao, Y.; Amar, S.; Pahwa, S.; Fields, G.; Kodadek, T. Rapid Lead Discovery through Iterative Screening of One Bead One Compound Libraries. *ACS Comb. Sci.* **2015**, *17* (1), 49–59.

(25) Zuckermann, R. N.; Kodadek, T. Peptoids as Potential Therapeutics. *Curr. Opin. Mol. Ther.* **2009**, *11*, 299–307.

(26) Gao, Y.; Kodadek, T. Direct Comparison of Linear and Macrocyclic

Compound Libraries as a Source of Protein Ligands. *ACS Comb. Sci.* **2015**, *17* (3), 190–195.

(27) Ovadia, O.; Linde, Y.; Haskell-Luevano, C.; Dirain, M. L.; Sheynis, T.; Jelinek, R.; Gilon, C.; Hoffman, A. The Effect of Backbone Cyclization on PK/PD Properties of Bioactive Peptide-Peptoid Hybrids: The Melanocortin Agonist Paradigm. *Bioorg. Med. Chem.* **2010**, *18* (2), 580–589.

(28) Demmer, O.; Frank, A. O.; Hagn, F.; Schottelius, M.; Marinelli, L.; Cosconati, S.; Brack-Werner, R.; Kremb, S.; Wester, H.-J.; Kessler, H. A Conformationally Frozen Peptoid Boosts CXCR4 Affinity and Anti-HIV Activity. *Angew. Chem. Int. Ed. Engl.* **2012**, *51* (32), 8110–8113.

(29) Shankaramma, S. C.; Moehle, K.; James, S.; Vrijbloed, J. W.; Obrecht, D.; Robinson, J. A.; Cavicchioni, G.; Wang, L.; Rosenberg, S.; Marlowe, C. K.; Spellmeyer, D. C.; Tan, R. R.; Frankel, A. D.; Santi, D. V.; Cohen, F. E.; Bartlett, P. A. A Family of Macrocyclic Antibiotics with a Mixed peptide–Peptoid Beta-Hairpin Backbone Conformation. *Chem. Commun.* **2003**, *8* (15), 1842–1843.

(30) Fowler, S. A.; Stacy, D. M.; Blackwell, H. E. Design and Synthesis of Macrocyclic Peptomers as Mimics of a Quorum Sensing Signal from Staphylococcus Aureus. *Org. Lett.* **2008**, *10* (12), 2329–2332.

(31) Olsen, C. A.; Montero, A.; Leman, L. J.; Ghadiri, M. R. Macrocyclic Peptoid-Peptide Hybrids as Inhibitors of Class I Histone Deacetylases. *ACS Med. Chem. Lett.* **2012**, *3* (9), 749–753.

(32) Renfrew, P. D.; Craven, T. W.; Butterfoss, G. L.; Kirshenbaum, K.; Bonneau, R. A Rotamer Library to Enable Modeling and Design of Peptoid Foldamers. *J. Am. Chem. Soc.* **2014**, *136* (24), 8772–8782.

(33) Fowler, S. A.; Blackwell, H. E. Structure–function Relationships in Peptoids: Recent Advances toward Deciphering the Structural Requirements for Biological Function. *Org. Biomol. Chem.* **2009**, *7* (8), 1508.

(34) Tan, N. C.; Yu, P.; Kwon, Y. U.; Kodadek, T. High-Throughput Evaluation of Relative Cell Permeability between Peptoids and Peptides. *Bioorganic Med. Chem.* **2008**, *16*, 5853–5861.

(35) Udugamasooriya, D. G.; Ritchie, C.; Brekken, R. A.; Kodadek, T. A Peptoid Antagonist of VEGF Receptor 2 Recognizes a "Hotspot" in the Extracellular Domain Distinct from the Hormone-Binding Site. *Bioorganic Med. Chem.* **2008**, *16*, 6338–6343.

(36) Udugamasooriya, D. G.; Dineen, S. P.; Brekken, R. A.; Kodadek, T. A peptoid "Antibody Surrogate" that Antagonizes VEGF Receptor 2 Activity. *J. Am. Chem. Soc.* **2008**, *130*, 5744–5752.

(37) Lim, H. S.; Archer, C. T.; Kodadek, T. Identification of a Peptoid Inhibitor of the Proteasome 19S Regulatory Particle. *J. Am. Chem. Soc.* **2007**, *129*, 7750–7751.

(38) White, T. R.; Renzelman, C. M.; Rand, A. C.; Rezai, T.; McEwen, C. M.; Gelev, V. M.; Turner, R. A.; Linington, R. G.; Leung, S. S. F.; Kalgutkar, A. S.; Bauman, J. N.; Zhang, Y.; Liras, S.; Price, D. A.; Mathiowetz, A. M.;

Jacobson, M. P.; Lokey, R. S. On-Resin N-Methylation of Cyclic Peptides for Discovery of Orally Bioavailable Scaffolds. *Nat. Chem. Biol.* **2011**, *7* (11).

(39) Wang, C. K.; Northfield, S. E.; Colless, B.; Chaousis, S.; Hamernig, I.; Lohman, R.-J.; Nielsen, D. S.; Schroeder, C. I.; Liras, S.; Price, D. A.; Fairlie, D. P.; Craik, D. J. Rational Design and Synthesis of an Orally Bioavailable Peptide Guided by NMR Amide Temperature Coefficients. *Proc. Natl. Acad. Sci.* **2014**, *111* (49), 17504–17509.

(40) Rand, A. C.; Leung, S. S. F.; Eng, H.; Rotter, C. J.; Sharma, R.; Kalgutkar, A. S.; Zhang, Y.; Varma, M. V; Farley, K. A.; Khunte, B.; Limberakis, C.; Price, D. A.; Liras, S.; Mathiowetz, A. M.; Jacobson, M. P.; Lokey, R. S. Optimizing PK Properties of Cyclic Peptides: The Effect of Side Chain Substitutions on Permeability and Clearance. *Medchemcomm* **2012**, *3* (10), 1282–1289.

(41) Lewis, I.; Schaefer, M.; Wagner, T.; Oberer, L.; Sager, E.; Wipfli, P.; Vorherr, T. A Detailed Investigation on Conformation, Permeability and PK Properties of Two Related Cyclohexapeptides. *Int. J. Pept. Res. Ther.* **2014**.

(42) Thansandote, P.; Harris, R. M.; Dexter, H. L.; Simpson, G. L.; Pal, S.; Upton, R. J.; Valko, K. Improving the Passive Permeability of Macrocyclic Peptides: Balancing Permeability with Other Physicochemical Properties. *Bioorg. Med. Chem.* **2015**, *23* (2), 322–327.

(43) Wang, C. K.; Northfield, S. E.; Swedberg, J. E.; Colless, B.; Chaousis, S.; Price, D. A.; Liras, S.; Craik, D. J. Exploring Experimental and Computational Markers of Cyclic Peptides: Charting Islands of Permeability. *Eur. J. Med.*

Chem. **2015**.

(44) Gavenonis, J.; Sheneman, B. A.; Siegert, T. R.; Eshelman, M. R.; Kritzer, J. A. Comprehensive Analysis of Loops at Protein-Protein Interfaces for Macrocycle Design. *Nat. Chem. Biol.* **2014**, 1–8.

(45) Sui, Q.; Borchardt, D.; Rabenstein, D. L. Kinetics and Equilibria of Cis/trans Isomerization of Backbone Amide Bonds in Peptoids. *J. Am. Chem. Soc.* **2007**, *129* (39), 12042–12048.

(46) Di, L.; Whitney-Pickett, C.; Umland, J. P.; Zhang, H.; Zhang, X.; Gebhard, D. F.; Lai, Y.; Federico, J. J.; Davidson, R. E.; Smith, R.; Reyner, E. L.; Lee, C.; Feng, B.; Rotter, C.; Varma, M. V; Kempshall, S.; Fenner, K.; El-Kattan, A. F.; Liston, T. E.; Troutman, M. D. Development of a New Permeability Assay Using Low-Efflux MDCKII Cells. *J. Pharm. Sci.* **2011**, *100* (11), 4974–4985.

(47) Koehorst, R. B. M.; Spruijt, R. B.; Vergeldt, F. J.; Hemminga, M. A. Lipid Bilayer Topology of the Transmembrane Alpha-Helix of M13 Major Coat Protein and Bilayer Polarity Profile by Site-Directed Fluorescence Spectroscopy. *Biophys. J.* **2004**, *87* (3), 1445–1455.

(48) Atasoylu, O.; Furst, G.; Risatti, C.; Smith III, A. B. The Solution Structure of (+)-Spongistatin 1 in DMSO. *Org. Lett.* **2010**, *12* (8), 1788–1791.

(49) Evans, D. A.; Bodkin, M. J.; Baker, S. R.; Sharman, G. J. Janocchio - a Java Applet for Viewing 3D Structures and Calculating NMR Couplings and NOEs. *Magn. Reson. Chem.* **2007**, *45* (7), 595–600.

(50) Rainaldi, M.; Moretto, V.; Crisma, M.; Peggion, E.; Mammi, S.; Toniolo, C.;

Cavicchioni, G. Peptoid Residues and Beta-Turn Formation. *J. Pept. Sci.* **2002**, *8* (6), 241–252.

(51) Butterfoss, G. L.; Drew, K.; Renfrew, P. D.; Kirshenbaum, K.; Bonneau, R. Conformational Preferences of Peptide-Peptoid Hybrid Oligomers. *Biopolymers* **2014**, *102* (5), 369–378.

(52) Ertl, P.; Rohde, B.; Selzer, P. Fast Calculation of Molecular Polar Surface Area as a Sum of Fragment-Based Contributions and Its Application to the Prediction of Drug Transport Properties. *J. Med. Chem.* **2000**, *43* (20), 3714–3717.

(53) Guimaraes, C. R. W.; Mathiowetz, A. M.; Shalaeva, M.; Goetz, G.; Liras, S. Use of 3D Properties to Characterize Beyond Rule-of-5 Property Space for Passive Permeation. *J. Chem. Inf. Model.* **2012**, *52* (4), 882–890.

(54) Goetz, G. H.; Philippe, L.; Shapiro, M. J. EPSA: A Novel Supercritical Fluid Chromatography Technique Enabling the Design of Permeable Cyclic Peptides. *ACS Med. Chem. Lett.* **2014**, *5* (10), 1167–1172.

(55) Ghose, A. K.; Crippen, G. M. Atomic Physicochemical Parameters for Three-Dimensional Structure-Directed Quantitative Structure-Activity Relationships I. Partition Coefficients as a Measure of Hydrophobicity. *J. Comput. Chem.* **1986**, *7* (4), 565–577.

(56) Callegari, E.; Malhotra, B.; Bungay, P. J.; Webster, R.; Fenner, K. S.; Kempshall, S.; LaPerle, J. L.; Michel, M. C.; Kay, G. G. A Comprehensive Non-Clinical Evaluation of the CNS Penetration Potential of Antimuscarinic

Agents for the Treatment of Overactive Bladder. *Br. J. Clin. Pharmacol.* **2011**, *72* (2), 235–246.

(57) Phillips, J. C.; Braun, R.; Wang, W.; Gumbart, J.; Tajkhorshid, E.; Villa, E.; Chipot, C.; Skeel, R. D.; Kale, L.; Schulten, K. Scalable Molecular Dynamics with NAMD. *J. Comput. Chem.* **2005**, *26* (16), 1781–1802.

3. NATURALLY DERIVED CYCLIC PEPTIDES: SYNTHESIS, PHYSIOCHEMICAL AND SPECTROSCOPIC ANALYSIS.

3.1. Foreword

This chapter contains text and figures from the following manuscripts:

Schwochert, J.; Lao, Y.; Pye, C. R.; Naylor, M. R.; Desai, P. V; Gonzalez Valcarcel, I. C.; Barrett, J. A.; Sawada, G.; Blanco, M.-J.; Lokey, R. S. Stereochemistry Balances Cell Permeability and Solubility in the Naturally Derived Phepropeptin Cyclic Peptides. *ACS Med. Chem. Lett.* **2016**, 7 (8), 757–761.

This work was completed as a collaboration between all authors; I prepared the manuscript and performed most of the spectroscopic analysis, Yongtong Lao performed most of the synthesis, Matthew Naylor performed some NMR experiments, Cameron Pye calculated computationally derived solvation energies and the team at Eli Lilly conducted ADME analysis.

3.2. Introduction

Research into macrocycles as an emerging class of pharmaceutically relevant molecules has increased in recent years. Advances in combinatorial chemistry and screening have yielded a number of potent macrocycles against challenging protein targets.[1–9] Although they often exhibit favorable target binding characteristics, with long off rates and high specificity[10–13], they generally tend to suffer from an inability to cross cellular membranes and are thus limited to extracellular targets. By contrast, some cyclic peptide natural products or derivatives thereof are cell permeable.[14] While Lipinski's Rule of 5 has provided a framework for predicting oral bioavailability in small molecules[15], these types of simple 2-dimensional descriptors do not predict the exceptional ADME characteristics of many large macrocyclic natural products.[14,16–18] This observation has led to a surge of interest in understanding the factors that govern ADME characteristics such as cell permeability, solubility and plasma stability, in medium- and large-ring macrocycles.

3.2.1. Structural Elements and Cell Permeability

In addition to being a rich class of natural products, cyclic peptides are relatively easy to synthesize and diversify, making them a centerpiece in "beyond-Rule of 5" (bRo5) chemical space. A variety of factors have been shown to affect membrane permeability in cyclic peptides, including side chain composition[16,19,20], N-methylation[21–23], β-branching[24,25], and the introduction of non-proteinogenic residues such as peptoid[26], statine, and vinylogous residues[27]. All of these modifications appear to improve permeability, at least in part by increasing lipophilicity.

3.2.2. Cyclosporine and Solvent Dependent Conformations

Cyclosporine A (CSA), an uncharged cyclic undecapeptide, has provided a compelling focal point for inquiry in this chemical space. Its solvent-dependent conformational behavior has been invoked as a potential cause of its exceptional passive membrane permeability and oral bioavailability[28]. We also observed a very large solvent-dependent conformational effect on aqueous solubility among synthetic analogs of the natural product sanguinamide A.[24] Yet although conformational flexibility has been observed in CSA as well as some other natural products[29], the effect of flexibility per se on physicochemical properties has not been studied in these natural systems.

3.3. Phepropeptins and Analogs

3.3.1. Introduction

The phepropeptins, Figure 3-1, are cyclic hexapeptides that were isolated from *Streptomyces* in a search for proteasome inhibitors.[30] Although the proteasome inhibitory activity of this series was modest, we hypothesized that the phepropeptins were nonetheless likely to exhibit favorable cell permeability. In particular, both the absence of polar or charged side chains as well as calculated octanol/water partition (ALogP)[31] coefficients between 3 and 5[32], suggested that the phepropeptins should have passive permeabilities close to those observed in similar cyclic hexapeptide systems.

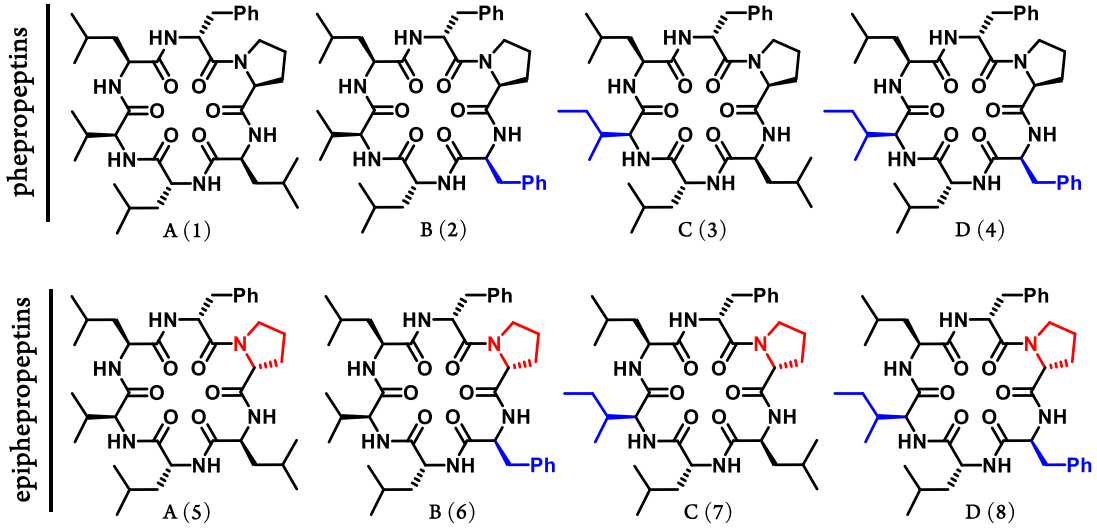

Figure 3-1 Structure of the phepropeptins and analogs

3.3.2. Synthesis

In an effort to determine a structure-property relationship for this class of natural products, we synthesized and tested various ADME properties of a series of phepropetin analogs as well as a congeneric series of epimers. The phepropeptins and analogs thereof were synthesized through automated solid phase peptide synthesis followed by solution phase cyclization. The 1D ^{1}H NMR spectra of the synthetic phepropeptins A, C, and D were identical to those reported for the natural products, confirming their assigned structures.[30] In addition to the natural phepropeptins, a series of epimers were synthesized incorporating a D-Pro instead of the naturally occurring L-Pro ("epiphepropeptins" **5** - **8**). The ^{1}H NMR spectra of the epimers differed substantially from those of the natural compounds; Figure 3-9, Figure 3-10, Figure 3-11, and Figure 3-12, indicating a major change in the conformation of the

macrocycles. The epiphepropeptins were also poorly soluble in $CDCl_3$, suggesting they are less lipophilic than their natural epimers.

3.3.3. ADME Properties

To quantify the effect of this stereoinversion on ADME properties, we measured experimental $LogD_{7.4}$ (octanol/water), solubility, cell permeability and plasma stability for both series. As seen in Table 3-1, all four of the side chain variants of the phepropeptins were rapidly permeable in an MDCK monolayer permeability assay, with permeation rates of 30-40 x 10^{-6} cm/s. The corresponding epiphepropeptins showed 2-4 fold slower permeability than the natural epimers, and, in contrast to the natural products, their permeabilities showed a ~2-fold variation among side chain variants. Although absorption is a complex process that is dependent on multiple factors, MDCK permeability has been shown to be a reasonable indicator of human absorption.[33] While the net impact of increasing MDCK permeability on oral absorption will depend on a given compound and the rate limiting steps for its absorption, the present work offers a potential strategy to modulate permeability toward probing the in vivo impact for a given drug discovery program. None of the compounds showed statistically significant degradation on incubation with human plasma for 30 min. Overall, thermodynamic aqueous solubility pH 7.4 ranged from 0.165 to 0.011 mg/mL for the compounds assessed. However, comparable solubility was observed for the matched pairs of the phepropeptin and epiphepropeptin series, Figure 3-2.

Table 3-1 ADME Properties of phepropeptins and epiphepropetins [a]thermodynamic aqueous solubility pH 7.4, [b]average of A-B and B-A apparent permeability, Papp, reported in cm/sec x10^{-6}

	Compound	ALogP	$LogD_{7.4}$	Solubility[a] (mg/mL)	MDCK Papp[b]
phepropeptins	A (**1**)	3.36	2.08	0.17	33
	B (**2**)	3.76	2.33	0.05	39
	C (**3**)	3.8	2.63	0.06	40
	D (**4**)	4.21	2.42	0.01	40
epiphepropeptins	A (**5**)	3.36	2.37	0.15	8
	B (**6**)	3.76	2.41	0.07	11
	C (**7**)	3.8	2.39	0.07	15
	D (**8**)	4.21	2.32	0.03	18

Regression-based 2-dimensional descriptors such as ALogP[31] (an atomistic version of the more familiar, group-based calculated octanol-water partition coefficient, cLogP), are necessarily the same for any pair of stereoisomers. Each phepropeptin analog and its epimer share the same ALogP value and are therefore predicted to have identical lipophilicities, Table 3-1. Thus, the observed differences between the two series must be due to 3-dimensional (e.g., conformational) effects. There was also little difference in *experimental* octanol-water partition coefficients ($LogD_{7.4}$) between these two compound sets; therefore, in this series neither calculated nor experimental octanol-water partition coefficients were predictive of the permeability differences observed between epimers.

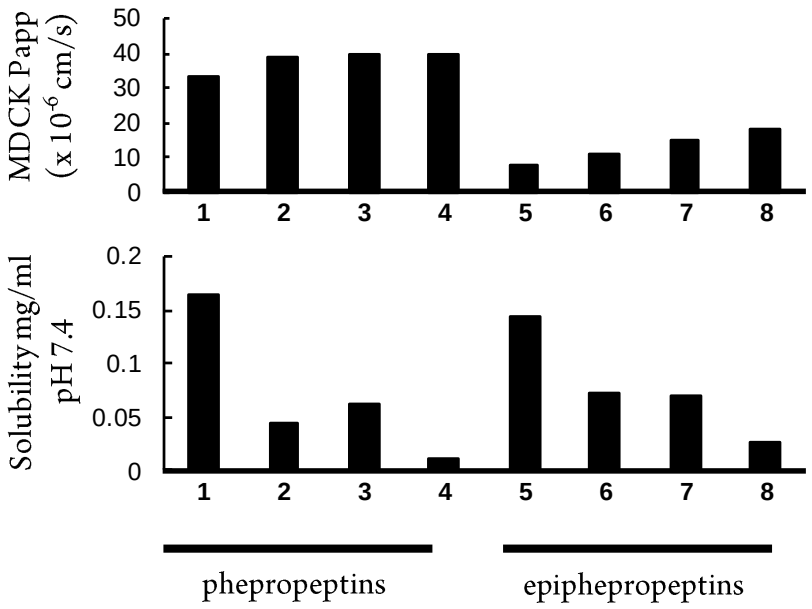

Figure 3-2 *In vitro* cell permeability and solubility for the phepropeptins and epimeric analogs.

3.3.4. NMR Analysis

3.3.4.1. Temperature Shift Analysis

To gain insight into the possible conformational basis for these observed differences, we turned to NMR in $CDCl_3$ and DMSO, solvents selected to mimic the lipid bilayer[34,35] and water, respectively. NMR temperature shift coefficients (Tc) have been used to probe intramolecular hydrogen bonding in cyclic peptides.[17,23,24,36] As temperature increases, solvent-exposed amide NH protons shift upfield, leading to large negative Tc values (<-4 ppb/K being considered solvent-exposed).[37] The number of solvent-exposed NH groups has been shown to negatively correlate with cell permeability in a number of model systems.[17,23,24,35,36]

To compare two matched pairs we conducted temperature coefficient experiments on **1**, **3**, **5** and **7** in chloroform. For both compounds with natural stereochemistry, **1** and **3**, only one or two amide protons are exposed. In the unnatural epimers, **5** and **7**, at least three amide protons are exposed, Figure 3-3. Interestingly **1** and **3** differ only by a valine to isoleucine substitution at position 6, but this leads to shielding of the Ile6's amide proton in compound **3**. Based on the solution structure of **3** presented later in this study the Ile γ-methyl may shield its own NH. Spectral overlap and limited solubility in chloroform prevented further characterization of the unnatural epimers. Nonetheless, the temperature shift data is consistent with the greater degree of passive permeability observed for the natural phepropeptins compared to their epimers.

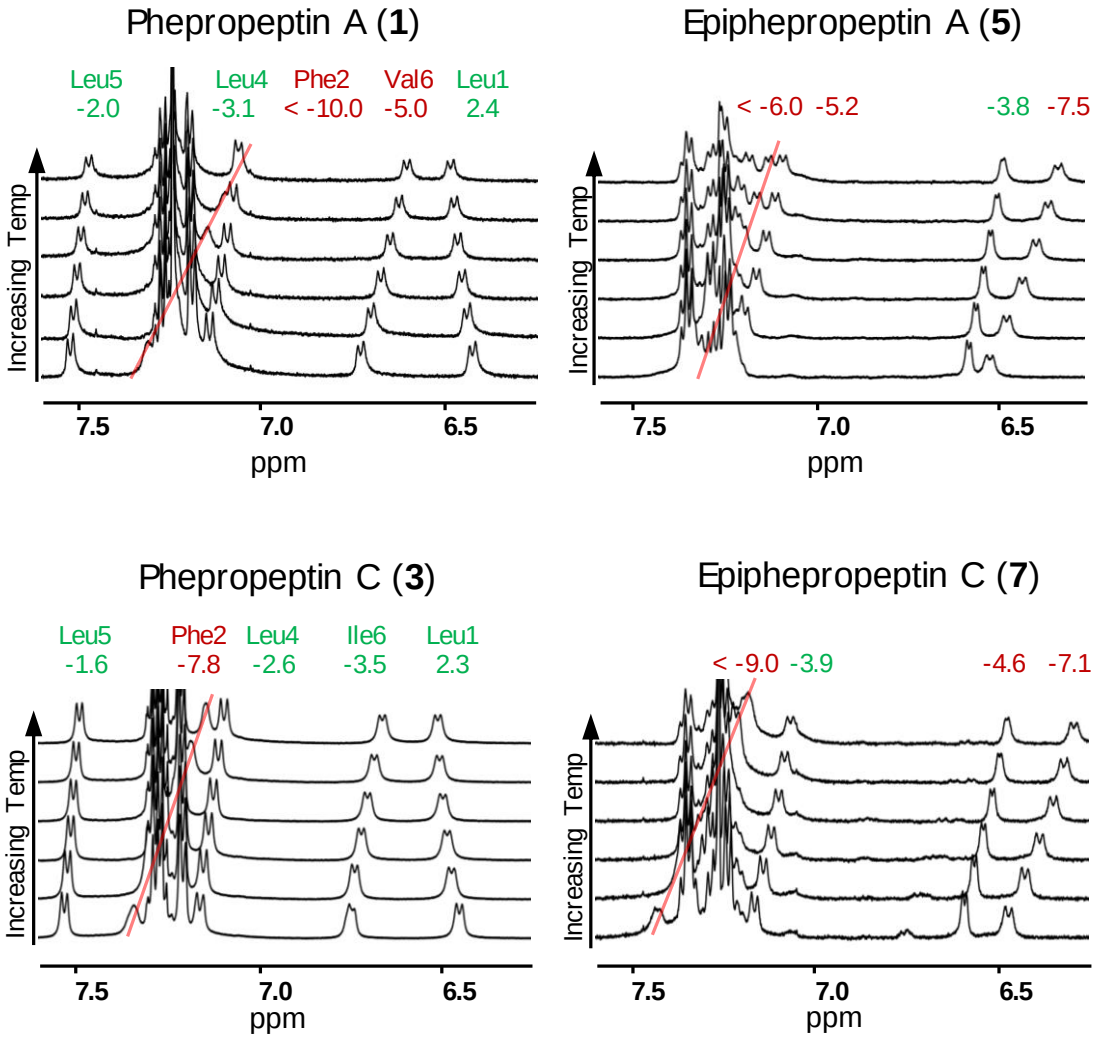

Figure 3-3 Temperature shift experiments for **1**, **3**, **5** and **7** in chloroform. Using the cutoff of -4 ppb/K peaks that are solvent exposed are noted in red, while those that are hidden from solvent are noted in green. Peaks that disappear and reappear are highlighted with a red line Note: only 4 peaks were observable for compounds **5** and **7**, with the 5th amide NH likely hidden under the phenylalanine sidechain protons at 7.2-7.3 ppm.

3.3.4.2. NMR Structure of Phepropetin C (3) in Chloroform

To further investigate the conformation of **3** in a low dielectric environment we sought to obtain a solution structure. We used ROESY and ^{3}J couplings obtained from

2D NMR experiments in $CDCl_3$, together with unrestrained molecular dynamics (MD) simulations. The conformation from the unrestrained MD simulations that showed the least deviation from experimental values is shown in Figure 3-4. In this conformation, only the amide NH of the Phe residue is exposed to solvent, consistent with the temperature shift data (highlighted in Figure 3-4 as a dashed circle). Although previous work in our lab and others has shown non-N-methylated cyclic hexapeptides can be cell permeable[20,38,39], no other examples of all-amide, non-N-methylated cyclic peptide natural products have been reported to show passive membrane permeability.

Based on these observations, we hypothesized that in addition to adopting a sufficiently membrane-permeable lipophilic conformation in a low dielectric environment, the phepropeptins may adopt a different more hydrophilic conformation when in a more polar solvent. This phenomenon has been well described for cyclosporine A and has been attributed to other natural products by inference.[29] Although it is often discussed in reference to the behavior of CSA and other bRo5 compounds[28], the effect of conformational flexibility on ADME properties has been studied in only a handful of model systems.[16,24,40] To explore the conformation of **3** in a polar environment we performed NMR experiments in DMSO, which was chosen because of its high dielectric constant and its ability to effectively solubilize lipophilic peptides.

a.

Phepropeptin C (**3**) $CDCl_3$			
Amide	Shift	*J*NH-HA	Δppb/K
Leu1	6.45	8.2	2.3
Phe2	7.34	br.	-7.8
Leu4	7.16	8.9	-2.6
Leu5	7.53	7.6	-1.6
Ile6	6.75	7.8	-3.5

b.

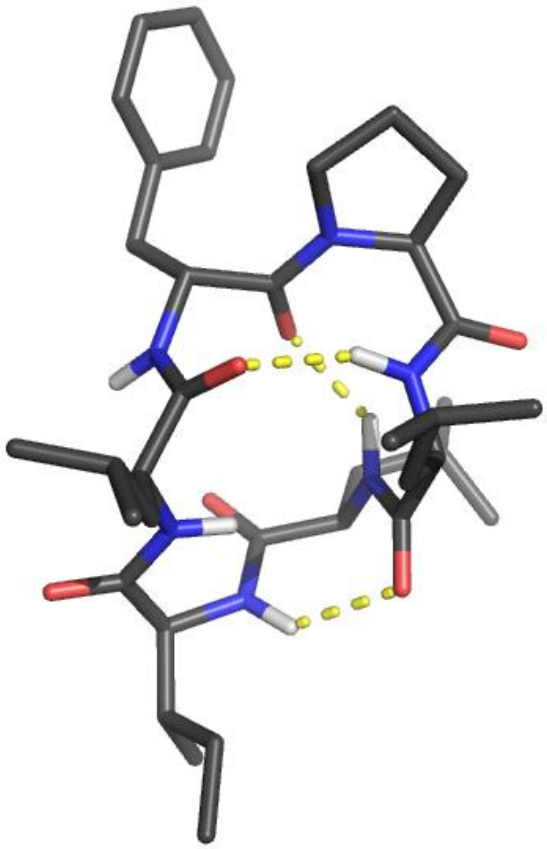

c.

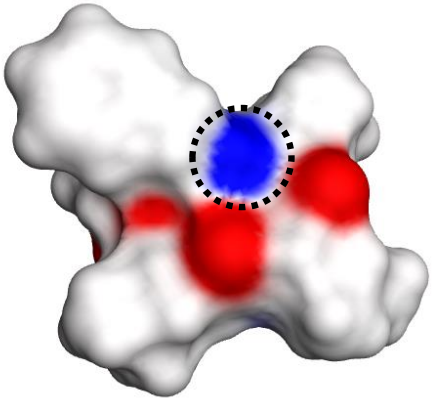

Figure 3-4 NMR structure of phepropeptin C (**3**) in chloroform a) table of NMR data for the NH protons of compound **3**, b) solution structure of **3** as found by molecular dynamics, ROESY, and 3*J* HNHA, c) surface showing solvent accessible polarity of the structure in b, with the solvent exposed NH of phenyalanine 2 highlighted with a dashed circle.

Typically, by introducing an intra-molecular hydrogen bond and/or shielding polar atoms one would expect to see an increase in lipophilicity which in turn may lead to increased permeability but a concomitant decrease in aqueous solubility.[41] Hence, it was interesting to note that the natural epimers with increased shielding of the NH groups maintained similar aqueous solubility as their corresponding unnatural epimers,

3.3.4.3. NMR Structure of Phepropeptin C in DMSO

a.

Phepropeptin C (**3**) DMSO			
Amide	Shift	*J*NH-HA	Δppb/K
Leu1	7.46	7.99	-3.4
Phe2	8.18	6.19	-6.9
Leu4	6.82	7.83	1.4
Leu5	8.32	5.12	-7.5
Ile6	8.19	8.14	-6.4

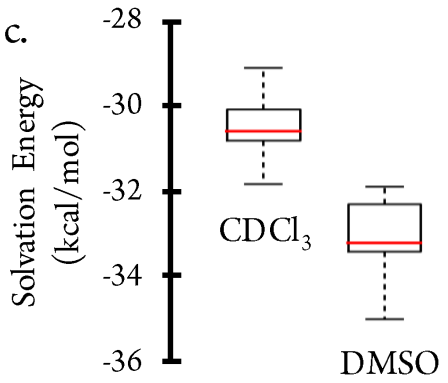

b.

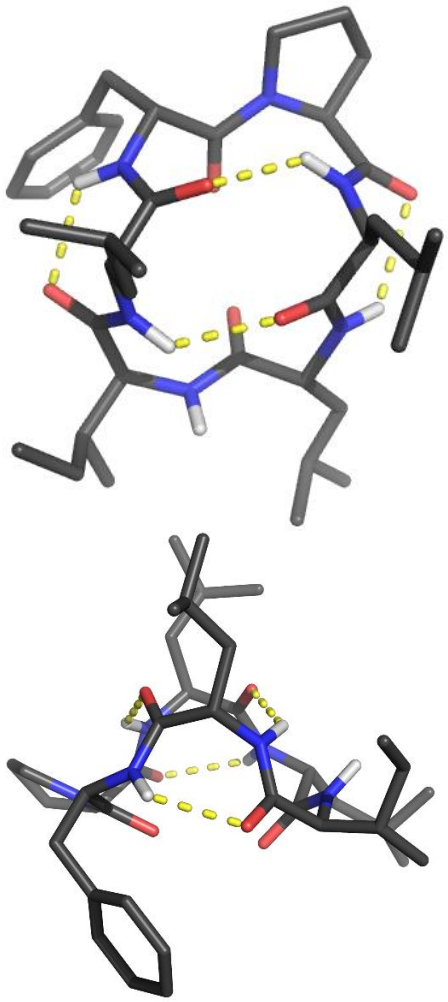

Figure 3-5 NMR structure of phepropeptin C (**3**) in DMSO a) table of NMR data for the NH protons of compound **3** in DMSO, b) two views of the solution structure of **3** in DMSO c) Box plots of solvation energy of the 10 best NMR structures in DMSO and chloroform.

While NMR temperature coefficient experiments for **3** in chloroform indicated a single, solvent-exposed NH, in DMSO three NH groups appeared to be solvent exposed Figure 3-5. After performing a complete spectral assignment followed by MD simulations in an implicit, high-dielectric solvent model, we obtained the solution

structure of **3** in DMSO. The lowest energy structure from the high-temperature MD simulation that was also consistent with the NH temperature coefficient data (which was 2nd-lowest conformation in energy overall) was selected as the starting point for the rt-MD simulation.

To our surprise, the solution structure in DMSO (Figure 5b) showed more intramolecular hydrogen bonds and a lower calculated polar surface area than the structure in chloroform, Figure 3-5. However, using a more refined model for calculating solvation energy[42], the high-dielectric conformation had a greater energy of solvation than the $CDCl_3$ conformation, Figure 3-5. Given that changes in solvent dependent conformations have been implicated in increased solubility in the past[24,41], one can speculate that **3** possesses a favorable balance of membrane permeability and water solubility because of its ability to equilibrate between polar and nonpolar conformations depending on its environment.

3.4. Methods for the Preparation and Analysis of Phepropeptins and Analogs

3.4.1. General Synthetic Methods

3.4.1.1. Loading of 2-Chlorotrityl resin

Fmoc-Xaa (10 mmol) was added to a flame dried round bottom flask and dried in a vacuum dessicator with phosphorous pentoxide overnight. Dry DCM (50 mL) was cannula transferred into the flask followed by DIPEA (2.5 mL) transferred via syringe. After sonication for 10 min, 5 g of 2-chlorotrityl resin was added under a stream of N_2 and allowed to shake for 4 h. Resin was capped with a 15 mL solution of 1:2:17 MeOH:DIPEA:DMF (3 x 15 min). Resin was washed with DMF (3 x 15 mL) followed by DCM (3 x 15 mL). Loading value was calculated by mass increase of dried, loaded resin.

3.4.1.2. Automated Peptide Synthesis

Linear peptide intermediates were synthesized on a Protein Technologies Prelude peptide synthesizer, using advanced programming mode and 60 mL reaction vessels. The reaction procedures are described below.

3.4.1.3. Automated On-Resin Fmoc Deprotection

Resin was immersed in 5 mL of a solution of 2% piperidine and 2% DBU in DMF for 10 min under N_2 agitation twice. Resin was washed with DMF (6 x 3 mL).

3.4.1.4. Peptide Cleavage

Complete linear peptides were cleaved off resin in 5 resin volumes of 2.5% TFA in DCM for 4 minutes three times with a 5 resin volume DCM wash in between each step. Solvent was removed under N_2 followed by dissolution in acetone or DCM and evaporation under reduced pressure. Residual TFA was removed *in vacuo* overnight.

3.4.1.5. Automated Amino Acid Coupling

Fmoc-Xaa (3 equiv), DIPEA (5 equiv), and HBTU (3 equiv) were added to the resin in 4.5 mL of DMF. The reaction was agitated via N_2 bubbling for 90 min. The resin was washed with DMF (6 x 3 mL) and DCM (3 x 3 mL).

3.4.1.6. Cyclization with COMU

Linear peptides were dissolved in 20 mL of dry acetonitrile with DIPEA (4 equiv) and added dropwise to a solution of (final concentration 1 mg crude peptide per mL) 1:1 THF/ACN containing COMU (2 equiv). Reactions were stirred from 0.5 to 24 h until complete cyclization was achieved as monitored by LCMS. The reaction was reduced *in vacuo* for purification via HPLC.

3.4.1.7. Purification of Peptides

COMU by-products were removed after solution phase cyclization on a Biotage Isolera Prime system equipped with a KP-C18-HS 30g column eluting with H_2O/Acetonitrile modified with 0.1% TFA.

3.4.2. Methods for *in vitro* ADME assays

3.4.2.1. Plasma stability assay

The plasma stability assay was designed based on the recommendations by Di et al[43]. The method utilized fast gradient elution LC-ESI/MS to estimate the percent loss of a substrate at 10 min and 30 min incubation periods at 37 °C. Reactions were performed in a 96-well plate format and were initiated with the addition of the substrate into the plasma and terminated by protein precipitation. Three time points (0 min, 10 min, 30 min) were sampled and only the signal for the parent [M+H]+ was monitored by LC-ESI/MS. The ratio of the 30 min to the 0 min and 10 min to the 0 min was converted to percent loss of parent remaining. All reactions were performed using a final substrate concentration of 2μM in 50:50 plasma:tris buffer, pH 7.4. The final organic solvent content was 2% DMSO.

3.4.2.2. Mechanistic permeability assay

MDCKII-MDR1 cells were obtained from NKI and maintained at 37 °C in 5% CO_2 and 95% RH using DMEM supplemented with 10% v/v FBS, 1% v/v l-glutamine, 200 μg/ml penicillin, and 100 μg/ml streptomycin sulfate. Stock flasks were split 1:10 every 3-4 days. Cells were plated for experiment at 50,000 cells/cm^2 in 12-well Transwell inserts. Cell culture medium was changed on days 3 and 5 (0.5 mL apical, 1.5 mL basolateral), and Permeability was measured on day 6.

Culture inserts were rinsed with Dulbecco's PBS + 10mM HEPES, pH 7.4, and then conditioned with 10uM cyclosporin for 30 min at 37 °C. Liquid volumes in the apical and basolateral compartments were 0.5 mL and 1.0 mL, respectively, throughout the assay. Cells were incubated 5 μM test compound at 37 °C with constant nutation (BD Clay Adams, VWR). After 60 minutes, the cell inserts were removed and samples taken from both apical and basolateral chambers. Cells were rinsed with cold buffer and extracted with 500uL MeOH. Samples were combined 3-in-1 and analyzed by LC/MS/MS with methods individually optimized for each cassette. Permeability was determined by the equation: Pe =(V/A)*(M/t) where V = volume in the apical compartment (mL), A = surface area of the filter area (1.13cm^2), M = change in mass in the basolateral compartment, and t = time (seconds). Permeability was measured in both directions - basolateral to apical and apical to basolateral. The apparent passive permeability (Papp) was calculated as the average value across the two directions.

3.4.2.3. Thermodynamic Solubility via "High Throughput Method"

Samples prepared in DMSO were dried for 12 h. The powder or film was re-dissolved in the solvent at different pH (2, 6 and 7.4) and DMSO control at 2mM target concentration. Samples are stirred for 20 h and filtered through a 0.7 μm GF filter. The filtrate was analyzed by HPLC assay for concentration against DMSO standard curve.

Note: Data is single point. Compound A (**5**) had low recovery control and data is considered estimated.

3.4.2.4. LogD 7.4

Miniaturized shake flask method with equimolar chemiluminescent nitrogen detection (CLND) of both octanol and aqueous phases through third party Analiza, Inc.

Note: Data is single point.

3.4.3. HPLC-MS of Phepropeptins and Analogs

HPLC-MS spectrum of Phepropeptin A (**1**)

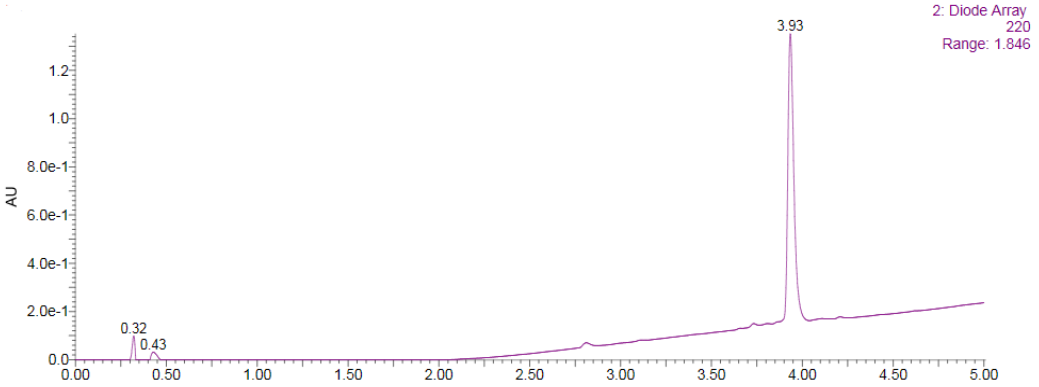

Extracted Mass Spectrum from major peak:

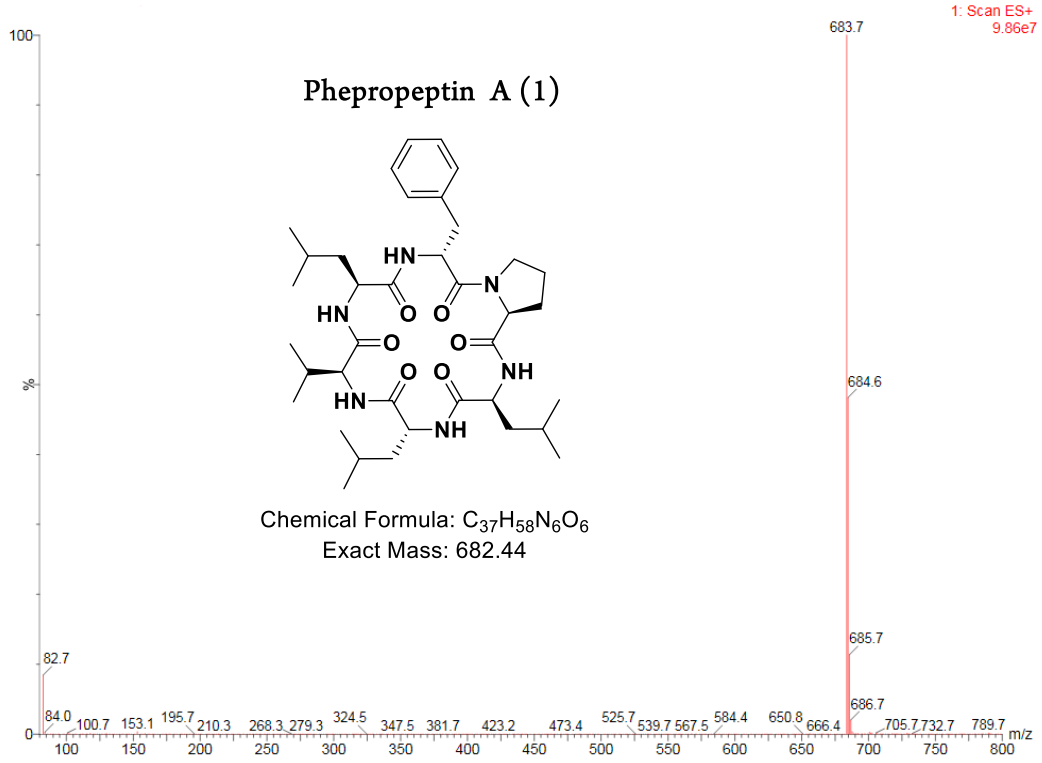

ESI cacld. for $C_{37}H_{58}N_6O_6[M+H]^+$ *m/z* = 683.4; found 683.7

HPLC-MS spectrum of Phepropeptin B (**2**)

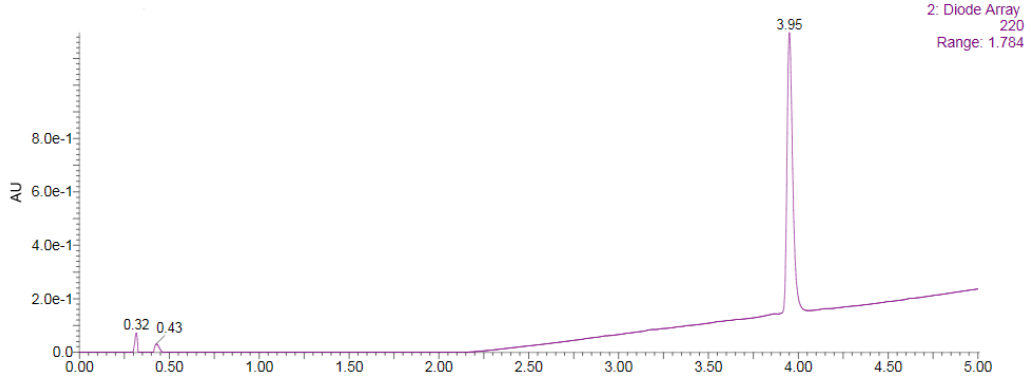

Extracted Mass Spectrum from major peak:

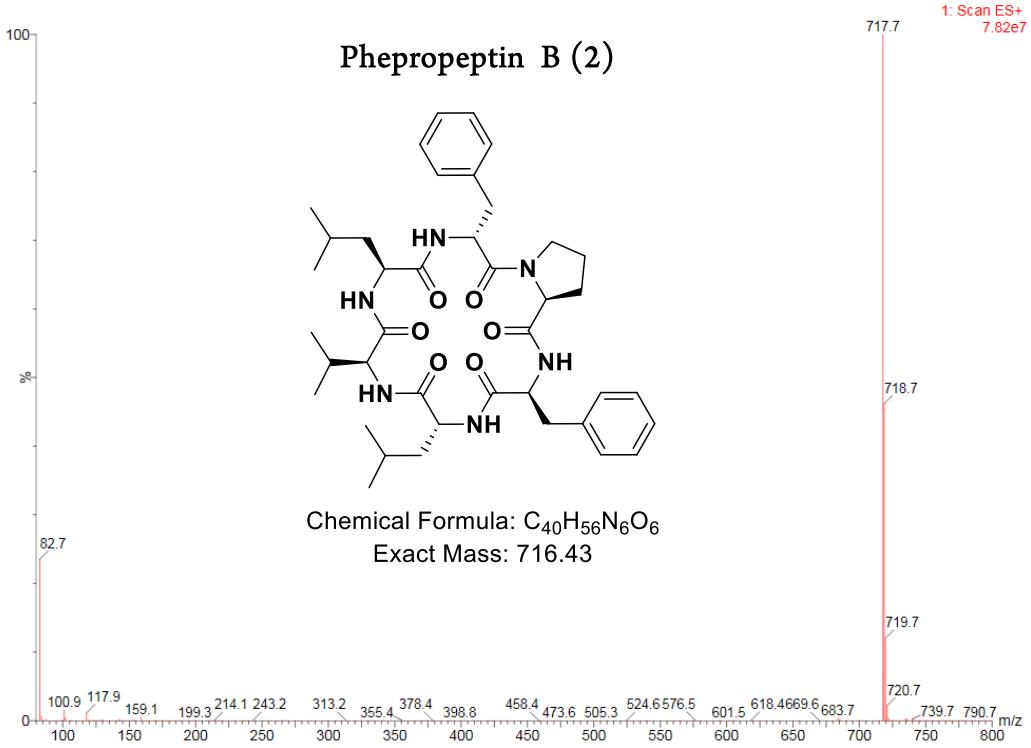

ESI cacld. for $C_{40}H_{56}N_6O_6[M+H]^+$ *m/z* = 717.4; found 717.7

HPLC-MS spectrum of Phepropeptin C (**3**)

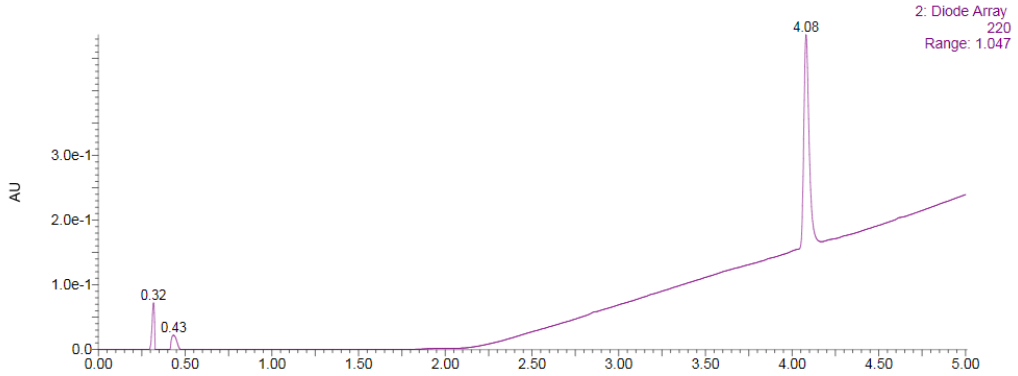

Extracted Mass Spectrum from major peak:

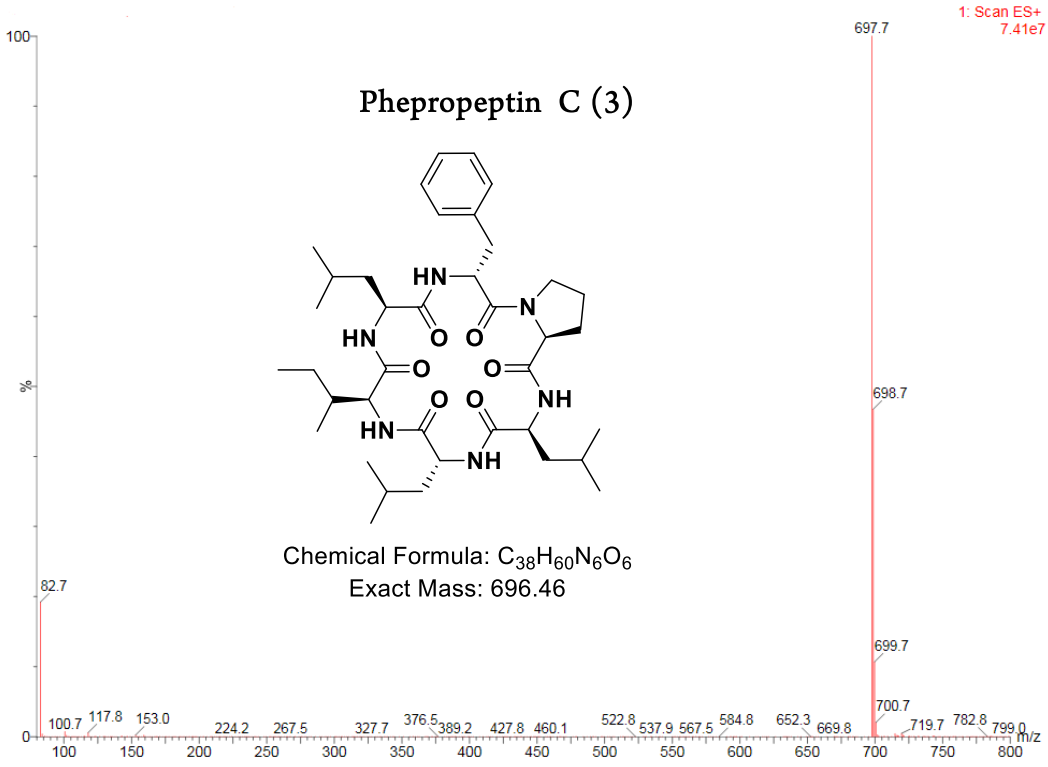

ESI calcd. for $C_{38}H_{60}N_6O_6[M+H]^+$ *m/z* = 697.5; found 697.7

HPLC-MS spectrum of Phepropeptin D (**4**)

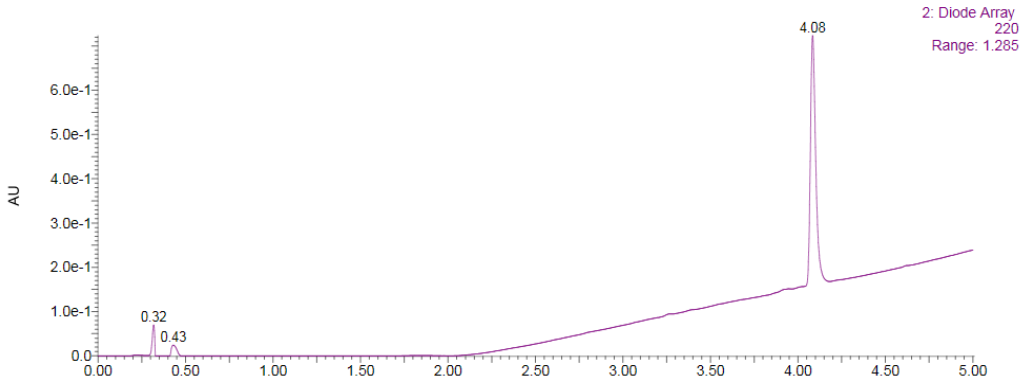

Extracted Mass Spectrum from major peak:

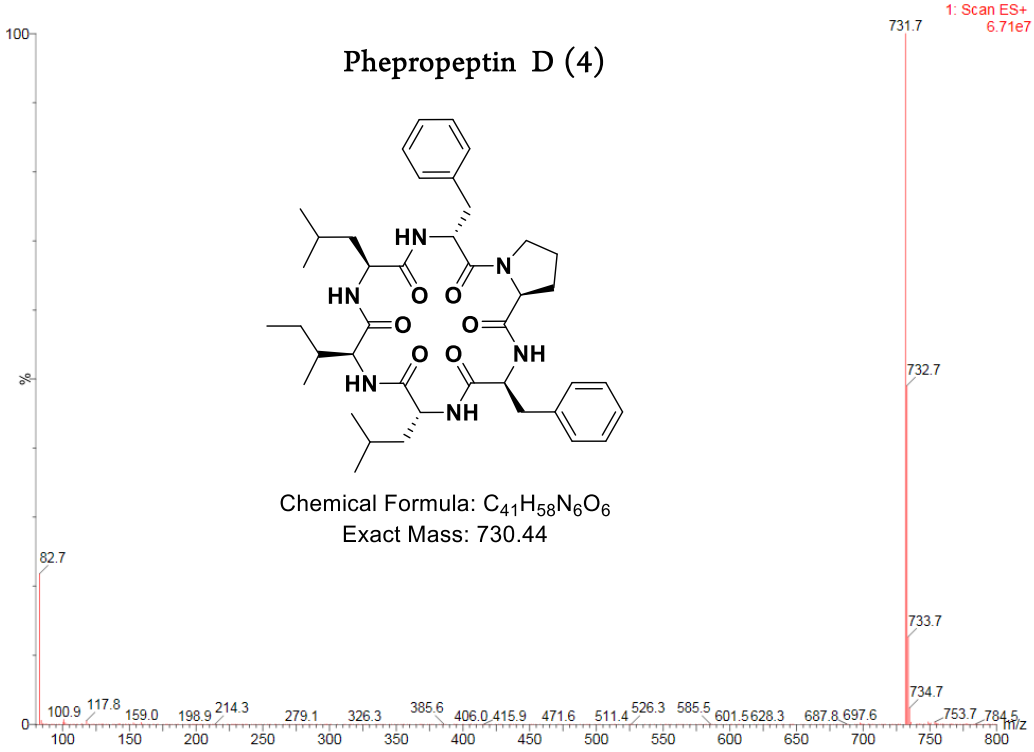

ESI calcld. for $C_{41}H_{58}N_6O_6[M+H]^+$ *m/z* = 731.4; found 731.4

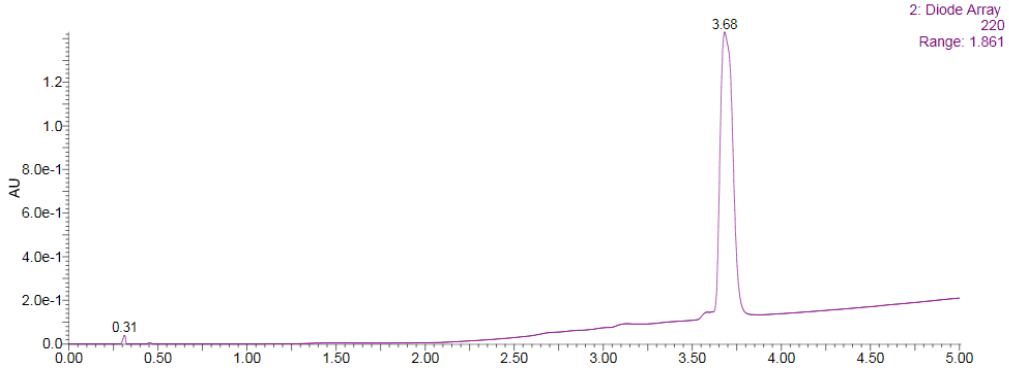

Extracted Mass Spectrum from major peak:

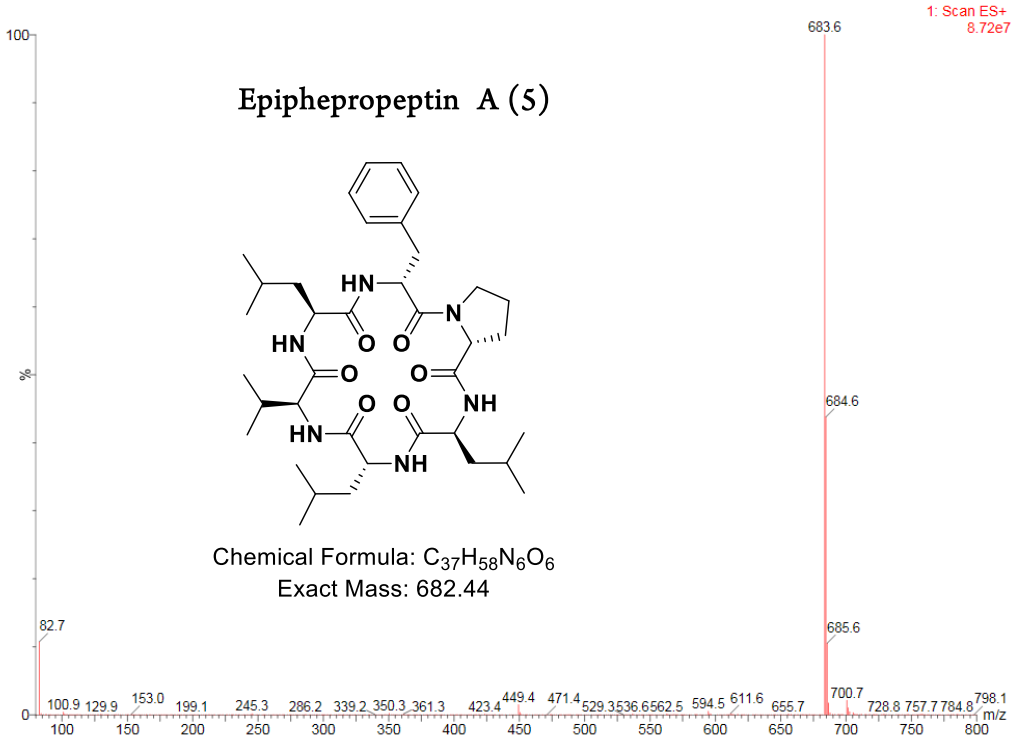

Epiphepropeptin A (5)

Chemical Formula: $C_{37}H_{58}N_6O_6$
Exact Mass: 682.44

ESI cacld. for $C_{37}H_{58}N_6O_6[M+H]^+$ *m/z* = 683.4; found 683.6

HPLC-MS spectrum of Epihepropeptin B (**6**)

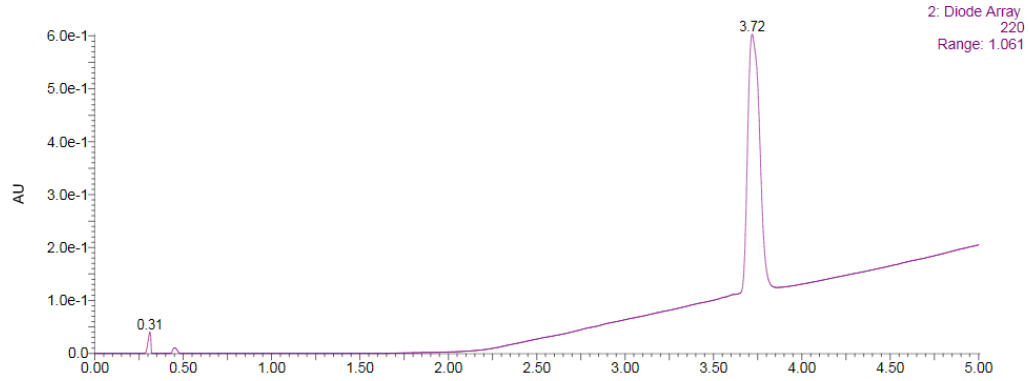

Extracted Mass Spectrum from major peak:

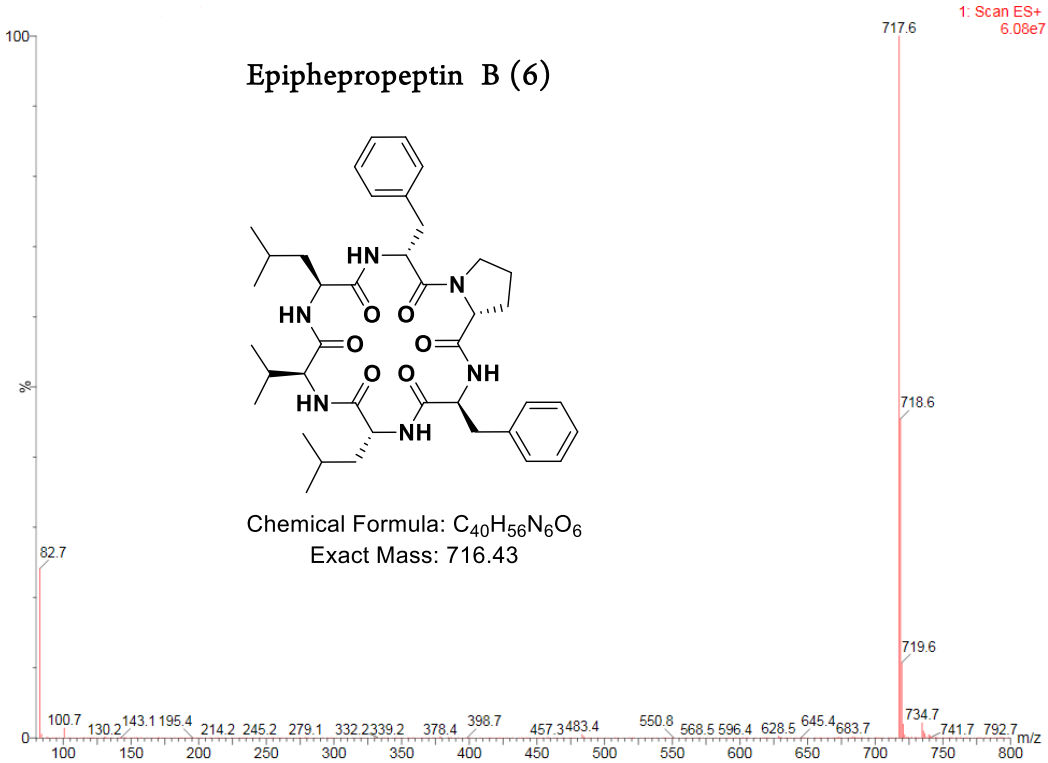

ESI cacld. for $C_{40}H_{56}N_6O_6[M+H]^+$ *m/z* = 717.4; found 717.6

HPLC-MS spectrum of Epihepropeptin C (**7**)

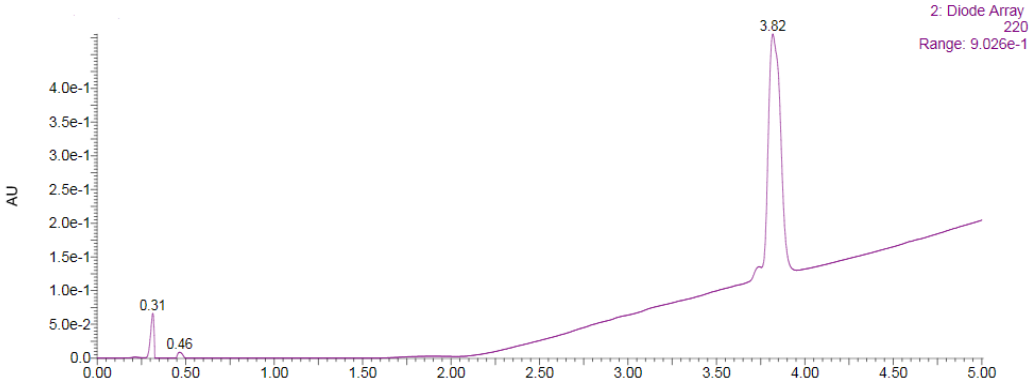

Extracted Mass Spectrum from major peak:

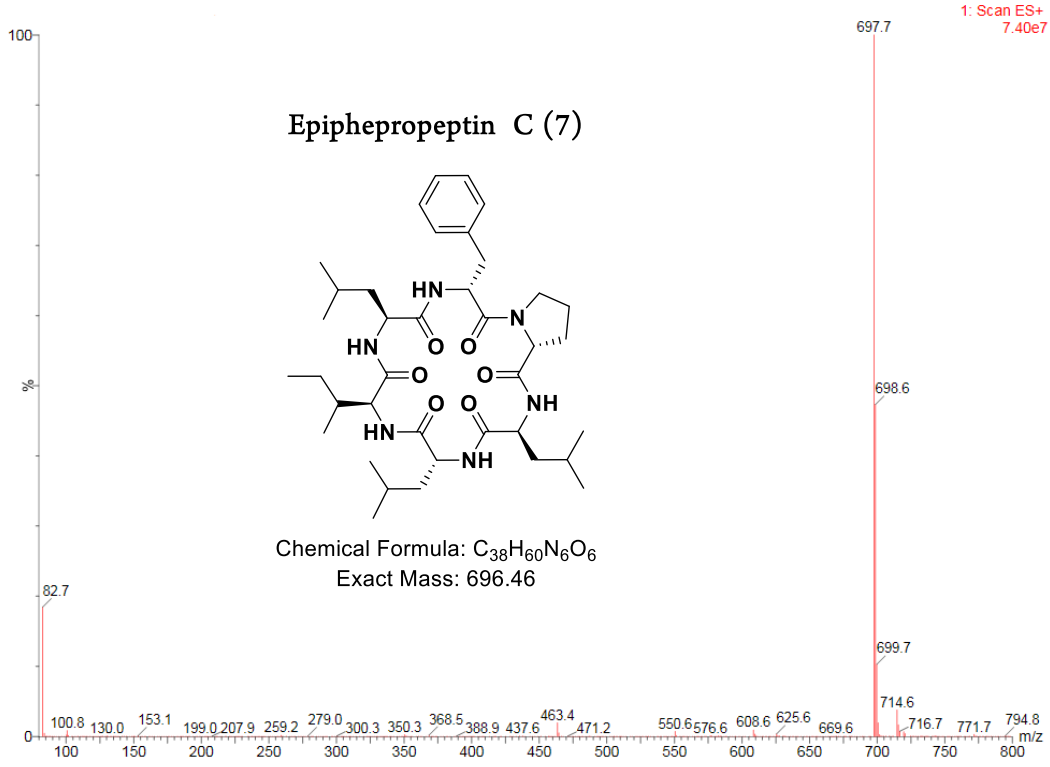

ESI calcld. for $C_{38}H_{60}N_6O_6[M+H]^+$ *m/z* = 697.5; found 697.7

HPLC-MS spectrum of Epihepropeptin D (**8**)

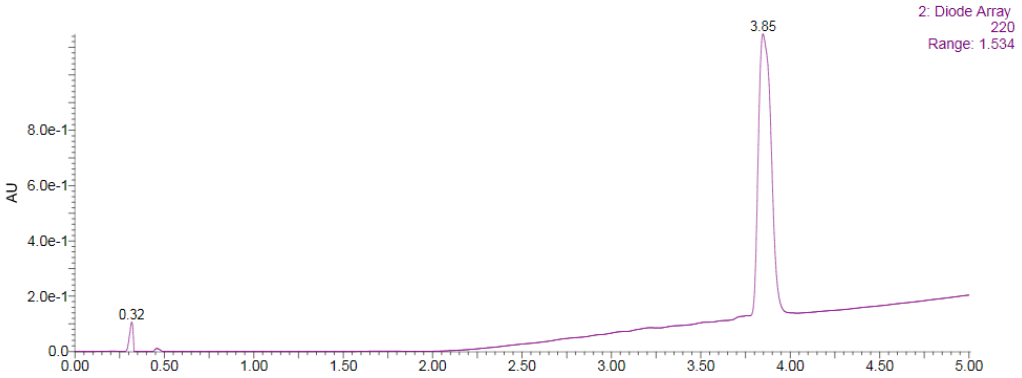

Extracted Mass Spectrum from major peak:

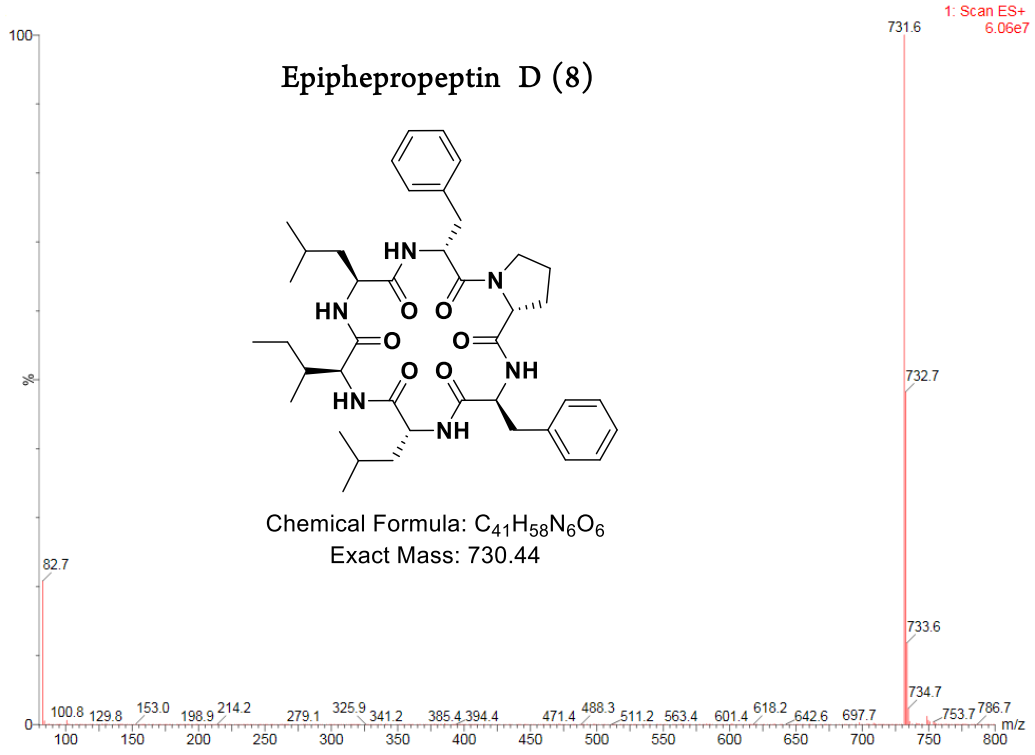

ESI calcld. for $C_{41}H_{58}N_6O_6[M+H]^+$ *m/z* = 731.4; found 731.6

3.4.4. NMR Solution Structures

3.4.4.1. NMR Parameters

ROESY spectra were acquired on a Varian/Agilent 600 MHz NMR with a Unity Inova console with a 5 mm triple resonances cold probe. ^{1}H spectra of compounds synthesized were acquired on an Agilent/Varian 500 MHz NMR with Unity Plus console and a 5 mm broadband probe or a 5 mm HX indirect detection probe. All spectra were acquired at 25 °C (600 MHz) or 15 °C (500 MHz) unless otherwise noted.

Previously reported peak assignments for compound phepropeptin C (**3**) in $CDCl_3$ were used for interpretation of the ROESY spectrum.

Our lab has found that in our hands a ROESY mixing time of 200 ms is optimal for peptides of this size (unpublished work), so this mixing time was used for phepropeptin C (**3**). The ROESY spectrum used in conformational analysis was gathered then for phepropeptin C (**3**) at a mixing time of 200 ms with a d1=1.0 with 16 scans at 25 °C.

3.4.4.2. Molecular Dynamics and Conformer Analysis:

To obtain starting conformations for comparison to the NMR data, the NAMD[44] molecular dynamics (MD) protocol was used, beginning with an arbitrary conformation, to generate a diverse family of minimized conformers. We used the CHARMM forcefield with MMFF94 partial charge estimation for the MD simulation, which was carried out for 5 ns at 2000 ˚K with a 1 fs time step. Snapshots were saved every 20 ps, leading to an ensemble of 250 snapshots. The resulting high temperature snapshots were energy minimized using the generalized Born implicit solvent model

with a dielectric of 4. The lowest energy snapshot of the 250 snapshots (plus 5 from an initial dynamics cascade) was used as the input for a room temperature simulation. This structure contained the trans proline configuration that was predicted by the NMR ^{13}C chemical shifts.[45] The room temperature run was carried out for 500 ns at 300 ˚K with a 2 fs time step. Snapshots were saved every 500 ps, leading to an ensemble of 1000 snapshots. The resulting snapshots were energy minimized using the generalized Born implicit solvent model with a dielectric of 4. Inter-proton distances and phi-angles were then analyzed and used for comparison with the NMR data.

3.4.4.3. NMR Processing and Comparison of Conformations:

The ROESY spectra was processed and sufficiently resolved crosspeaks were integrated. As a reference the NOE between geminal proline delta protons was set to 1.76 angstroms. The following equation was used to calculate the 16 experimental distances used for further analysis:

$$r_{ij} = r_{ref} \sqrt[6]{\frac{I_{ref}}{I_{ij}}}$$

J-couplings were gathered from the ^{1}H chloroform spectra. To the phi angles of conformations to the 3J HNHA values the equation from Wang and Bax[46] was used:

$$^{3}J_{HNH\alpha} = 6.98\,cos^{2}(Phi - 60) - 1.38\cos(Phi - 60) + 1.72$$

The absolute value of the difference between the observed and experimental distances (in angstroms) and coupling constants (in hertz) was evaluated for all conformations. The RMSD for all conformers was calculated and the conformation with the lowest RMSD also had the 3rd lowest total error, this

structure was chosen at the NMR structure, Table 3-4. Additionally, the 10 structures with the lowest deviation also converged on that same structure,

Figure 3-7.

The analysis above was repeated for the structure of phepropeptin C (**3**) in DMSO, but the dielectric constant was set to 50 for both dynamics runs and the minimization steps.

Solvation free energies for the 10 conformations with the least NMR deviation (in DMSO and chloroform) were calculated the Szybki program by Openeye (Szybki 1.8.0.2 OpenEye Scientific Software http://www.eyesopen.com) which makes use of a Poisson-Boltzmann solver and the MMFF94 forcefield to evaluate the free energy of solvation from vacuum to a water dielectric.

Solvent accessible surface area is calculated assuming a solvent probe radius of 1.4 angstroms. Polar solvent accessible surface is calculated area for each molecule using a 3D method (Accerlys Software, Biovia corp.). Atoms considered polar are N, O, P, S, hydrogens attached to them, and any atom with a formal charge.

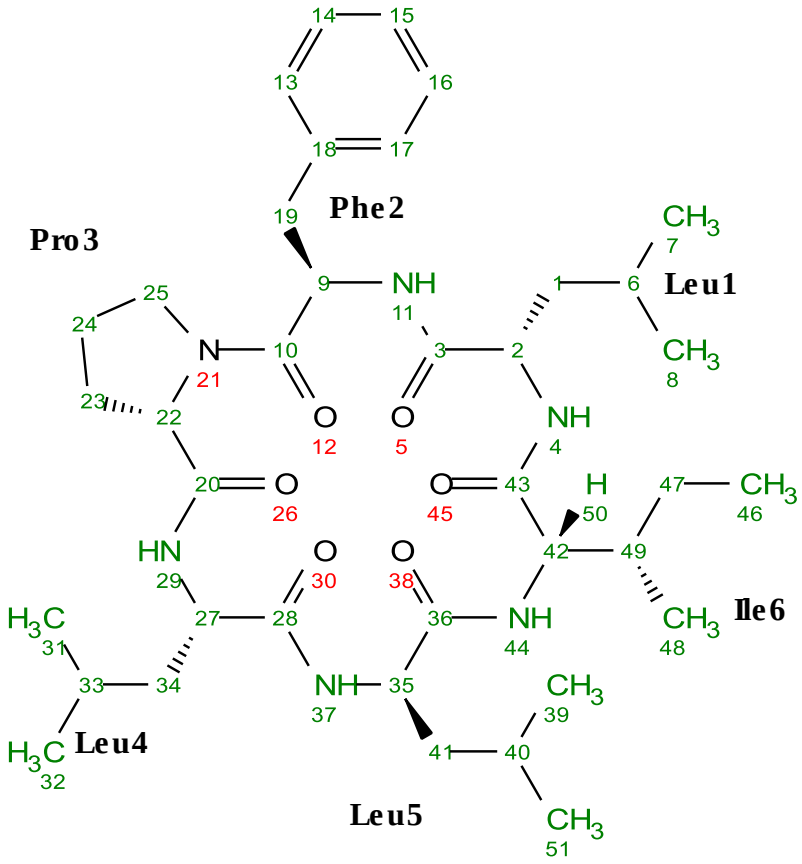

Figure 3-6 Numbering Scheme for Phepropeptin C (**3**)

Table 3-2 Experimental ROESY distances and computational structure (650) in $CDCl_3$.

Atom Pair	Norm Int.	Exp. Distance	Comp. Distance	Δ Å
44-35	29.84	2.36	2.25	0.10
37-44	1.23	4.01	3.79	0.22
37-27	15.91	2.62	3.15	0.53
29-37	15.48	2.63	2.54	0.09
29-25	8.50	2.91	3.39	0.48
29-22	3.41	3.38	3.39	0.01
29-9	2.13	3.66	3.49	0.17
29-4	2.32	3.61	3.56	0.04
37-4	2.55	3.55	3.36	0.19
25-19*	2.93	3.46	4.40	0.95
13-25	5.88	3.09	3.62	0.53
11-2	9.04	2.88	2.29	0.59
25-9*	45.16	2.13	2.13	0.00
4-49	1.72	3.79	4.26	0.47
4-47	2.00	3.70	3.20	0.50
4-35	0.81	4.30	3.83	0.47
25-25‡	161.01	1.78	NA	NA

*= denotes average of 2 or more diastereotopic protons

‡=denotes geminal protons used as standard

Table 3-3 Experimental coupling constants and computational structure (650) in $CDCl_3$.

Residue	Exp. Coupling	Comp. Coupling	Δ hertz
L1 ^{3}JHN-HA	8.22	8.94	0.7
F2 ^{3}JHN-HA	Broad	Not calculated	NA
L4 ^{3}JHN-HA	8.89	8.55	0.3
L5 ^{3}JHN-HA	7.57	8.03	0.5
I6 ^{3}JHN-HA	7.75	7.40	0.3

Table 3-4 10 lowest computational structures by RMSD and average over the entire run in $CDCl_3$.

Frame	CHARMm Energy	Total ROE Error	Total Jcoupling Error	Combined Error	RMSD
650	-22.0	5.4	1.9	5.8	0.44
501	-21.7	5.2	2.4	5.8	0.50
783	-22.2	5.6	2.4	6.2	0.50
80	-21.3	6.2	1.1	6.5	0.50
117	-24.2	5.9	2.4	6.5	0.50
815	-22.4	5.2	3.1	6.0	0.51
648	-20.7	5.1	2.5	5.7	0.51
107	-23.9	5.8	2.7	6.5	0.51
113	-20.1	6.3	1.4	6.6	0.53
553	-19.6	4.8	2.9	5.5	0.53
All Frames	-21.9	7.0	3.4	7.9	0.85

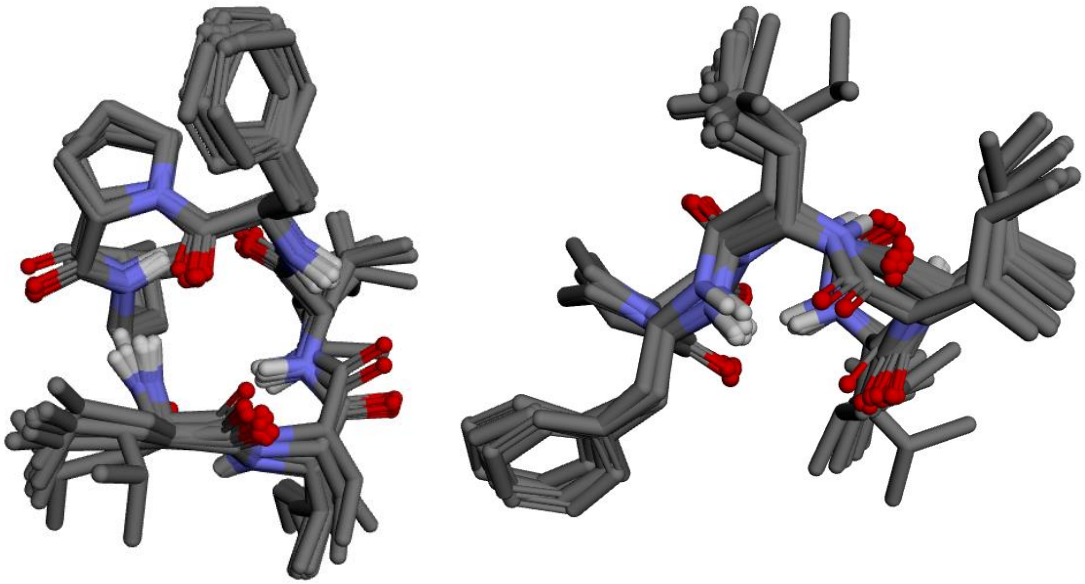

Figure 3-7 Overlays of the 10 lowest RMSD structure in CDCl3.

Table 3-5 phepropeptin C (**3**) assignment in DMSO

Leu1	^{1}H	^{13}C
Hα	4.37	51.41
Hβ	1.47	41.8
Hβ'	1.47	
Hγ	1.39	24.59
Hδ	0.78	~23
Hδ'	0.85	~23
NH	7.46	NA

Phe2	^{1}H	^{13}C
Hα	4.51	5321
Hβ	2.92	36.7
Hβ'	2.79	
Hδ	7.21	129.73
Hε	7.26	128.57
Hζ	7.21	126.98
NH	8.18	NA

Leu4	^{1}H	^{13}C
Hα	4.4	50.9
Hβ	1.45	42.5
Hβ'	1.45	
Hγ	1.43	24.92
Hδ	0.85	~23
Hδ'	0.87	~23
NH	6.82	NA

Leu5	^{1}H	^{13}C
Hα	4.23	52.43
Hβ	1.47	39.87
Hβ'	1.44	
Hγ	7.58	24.55
Hδ	0.85	~23
Hδ'	0.92	~23
NH	8.32	NA

Pro3	^{1}H	^{13}C
Hα	4.13	60.81
Hβ	1.82	29.72
Hβ'	1.8	
Hγ	1.65	24.32
Hγ'	1.65	
Hδ	3.57	47.1
Hδ'	3.03	

Tertiary	^{13}C
Leu1 CO	171.49
Phe2 CO	170.77
Phe2 Cγ	137.42
Pro3 CO	170.68
Leu4 CO	171.83
Leu5 CO	173.13
Ile6 CO	170.74

Ile6	^{1}H	^{13}C
Hα	4.12	58.24
Hβ	2.03	35.93
Hγ-Me	0.83	16.15
Hγ	1.28	24.25
Hγ'	1.23	
Hδ'	0.82	12.2
NH	8.19	NA

Table 3-6 Experimental ROESY distances and computational structure (251) in DMSO.

Atom Pair	Norm Int.	Exp. Distance	Comp. Distance	Δ Å
37-27	24.89	2.38	2.26	0.12
37-4	0.78	4.24	4.79	0.55
37-29	3.44	3.31	3.82	0.51
44-35	43.14	2.17	2.08	0.09
11-29	1.66	3.74	4.66	0.92
11-2	23.56	2.40	2.24	0.16
11-19*	11.40	2.71	3.06	0.35
4-29	0.84	4.19	4.69	0.50
4-50	2.19	3.57	3.44	0.13
4-35	1.04	4.04	3.28	0.76
4-49	1.91	3.65	4.13	0.47
13-25	0.61	4.42	4.82	0.40
29-24	2.83	3.42	3.70	0.28
29-22	1.58	3.77	3.40	0.37
29-25	5.67	3.05	3.18	0.13
9-25*	36.74	2.23	2.20	0.03
25-25‡	142.44	1.78		NA

*= denotes average of 2 or more diastereotopic peaks

‡=denotes geminal protons used as standard

Table 3-7 Experimental coupling constants and computational structure (251) in DMSO.

Residue	Exp. Coupling	Comp. Coupling	Δ hertz
L1 ^{3}JHN-HA	7.99	8.07	0.1
F2 ^{3}JHN-HA	*6.19	5.08	1.1
L4 ^{3}JHN-HA	7.83	8.63	0.8
L5 ^{3}JHN-HA	5.12	5.62	0.5
I6 ^{3}JHN-HA	*8.14	7.55	0.6

*= denotes measurement at 35°C, spectral overlap at 25°C prevents accurate calculation

Table 3-8 10 lowest computational structures by RMSD and average over the entire run in DMSO.

Frame	CHARMM Energy	Total ROE Error	Total Jcoupling Error	Combined Error	RMSD
251	-4.7	5.8	3.1	6.7	0.52
466	-6.0	4.4	3.8	5.6	0.53
906	-6.5	5.8	3.8	6.9	0.56
747	-5.3	5.2	3.9	6.4	0.59
678	-4.9	4.9	4.5	6.3	0.59
634	-7.2	4.0	4.4	5.3	0.60
675	-5.2	5.2	4.5	6.6	0.62
53	-5.0	4.7	4.2	6.0	0.63
775	-8.2	4.6	4.9	6.2	0.64
884	-5.7	4.5	5.1	6.1	0.64
All Frames	-8.9	8.9	7.4	10.7	1.29

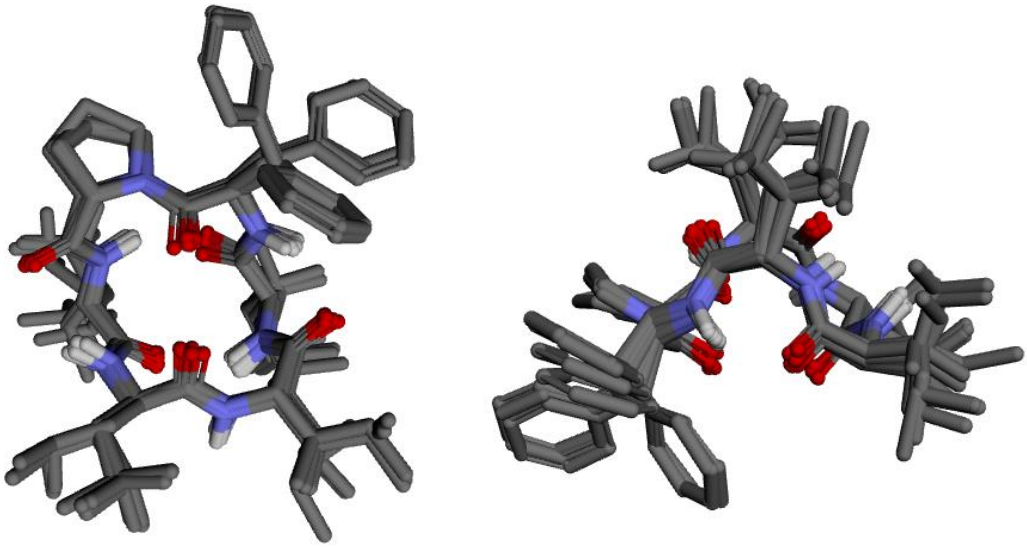

Figure 3-8 Overlays of the 10 lowest RMSD structures in DMSO.

Table 3-9 Temperature Coefficient Data in ppb/K for Phepropeptin A (**3**)

Compound 1			
$CDCl_3$			
Residue	**Chemical Shift**	**Slope**	**R^2**
Leu1	6.43	2.38	0.99
Val6	6.73	-5.00	1.00
Leu4	7.14	-3.14	1.00
Phe2	7.31	-10.44	1.00
Leu5	7.52	-2.02	1.00

Compound 1		
DMSO		
Chemical Shift	**Slope**	**R^2**
6.797	0.59	0.95
7.449	-3.66	1.00
8.097	-7.40	1.00
8.123	-6.60	1.00
8.367	-7.60	1.00

Table 3-10 Temperature Coefficient Data in ppb/K for Phepropeptin C (**3**)

Compound 3			
$CDCl_3$			
Residue	**Chemical Shift**	**Slope**	**R^2**
Leu1	6.45	2.29	0.96
Ile6	6.75	-3.53	0.99
Leu4	7.16	-2.63	1.00
Phe2	7.34	-7.82	1.00
Leu5	7.53	-1.60	1.00

Compound 3			
DMSO			
Residue	**Chemical Shift**	**Slope**	**R^2**
Leu4	6.82	1.45	1.00
Leu1	7.45	-3.35	1.00
Phe2	8.12	-6.94	1.00
Ile6	8.14	-6.38	1.00
Leu5	8.30	-7.48	1.00

Table 3-11 Temperature Coefficient Data in ppb/K for Epiphepropeptin A (**5**)

Compound 5		
$CDCl_3$		
Chemical Shift	**Slope**	**R^2**
6.52	-7.53	0.99
6.57	-3.81	1.00
7.15	-6.45	2 points
7.19	-5.20	0.99

Table 3-12 Temperature Coefficient Data in ppb/K for Epiphepropeptin C (**7**)

Compound 7		
$CDCl_3$		
Chemical Shift	**Slope**	**R^2**
6.47	-7.12	0.99
6.59	-4.64	1.00
7.16	-3.91	0.99
7.43	-9.81	2 points

3.4.1. Selected NMR Spectra

1 ^{1}H $CDCl_3$

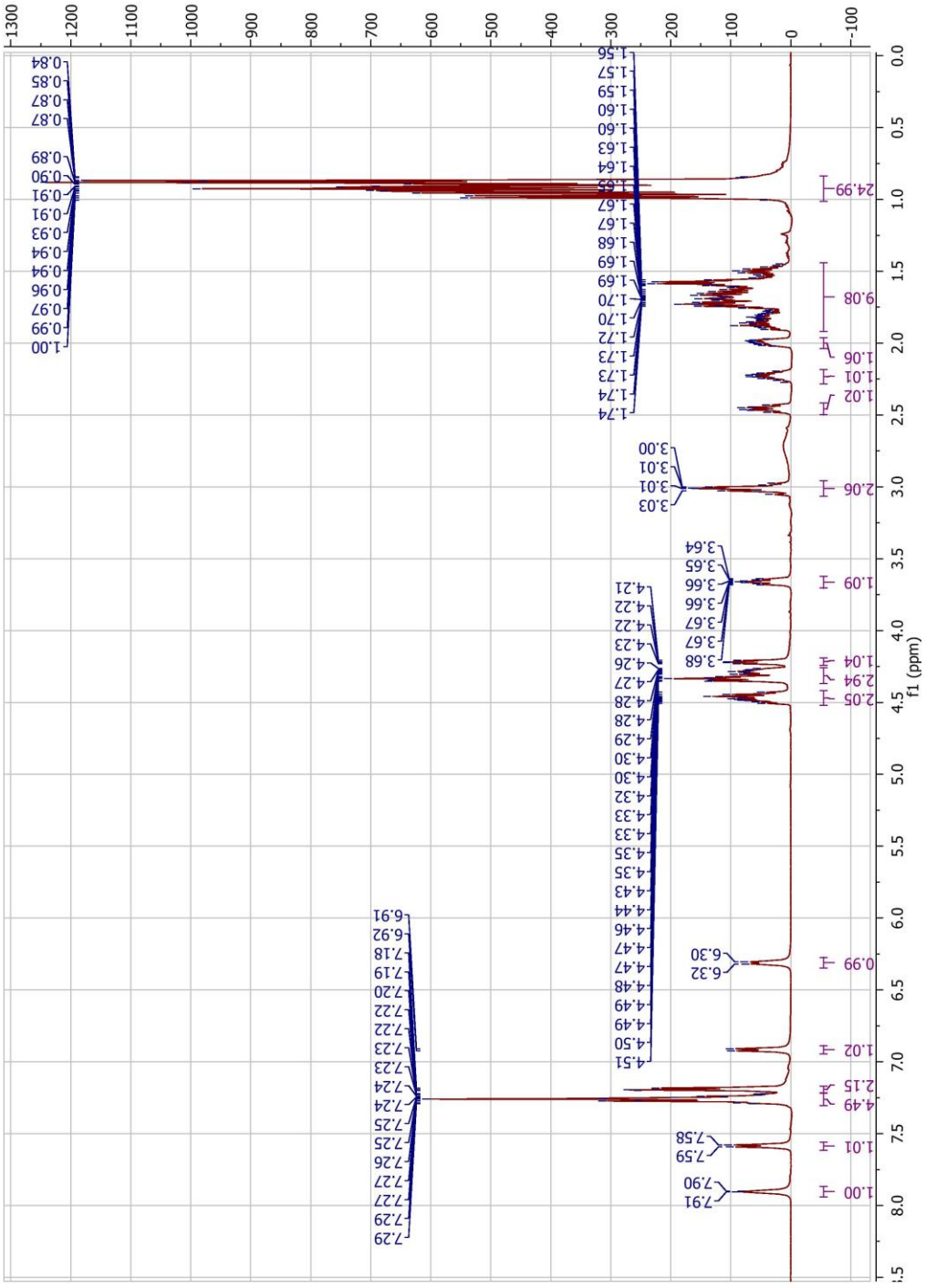

2 ^{1}H $CDCl_3$

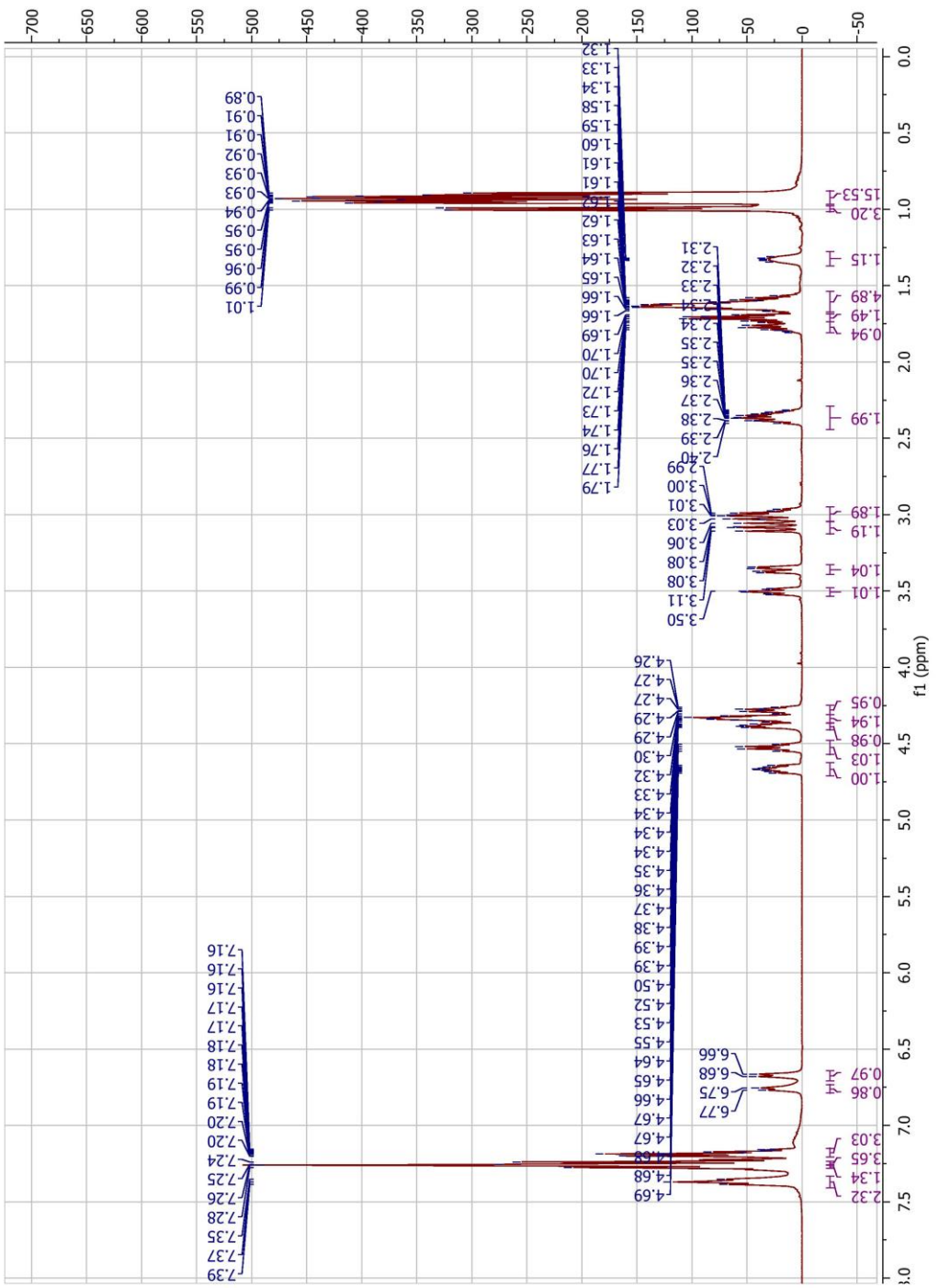

3 ^{1}H $CDCl_3$

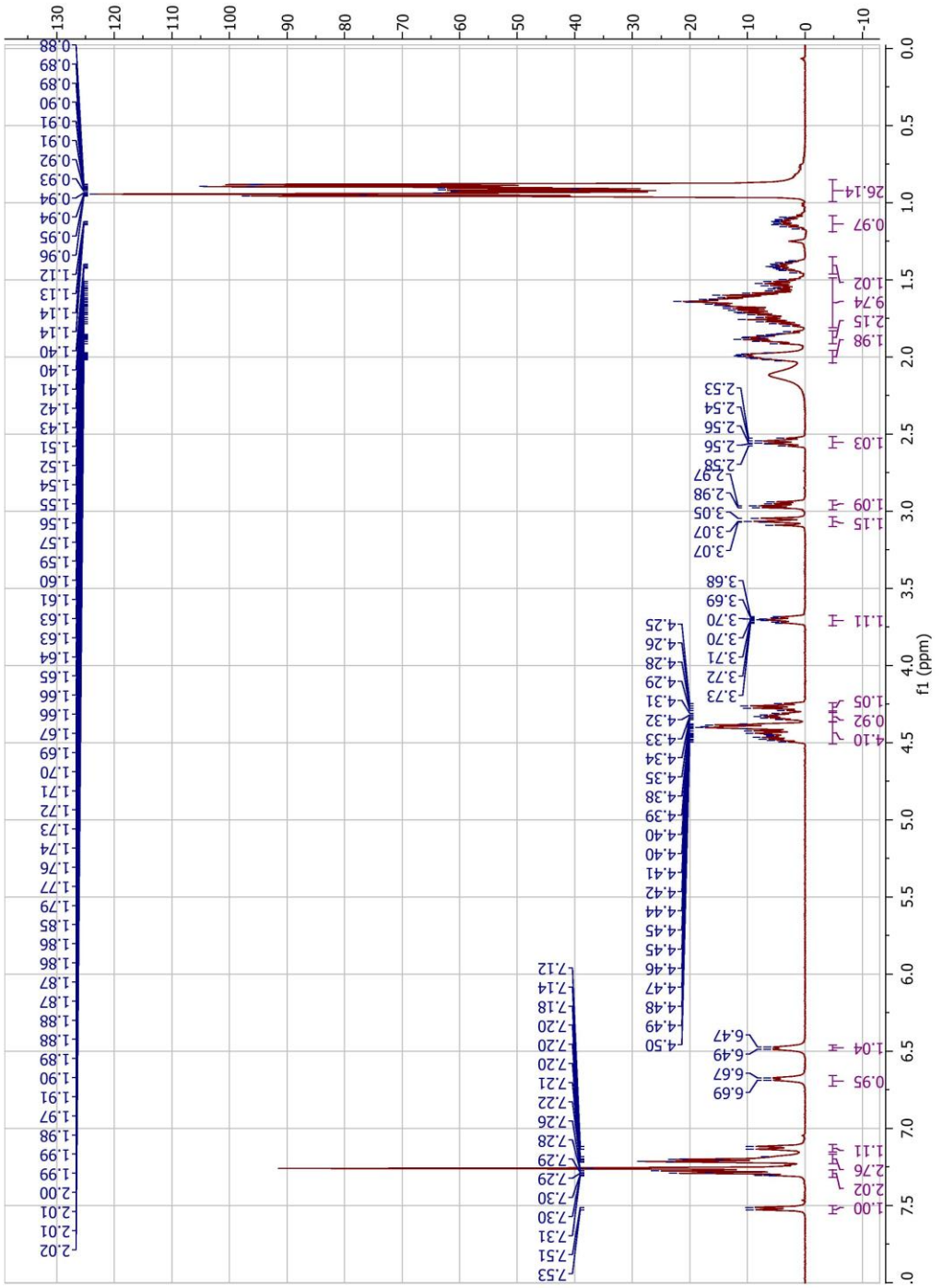

4 ^{1}H $CDCl_3$

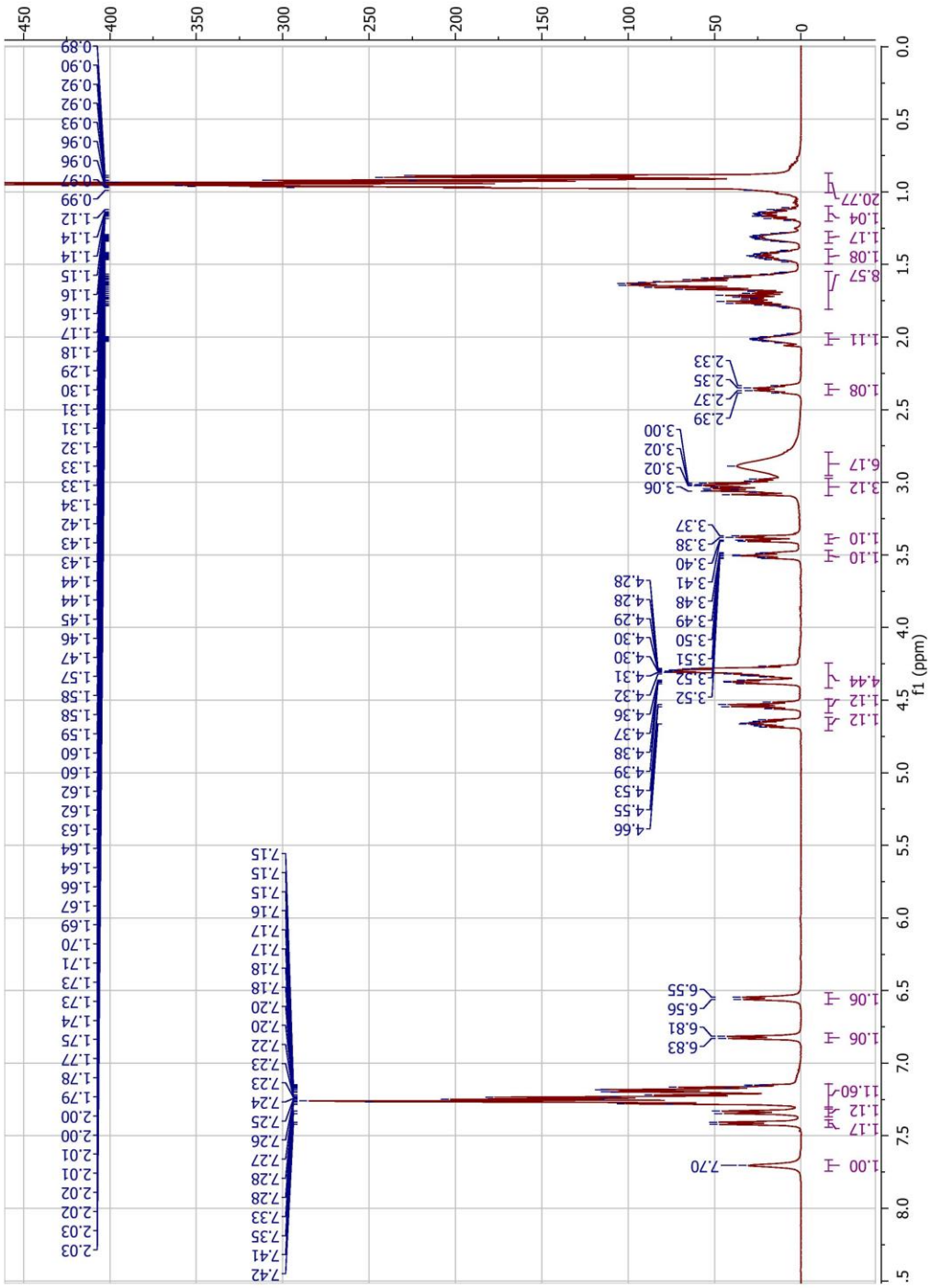

5 1H d6 DMSO (2 conformers)

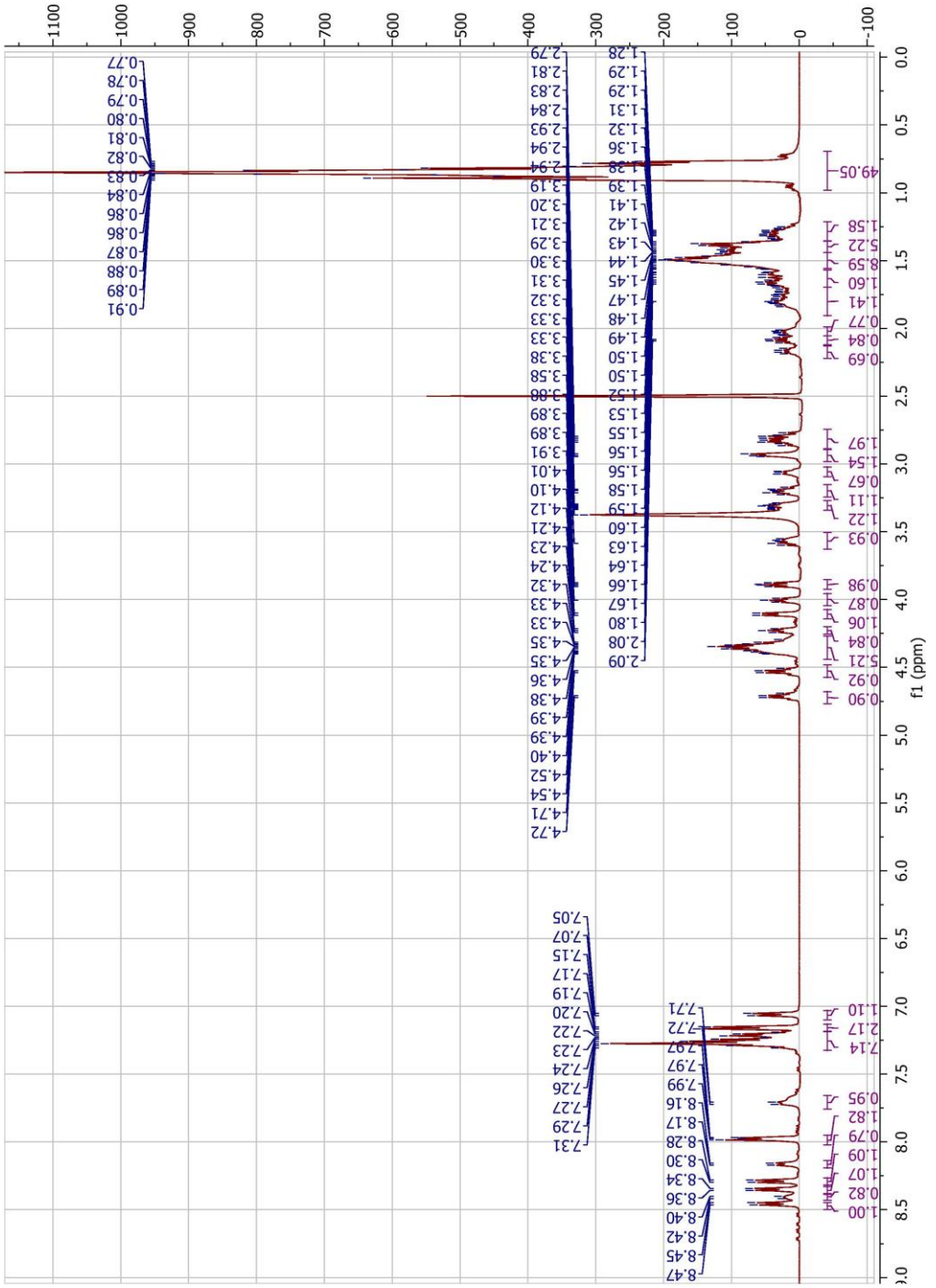

6 ^{1}H *d*6 DMSO (2 conformers)

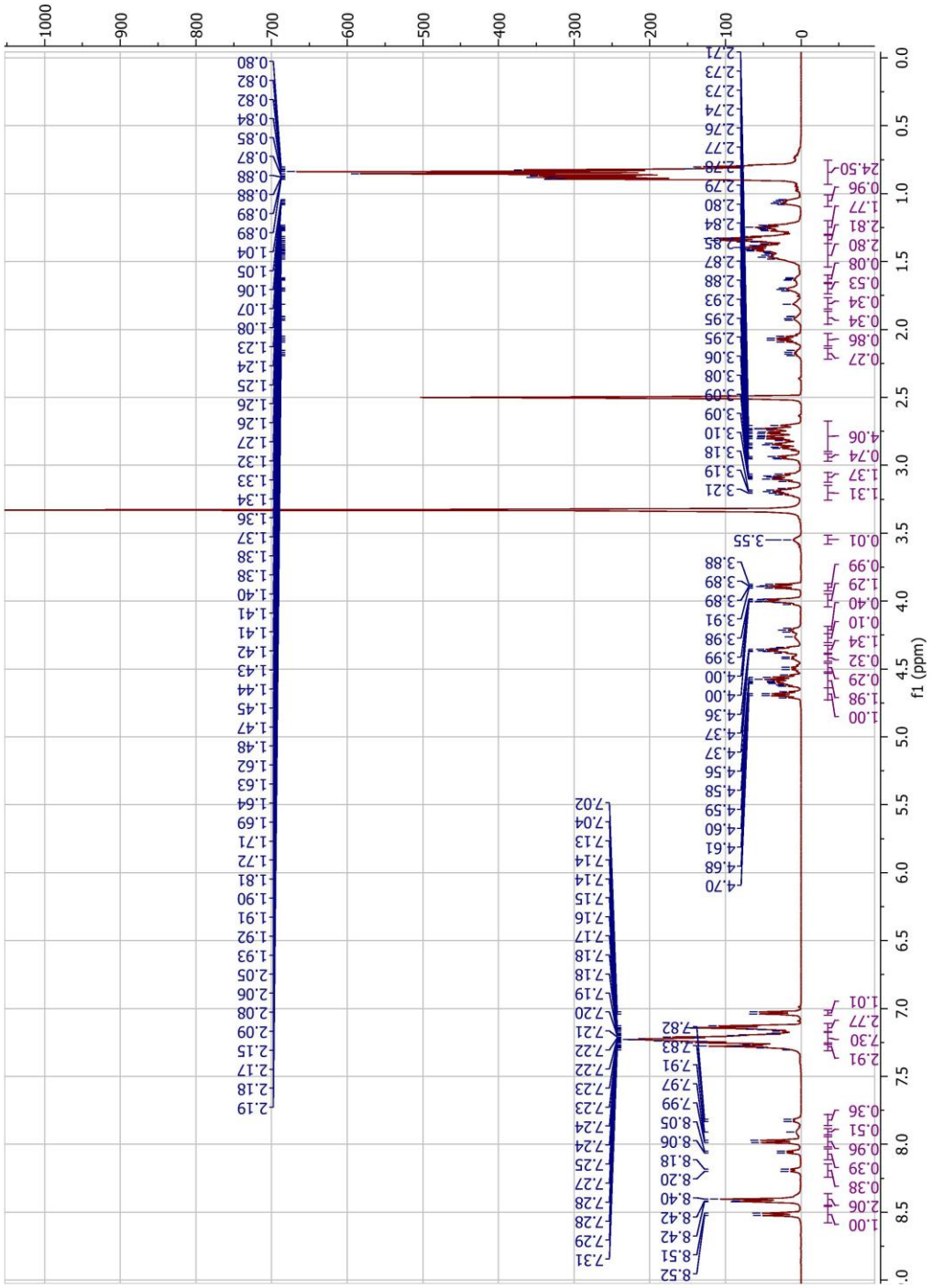

7 ^{1}H *d*6 DMSO (2 conformers)

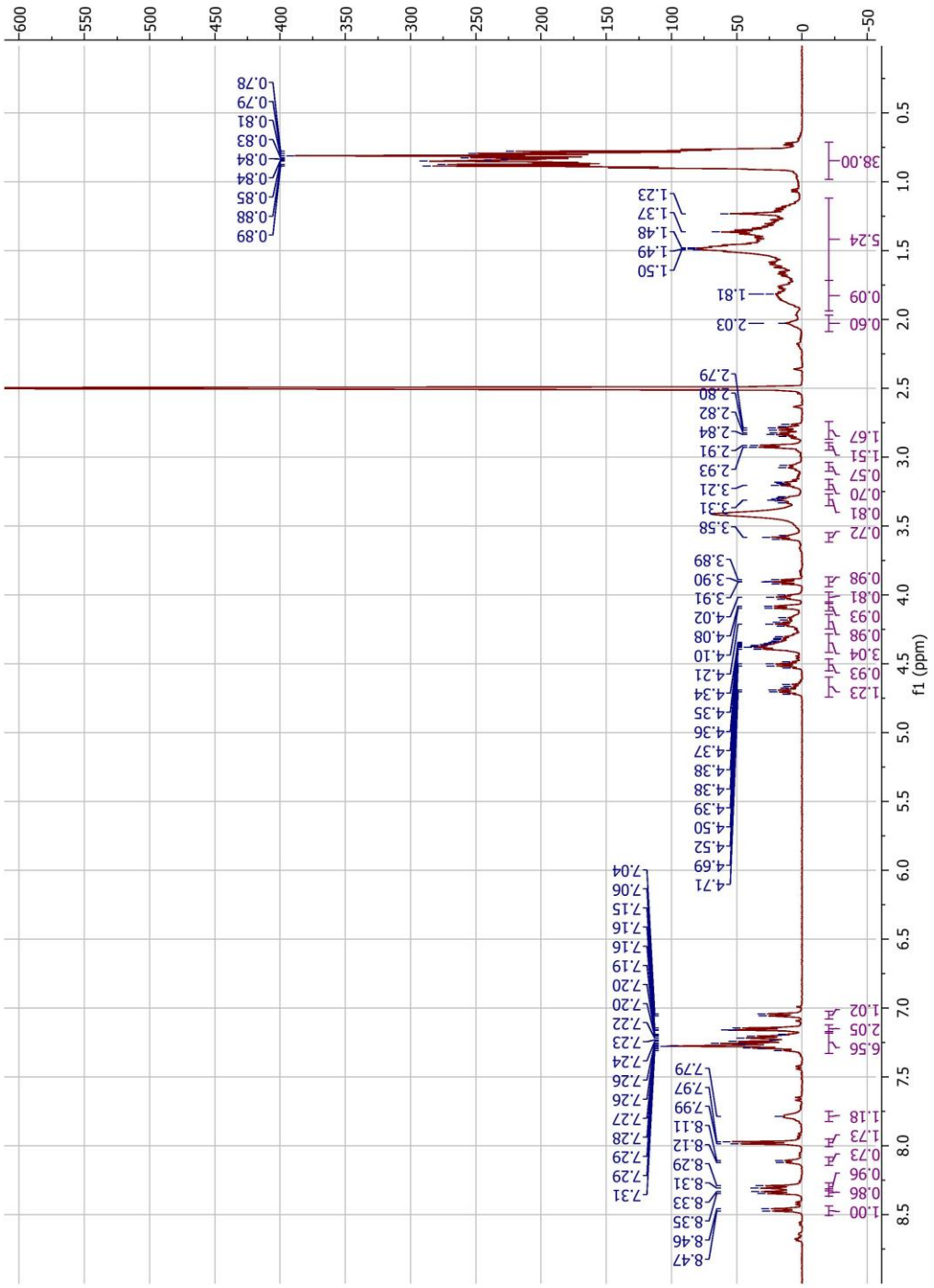

8 ^{1}H *d*6 DMSO (2 conformers)

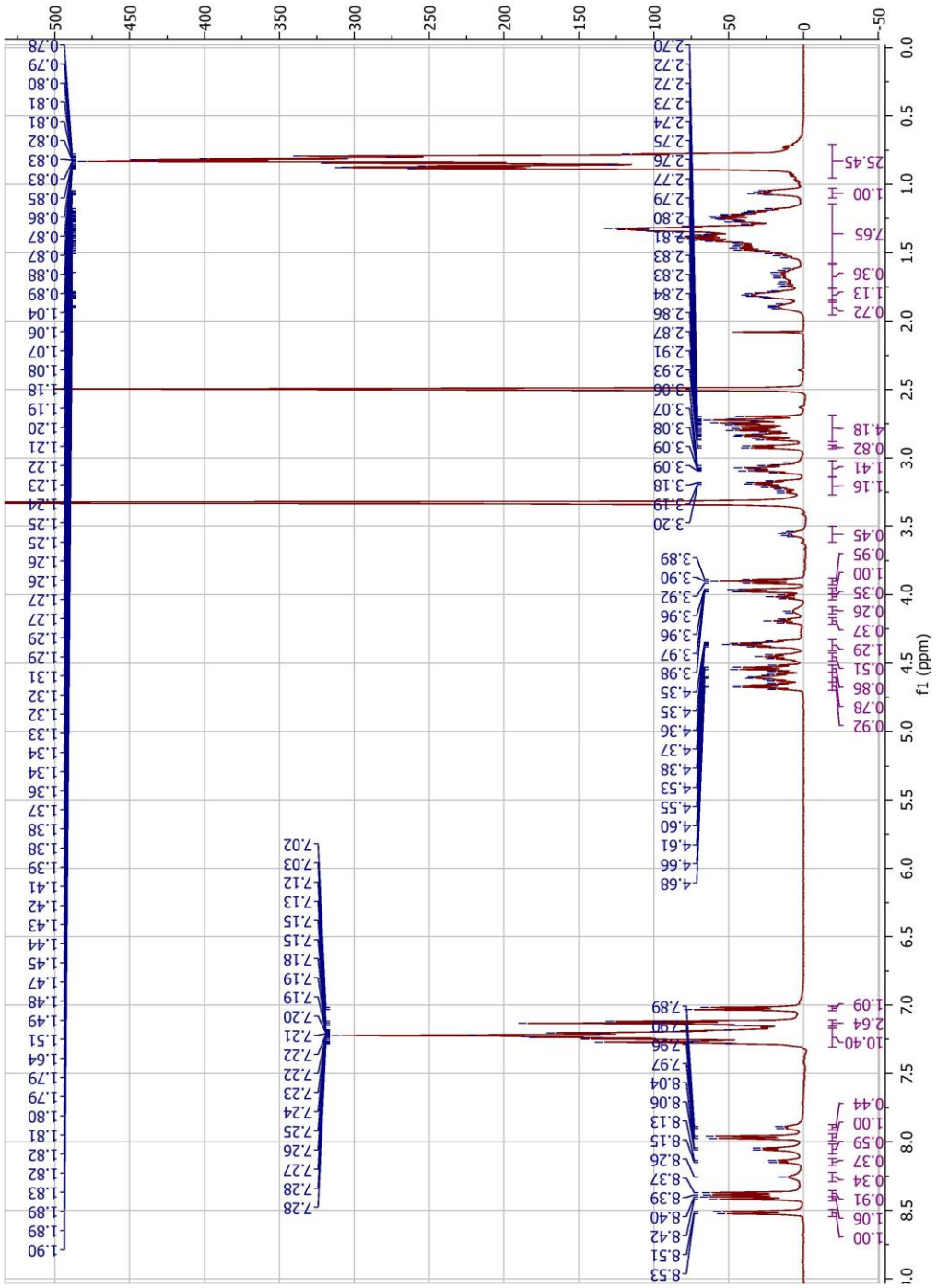

3.4.1.1. Pairwise Comparisson in Chloroform of Epimers

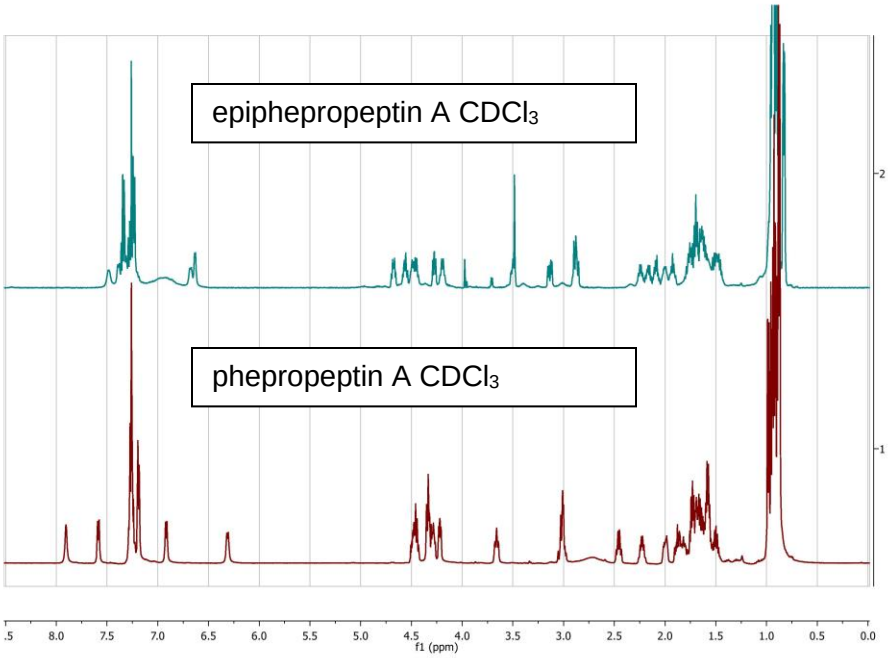

Figure 3-9 Comparisson of Phepropeptin A and Epiphepropeptin A in Chloroform

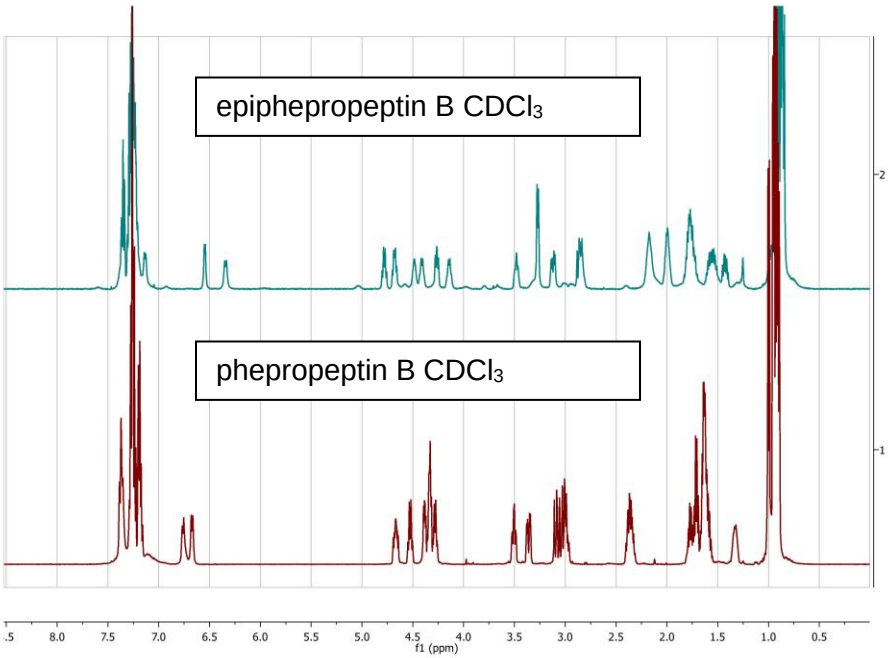

Figure 3-10 Comparisson of Phepropeptin B and Epiphepropeptin B in Cholroform

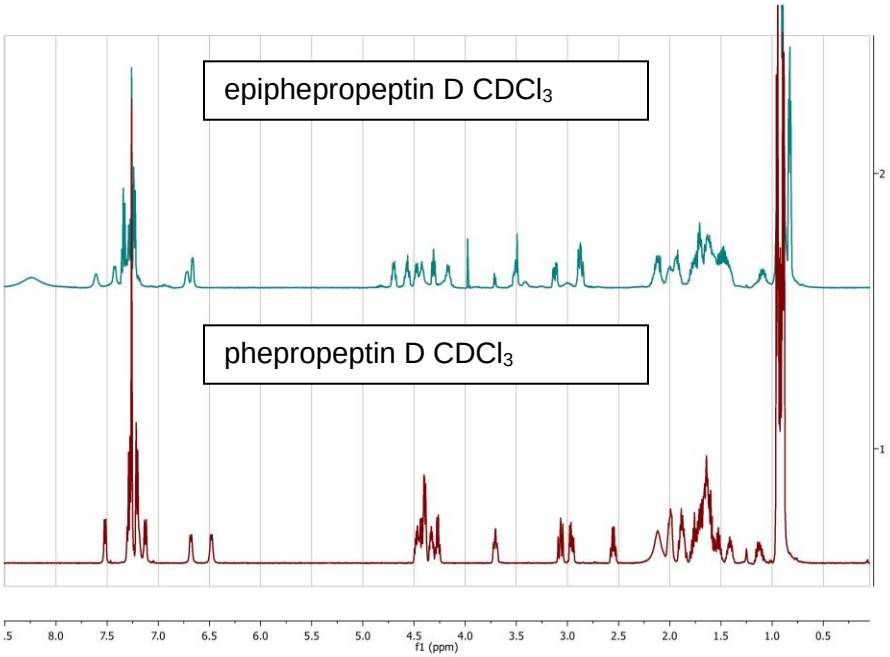

Figure 3-11 Comparisson of Phepropeptin C and Epiphepropeptin C in Chloroform

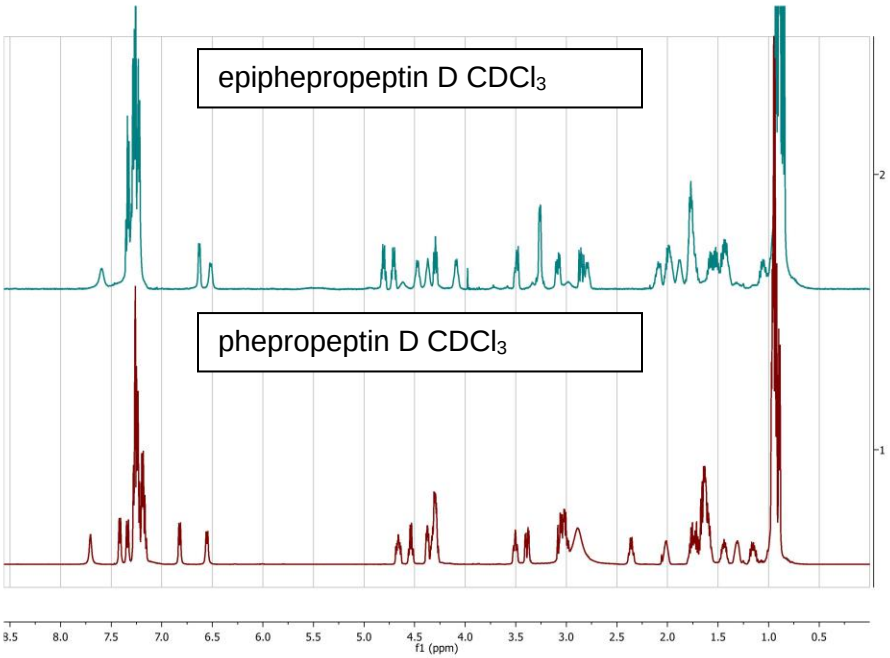

Figure 3-12 Comparisson of Phepropeptin D and Epiphepropeptin D in Chloroform

3 ROESY $CDCl_3$

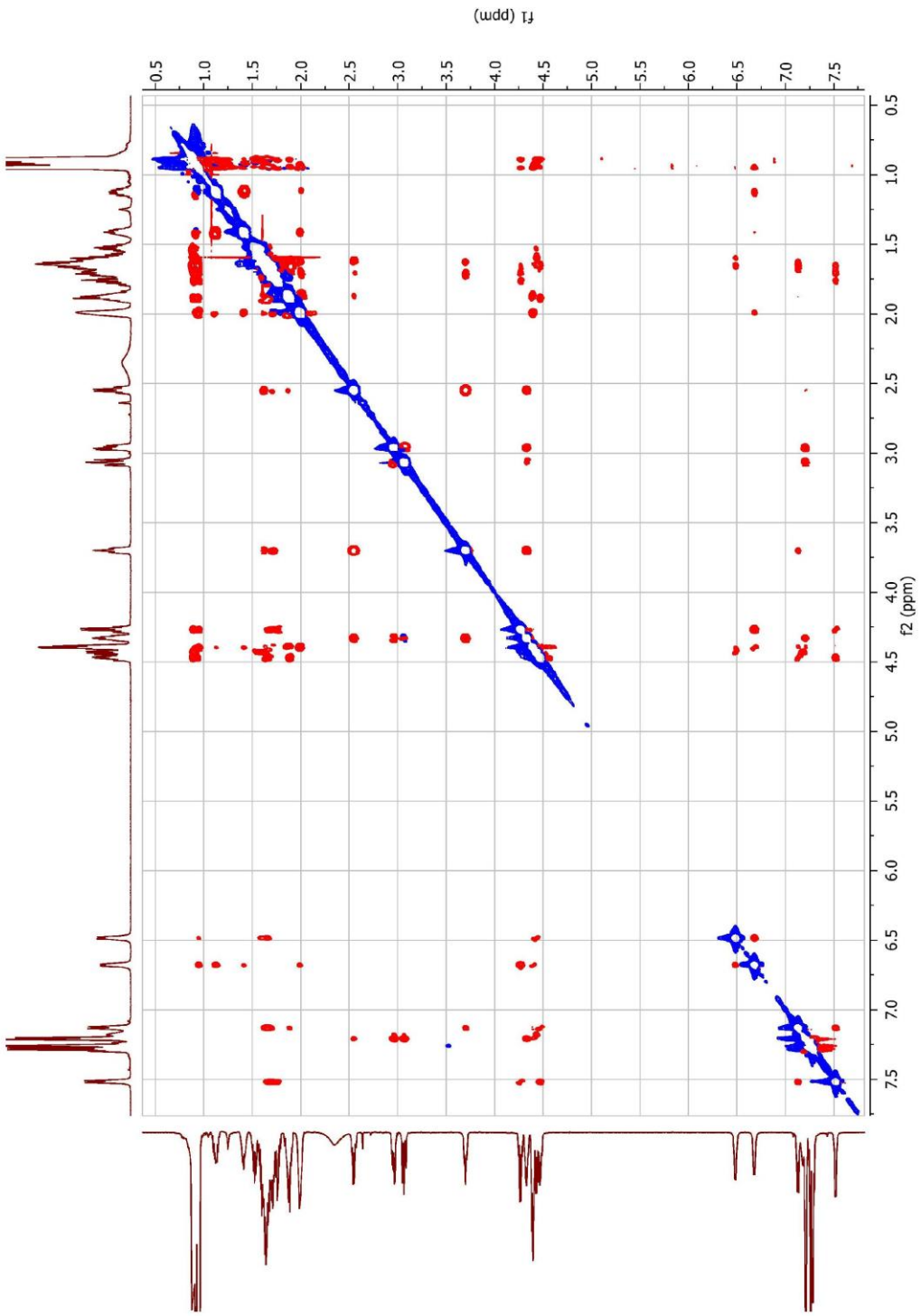

3 ^{1}H (*d*6 DMSO)

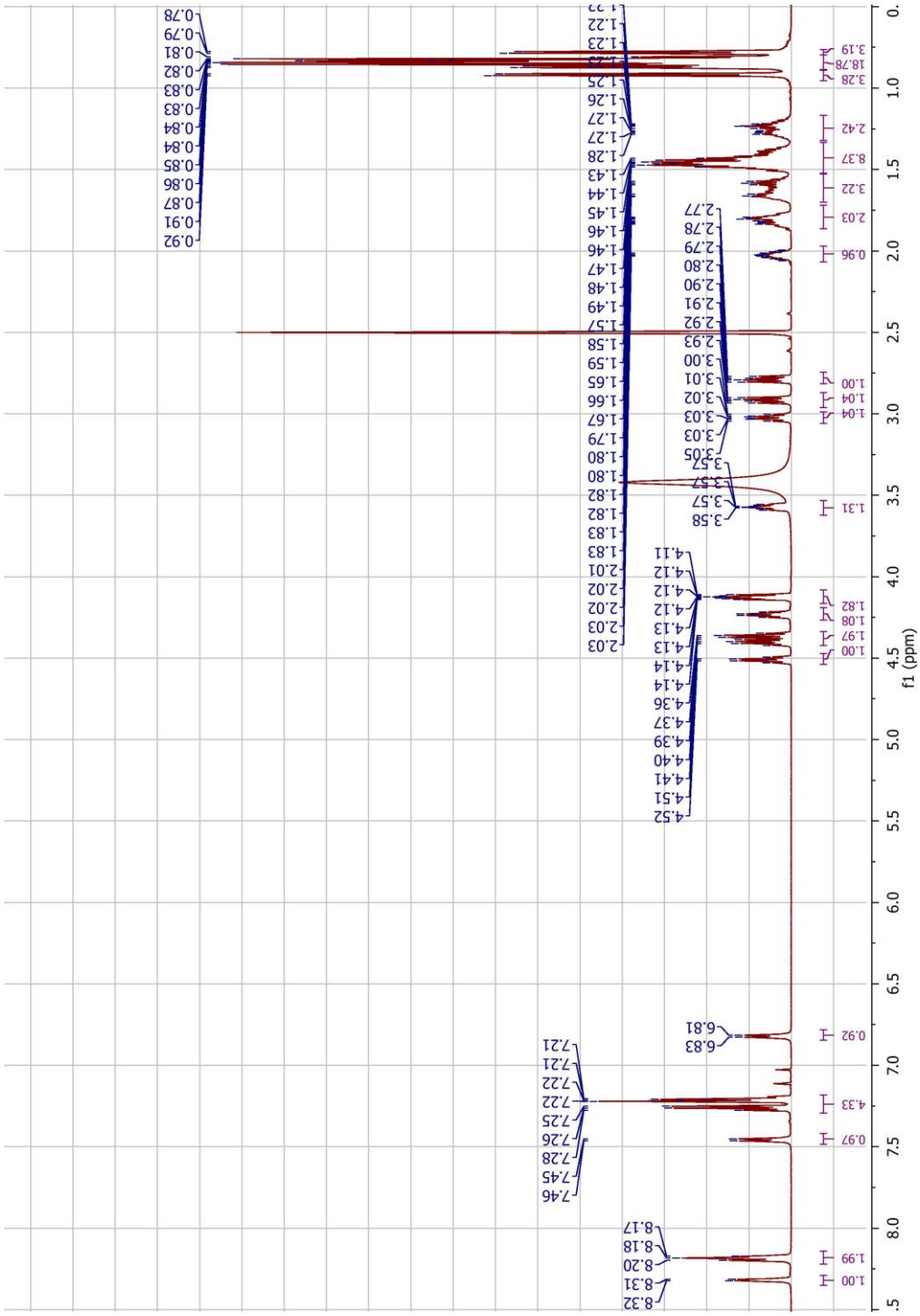

3 COSY (*d*6 DMSO)

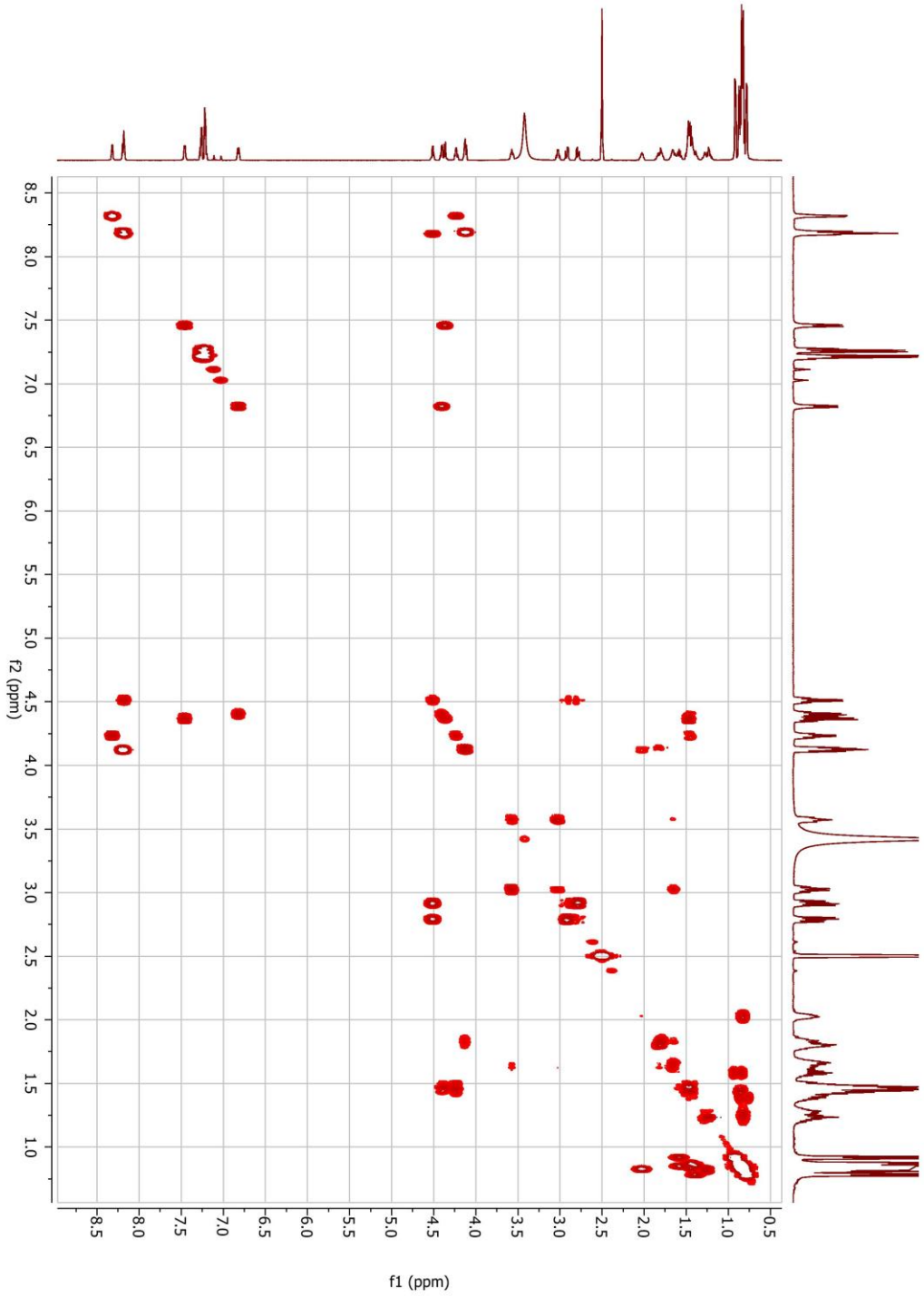

3 TOCSY (*d*6 DMSO)

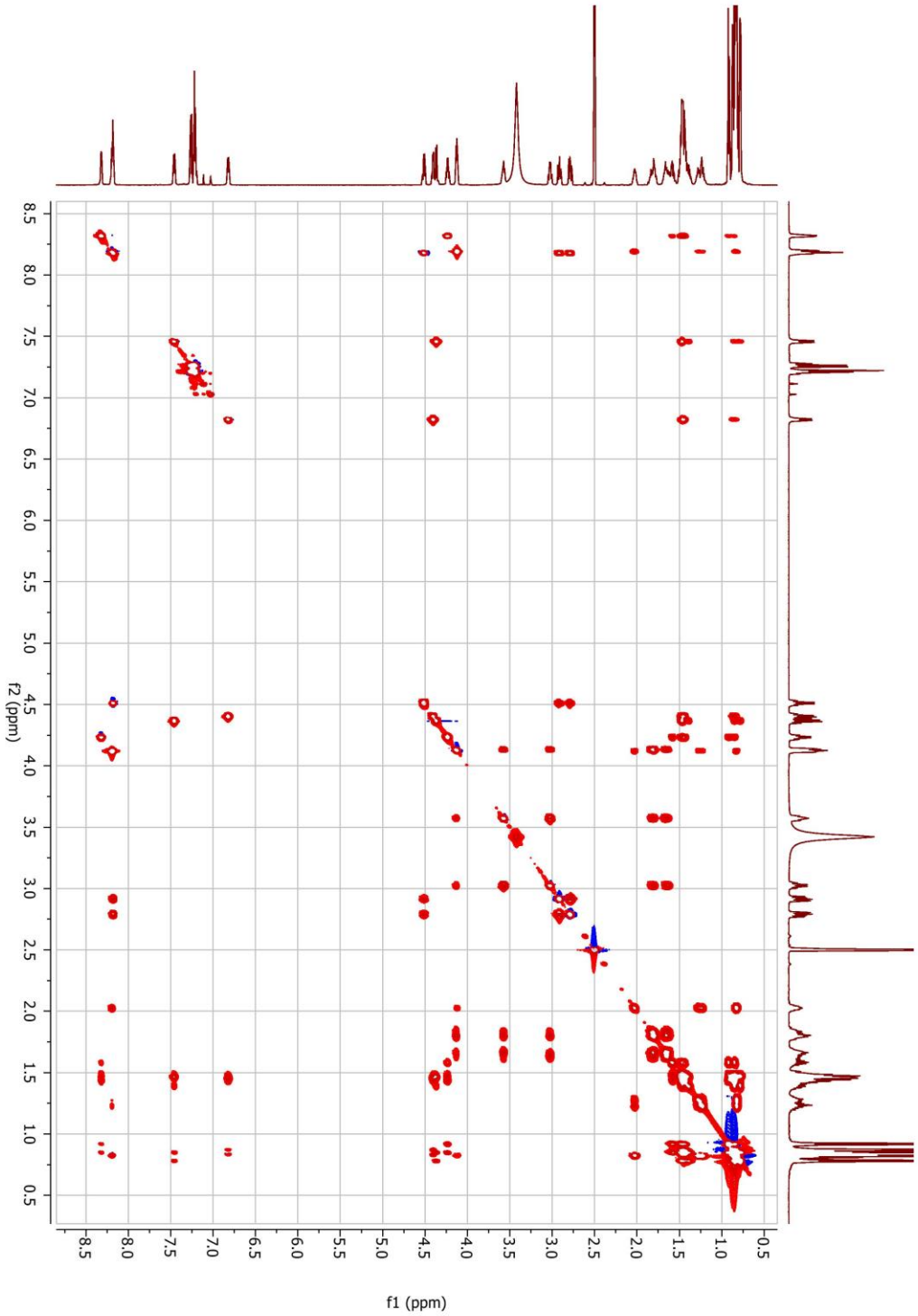

3 HSQC (*d*6 DMSO)

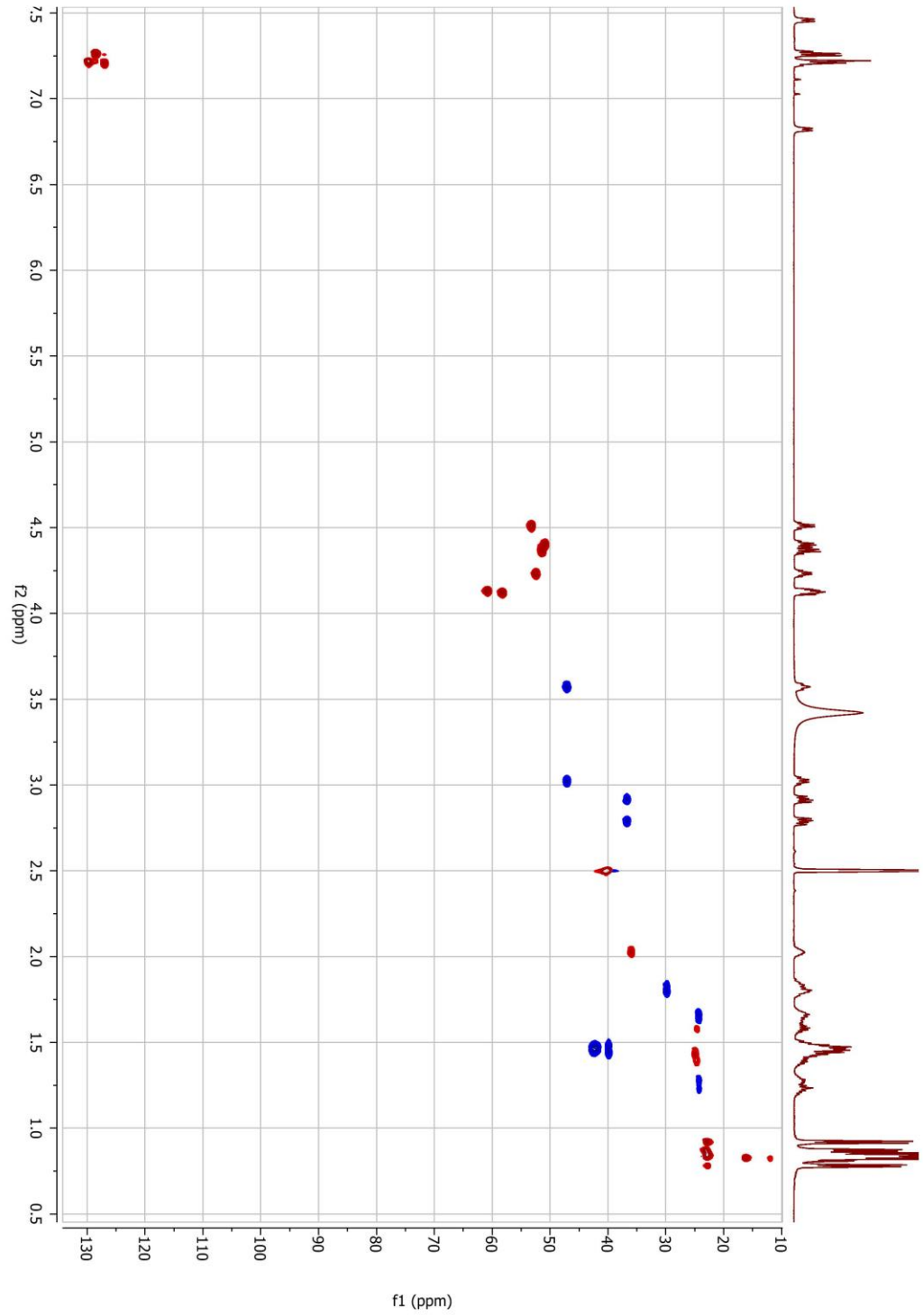

3 HMBC (*d*6 DMSO)

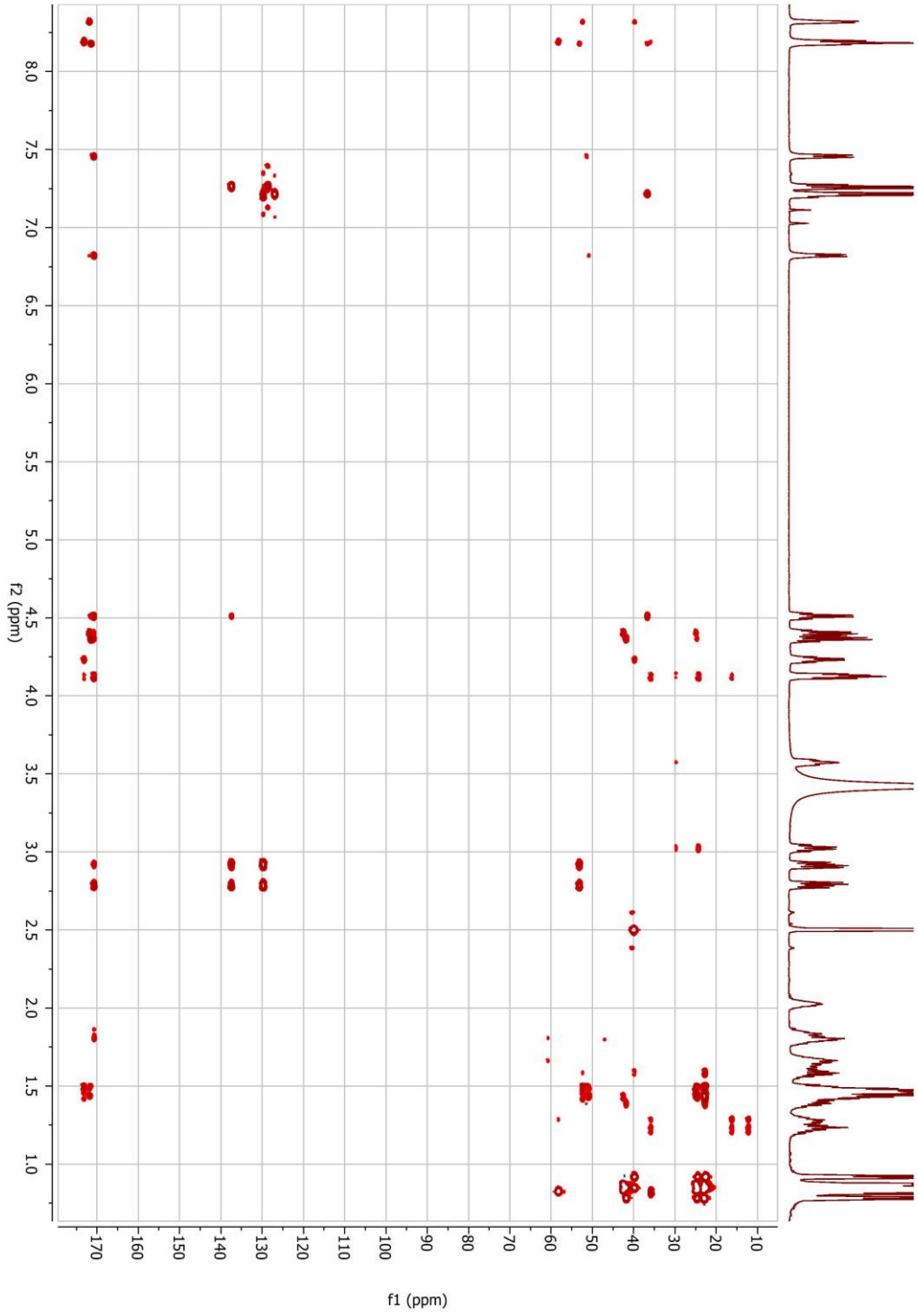

3 ROESY (*d*6 DMSO)

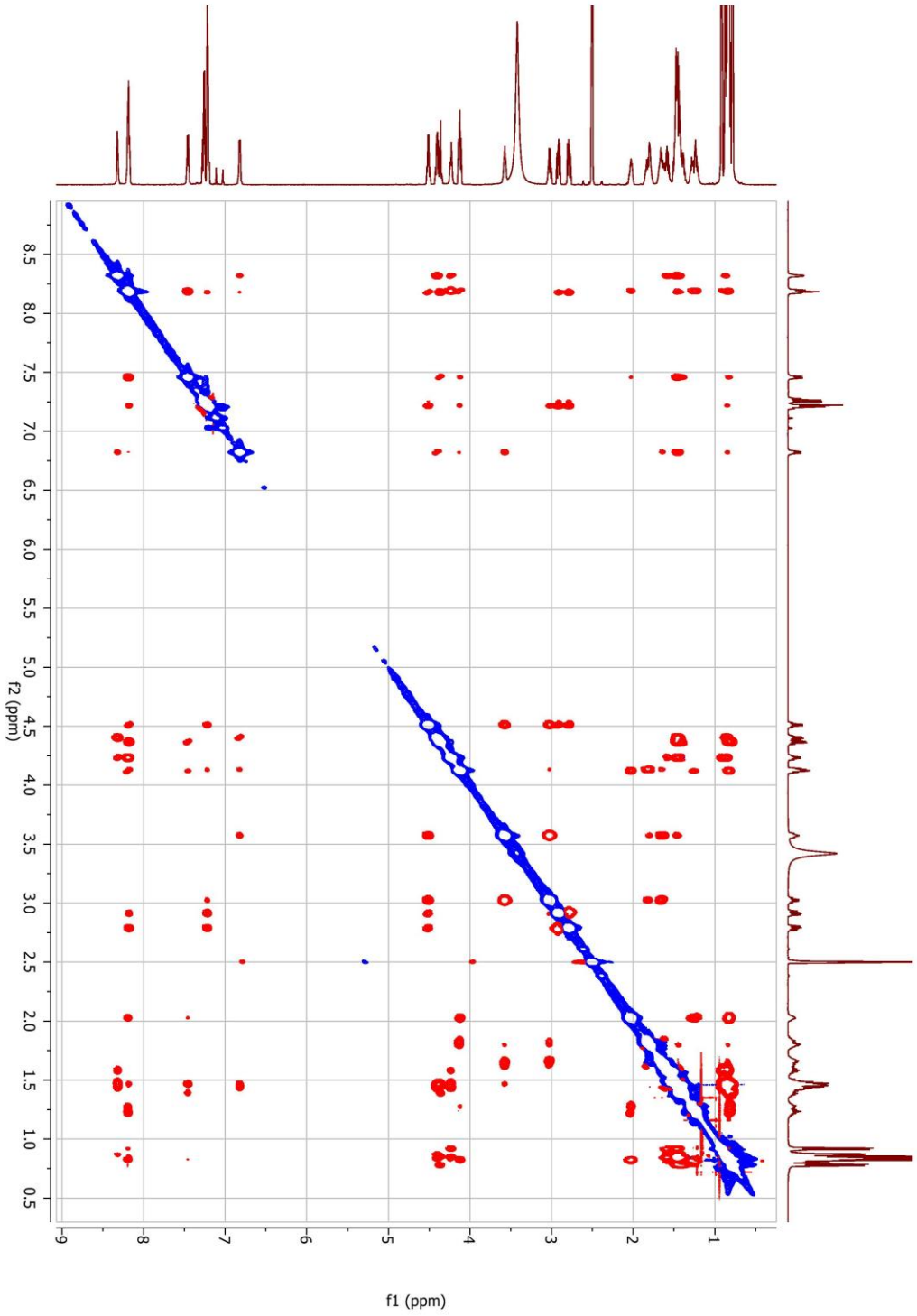

3.5. Other Natural Products

3.5.1. Introduction

While there have been several studies conducted in the Lokey Lab[18,24,47,48] and others[25,49,50] on the cell permeability of cyclic peptide natural products they are still heavily outnumbered by the number of studies focused on purely synthetic model systems[51]. A primary reason for this is the difficulty in obtaining substantial amounts of natural products as both the growth (or harvesting) of their source organisms and the subsequent purification is challenging and time consuming. It is rare to have enough of a natural product where conducting destructive assays focusing on pharmacokinetics are a priority, especially in natural products labs which traditionally focus on bioactivity.

To address this, Cameron Pye, in unpublished work, mined the Antimarin database for cyclic peptide natural products. After computational trimming for predicted ADME properties a list of "potentially permeable" cyclic peptides were produced. Manual curation of this list for synthetic tractability lead to a small, < 200, list of cyclic peptides which both appeared to be passively permeable by 2-dimensional descriptors and possessed facile synthetic routes. To explore these natural products as potential scaffolds whose characterization would lead to further insights into the pharmacokinetic properties of natural products a number of these compounds were synthesized.

In addition to providing material to test for pharmacokinetic properties the total synthesis of natural products provides the following: an opportunity to confirm the proposed structure, a path to synthesis of new analogs, and a re-evaluation of their biological activity. The natural products cylindrocyclin A, stylissamide G, cordyheptapeptide B, and scytalidamide A were synthesized as a part of a study into the effect of size on membrane translocation in macrocycles. These compounds were included as diverse scaffolds to confirm the generality of the size-dependence observed by Pye et al.[48] in purely synthetic model systems. All compounds had permeabilities within an order of magnitude of that of CSA, > -7 cm/s^2 log Pe, in the PAMPA assay, with only scytalidamide A outperforming it. All of them, except for stylissamide G, had very low soluble fractions, which appears to be limiting their observed permeabilities.

3.5.2. Cylindrocyclin

3.5.2.1. Introduction

The natural product cylindrocyclin was initially reported by Weber et al. in 2006.[52] It was isolated from the fungus *Cylindrocarpon* sp. which was collected from a twig in France by Prof. H. Anke (IBWF). Fermentation and methanolic extraction followed by multiple chromatographic separations yielded cyclindrocyclin A. It was reported to have modest, > 10 uM IC_{50}, cytotoxic activity against a panel of 6 mammalian cell lines and no antimicrobial, nematicidal, or phytoxicity in any of the organisms tested. None the less, it represents a unique structure not unlike that of cyclosporine A. With 9 amino

acids, all of which are aliphatic, and 4 *N*-methylated residues it fits the description for a "potentially permeable peptide", Figure 3-13. Its molecular weight of 948.3 Da also puts its outside the "extended rule of 5" space that most synthetic cell permeable cyclic peptides fall into.

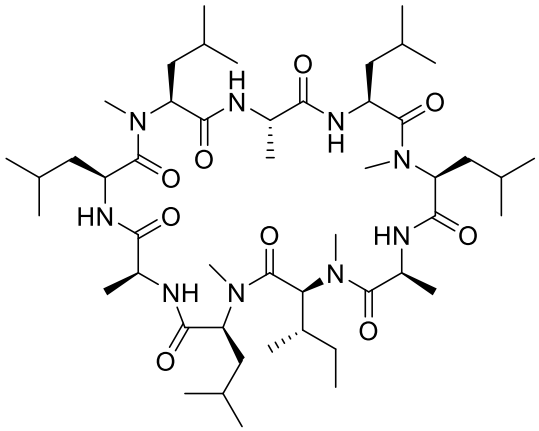

Figure 3-13 Structure of cylindrocyclin A

3.5.2.2. Synthesis

The synthesis of cylindrocyclin A was conducted using classic FMOC-solid phase peptide synthesis, Figure 3-14. In general couplings went to completion using HATU and microwave heating, with the exception of *N*-Me-isoleucine onto *N*-Me-leucine. Consecutive N-methylated amino acids are known to cause inefficient couplings. To address this the much more reactive acyl-chloride was generated using Bis(trichloromethyl) carbonate (BTC)[53] which efficiently yielded to the tri-peptide. Cyclization in solution with the reagent COMU, flash purification, and finally HPLC purification lead to pure cyclindrocyclin. Interesting, like cyclosporine A, cylindrocyclin exhibits a broad peak shape on the chromatographic timescale, which

may be a sign of multiple conformations with different physical properties, especially given its uncharged nature. A comparison to the published NMR chemical shifts yielded a match, confirming the reported structure.

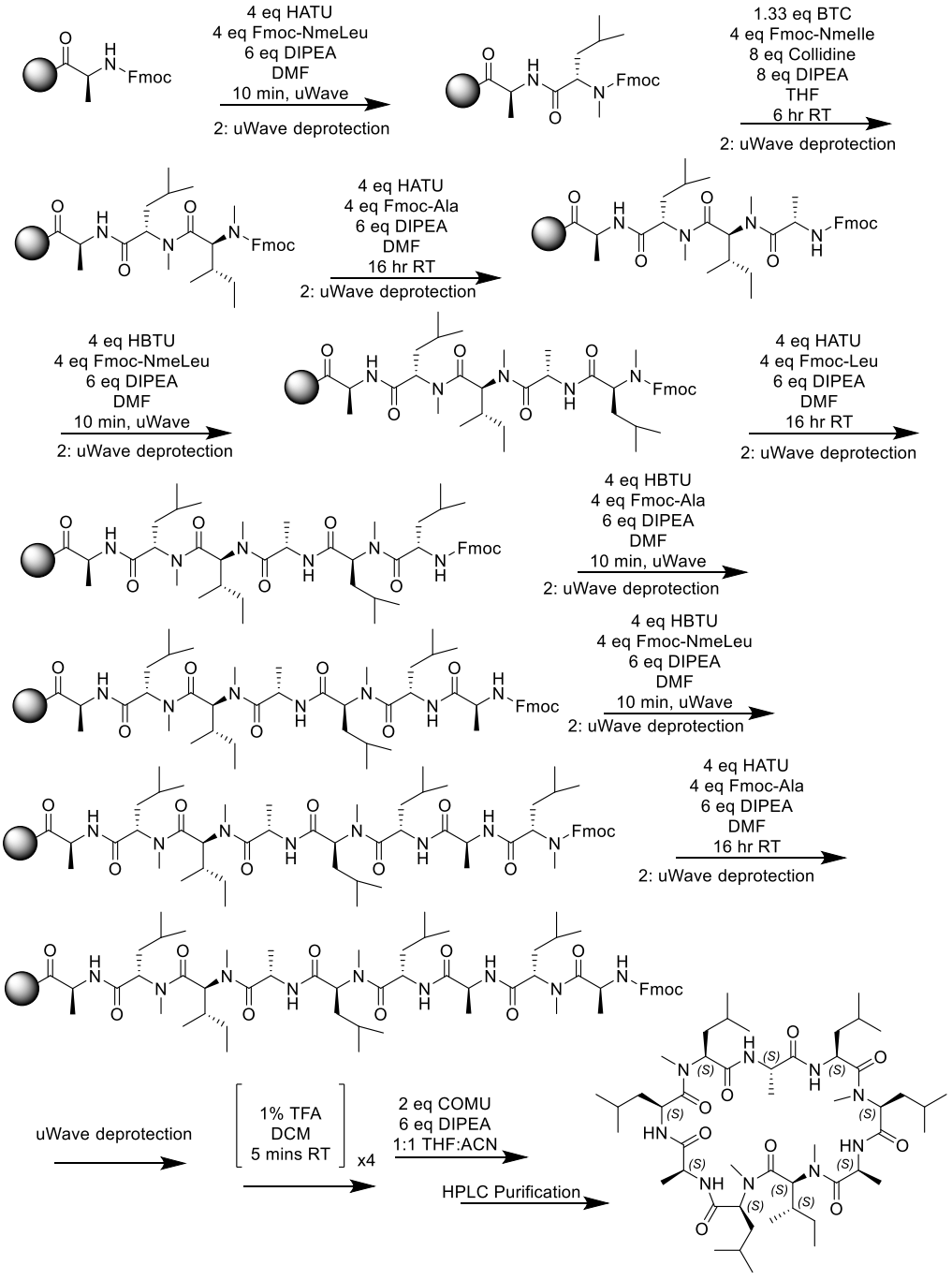

Figure 3-14 Synthesis of cylindrocyclin A

3.5.2.3. NMR Analysis

To explore its ability to form intramolecular hydrogen bonds in a low dielectric environment temperature shift analysis was conducted in chloroform. Additionally, since it has been speculated that many natural products may have solvent dependent conformations which may be a way of balancing solubility and permeability the temperature shift analysis was also conducted in DMSO which is much more polar than chloroform. In chloroform cylindrocyclin has all its amide protons shielded from solvent as indicated by temperature shift analysis[37]; in contrast 2 of its 5 protons are solvent exposed in DMSO, Table 3-13. Curiously, there appear to be two major conformations in slow exchange on the NMR time scale in both solvents. Upon visual inspection, in chloroform the major conformation seems to hide its amides better than the minor conformation. In contrast, in DMSO the major conformation exposes a number of its NHs while the minor conformation appears to do so to a lesser degree, although spectral overlap precludes detailed analysis, Figure 3-15.

Table 3-13 Temperature Shift Analysis of Cylindrocyclin A

Chloroform		
ppm	**Slope**	**R2**
6.74	-0.64	1.00
7.23	-0.85	1.00
7.56	0.17	0.93
8.12	-2.21	1.00
8.17	-2.07	1.00

DMSO		
ppm	**Slope**	**R2**
7.36	-5.51	1.00
7.70	-5.17	1.00
7.97	-0.92	0.98
8.40	2.20	0.96
8.85	-2.35	0.99

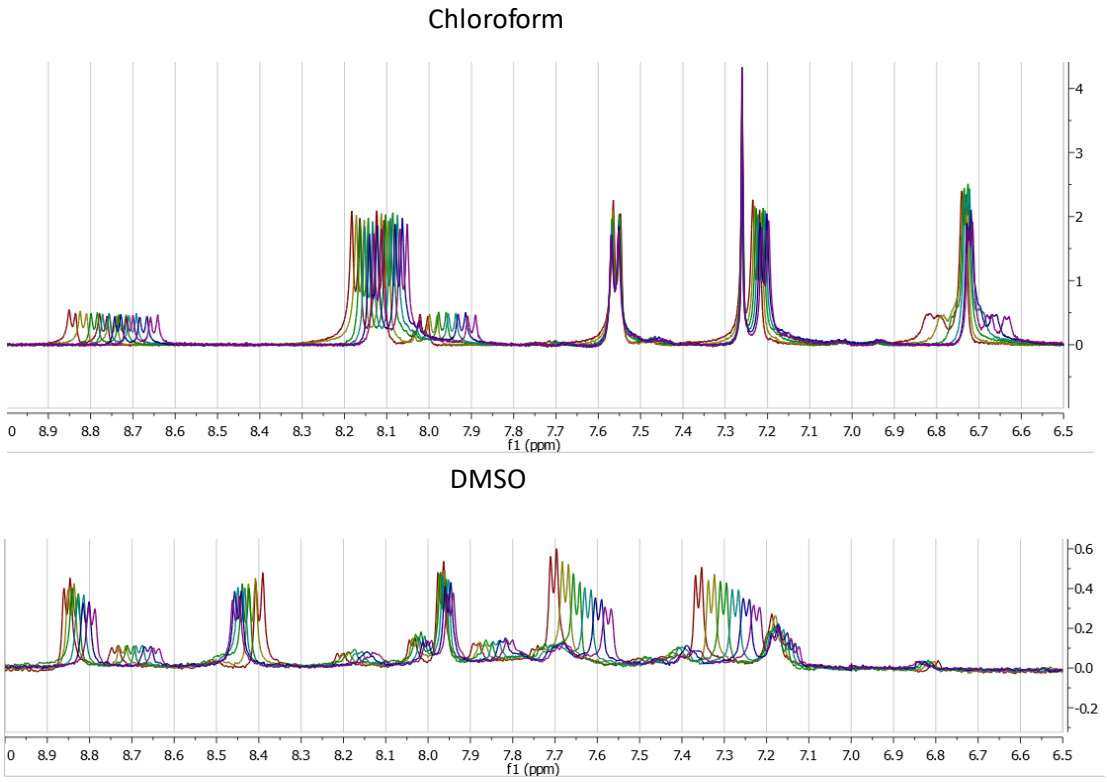

Figure 3-15 Variable Temperature NMR Spectra for Cylindrocyclin A

3.5.2.4. Conclusion

In conclusion cylindrocyclin A represents a novel scaffold with a dynamic hydrogen bonding pattern depending on the solvent environment. Further investigations into the 3 dimensional structure will undoubtedly find a unique conformation, one that will likely be dependent on the polarity of the solvent environment.

3.5.3. Stylissamide G

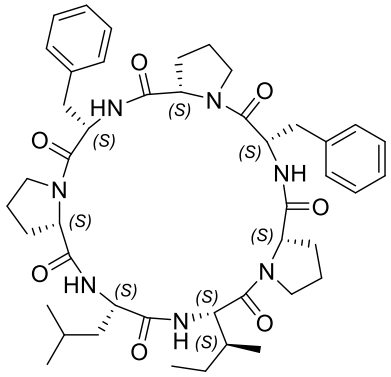

Figure 3-16 Structure of Stylissamide G

Stylissamide G, Figure 3-16, was initially isolated from a extract of the sponge *Stylissa caribica* collected in the Caribbean Sea.[54] Stylissamide G is reminiscent of other proline rich cyclic peptide natural products[55] and is of interest since its hydrophobic nature suggests that it might be passively permeable. In 2014 its synthesis was completed via solution phase BOC chemistry by Fang et al. confirming the initially published structure as well as further characterizing its biological activity.[55] Since stylissamde G doesn't contain any methylated amides or unnatural residues it's synthesis was completed using standard microwave assisted FMOC SPPS followed by solution phase cyclization, Figure 3-17. Its NMR spectrum matched the previously reported spectra.[54]

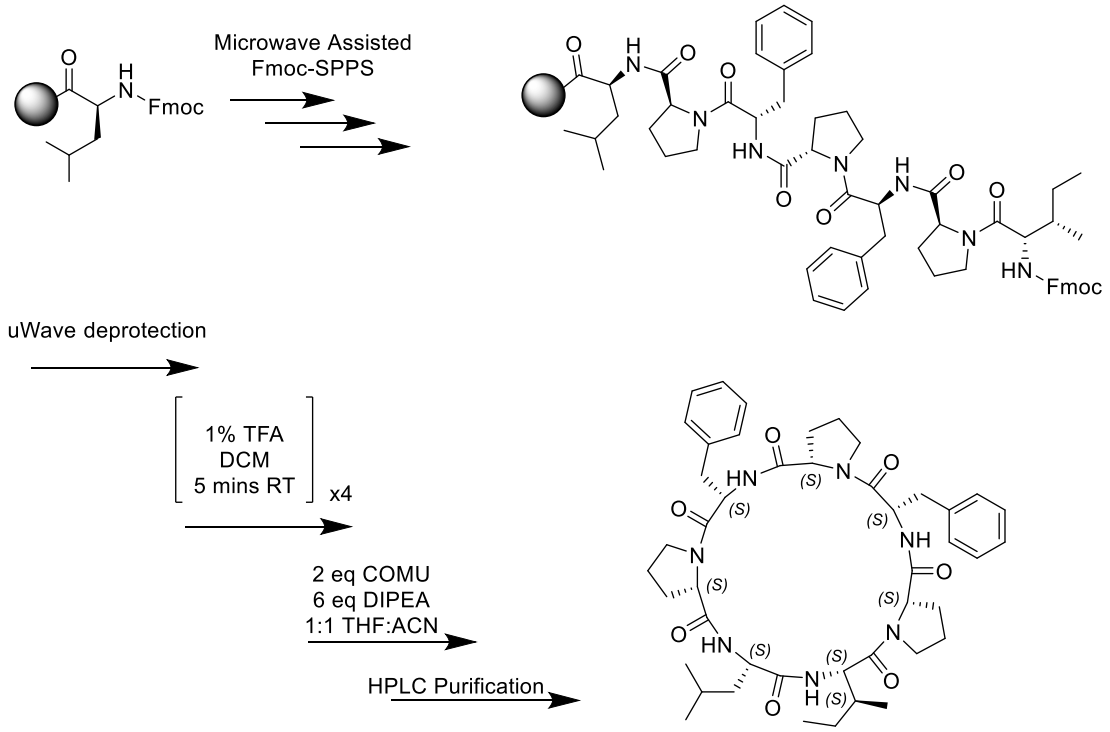

Figure 3-17 Total Synthesis of Stylissamide G

3.5.4. Cordyheptapeptide B

Cordyheptapeptides A and B, Figure 3-18, are cyclic heptapeptide natural products that include both D-amino acids as well as *N*-methylation, two classic hallmarks of cell permeability. They were initially isolated from the pathogenic fungus *Cordyceps pseudomilitaris*.[56] Cordyheptapeptide A showed potent cytotoxity in a panel of 4 mammalian cell lines, IC_{50} values < 1 μM, while cordyheptapeptide B was slightly less potent with IC_{50} values < 3.2 μM. Cordyheptapeptide B was synthesized by Dahiya et al. in 2016 via solution phase BOC peptide chemistry confirming the originally reported structure.[57]

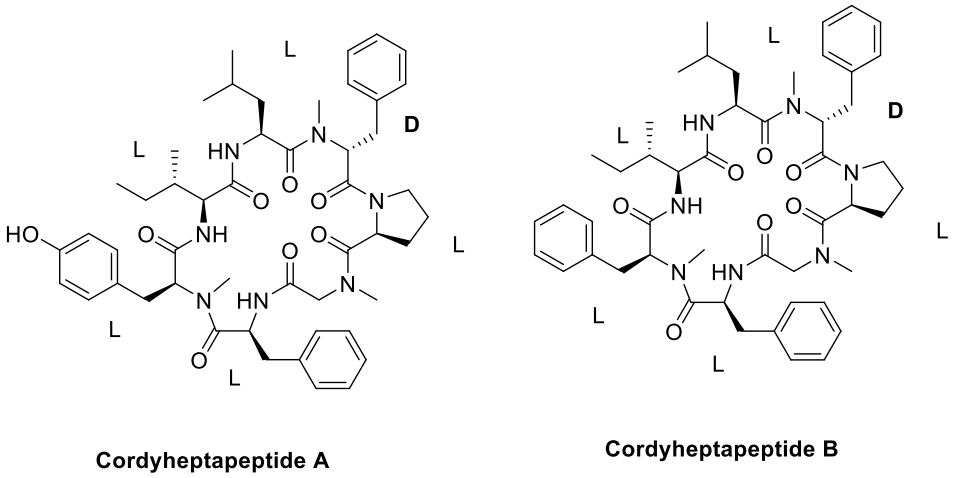

Figure 3-18 Cordyheptapeptides A and B

Later a number of analogs of the cordyheptapeptides, C-E, were isolated by Chen et al.[58] This report included a crystal structure of cordyheptapeptide C, which shares the same backbone scaffold as cordyheptapeptides A and B. Curiously it shows a number of intramolecular hydrogen bonds and a beta-turn/beta bulge motif. While cordyheptapeptide A has more potent biological activity, the presence of a *N*-methylated tyrosine requires tedious in-sequence methylation. Cordyheptapeptide B, which includes an *N*-methylated phenylalanine instead, was chosen for this study to simplify the synthesis. However, the total synthesis of cordyheptapeptide A, unpublished, was achieved and will be reported in due course by Quinn Edmonson in the Lokey Lab. The facile synthetic route of cordyheptapeptide B encouraged us to synthesize it as a potentially permeable peptide. Its synthesis was accomplished by microwave assisted solid phase peptide synthesis using pre-methylated amino acids, Figure 3-20. NMR spectrum matched the previously reported spectra.

Pharmacokinetic and biological activity of these compounds will be explored and reported in due course.

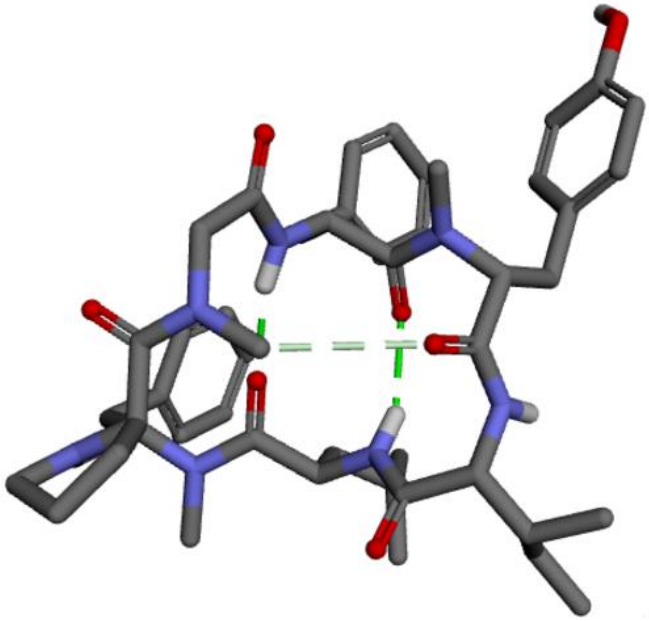

Figure 3-19 Crystal Structure of Cordyheptapeptide C reported by Chen et al.

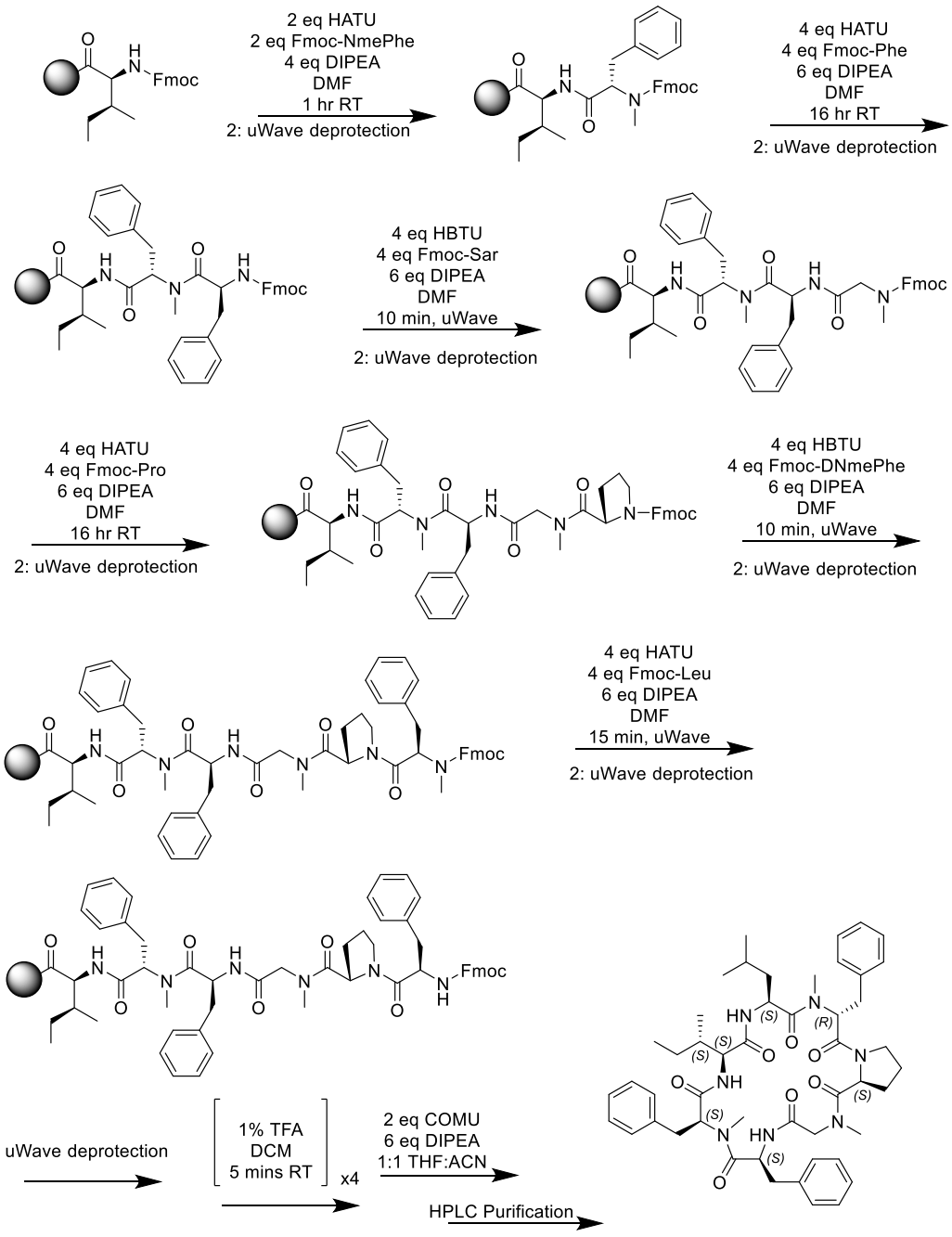

Figure 3-20 Total Synthesis of Cordyheptapeptide B

3.5.5. Scytalidamide A

Scytalidamides A and B were initially isolated from an algae associated *Scytalidium* fungus by Tan et al. in 2003.[59] The defining structural elements of the cyclic heptapeptides are an α-aminoisobutyric acid residue (Aib) , an *N*-methylated leucine and phenylalanine as well as a *trans* 4-methyl-proline in the case of scytalidamide B. Both compounds were tested against the NCI 60 panel of human cancer cell lines and displayed modest activity, IC_{50} values of < 5 μM for at least one cell line. The most interesting aspect, from a pharmacokinetic perspective, was the NMR analysis that was conducted. It was found that both compounds have 3 to 4 intramolecular hydrogen bonds by temperature coefficient analysis in chloroform but only 2 in DMSO. This hints at solvent dependent conformations which have been proposed as a general feature of cell permeable cyclic peptide natural products. Additionally, the solution conformation in chloroform was also obtained which showed three intramolecular hydrogen bonds, confirming the temperature shift analysis that showed three of the four residues were strongly shielded from solvent while the Aib residue is not engaged in a hydrogen bond.

The total synthesis of scytalidamide A was achieved in 2003 by Gu et al. via solid phase peptide synthesis confirming the published structure.[60] The presence of intramolecular hydrogen bonds prompted us to investigate scytalidamide A as a potentially permeable peptide. Its total synthesis was accomplished via solid phase peptide synthesis, Figure 3-21, however using a different linker strategy than Gu et al. A difficult coupling between the sterically hindered Aib residue and an incoming N-

methylated leucine required the use of the reagent BTC.[53] Cleavage from resin and solution phase cyclization yielded scytalidamide A whose NMR spectrum matched the previously reported spectra.

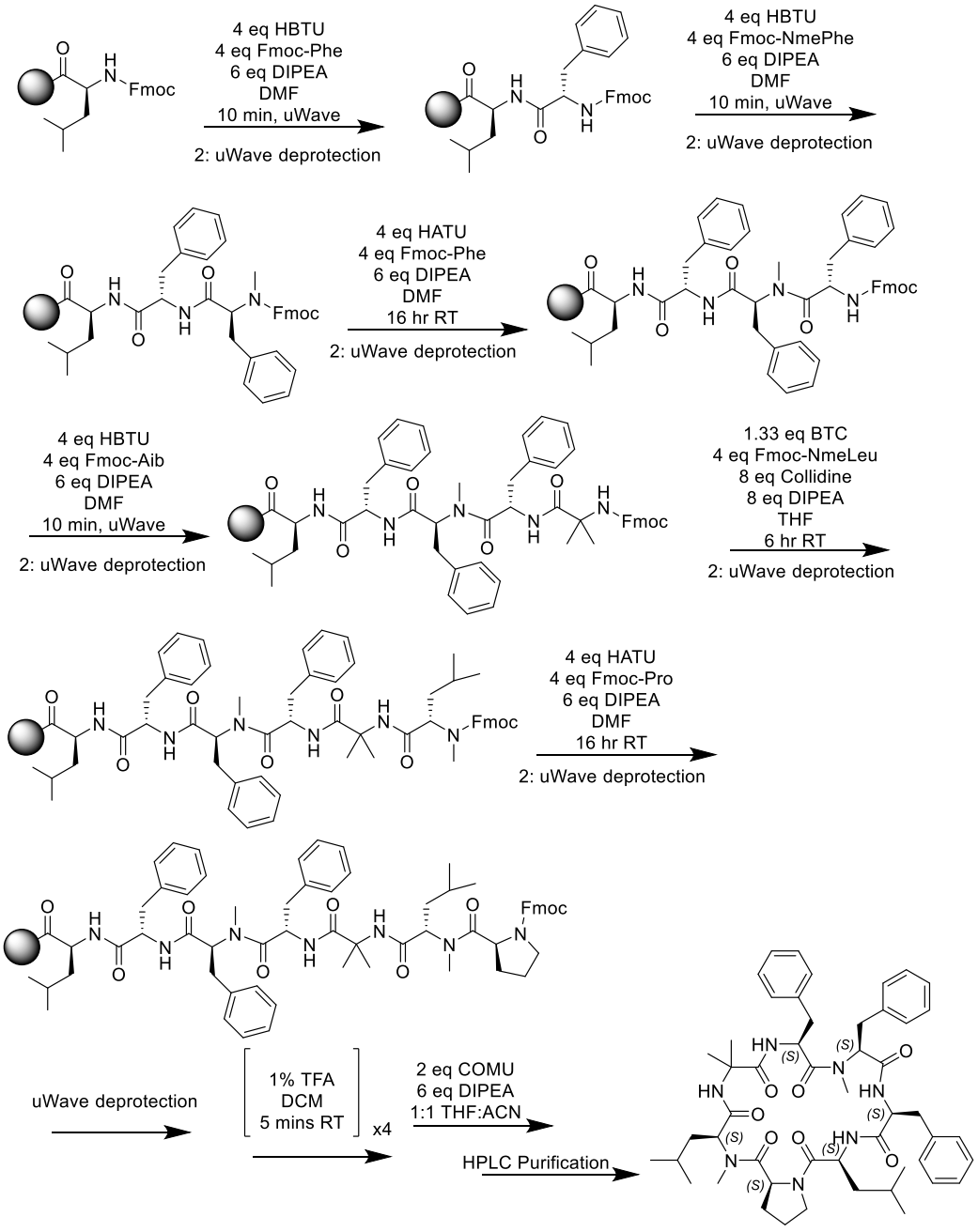

Figure 3-21 Total Synthesis of Scytalidamide A

3.6. Abbreviations

ACN, acetonitrile; BTC, Bis(trichloromethyl) carbonate; COMU, (1-Cyano-2-ethoxy-2-oxoethylidenaminooxy)dimethylamino-morpholino-carbenium hexafluorophosphate; DBU, 1,8- Diazabicyclo[5.4.0]undec-7-ene; DCM, dichloromethane; DIAD, diisopropyl azodicarboxylate; DMF, N,N-dimethylformamide; DIC, diisopropylcarbodiimide; DIPEA, diisopropylethylamine, DMSO, dimethylsulfoxide; DVB, divinylbenzene; EtOH, ethanol; Fmoc, 9-fluorenylmethoxycarbonyl; HBTU, N,N,N',N'-Tetramethyl-O-(1H-benzotriazol-1-yl)-uronium hexafluorophosphate; HOAt, 1-hydroxy-7-azabenzotriazole; IR, infrared; LCMS, liquid chromatography mass spectrometry; MeOH, methanol; N2, nitrogen; NMP, 1-methyl-2-pyrrolidinone; PTFE, Polytetrafluoroethylene; PyBOP, (benzotriazol-1-yloxy)tripyrrolidinophosphonium hexafluorophosphate; RP, reverse phase; SPPS, solid phase peptide synthesis; TFA, trifluoroacetic acid; THF, tetrahydrofuran

3.7. Methods for Natural Product Synthesis

3.7.1. General Synthetic Strategies

Peptides were prepared with the following procedures; stylissamide G, cordyheptapeptide B, scytallidamide B, and cylindrocyclin were prepared using microwave assisted peptide couplings with installation of pre-methylated amino acids followed by solution phase cyclization with COMU.

3.7.2. Loading of 2-Chlorotrityl resin

Fmoc-Xaa (10 mmol) was added to a flame dried round bottom flask and dried in a vacuum dessicator with phosphorous pentoxide overnight. 50mL of dry DCM was cannula transferred into the flask followed by 2.5 mL of DIPEA transferred via syringe. After sonication for 10 min, 2-chlorotrityl resin (5 g) was added under a stream of N_2 and allowed to shake for 4 h. Resin was capped with a 15 mL solution of 1:2:17 MeOH:DIPEA:DMF (3 x 15 min). Resin was washed with DMF (3 x 15 mL) followed by DCM (3 x 15 mL). Loading value was calculated by mass increase of dried, loaded resin.

3.7.3. Microwave Reaction Conditions

Microwave assisted reactions were done in a CEM Discover microwave reactor with an open reaction vessel. Reactions were heated to 50 °C with 12 watts of power while temperature was monitored with an IR probe from within the reaction vessel.

3.7.4. Amino Acid Coupling under Microwave Condtions

A solution of Fmoc-Xaa, (4 equiv) HBTU (4 equiv), HOAt (4 equiv), and DIPEA (6 equiv) in DMF was allowed to pre-react for 5 min. This solution was added to the deprotected peptide on-resin and allowed to react for 10 min at 50 °C under microwave heating. The solution was drained and resin was washed 3 times with DMF (3 x 3 mL)

and DCM (3 x 3 mL). The reaction was monitored by LCMS and repeated until starting material was no longer observed.

3.7.5. Amino Acid Coupling onto Sterically Demanding Amino Acids under Microwave Conditions

A solution of Fmoc-Xaa (4 equiv), HATU (4 equiv), and DIPEA (6 equiv) in DMF was allowed to pre-react for 5 min. This solution was added to the deprotected peptide on-resin and allowed to react for 30 min at 50 °C under microwave heating. The solution was drained and resin was washed DMF (3 x 3 mL) and DCM (3 x 3 mL). The reaction was monitored by LCMS and repeated until starting material was no longer observed.

3.7.6. Difficult Amino Acid Coupling with BTC

A solution of BTC (1.33 equiv) and Fmoc-Xaa (4 equiv) in dry THF was allowed to pre-react for 1 min. A solution of DIPEA (8 equiv) in a minimum volume of THF was added to the resin that had been washed 3x with dry THF. To the solution of BTC and Fmoc-Xaa collidine (8 equiv) was added. After pre-reaction for 1 min this solution was added to the resin and the reaction was allowed to proceed for 6 hours under an atmosphere of dry Ar. The solution was drained and resin was washed DMF (3 x 3 mL) and DCM (3 x 3 mL). The reaction was monitored by LCMS and repeated until starting material was no longer observed.

3.7.7. Removal of the *N*-Fmoc Protecting Group Under Microwave Conditions

A solution of 2% piperidine and 2% DBU in DMF was added to the resin. The reaction was allowed to react for 5 min at 50 °C under microwave heating then drained. The resin was washed with DMF (3 x 3 mL) and DCM (3 x 3 mL).

3.7.8. Peptide Cleavage

Complete linear peptides were cleaved off resin in 5 resin volumes of 2.5% TFA in DCM for 4 minutes three times with a 5 resin volume DCM wash in between each step. Solvent was removed under N_2 followed by dissolution in acetone or DCM and evaporation under reduced pressure. Residual TFA was removed *in vacuo* overnight.

3.7.9. Cyclization with COMU

Linear peptides were dissolved in 20 mL of dry acetonitrile with DIPEA (4 equiv) and added dropwise to a solution of (final concentration 1 mg crude peptide per mL) 1:1 THF/ACN containing COMU (2 equiv). Reactions were stirred from 0.5 to 24 h until complete cyclization was achieved as monitored by LCMS. The reaction was reduced *in vacuo* for purification via HPLC.

3.7.10. Purification of Peptides

COMU by-products were removed after solution phase cyclization on a Biotage Isolera Prime system equipped with a KP-C18-HS 12g column eluting with H-2O/Acetonitrile modified with 0.1% TFA. Peptides were further purified when necessary on a Waters mass-directed prep system equipped with an XBridge BEH130 5µm 19x150 C18 column eluting with H_2O/Acetonitrile modified with 0.1% formic acid.

3.7.11. NMR Analysis

Spectra were acquired on either a Varian/Agilent 600 MHz NMR with a Unity Inova console with a 5 mm triple resonances cold probe or on an Agilent/Varian 500 MHz NMR with Unity Plus console and a 5 mm broadband probe or a 5 mm HX indirect detection probe.

3.7.12. HPLC-MS Characterization

HPLC-MS Spectrum for Cordyheptapeptide B

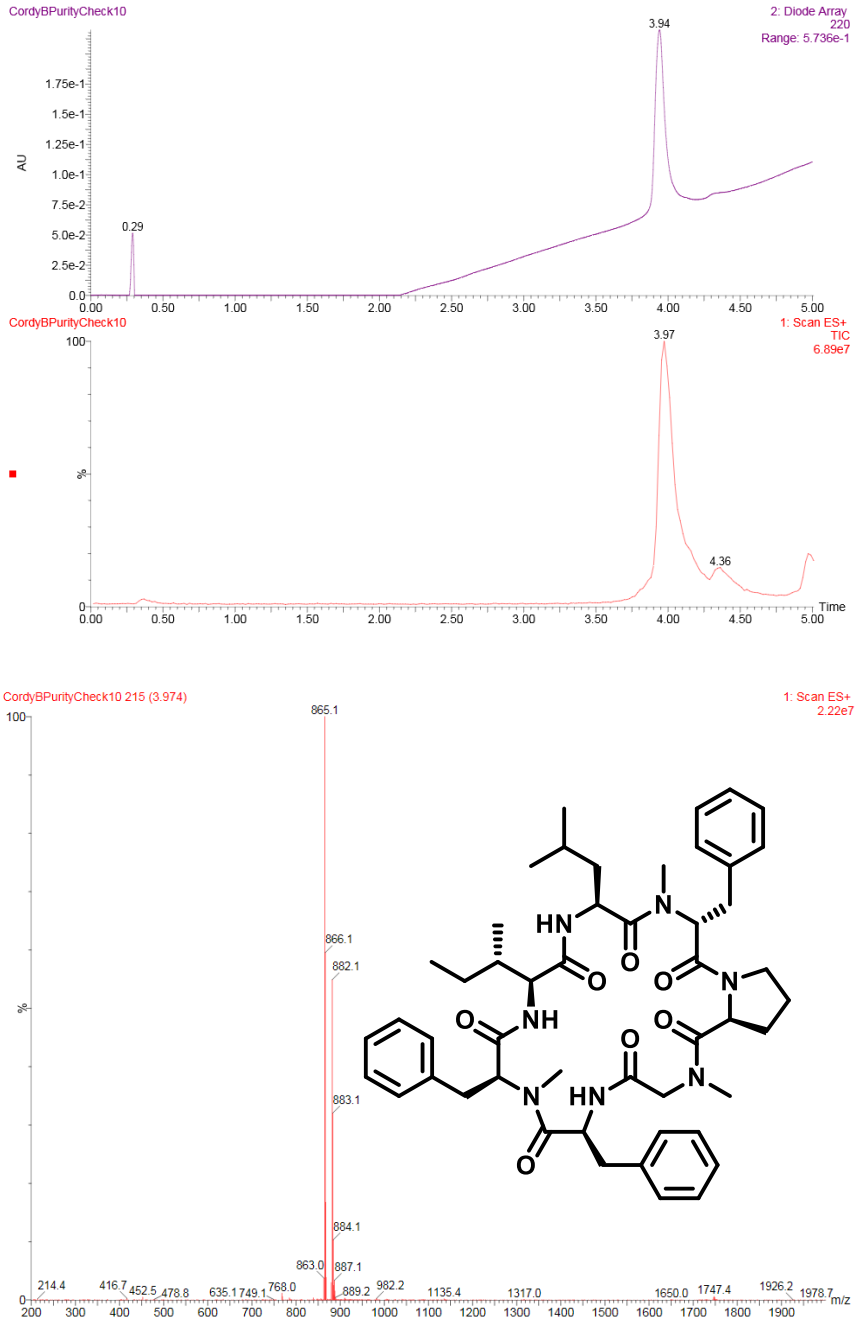

HPLC-MS Spectrum for Scytalidamide A

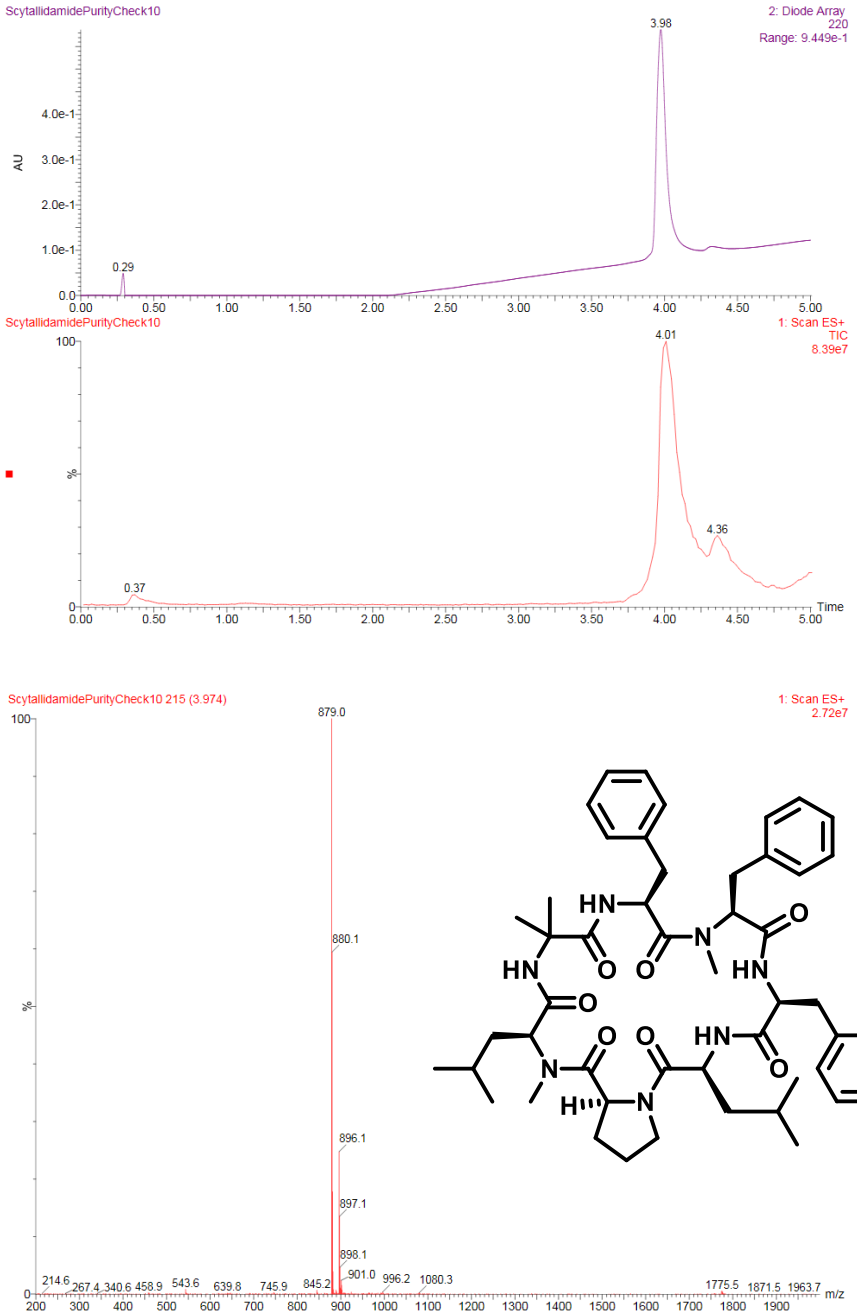

HPLC-MS Spectrum for Styllisamide G

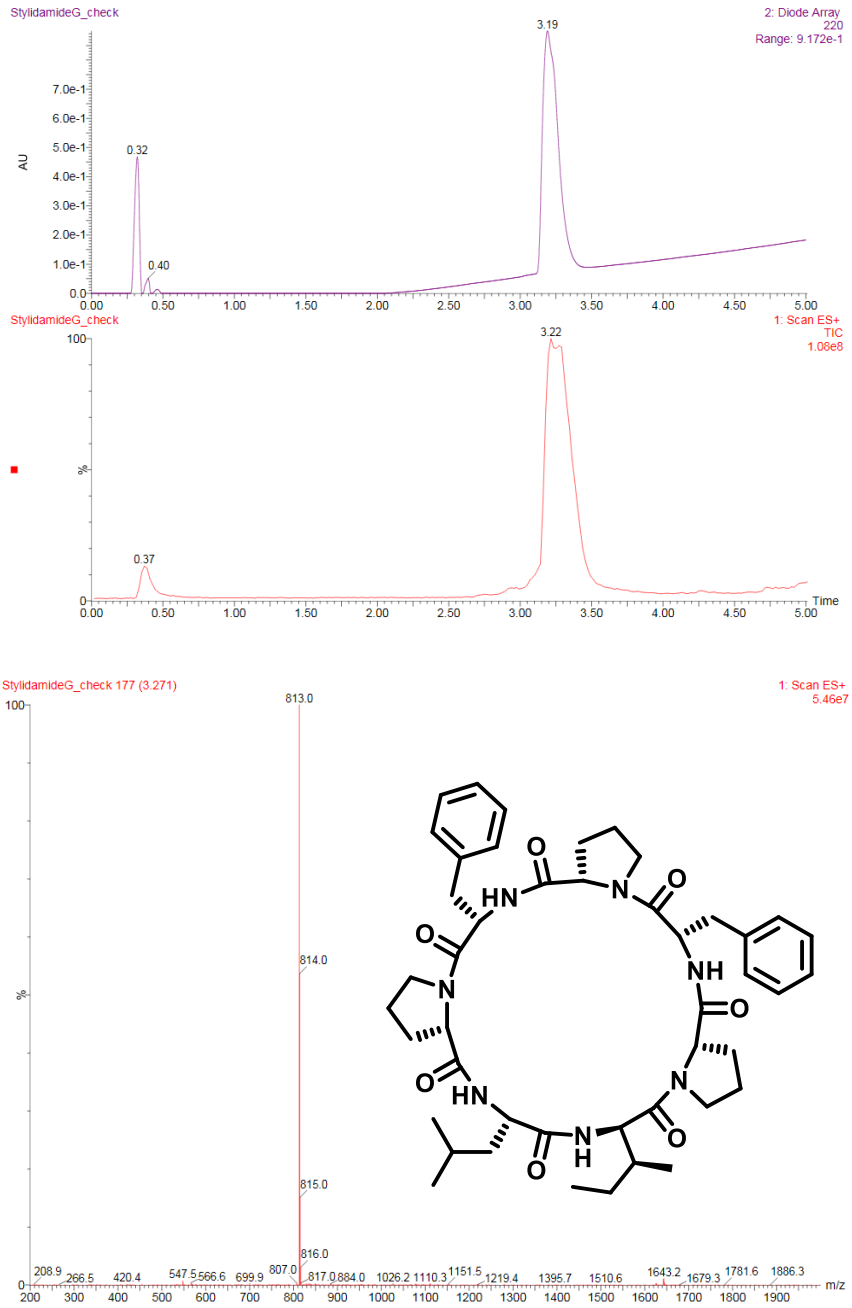

HPLC-MS Spectrum for Cylindrocyclin A

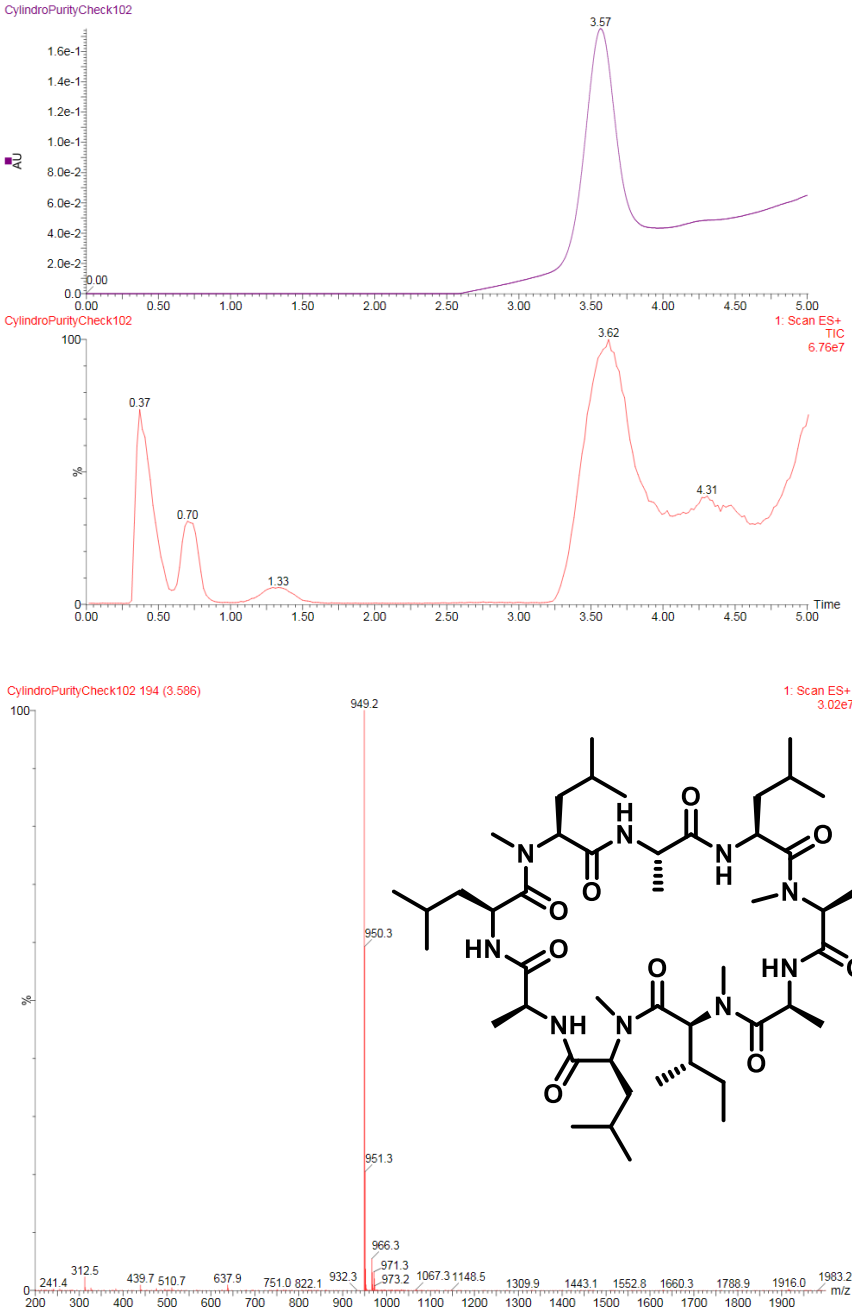

3.7.13. Selected NMR Spectra

NMR Spectrum for Cordyheptapeptide B in $CDCl_3$

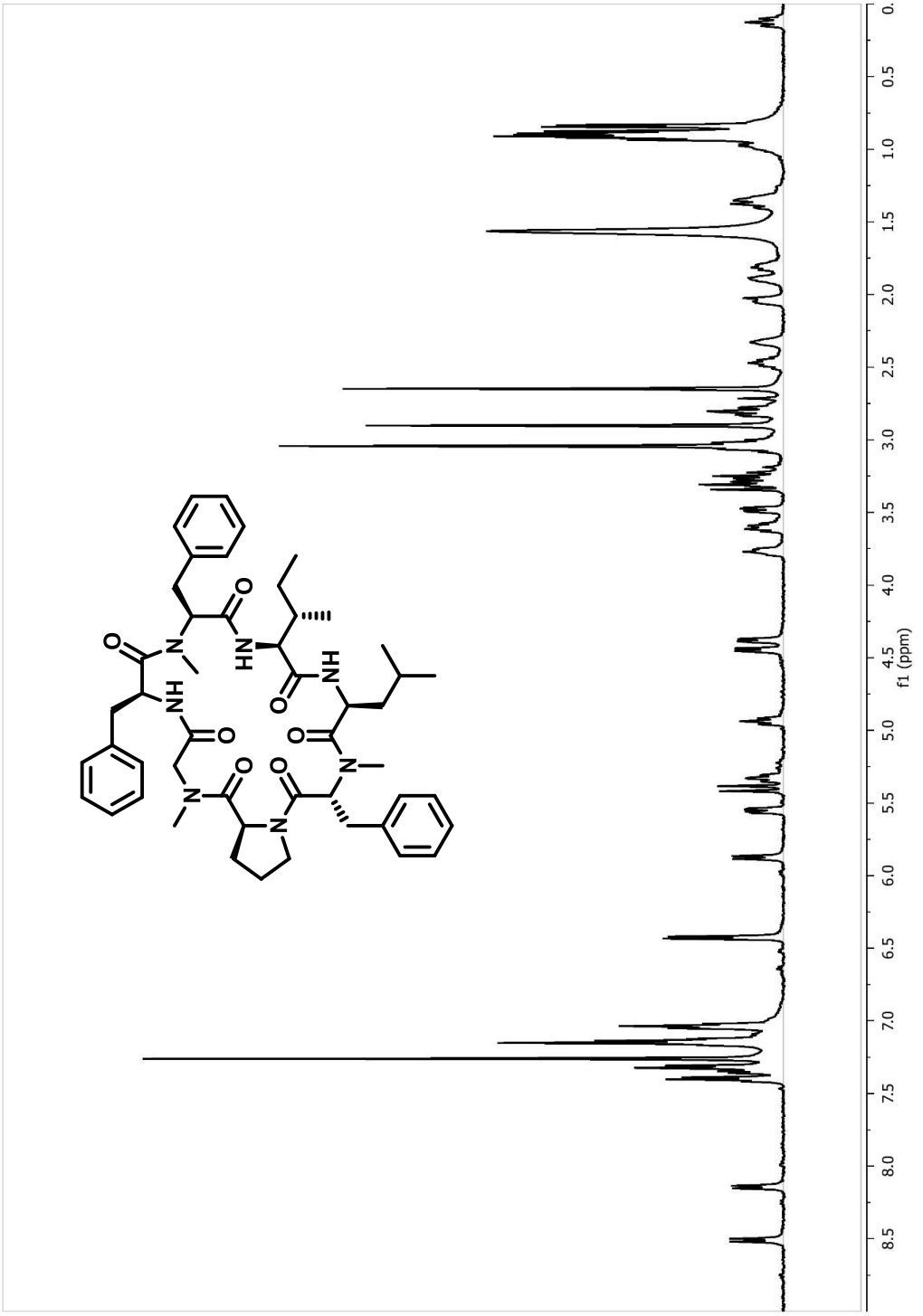

NMR Spectrum for Scytalidamide A in Pyridine *d*5

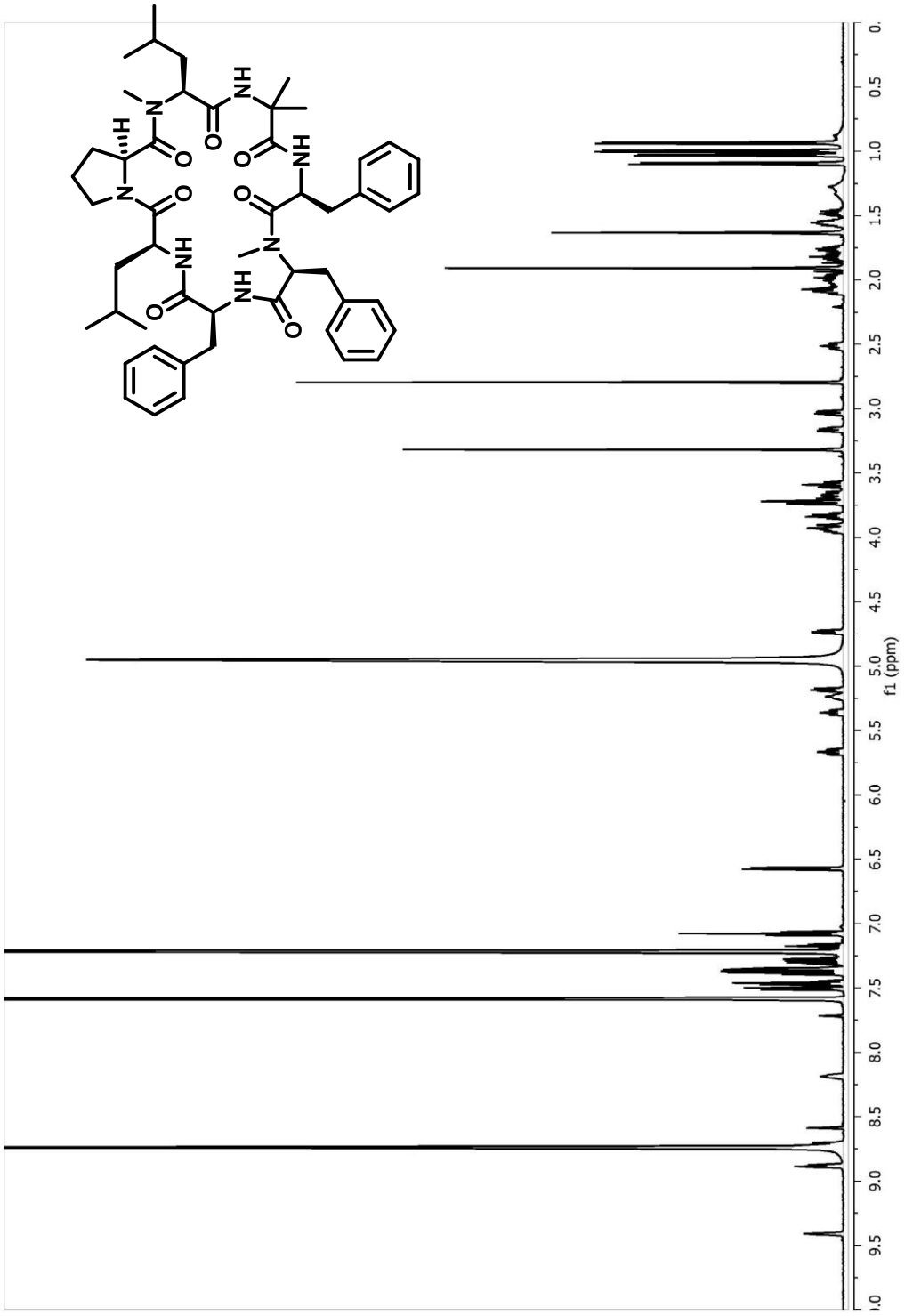

NMR Spectrum for Styllisamide G in DMSO *d*6

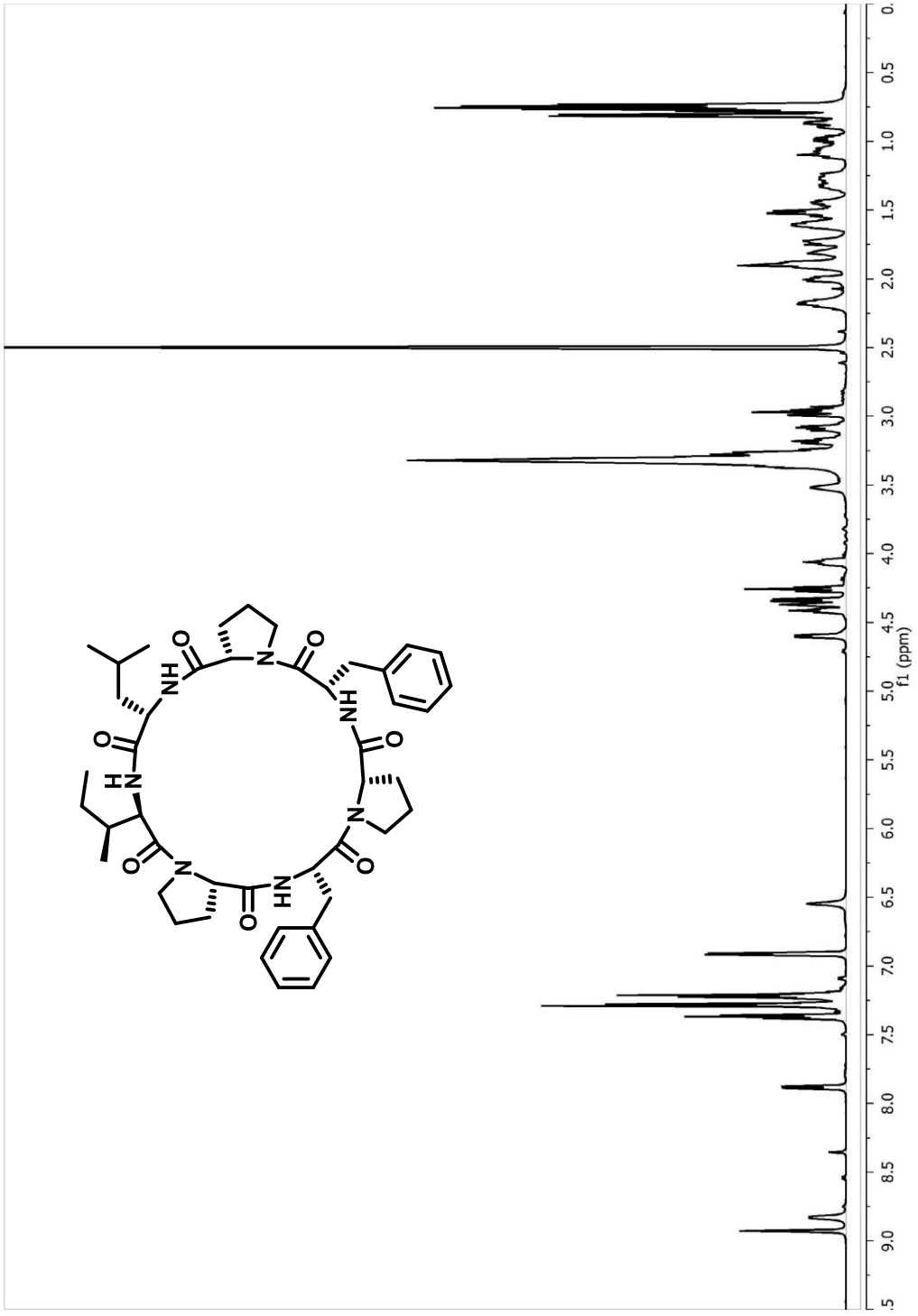

NMR Spectrum for Cylindrocyclin A in $CDCl_3$

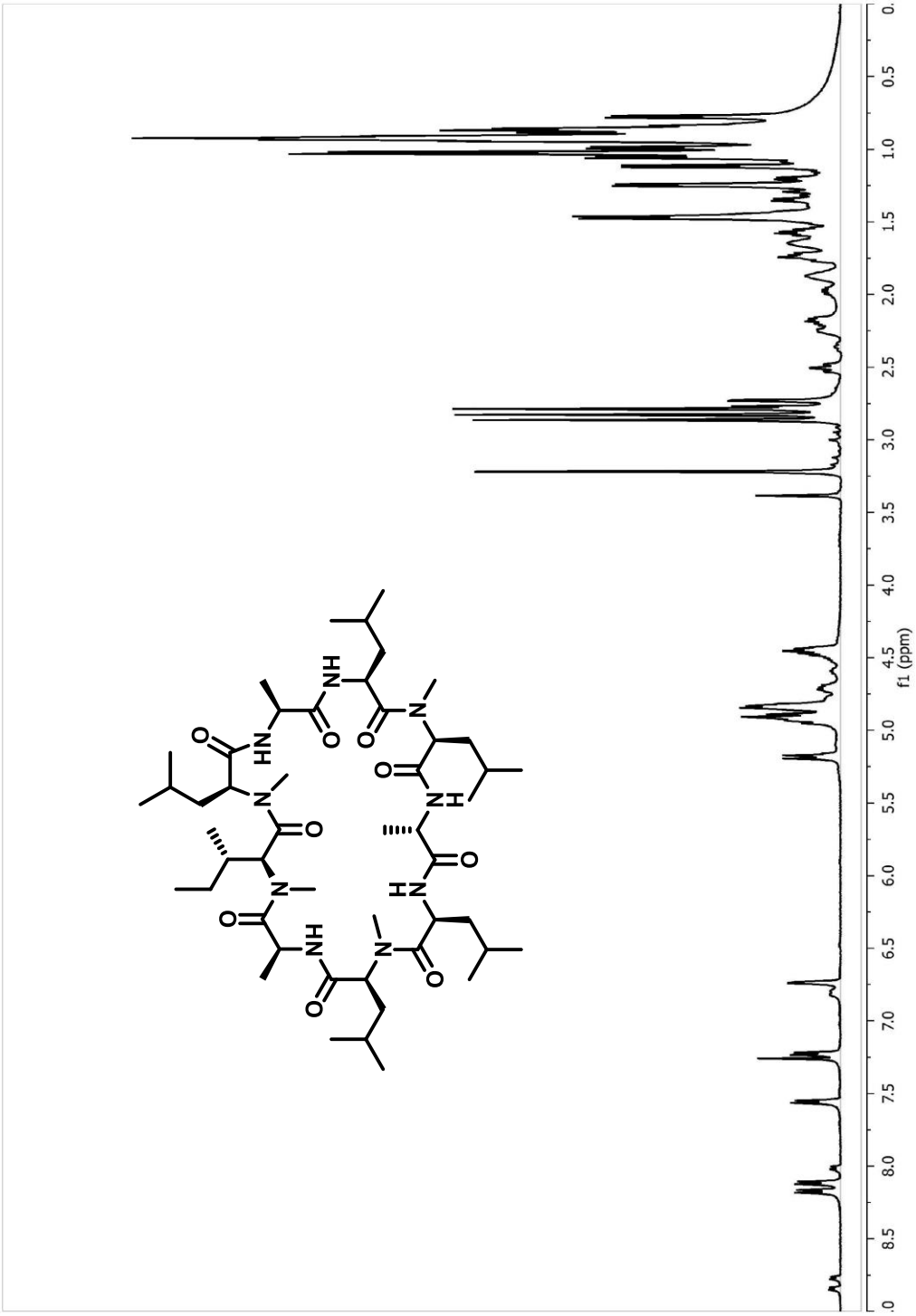

3.8. Conclusions

As the number of known bRo5 molecules exhibiting favorable PK grows, our understanding of this chemical space increases. For conformation-dependent effects, simple 2-D metrics are limited in their predictive power, while more in-depth conformational analysis may be required to probe the physiochemical factors underlying the properties of large molecules. As with typical small molecules, polarity may need to be adjusted to generate favorable solubility and permeability profiles in a drug discovery context.[61] Inspiration from natural products has led to cyclization, N-methylation, and unnatural stereochemistry as the first tools for increasing the permeability and stability of peptides. In the same way, the solvent dependent behavior of some natural products may provide inspiration for future efforts in macrocyclic design. Indeed, there are thousands of cyclic peptide natural products, comprising hundreds of unique scaffolds, which upon further study may reveal new insights into the relationship between structure and properties in this interesting chemical space. In summary, with this small set of compounds we present an approach for focusing on the natural stereochemistry of cyclic peptides as a way to increase permeability. Further studies on cyclic peptide natural products might help to reveal additional key features for understanding structure−property relationships in this chemical space.

3.9. References

(1) Morioka, T.; Loik, N. D.; Hipolito, C. J.; Goto, Y.; Suga, H. Selection-Based Discovery of Macrocyclic Peptides for the Next Generation Therapeutics. *Curr. Opin. Chem. Biol.* **2015**, *26*, 34–41.

(2) Young, T. S.; Young, D. D.; Ahmad, I.; Louis, J. M.; Benkovic, S. J.; Schultz, P. G. Evolution of Cyclic Peptide Protease Inhibitors. *Proc. Natl. Acad. Sci.* **2011**, *108* (27), 11052–11056.

(3) Morimoto, J.; Hayashi, Y.; Suga, H. Discovery of Macrocyclic Peptides Armed with a Mechanism-Based Warhead: Isoform-Selective Inhibition of Human Deacetylase SIRT2. *Angew. Chem. Int. Ed. Engl.* **2012**, *51* (14), 3423–3427.

(4) Hayashi, Y.; Morimoto, J.; Suga, H. In Vitro Selection of Anti-Akt2 Thioether-Macrocyclic Peptides Leading to Isoform-Selective Inhibitors. *ACS Chem. Biol.* **2012**, *7* (3), 607–613.

(5) Yamagishi, Y.; Shoji, I.; Miyagawa, S.; Kawakami, T.; Katoh, T.; Goto, Y.; Suga, H. Natural Product-like Macrocyclic N-Methyl-Peptide Inhibitors against a Ubiquitin Ligase Uncovered from a Ribosome-Expressed de Novo Library. *Chem. Biol.* **2011**, *18* (12), 1562–1570.

(6) Heinis, C.; Rutherford, T.; Freund, S.; Winter, G. Phage-Encoded Combinatorial Chemical Libraries Based on Bicyclic Peptides. *Nat. Chem. Biol.* **2009**, *5* (7), 502–507.

(7) White, E. R.; Sun, L.; Ma, Z.; Beckta, J. M.; Danzig, B. A.; Hacker, D. E.;

Huie, M.; Williams, D. C.; Edwards, R. A.; Valerie, K.; Glover, J. N. M.; Hartman, M. C. T. Peptide Library Approach to Uncover Phosphomimetic Inhibitors of the BRCA1 C-Terminal Domain. *ACS Chem. Biol.* **2015**, *10* (5), 1198–1208.

(8) Trinh, T. B.; Upadhyaya, P.; Qian, Z.; Pei, D. Discovery of a Direct Ras Inhibitor by Screening a Combinatorial Library of Cell-Permeable Bicyclic Peptides. *ACS Comb. Sci.* **2016**, *18* (1), 75–85.

(9) Jiang, B.; Pei, D. A Selective, Cell-Permeable Nonphosphorylated Bicyclic Peptidyl Inhibitor against Peptidyl-Prolyl Isomerase Pin1. *J. Med. Chem.* **2015**, *58* (15), 6306–6312.

(10) Tsomaia, N. Peptide Therapeutics: Targeting the Undruggable Space. *Eur. J. Med. Chem.* **2015**, *94*, 459–470.

(11) Bhat, A.; Roberts, L. R.; Dwyer, J. J. Lead Discovery and Optimization Strategies for Peptide Macrocycles. *Eur. J. Med. Chem.* **2015**, *94*, 471–479.

(12) Villar, E. A.; Beglov, D.; Chennamadhavuni, S.; Porco, J. A.; Kozakov, D.; Vajda, S.; Whitty, A. How Proteins Bind Macrocycles. *Nat. Chem. Biol.* **2014**, *10* (9), 723–731.

(13) Doak, B. C.; Zheng, J.; Dobritzsch, D.; Kihlberg, J. How Beyond Rule of 5 Drugs and Clinical Candidates Bind to Their Targets. *J. Med. Chem.* **2016**, *59* (6), 2312–2327.

(14) Doak, B. C.; Over, B.; Giordanetto, F.; Kihlberg, J. Oral Druggable Space beyond the Rule of 5: Insights from Drugs and Clinical Candidates. *Chem.*

Biol. **2014**, *21* (9), 1115–1142.

(15) Lipinski, C. A.; Lombardo, F.; Dominy, B. W.; Feeney, P. J. Experimental and Computational Approaches to Estimate Solubility and Permeability in Drug Discovery and Development Settings. *Adv. Drug Deliv. Rev.* **2001**, *46* (1–3), 3–26.

(16) Wang, C. K.; Northfield, S. E.; Swedberg, J. E.; Colless, B.; Chaousis, S.; Price, D. A.; Liras, S.; Craik, D. J. Exploring Experimental and Computational Markers of Cyclic Peptides: Charting Islands of Permeability. *Eur. J. Med. Chem.* **2015**, *97*, 202–213.

(17) Over, B.; McCarren, P.; Artursson, P.; Foley, M.; Giordanetto, F.; Grönberg, G.; Hilgendorf, C.; Lee, M. D.; Matsson, P.; Muncipinto, G.; Pellisson, M.; Perry, M. W. D.; Svensson, R.; Duvall, J. R.; Kihlberg, J. Impact of Stereospecific Intramolecular Hydrogen Bonding on Cell Permeability and Physicochemical Properties. *J. Med. Chem.* **2014**, *57* (6), 2746–2754.

(18) Ahlbach, C. L.; Lexa, K. W.; Bockus, A. T.; Chen, V.; Crews, P.; Jacobson, M. P.; Lokey, R. S. Beyond Cyclosporine A: Conformation-Dependent Passive Membrane Permeabilities of Cyclic Peptide Natural Products. *Future Med. Chem.* **2015**, 1–10.

(19) Rand, A. C.; Leung, S. S. F.; Eng, H.; Rotter, C. J.; Sharma, R.; Kalgutkar, A. S.; Zhang, Y.; Varma, M. V; Farley, K. A.; Khunte, B.; Limberakis, C.; Price, D. A.; Liras, S.; Mathiowetz, A. M.; Jacobson, M. P.; Lokey, R. S. Optimizing PK Properties of Cyclic Peptides: The Effect of Side Chain Substitutions on

Permeability and Clearance. *Medchemcomm* **2012**, *3* (10), 1282–1289.

(20) Hewitt, W. M.; Leung, S. S. F.; Pye, C. R.; Ponkey, A. R.; Bednarek, M.; Jacobson, M. P.; Lokey, R. S. Cell-Permeable Cyclic Peptides from Synthetic Libraries Inspired by Natural Products. *J. Am. Chem. Soc.* **2015**, *137* (2), 715–721.

(21) Chatterjee, J.; Gilon, C.; Hoffman, A.; Kessler, H. N-Methylation of Peptides: A New Perspective in Medicinal Chemistry. *Acc. Chem. Res.* **2008**, *41* (10), 1331–1342.

(22) White, T. R.; Renzelman, C. M.; Rand, A. C.; Rezai, T.; McEwen, C. M.; Gelev, V. M.; Turner, R. A.; Linington, R. G.; Leung, S. S. F.; Kalgutkar, A. S.; Bauman, J. N.; Zhang, Y.; Liras, S.; Price, D. A.; Mathiowetz, A. M.; Jacobson, M. P.; Lokey, R. S. On-Resin N-Methylation of Cyclic Peptides for Discovery of Orally Bioavailable Scaffolds. *Nat. Chem. Biol.* **2011**, *7* (11).

(23) Wang, C. K.; Northfield, S. E.; Colless, B.; Chaousis, S.; Hamernig, I.; Lohman, R.-J.; Nielsen, D. S.; Schroeder, C. I.; Liras, S.; Price, D. A.; Fairlie, D. P.; Craik, D. J. Rational Design and Synthesis of an Orally Bioavailable Peptide Guided by NMR Amide Temperature Coefficients. *Proc. Natl. Acad. Sci.* **2014**, *111* (49), 17504–17509.

(24) Bockus, A. T.; Schwochert, J. A.; Pye, C. R.; Townsend, C. E.; Sok, V.; Bednarek, M. A.; Lokey, R. S. Going Out on a Limb: Delineating The Effects of β-Branching, N-Methylation, and Side Chain Size on the Passive Permeability, Solubility, and Flexibility of Sanguinamide A Analogues. *J.*

Med. Chem. **2015**, *58* (18), 7409–7418.

(25) Nielsen, D. S.; Hoang, H. N.; Lohman, R.-J.; Hill, T. A.; Lucke, A. J.; Craik, D. J.; Edmonds, D. J.; Griffith, D. A.; Rotter, C. J.; Ruggeri, R. B.; Price, D. A.; Liras, S.; Fairlie, D. P. Improving on Nature: Making a Cyclic Heptapeptide Orally Bioavailable. *Angew. Chem. Int. Ed. Engl.* **2014**, *53* (45), 12059–12063.

(26) Schwochert, J.; Turner, R.; Thang, M.; Berkeley, R. F.; Ponkey, A. R.; Rodriguez, K. M.; Leung, S. S. F.; Khunte, B.; Goetz, G.; Limberakis, C.; Kalgutkar, A. S.; Eng, H.; Shapiro, M. J.; Mathiowetz, A. M.; Price, D. A.; Liras, S.; Jacobson, M. P.; Lokey, R. S. Peptide to Peptoid Substitutions Increase Cell Permeability in Cyclic Hexapeptides. *Org. Lett.* **2015**, *17* (12), 2928–2931.

(27) Bockus, A. T.; Lexa, K. W.; Pye, C. R.; Kalgutkar, A. S.; Gardner, J. W.; Hund, K. C. R.; Hewitt, W. M.; Schwochert, J. A.; Glassey, E.; Price, D. A.; Mathiowetz, A. M.; Liras, S.; Jacobson, M. P.; Lokey, R. S. Probing the Physicochemical Boundaries of Cell Permeability and Oral Bioavailability in Lipophilic Macrocycles Inspired by Natural Products. *J. Med. Chem.* **2015**, *58* (11), 4581–4589.

(28) Whitty, A.; Zhong, M.; Viarengo, L.; Beglov, D.; Hall, D. R.; Vajda, S. Quantifying the Chameleonic Properties of Macrocycles and Other High-Molecular-Weight Drugs. *Drug Discov. Today* **2016**, *21* (5), 712–717.

(29) Bockus, A. T.; McEwen, C. M.; Lokey, R. S. Form and Function in Cyclic

Peptide Natural Products: A Pharmacokinetic Perspective. *Curr. Top. Med. Chem.* **2013**, *13* (7), 821–836.

(30) Sekizawa, R.; Momose, I.; Kinoshita, N.; Naganawa, H.; Hamada, M.; Muraoka, Y.; Iinuma, H.; Takeuchi, T. Isolation and Structural Determination of Phepropeptins A, B, C, and D, New Proteasome Inhibitors, Produced by Streptomyces Sp. *J. Antibiot. (Tokyo).* **2001**, *54* (11), 874–881.

(31) Ghose, A. K.; Viswanadhan, V. N.; Wendoloski, J. J. Prediction of Hydrophobic (Lipophilic) Properties of Small Organic Molecules Using Fragmental Methods: An Analysis of ALOGP and CLOGP Methods. *J. Phys. Chem. A* **1998**, *102* (21), 3762–3772.

(32) Waring, M. J. Defining Optimum Lipophilicity and Molecular Weight Ranges for Drug Candidates-Molecular Weight Dependent Lower logD Limits Based on Permeability. *Bioorg. Med. Chem. Lett.* **2009**, *19* (10), 2844–2851.

(33) Irvine, J. D.; Takahashi, L.; Lockhart, K.; Cheong, J.; Tolan, J. W.; Selick, H. E.; Grove, J. R. MDCK (Madin-Darby Canine Kidney) Cells: A Tool for Membrane Permeability Screening. *J. Pharm. Sci.* **1999**, *88* (1), 28–33.

(34) Koehorst, R. B. M.; Spruijt, R. B.; Vergeldt, F. J.; Hemminga, M. A. Lipid Bilayer Topology of the Transmembrane Alpha-Helix of M13 Major Coat Protein and Bilayer Polarity Profile by Site-Directed Fluorescence Spectroscopy. *Biophys. J.* **2004**, *87* (3), 1445–1455.

(35) Wang, C. K.; Northfield, S. E.; Swedberg, J. E.; Colless, B.; Chaousis, S.; Price, D. A.; Liras, S.; Craik, D. J. Exploring Experimental and Computational

Markers of Cyclic Peptides: Charting Islands of Permeability. *Eur. J. Med. Chem.* **2015**.

(36) Desai, P. V; Raub, T. J.; Blanco, M.-J. How Hydrogen Bonds Impact P-Glycoprotein Transport and Permeability. *Bioorg. Med. Chem. Lett.* **2012**, *22* (21), 6540–6548.

(37) Cierpicki, T.; Otlewski, J. Amide Proton Temperature Coefficients as Hydrogen Bond Indicators in Proteins. *J. Biomol. NMR 21* (3), 249–261.

(38) Rezai, T.; Bock, J. E.; Zhou, M. V; Kalyanaraman, C.; Lokey, R. S.; Jacobson, M. P. Conformational Flexibility, Internal Hydrogen Bonding, and Passive Membrane Permeability: Successful in Silico Prediction of the Relative Permeabilities of Cyclic Peptides. *J. Am. Chem. Soc.* **2006**, *128* (43), 14073–14080.

(39) Hill, T. A.; Lohman, R.-J.; Hoang, H. N.; Nielsen, D. S.; Scully, C. C. G.; Kok, W. M.; Liu, L.; Lucke, A. J.; Stoermer, M. J.; Schroeder, C. I.; Chaousis, S.; Colless, B.; Bernhardt, P. V; Edmonds, D. J.; Griffith, D. A.; Rotter, C. J.; Ruggeri, R. B.; Price, D. A.; Liras, S.; Craik, D. J.; Fairlie, D. P. Cyclic Penta- and Hexaleucine Peptides without N-Methylation Are Orally Absorbed. *ACS Med. Chem. Lett.* **2014**, *5* (10), 1148–1151.

(40) Nielsen, D. S.; Lohman, R.-J.; Hoang, H. N.; Hill, T. A.; Jones, A.; Lucke, A. J.; Fairlie, D. P. Flexibility versus Rigidity for Orally Bioavailable Cyclic Hexapeptides. *Chembiochem* **2015**, *16* (16), 2289–2293.

(41) Kuhn, B.; Mohr, P.; Stahl, M. Intramolecular Hydrogen Bonding in Medicinal

Chemistry. *J. Med. Chem.* **2010**, *53* (6), 2601–2611.

(42) Grant, J. A.; Pickup, B. T.; Nicholls, A. A Smooth Permittivity Function for Poisson-Boltzmann Solvation Methods. *J. Comput. Chem.* **2001**, *22* (6), 608–640.

(43) Di, L.; Kerns, E. H.; Hong, Y.; Chen, H. Development and Application of High Throughput Plasma Stability Assay for Drug Discovery. *Int. J. Pharm.* **2005**, *297* (1–2), 110–119.

(44) Phillips, J. C.; Braun, R.; Wang, W.; Gumbart, J.; Tajkhorshid, E.; Villa, E.; Chipot, C.; Skeel, R. D.; Kale, L.; Schulten, K. Scalable Molecular Dynamics with NAMD. *J. Comput. Chem.* **2005**, *26* (16), 1781–1802.

(45) Shen, Y.; Bax, A. Prediction of Xaa-Pro Peptide Bond Conformation from Sequence and Chemical Shifts. *J. Biomol. NMR* **2010**, *46* (3), 199–204.

(46) Wang, A. C.; Bax, A. Determination of the Backbone Dihedral Angles φ in Human Ubiquitin from Reparametrized Empirical Karplus Equations. *J. Am. Chem. Soc.* **1996**, *118* (10), 2483–2494.

(47) Schwochert, J.; Lao, Y.; Pye, C. R.; Naylor, M. R.; Desai, P. V; Gonzalez Valcarcel, I. C.; Barrett, J. A.; Sawada, G.; Blanco, M.-J.; Lokey, R. S. Stereochemistry Balances Cell Permeability and Solubility in the Naturally Derived Phepropeptin Cyclic Peptides. *ACS Med. Chem. Lett.* **2016**, *7* (8), 757–761.

(48) Pye, C. R.; Hewitt, W. M.; Schwochert, J.; Haddad, T. D.; Townsend, C. E.; Etienne, L.; Lao, Y.; Limberakis, C.; Furukawa, A.; Mathiowetz, A. M.; Price,

D. A.; Liras, S.; Lokey, R. S. Nonclassical Size Dependence of Permeation Defines Bounds for Passive Adsorption of Large Drug Molecules. *J. Med. Chem.* **2017**, *60* (5), 1665–1672.

(49) Nielsen, D. S.; Hoang, H. N.; Lohman, R.-J.; Diness, F.; Fairlie, D. P. Total Synthesis, Structure, and Oral Absorption of a Thiazole Cyclic Peptide, Sanguinamide A. *Org. Lett.* **2012**, *14* (22), 5720–5723.

(50) Bockus, A. T.; McEwen, C. M.; Lokey, R. S. Form and Function in Cyclic Peptide Natural Products: A Pharmacokinetic Perspective. *Curr. Top. Med. Chem.* **2013**, *13* (7), 821–836.

(51) Wang, C. K.; Craik, D. J. Cyclic Peptide Oral Bioavailability: Lessons from the Past. *Biopolymers* **2016**, *106* (6), 901–909.

(52) Weber, D.; Erosa, G.; Sterner, O.; Anke, T. Cylindrocyclin A, a New Cytotoxic Cyclopeptide from Cylindrocarpon Sp. *J. Antibiot. (Tokyo).* **2006**, *59* (8), 495–499.

(53) Thern, B.; Rudolph, J.; Jung, G. Triphosgene as Highly Efficient Reagent for the Solid-Phase Coupling of N-Alkylated Amino Acids—total Synthesis of Cyclosporin O. *Tetrahedron Lett.* **2002**, *43* (28), 5013–5016.

(54) Wang, X.; Morinaka, B. I.; Molinski, T. F. Structures and Solution Conformational Dynamics of Stylissamides G and H from the Bahamian Sponge *Stylissa Caribica*. *J. Nat. Prod.* **2014**, *77* (3), 625–630.

(55) Fang, W.-Y.; Dahiya, R.; Qin, H.-L.; Mourya, R.; Maharaj, S. Natural Proline-Rich Cyclopolypeptides from Marine Organisms: Chemistry, Synthetic

Methodologies and Biological Status. *Mar. Drugs* **2016**, *14* (11), 194.

(56) Isaka, M.; Srisanoh, U.; Lartpornmatulee, N.; Boonruangprapa, T. ES-242 Derivatives and Cycloheptapeptides from Cordyceps Sp. Strains BCC 16173 and BCC 16176. *J. Nat. Prod.* **2007**, *70* (10), 1601–1604.

(57) Dahiya, R.; Singh, S.; Sharma, A.; Chennupati, S.; Maharaj, S. First Total Synthesis and Biological Screening of a Proline-Rich Cyclopeptide from a Caribbean Marine Sponge. *Mar. Drugs* **2016**, *14* (12), 228.

(58) Chen, Z.; Song, Y.; Chen, Y.; Huang, H.; Zhang, W.; Ju, J. Cyclic Heptapeptides, Cordyheptapeptides C–E, from the Marine-Derived Fungus *Acremonium Persicinum* SCSIO 115 and Their Cytotoxic Activities. *J. Nat. Prod.* **2012**, *75* (6), 1215–1219.

(59) Tan, L. T.; Cheng, X. C.; Jensen, P. R.; Fenical, W. Scytalidamides A and B, New Cytotoxic Cyclic Heptapeptides from a Marine Fungus of the Genus Scytalidium. *J. Org. Chem.* **2003**, *68* (23), 8767–8773.

(60) Gu, W.; Silverman, R. B. Solid-Phase Total Synthesis of Scytalidamide A. *J. Org. Chem.* **2003**, *68* (23), 8774–8779.

(61) Di, L.; Fish, P. V; Mano, T. Bridging Solubility between Drug Discovery and Development. *Drug Discov. Today* **2012**, *17* (9–10), 486–495.

4. BIBLIOGRAPHY

Ahlbach, C.L., Lexa, K.W., Bockus, A.T., Chen, V., Crews, P., Jacobson, M.P., Lokey, R.S.,. Beyond cyclosporine A: conformation-dependent passive membrane permeabilities of cyclic peptide natural products. *Future Med. Chem.* **2015**, 1–10. doi:10.4155/fmc.15.78

Atasoylu, O., Furst, G., Risatti, C., Smith III, A.B.,. The Solution Structure of (+)-Spongistatin 1 in DMSO. *Org. Lett.* **2010**, *12* (8), 1788–1791. doi:10.1021/ol100417d

Beck, J.G., Chatterjee, J., Laufer, B., Kiran, M.U., Frank, A.O., Neubauer, S., Ovadia, O., Greenberg, S., Gilon, C., Hoffman, A., Kessler, H.,. Intestinal Permeability of Cyclic Peptides: Common Key Backbone Motifs Identified. *J. Am. Chem. Soc.* **2012**, *134* (29), 12125–12133. doi:10.1021/ja303200d

Bhat, A., Roberts, L.R., Dwyer, J.J.,. Lead discovery and optimization strategies for peptide macrocycles. *Eur. J. Med. Chem.* **2015**, *94*, 471–9. doi:10.1016/j.ejmech.2014.07.083

Biron, E., Chatterjee, J., Ovadia, O., Langenegger, D., Brueggen, J., Hoyer, D., Schmid, H.A., Jelinek, R., Gilon, C., Hoffman, A., Kessler, H.,. Improving oral bioavailability of peptides by multiple N-methylation: Somatostatin analogues. *Angew. Chem. Int. Ed. Engl.* **2008**, *47* (14), 2595–2599. doi:10.1002/anie.200705797

Biron, E., Kessler, H.,. Convenient synthesis of N-methylamino acids compatible with Fmoc solid-phase peptide synthesis. *J. Org. Chem.* **2005**, *70* (13), 5183–

5189. doi:10.1021/jo050477z

Bockus, A.T., Lexa, K.W., Pye, C.R., Kalgutkar, A.S., Gardner, J.W., Hund, K.C.R., Hewitt, W.M., Schwochert, J.A., Glassey, E., Price, D.A., Mathiowetz, A.M., Liras, S., Jacobson, M.P., Lokey, R.S.,. Probing the Physicochemical Boundaries of Cell Permeability and Oral Bioavailability in Lipophilic Macrocycles Inspired by Natural Products. *J. Med. Chem.* **2015**, *58* (11), 4581–9. doi:10.1021/acs.jmedchem.5b00128

Bockus, A.T., McEwen, C.M., Lokey, R.S.,. Form and Function in Cyclic Peptide Natural Products: A Pharmacokinetic Perspective. *Curr. Top. Med. Chem.* **2013**, *13* (7), 821–836.

Bockus, A.T., Schwochert, J.A., Pye, C.R., Townsend, C.E., Sok, V., Bednarek, M.A., Lokey, R.S.,. Going Out on a Limb: Delineating The Effects of β-Branching, N-Methylation, and Side Chain Size on the Passive Permeability, Solubility, and Flexibility of Sanguinamide A Analogues. *J. Med. Chem.* **2015**, *58* (18), 7409–18. doi:10.1021/acs.jmedchem.5b00919

Burgi, H.B., Dunitz, J.D., Lehn, J.M., Wipff, G.,. Stereochemistry of reaction paths at carbonyl centres. *Tetrahedron* **1974**, *30* (12), 1563–1572. doi:10.1016/s0040-4020(01)90678-7

Butterfoss, G.L., Drew, K., Renfrew, P.D., Kirshenbaum, K., Bonneau, R.,. Conformational preferences of peptide-peptoid hybrid oligomers. *Biopolymers* **2014**, *102* (5), 369–78. doi:10.1002/bip.22516

Callegari, E., Malhotra, B., Bungay, P.J., Webster, R., Fenner, K.S., Kempshall, S.,

LaPerle, J.L., Michel, M.C., Kay, G.G.,. A comprehensive non-clinical evaluation of the CNS penetration potential of antimuscarinic agents for the treatment of overactive bladder. *Br. J. Clin. Pharmacol.* **2011**, *72* (2), 235–246. doi:10.1111/j.1365-2125.2011.03961.x

Capon, R.J., Skene, C., Stewart, M., Ford, J., O'Hair, R.A.J., Williams, L., Lacey, E., Gill, J.H., Heiland, K., Friedel, T.,. Aspergillicins A-E: five novel depsipeptides from the marine-derived fungus Aspergillus carneus. *Org. Biomol. Chem.* **2003**, *1* (11), 1856–1862. doi:10.1039/b302306k

Carpino, L.A., Krause, E., Sferdean, C.D., Bienert, M., Beyermann, M.,. Dramatically enhanced N→O acyl migration during the trifluoroacetic acid-based deprotection step in solid phase peptide synthesis. *Tetrahedron Lett.* **2005**, *46* (8), 1361–1364. doi:10.1016/j.tetlet.2004.12.089

Chatterjee, J., Gilon, C., Hoffman, A., Kessler, H.,. N-Methylation of Peptides: A New Perspective in Medicinal Chemistry. *Acc. Chem. Res.* **2008**, *41* (10), 1331–1342. doi:10.1021/ar8000603

Chatterjee, J., Mierke, D.F., Kessler, H.,. Conformational preference and potential templates of N-methylated cyclic pentaalanine peptides. *Chem. Eur. J.* **2008**, *14* (5), 1508–1517. doi:10.1002/chem.200701029

Chen, Z., Song, Y., Chen, Y., Huang, H., Zhang, W., Ju, J.,. Cyclic Heptapeptides, Cordyheptapeptides C–E, from the Marine-Derived Fungus *Acremonium persicinum* SCSIO 115 and Their Cytotoxic Activities. *J. Nat. Prod.* **2012**, *75* (6), 1215–1219. doi:10.1021/np300152d

Cicero, D.O., Barbato, G., Bazzo, R.,. Nmr Analysis of Molecular Flexibility in Solution - a New Method for the Study of Complex Distributions of Rapidly Exchanging Conformations - Application to a 13-Residue Peptide with an 8-Residue Loop. *J. Am. Chem. Soc.* **1995**, *117* (3), 1027–1033. doi:Doi 10.1021/Ja00108a019

Cierpicki, T., Otlewski, J.,. Amide proton temperature coefficients as hydrogen bond indicators in proteins. *J. Biomol. NMR* n.d. *21* (3), 249–261. doi:10.1023/A:1012911329730

Dahiya, R., Singh, S., Sharma, A., Chennupati, S., Maharaj, S.,. First Total Synthesis and Biological Screening of a Proline-Rich Cyclopeptide from a Caribbean Marine Sponge. *Mar. Drugs* **2016**, *14* (12), 228. doi:10.3390/md14120228

De León-Rodríguez, L.M., Lubag, A., Udugamasooriya, D.G., Proneth, B., Brekken, R.A., Sun, X., Kodadek, T., Dean Sherry, A.,. MRI detection of VEGFR2 in vivo using a low molecular weight peptoid-(Gd)8-dendron for targeting. *J. Am. Chem. Soc.* **2010**, *132*, 12829–12831. doi:10.1021/ja105563a

Demmer, O., Frank, A.O., Hagn, F., Schottelius, M., Marinelli, L., Cosconati, S., Brack-Werner, R., Kremb, S., Wester, H.-J., Kessler, H.,. A conformationally frozen peptoid boosts CXCR4 affinity and anti-HIV activity. *Angew. Chem. Int. Ed. Engl.* **2012**, *51* (32), 8110–3. doi:10.1002/anie.201202090

Desai, P. V, Raub, T.J., Blanco, M.-J.,. How hydrogen bonds impact P-glycoprotein transport and permeability. *Bioorg. Med. Chem. Lett.* **2012**, *22* (21), 6540–8. doi:10.1016/j.bmcl.2012.08.059

Di, L., Fish, P. V, Mano, T.,. Bridging solubility between drug discovery and development. *Drug Discov. Today* **2012**, *17* (9–10), 486–95. doi:10.1016/j.drudis.2011.11.007

Di, L., Kerns, E.H., Hong, Y., Chen, H.,. Development and application of high throughput plasma stability assay for drug discovery. *Int. J. Pharm.* **2005**, *297* (1–2), 110–9. doi:10.1016/j.ijpharm.2005.03.022

Di, L., Whitney-Pickett, C., Umland, J.P., Zhang, H., Zhang, X., Gebhard, D.F., Lai, Y., Federico, J.J., Davidson, R.E., Smith, R., Reyner, E.L., Lee, C., Feng, B., Rotter, C., Varma, M. V, Kempshall, S., Fenner, K., El-Kattan, A.F., Liston, T.E., Troutman, M.D.,. Development of a new permeability assay using low-efflux MDCKII cells. *J. Pharm. Sci.* **2011**, *100* (11), 4974–85. doi:10.1002/jps.22674

Doak, B.C., Over, B., Giordanetto, F., Kihlberg, J.,. Oral druggable space beyond the rule of 5: insights from drugs and clinical candidates. *Chem. Biol.* **2014**, *21* (9), 1115–42. doi:10.1016/j.chembiol.2014.08.013

Doak, B.C., Zheng, J., Dobritzsch, D., Kihlberg, J.,. How Beyond Rule of 5 Drugs and Clinical Candidates Bind to Their Targets. *J. Med. Chem.* **2016**, *59* (6), 2312–27. doi:10.1021/acs.jmedchem.5b01286

Driggers, E.M., Hale, S.P., Lee, J., Terrett, N.K.,. The exploration of macrocycles for drug discovery - an underexploited structural class. *Nat. Rev. Drug Discov.* **2008**, *7* (7), 608–624. doi:10.1038/nrd2590

Driggers, E.M., Hale, S.P., Lee, J., Terrett, N.K.,. The exploration of macrocycles for

drug discovery--an underexploited structural class. *Nat. Rev. Drug Discov.* **2008**, *7* (7), 608–24. doi:10.1038/nrd2590

Ertl, P., Rohde, B., Selzer, P.,. Fast Calculation of Molecular Polar Surface Area as a Sum of Fragment-Based Contributions and Its Application to the Prediction of Drug Transport Properties. *J. Med. Chem.* **2000**, *43* (20), 3714–3717. doi:10.1021/jm000942e

Evans, D.A., Bodkin, M.J., Baker, S.R., Sharman, G.J.,. Janocchio - a Java applet for viewing 3D structures and calculating NMR couplings and NOEs. *Magn. Reson. Chem.* **2007**, *45* (7), 595–600. doi:10.1002/mrc.2016

Fang, W.-Y., Dahiya, R., Qin, H.-L., Mourya, R., Maharaj, S.,. Natural Proline-Rich Cyclopolypeptides from Marine Organisms: Chemistry, Synthetic Methodologies and Biological Status. *Mar. Drugs* **2016**, *14* (11), 194. doi:10.3390/md14110194

Fowler, S.A., Blackwell, H.E.,. Structure–function relationships in peptoids: Recent advances toward deciphering the structural requirements for biological function. *Org. Biomol. Chem.* **2009**, *7* (8), 1508. doi:10.1039/b817980h

Fowler, S.A., Stacy, D.M., Blackwell, H.E.,. Design and synthesis of macrocyclic peptomers as mimics of a quorum sensing signal from Staphylococcus aureus. *Org. Lett.* **2008**, *10* (12), 2329–2332. doi:10.1021/ol800908h

Gao, Y., Amar, S., Pahwa, S., Fields, G., Kodadek, T.,. Rapid lead discovery through iterative screening of one bead one compound libraries. *ACS Comb. Sci.* **2015**, *17* (1), 49–59. doi:10.1021/co500154e

Gao, Y., Kodadek, T.,. Direct comparison of linear and macrocyclic compound libraries as a source of protein ligands. *ACS Comb. Sci.* **2015**, *17* (3), 190–5. doi:10.1021/co500161c

Gavenonis, J., Sheneman, B.A., Siegert, T.R., Eshelman, M.R., Kritzer, J.A.,. Comprehensive analysis of loops at protein-protein interfaces for macrocycle design. *Nat. Chem. Biol.* **2014**, 1–8. doi:10.1038/nchembio.1580

Georghiou, G., Kleiner, R.E., Pulkoski-Gross, M., Liu, D.R., Seeliger, M.A.,. Highly specific, bisubstrate-competitive Src inhibitors from DNA-templated macrocycles. *Nat. Chem. Biol.* **2012**, *8* (4), 366–374. doi:10.1038/nchembio.792

Ghose, A.K., Crippen, G.M.,. Atomic Physicochemical Parameters for Three-Dimensional Structure-Directed Quantitative Structure-Activity Relationships I. Partition Coefficients as a Measure of Hydrophobicity. *J. Comput. Chem.* **1986**, *7* (4), 565–577. doi:10.1002/jcc.540070419

Ghose, A.K., Viswanadhan, V.N., Wendoloski, J.J.,. Prediction of Hydrophobic (Lipophilic) Properties of Small Organic Molecules Using Fragmental Methods: An Analysis of ALOGP and CLOGP Methods. *J. Phys. Chem. A* **1998**, *102* (21), 3762–3772. doi:10.1021/jp980230o

Goetz, G.H., Philippe, L., Shapiro, M.J.,. EPSA: A Novel Supercritical Fluid Chromatography Technique Enabling the Design of Permeable Cyclic Peptides. *ACS Med. Chem. Lett.* **2014**, *5* (10), 1167–72. doi:10.1021/ml500239m

Grant, J.A., Pickup, B.T., Nicholls, A.,. A smooth permittivity function for Poisson-Boltzmann solvation methods. *J. Comput. Chem.* **2001**, *22* (6), 608–640.

doi:10.1002/jcc.1032

Grundmann, F., Kaiser, M., Kurz, M., Schiell, M., Batzer, A., Bode, H.B.,. Structure determination of the bioactive depsipeptide xenobactin from Xenorhabdus sp PB30.3. *Rsc Adv.* **2013**, *3* (44), 22072–22077. doi:10.1039/c3ra44721a

Gu, W., Silverman, R.B.,. Solid-Phase Total Synthesis of Scytalidamide A. *J. Org. Chem.* **2003**, *68* (23), 8774–8779. doi:10.1021/jo0346712

Guimaraes, C.R.W., Mathiowetz, A.M., Shalaeva, M., Goetz, G., Liras, S.,. Use of 3D Properties to Characterize Beyond Rule-of-5 Property Space for Passive Permeation. *J. Chem. Inf. Model.* **2012**, *52* (4), 882–890. doi:10.1021/ci300010y

Hara, T., Durell, S.R., Myers, M.C., Appella, D.H.,. Probing the structural requirements of peptoids that inhibit HDM2-p53 interactions. *J. Am. Chem. Soc.* **2006**, *128*, 1995–2004. doi:10.1021/ja056344c

Hayashi, Y., Morimoto, J., Suga, H.,. In Vitro Selection of Anti-Akt2 Thioether-Macrocyclic Peptides Leading to Isoform-Selective Inhibitors. *ACS Chem. Biol.* **2012**, *7* (3), 607–613. doi:10.1021/cb200388k

Heinis, C., Rutherford, T., Freund, S., Winter, G.,. Phage-encoded combinatorial chemical libraries based on bicyclic peptides. *Nat. Chem. Biol.* **2009**, *5* (7), 502–507. doi:10.1038/nchembio.184

Hewitt, W.M., Leung, S.S.F., Pye, C.R., Ponkey, A.R., Bednarek, M., Jacobson, M.P., Lokey, R.S.,. Cell-permeable cyclic peptides from synthetic libraries inspired by natural products. *J. Am. Chem. Soc.* **2015**, *137* (2), 715–21. doi:10.1021/ja508766b

Hill, T.A., Lohman, R.-J., Hoang, H.N., Nielsen, D.S., Scully, C.C.G., Kok, W.M., Liu, L., Lucke, A.J., Stoermer, M.J., Schroeder, C.I., Chaousis, S., Colless, B., Bernhardt, P. V, Edmonds, D.J., Griffith, D.A., Rotter, C.J., Ruggeri, R.B., Price, D.A., Liras, S., Craik, D.J., Fairlie, D.P.,. Cyclic Penta- and Hexaleucine Peptides without N-Methylation Are Orally Absorbed. *ACS Med. Chem. Lett.* **2014**, *5* (10), 1148–51. doi:10.1021/ml5002823

Hopkins, A.L., Groom, C.R.,. The druggable genome. *Nat. Rev. Drug Discov.* **2002**, *1* (9), 727–30. doi:10.1038/nrd892

Irvine, J.D., Takahashi, L., Lockhart, K., Cheong, J., Tolan, J.W., Selick, H.E., Grove, J.R.,. MDCK (Madin-Darby canine kidney) cells: A tool for membrane permeability screening. *J. Pharm. Sci.* **1999**, *88* (1), 28–33. doi:10.1021/js9803205

Isaka, M., Srisanoh, U., Lartpornmatulee, N., Boonruangprapa, T.,. ES-242 derivatives and cycloheptapeptides from Cordyceps sp. strains BCC 16173 and BCC 16176. *J. Nat. Prod.* **2007**, *70* (10), 1601–4. doi:10.1021/np070357h

Jiang, B., Pei, D.,. A Selective, Cell-Permeable Nonphosphorylated Bicyclic Peptidyl Inhibitor against Peptidyl-Prolyl Isomerase Pin1. *J. Med. Chem.* **2015**, *58* (15), 6306–12. doi:10.1021/acs.jmedchem.5b00411

Jimenez, J.C., Lopez-Macia, A., Gracia, C., Varon, S., Carrascal, M., Caba, J.M., Royo, M., Francesch, A.M., Cuevas, C., Giralt, E., Albericio, F.,. Structure-activity relationship of kahalalide F synthetic analogues. *J. Med. Chem.* **2008**, *51* (16), 4920–4931. doi:10.1021/jm8000828

Knight, A.S., Zhou, E.Y., Pelton, J.G., Francis, M.B.,. Selective chromium(VI) ligands identified using combinatorial peptoid libraries. *J. Am. Chem. Soc.* **2013**, *135* (46), 17488–93. doi:10.1021/ja408788t

Knipp, G.T., Vander Velde, D.G., Siahaan, T.J., Borchardt, R.T.,. The effect of beta-turn structure on the passive diffusion of peptides across caco-2 cell monolayers. *Pharm. Res.* **1997**, *14*, 1332–1340. doi:10.1023/A:1012152117703

Koehorst, R.B.M., Spruijt, R.B., Vergeldt, F.J., Hemminga, M.A.,. Lipid bilayer topology of the transmembrane alpha-helix of M13 Major coat protein and bilayer polarity profile by site-directed fluorescence spectroscopy. *Biophys. J.* **2004**, *87* (3), 1445–55. doi:10.1529/biophysj.104.043208

Kuhn, B., Mohr, P., Stahl, M.,. Intramolecular hydrogen bonding in medicinal chemistry. *J. Med. Chem.* **2010**, *53* (6), 2601–11. doi:10.1021/jm100087s

Lewis, I., Schaefer, M., Wagner, T., Oberer, L., Sager, E., Wipfli, P., Vorherr, T.,. A Detailed Investigation on Conformation, Permeability and PK Properties of Two Related Cyclohexapeptides. *Int. J. Pept. Res. Ther.* **2014**,. doi:10.1007/s10989-014-9447-3

Lim, H.-S., Archer, C.T., Kim, Y.-C., Hutchens, T., Kodadek, T.,. Rapid identification of the pharmacophore in a peptoid inhibitor of the proteasome regulatory particle. *Chem. Commun. (Camb).* **2008**, (9), 1064–6. doi:10.1039/b717861a

Lim, H.S., Archer, C.T., Kodadek, T.,. Identification of a peptoid inhibitor of the proteasome 19S regulatory particle. *J. Am. Chem. Soc.* **2007**, *129*, 7750–7751.

doi:10.1021/ja072027p

Lipinski, C.A., Lombardo, F., Dominy, B.W., Feeney, P.J.,. Experimental and computational approaches to estimate solubility and permeability in drug discovery and development settings. *Adv. Drug Deliv. Rev.* **2001**, *46* (1–3), 3–26. doi:10.1016/S0169-409X(00)00129-0

Liu, T., Joo, S.H., Voorhees, J.L., Brooks, C.L., Pei, D.,. Synthesis and screening of a cyclic peptide library: discovery of small-molecule ligands against human prolactin receptor. *Bioorg. Med. Chem.* **2009**, *17* (3), 1026–33. doi:10.1016/j.bmc.2008.01.015

Lynn, K.D., Udugamasooriya, D.G., Roland, C.L., Castrillon, D.H., Kodadek, T.J., Brekken, R.A.,. GU81, a VEGFR2 antagonist peptoid, enhances the anti-tumor activity of doxorubicin in the murine MMTV-PyMT transgenic model of breast cancer. *BMC Cancer* **2010**, *10*, 397. doi:10.1186/1471-2407-10-397

Mas-Moruno, C., Cruz, L.J., Mora, P., Francesch, A., Messeguer, A., Pérez-Payá, E., Albericio, F.,. Smallest peptoids with antiproliferative activity on human neoplastic cells. *J. Med. Chem.* **2007**, *50*, 2443–2449. doi:10.1021/jm061166z

Mauger, A.B., Stuart, O.A.,. Synthesis of an actinomycin-related peptide lactone from the corresponding cyclic pentapeptide by N,O-acyl shift. *Int. J. Pept. Protein Res.* **1989**, *34* (3), 196–199.

Merrifield, R.B.,. Solid Phase Peptide Synthesis. I. The Synthesis of a Tetrapeptide. *J. Am. Chem. Soc.* **1963**, *85* (14), 2149–2154. doi:10.1021/ja00897a025

Montoliu, C., Humet, M., Canales, J.-J., Burda, J., Planells-Cases, R., Sánchez-Baeza,

F., Carbonell, T., Pérez-Payá, E., Messeguer, A., Ferrer-Montiel, A., Felipo, V.,. Prevention of in vivo excitotoxicity by a family of trialkylglycines, a novel class of neuroprotectants. *J. Pharmacol. Exp. Ther.* **2002**, *301*, 29–36. doi:10.1124/jpet.301.1.29

Morimoto, J., Hayashi, Y., Suga, H.,. Discovery of macrocyclic peptides armed with a mechanism-based warhead: isoform-selective inhibition of human deacetylase SIRT2. *Angew. Chem. Int. Ed. Engl.* **2012**, *51* (14), 3423–7. doi:10.1002/anie.201108118

Morioka, T., Loik, N.D., Hipolito, C.J., Goto, Y., Suga, H.,. Selection-based discovery of macrocyclic peptides for the Next generation therapeutics. *Curr. Opin. Chem. Biol.* **2015**, *26*, 34–41. doi:10.1016/j.cbpa.2015.01.023

Munoz-Alonso, M.J., Gonzalez-Santiago, L., Martinez, T., Losada, A., Galmarini, C.M., Munoz, A.,. The mechanism of action of plitidepsin. *Curr. Opin. Investig. Drugs* **2009**, *10* (6), 536–542.

Murphy, J.E., Uno, T., Hamer, J.D., Cohen, F.E., Dwarki, V., Zuckermann, R.N.,. A combinatorial approach to the discovery of efficient cationic peptoid reagents for gene delivery. *Proc. Natl. Acad. Sci.* **1998**, *95* (4), 1517–1522. doi:10.1073/pnas.95.4.1517

Nielsen, D.S., Hoang, H.N., Lohman, R.-J., Diness, F., Fairlie, D.P.,. Total synthesis, structure, and oral absorption of a thiazole cyclic peptide, sanguinamide A. *Org. Lett.* **2012**, *14* (22), 5720–3. doi:10.1021/ol3027347

Nielsen, D.S., Hoang, H.N., Lohman, R.-J., Hill, T.A., Lucke, A.J., Craik, D.J.,

Edmonds, D.J., Griffith, D.A., Rotter, C.J., Ruggeri, R.B., Price, D.A., Liras, S., Fairlie, D.P.,. Improving on nature: making a cyclic heptapeptide orally bioavailable. *Angew. Chem. Int. Ed. Engl.* **2014**, *53* (45), 12059–63. doi:10.1002/anie.201405364

Nielsen, D.S., Lohman, R.-J., Hoang, H.N., Hill, T.A., Jones, A., Lucke, A.J., Fairlie, D.P.,. Flexibility versus Rigidity for Orally Bioavailable Cyclic Hexapeptides. *Chembiochem* **2015**, *16* (16), 2289–93. doi:10.1002/cbic.201500441

Okino, T., Murakami, M., Haraguchi, R., Munekata, H., Matsuda, H., Yamaguchi, K.,. Micropeptins A and B, plasmin and trypsin inhibitors from the blue-green alga Microcystis aeruginosa. *Tetrahedron Lett.* **1993**, *34* (50), 8131–8134. doi:10.1016/S0040-4039(00)61471-5

Oliyai, R., Stella, V.J.,. Kinetics and mechanism of isomerization of cyclosporin A. *Pharm Res* **1992**, *9* (5), 617–622.

Olsen, C.A., Montero, A., Leman, L.J., Ghadiri, M.R.,. Macrocyclic peptoid-Peptide hybrids as inhibitors of class I histone deacetylases. *ACS Med. Chem. Lett.* **2012**, *3* (9), 749–53. doi:10.1021/ml300162r

Ovadia, O., Linde, Y., Haskell-Luevano, C., Dirain, M.L., Sheynis, T., Jelinek, R., Gilon, C., Hoffman, A.,. The effect of backbone cyclization on PK/PD properties of bioactive peptide-peptoid hybrids: The melanocortin agonist paradigm. *Bioorg. Med. Chem.* **2010**, *18* (2), 580–589. doi:10.1016/j.bmc.2009.12.010

Over, B., McCarren, P., Artursson, P., Foley, M., Giordanetto, F., Grönberg, G., Hilgendorf, C., Lee, M.D., Matsson, P., Muncipinto, G., Pellisson, M., Perry,

M.W.D., Svensson, R., Duvall, J.R., Kihlberg, J.,. Impact of stereospecific intramolecular hydrogen bonding on cell permeability and physicochemical properties. *J. Med. Chem.* **2014**, *57* (6), 2746–54. doi:10.1021/jm500059t

Pelay-Gimeno, M., Tulla-Puche, J., Albericio, F.,. "Head-to-Side-Chain" Cyclodepsipeptides of Marine Origin. *Mar. Drugs* **2013**, *11* (5), 1693–1717. doi:10.3390/md11051693

Peypoux, F., Bonmatin, J.M., Wallach, J.,. Recent trends in the biochemistry of surfactin. *Appl. Microbiol. Biotechnol.* **1999**, *51* (5), 553–563.

Phillips, J.C., Braun, R., Wang, W., Gumbart, J., Tajkhorshid, E., Villa, E., Chipot, C., Skeel, R.D., Kale, L., Schulten, K.,. Scalable molecular dynamics with NAMD. *J. Comput. Chem.* **2005**, *26* (16), 1781–1802. doi:10.1002/jcc.20289

Pye, C.R., Hewitt, W.M., Schwochert, J., Haddad, T.D., Townsend, C.E., Etienne, L., Lao, Y., Limberakis, C., Furukawa, A., Mathiowetz, A.M., Price, D.A., Liras, S., Lokey, R.S.,. Nonclassical Size Dependence of Permeation Defines Bounds for Passive Adsorption of Large Drug Molecules. *J. Med. Chem.* **2017**, *60* (5), 1665–1672. doi:10.1021/acs.jmedchem.6b01483

Raiford, L.C., Couturn, J.R.,. The migration of acyl from nitrogen to oxygen. *J. Am. Chem. Soc.* **1922**, *44*, 1792–1798. doi:10.1021/ja01429a025

Rainaldi, M., Moretto, V., Crisma, M., Peggion, E., Mammi, S., Toniolo, C., Cavicchioni, G.,. Peptoid residues and beta-turn formation. *J. Pept. Sci.* **2002**, *8* (6), 241–52. doi:10.1002/psc.392

Raj, M., Bullock, B.N., Arora, P.S.,. Plucking the high hanging fruit: a systematic

approach for targeting protein-protein interactions. *Bioorg. Med. Chem.* **2013**, *21* (14), 4051–7. doi:10.1016/j.bmc.2012.11.023

Rand, A.C., Leung, S.S.F., Eng, H., Rotter, C.J., Sharma, R., Kalgutkar, A.S., Zhang, Y., Varma, M. V, Farley, K.A., Khunte, B., Limberakis, C., Price, D.A., Liras, S., Mathiowetz, A.M., Jacobson, M.P., Lokey, R.S.,. Optimizing PK properties of cyclic peptides: the effect of side chain substitutions on permeability and clearance. *Medchemcomm* **2012**, *3* (10), 1282–1289. doi:10.1039/c2md20203d

Renfrew, P.D., Craven, T.W., Butterfoss, G.L., Kirshenbaum, K., Bonneau, R.,. A rotamer library to enable modeling and design of peptoid foldamers. *J. Am. Chem. Soc.* **2014**, *136* (24), 8772–82. doi:10.1021/ja503776z

Rezai, T., Bock, J.E., Zhou, M. V., Kalyanaraman, C., Lokey, R.S., Jacobson, M.P.,. Conformational flexibility, internal hydrogen bonding, and passive membrane permeability: Successful in silico prediction of the relative permeabilities of cyclic peptides. *J. Am. Chem. Soc.* **2006**, *128*, 14073–14080. doi:10.1021/ja063076p

Schwochert, J., Lao, Y., Pye, C.R., Naylor, M.R., Desai, P. V, Gonzalez Valcarcel, I.C., Barrett, J.A., Sawada, G., Blanco, M.-J., Lokey, R.S.,. Stereochemistry Balances Cell Permeability and Solubility in the Naturally Derived Phepropeptin Cyclic Peptides. *ACS Med. Chem. Lett.* **2016**, *7* (8), 757–61. doi:10.1021/acsmedchemlett.6b00100

Schwochert, J., Turner, R., Thang, M., Berkeley, R.F., Ponkey, A.R., Rodriguez, K.M., Leung, S.S.F., Khunte, B., Goetz, G., Limberakis, C., Kalgutkar, A.S.,

Eng, H., Shapiro, M.J., Mathiowetz, A.M., Price, D.A., Liras, S., Jacobson, M.P., Lokey, R.S.,. Peptide to Peptoid Substitutions Increase Cell Permeability in Cyclic Hexapeptides. *Org. Lett.* **2015**, *17* (12), 2928–31. doi:10.1021/acs.orglett.5b01162

Sekizawa, R., Momose, I., Kinoshita, N., Naganawa, H., Hamada, M., Muraoka, Y., Iinuma, H., Takeuchi, T.,. Isolation and structural determination of phepropeptins A, B, C, and D, new proteasome inhibitors, produced by Streptomyces sp. *J. Antibiot. (Tokyo).* **2001**, *54* (11), 874–81.

Shankaramma, S.C., Moehle, K., James, S., Vrijbloed, J.W., Obrecht, D., Robinson, J.A., Cavicchioni, G., Wang, L., Rosenberg, S., Marlowe, C.K., Spellmeyer, D.C., Tan, R.R., Frankel, A.D., Santi, D. V., Cohen, F.E., Bartlett, P.A.,. A family of macrocyclic antibiotics with a mixed peptide–Peptoid beta-hairpin backbone conformation. *Chem. Commun.* **2003**, *8* (15), 1842–1843. doi:10.1039/B304310J

Shen, Y., Bax, A.,. Prediction of Xaa-Pro peptide bond conformation from sequence and chemical shifts. *J. Biomol. NMR* **2010**, *46* (3), 199–204. doi:10.1007/s10858-009-9395-y

Skwarczynski, M., Kiso, Y.,. Application of the O-N intramolecular acyl migration reaction in medicinal chemistry. *Curr Med Chem* **2007**, *14* (26), 2813–2823.

Sui, Q., Borchardt, D., Rabenstein, D.L.,. Kinetics and equilibria of cis/trans isomerization of backbone amide bonds in peptoids. *J. Am. Chem. Soc.* **2007**, *129* (39), 12042–8. doi:10.1021/ja0740925

Tan, H.W., Tay, S.T.,. The inhibitory effects of aureobasidin A on Candida planktonic and biofilm cells. *Mycoses* **2013**, *56* (2), 150–156. doi:10.1111/j.1439-0507.2012.02225.x

Tan, L.T., Cheng, X.C., Jensen, P.R., Fenical, W.,. Scytalidamides A and B, New Cytotoxic Cyclic Heptapeptides from a Marine Fungus of the Genus Scytalidium. *J. Org. Chem.* **2003**, *68* (23), 8767–8773. doi:10.1021/jo030191z

Tan, N.C., Yu, P., Kwon, Y.U., Kodadek, T.,. High-throughput evaluation of relative cell permeability between peptoids and peptides. *Bioorganic Med. Chem.* **2008**, *16*, 5853–5861. doi:10.1016/j.bmc.2008.04.074

Thansandote, P., Harris, R.M., Dexter, H.L., Simpson, G.L., Pal, S., Upton, R.J., Valko, K.,. Improving the passive permeability of macrocyclic peptides: Balancing permeability with other physicochemical properties. *Bioorg. Med. Chem.* **2015**, *23* (2), 322–327. doi:10.1016/j.bmc.2014.11.034

Thern, B., Rudolph, J., Jung, G.,. Triphosgene as highly efficient reagent for the solid-phase coupling of N-alkylated amino acids—total synthesis of cyclosporin O. *Tetrahedron Lett.* **2002**, *43* (28), 5013–5016. doi:10.1016/S0040-4039(02)00657-3

Trinh, T.B., Upadhyaya, P., Qian, Z., Pei, D.,. Discovery of a Direct Ras Inhibitor by Screening a Combinatorial Library of Cell-Permeable Bicyclic Peptides. *ACS Comb. Sci.* **2016**, *18* (1), 75–85. doi:10.1021/acscombsci.5b00164

Tsomaia, N.,. Peptide therapeutics: targeting the undruggable space. *Eur. J. Med. Chem.* **2015**, *94*, 459–70. doi:10.1016/j.ejmech.2015.01.014

Turner, R.A., Hauksson, N.E., Gipe, J.H., Lokey, R.S.,. Selective, On-Resin N-Methylation of Peptide N-Trifluoroacetamides. *Org. Lett.* **2013**, *15* (19), 5012–5015. doi:10.1021/ol402341u

Udugamasooriya, D.G., Dineen, S.P., Brekken, R.A., Kodadek, T.,. A peptoid "Antibody surrogate" that antagonizes VEGF receptor 2 activity. *J. Am. Chem. Soc.* **2008**, *130*, 5744–5752. doi:10.1021/ja711193x

Udugamasooriya, D.G., Ritchie, C., Brekken, R.A., Kodadek, T.,. A peptoid antagonist of VEGF Receptor 2 recognizes a "hotspot" in the extracellular domain distinct from the hormone-binding site. *Bioorganic Med. Chem.* **2008**, *16*, 6338–6343. doi:10.1016/j.bmc.2008.05.015

van Zoelen, W., Buss, H.G., Ellebracht, N.C., Lynd, N.A., Fischer, D.A., Finlay, J., Hill, S., Callow, M.E., Callow, J.A., Kramer, E.J., Zuckermann, R.N., Segalman, R.A.,. Sequence of Hydrophobic and Hydrophilic Residues in Amphiphilic Polymer Coatings Affects Surface Structure and Marine Antifouling/Fouling Release Properties. *ACS Macro Lett.* **2014**, *3* (4), 364–368. doi:10.1021/mz500090n

Villar, E.A., Beglov, D., Chennamadhavuni, S., Porco, J.A., Kozakov, D., Vajda, S., Whitty, A.,. How proteins bind macrocycles. *Nat. Chem. Biol.* **2014**, *10* (9), 723–731. doi:10.1038/nchembio.1584

Wang, A.C., Bax, A.,. Determination of the Backbone Dihedral Angles φ in Human Ubiquitin from Reparametrized Empirical Karplus Equations. *J. Am. Chem. Soc.* **1996**, *118* (10), 2483–2494. doi:10.1021/ja9535524

Wang, C.K., Craik, D.J.,. Cyclic peptide oral bioavailability: Lessons from the past. *Biopolymers* **2016**, *106* (6), 901–909. doi:10.1002/bip.22878

Wang, C.K., Northfield, S.E., Colless, B., Chaousis, S., Hamernig, I., Lohman, R.-J., Nielsen, D.S., Schroeder, C.I., Liras, S., Price, D.A., Fairlie, D.P., Craik, D.J.,. Rational design and synthesis of an orally bioavailable peptide guided by NMR amide temperature coefficients. *Proc. Natl. Acad. Sci.* **2014**, *111* (49), 17504–17509. doi:10.1073/pnas.1417611111

Wang, C.K., Northfield, S.E., Swedberg, J.E., Colless, B., Chaousis, S., Price, D.A., Liras, S., Craik, D.J.,. Exploring experimental and computational markers of cyclic peptides: Charting islands of permeability. *Eur. J. Med. Chem.* **2015**, *97*, 202–13. doi:10.1016/j.ejmech.2015.04.049

Wang, X., Morinaka, B.I., Molinski, T.F.,. Structures and Solution Conformational Dynamics of Stylissamides G and H from the Bahamian Sponge *Stylissa caribica*. *J. Nat. Prod.* **2014**, *77* (3), 625–630. doi:10.1021/np400891s

Waring, M.J.,. Defining optimum lipophilicity and molecular weight ranges for drug candidates-Molecular weight dependent lower logD limits based on permeability. *Bioorg. Med. Chem. Lett.* **2009**, *19* (10), 2844–51. doi:10.1016/j.bmcl.2009.03.109

Weber, D., Erosa, G., Sterner, O., Anke, T.,. Cylindrocyclin A, a new cytotoxic cyclopeptide from Cylindrocarpon sp. *J. Antibiot. (Tokyo).* **2006**, *59* (8), 495–9. doi:10.1038/ja.2006.69

Wei, D.G., Chiang, V., Fyne, E., Balakrishnan, M., Barnes, T., Graupe, M.,

Hesselgesser, J., Irrinki, A., Murry, J.P., Stepan, G., Stray, K.M., Tsai, A., Yu, H., Spindler, J., Kearney, M., Spina, C.A., McMahon, D., Lalezari, J., Sloan, D., Mellors, J., Geleziunas, R., Cihlar, T.,. Histone Deacetylase Inhibitor Romidepsin Induces HIV Expression in CD4 T Cells from Patients on Suppressive Antiretroviral Therapy at Concentrations Achieved by Clinical Dosing. *Plos Pathog.* **2014**, *10* (4). doi:10.1371/journal.ppat.1004071

Westendorf, C., Schmidt, A., Coin, I., Furkert, J., Ridelis, I., Zampatis, D., Rutz, C., Wiesner, B., Rosenthal, W., Beyermann, M., Schuelein, R.,. Inhibition of Biosynthesis of Human Endothelin B Receptor by the Cyclodepsipeptide Cotransin. *J. Biol. Chem.* **2011**, *286* (41), 35588–35600. doi:10.1074/jbc.M111.239244

White, E.R., Sun, L., Ma, Z., Beckta, J.M., Danzig, B.A., Hacker, D.E., Huie, M., Williams, D.C., Edwards, R.A., Valerie, K., Glover, J.N.M., Hartman, M.C.T.,. Peptide library approach to uncover phosphomimetic inhibitors of the BRCA1 C-terminal domain. *ACS Chem. Biol.* **2015**, *10* (5), 1198–208. doi:10.1021/cb500757u

White, T.R., Renzelman, C.M., Rand, A.C., Rezai, T., McEwen, C.M., Gelev, V.M., Turner, R.A., Linington, R.G., Leung, S.S.F., Kalgutkar, A.S., Bauman, J.N., Zhang, Y., Liras, S., Price, D.A., Mathiowetz, A.M., Jacobson, M.P., Lokey, R.S.,. On-resin N-methylation of cyclic peptides for discovery of orally bioavailable scaffolds. *Nat. Chem. Biol.* **2011**, *7* (11). doi:10.1038/nchembio.664

Whitty, A., Zhong, M., Viarengo, L., Beglov, D., Hall, D.R., Vajda, S.,. Quantifying

the chameleonic properties of macrocycles and other high-molecular-weight drugs. *Drug Discov. Today* **2016**, *21* (5), 712–7. doi:10.1016/j.drudis.2016.02.005

Yamagishi, Y., Shoji, I., Miyagawa, S., Kawakami, T., Katoh, T., Goto, Y., Suga, H.,. Natural product-like macrocyclic N-methyl-peptide inhibitors against a ubiquitin ligase uncovered from a ribosome-expressed de novo library. *Chem. Biol.* **2011**, *18* (12), 1562–70. doi:10.1016/j.chembiol.2011.09.013

Young, T.S., Young, D.D., Ahmad, I., Louis, J.M., Benkovic, S.J., Schultz, P.G.,. Evolution of cyclic peptide protease inhibitors. *Proc. Natl. Acad. Sci.* **2011**, *108* (27), 11052–11056. doi:10.1073/pnas.1108045108

Zuckermann, R.N., Kerr, J.M., Kent, S.B.H., Moos, W.H.,. Efficient method for the preparation of peptoids [oligo(N-substituted glycines)] by submonomer solid-phase synthesis. *J. Am. Chem. Soc.* **1992**, *114* (26), 10646–10647. doi:10.1021/ja00052a076

Zuckermann, R.N., Kodadek, T.,. Peptoids as potential therapeutics. *Curr. Opin. Mol. Ther.* **2009**, *11*, 299–307.